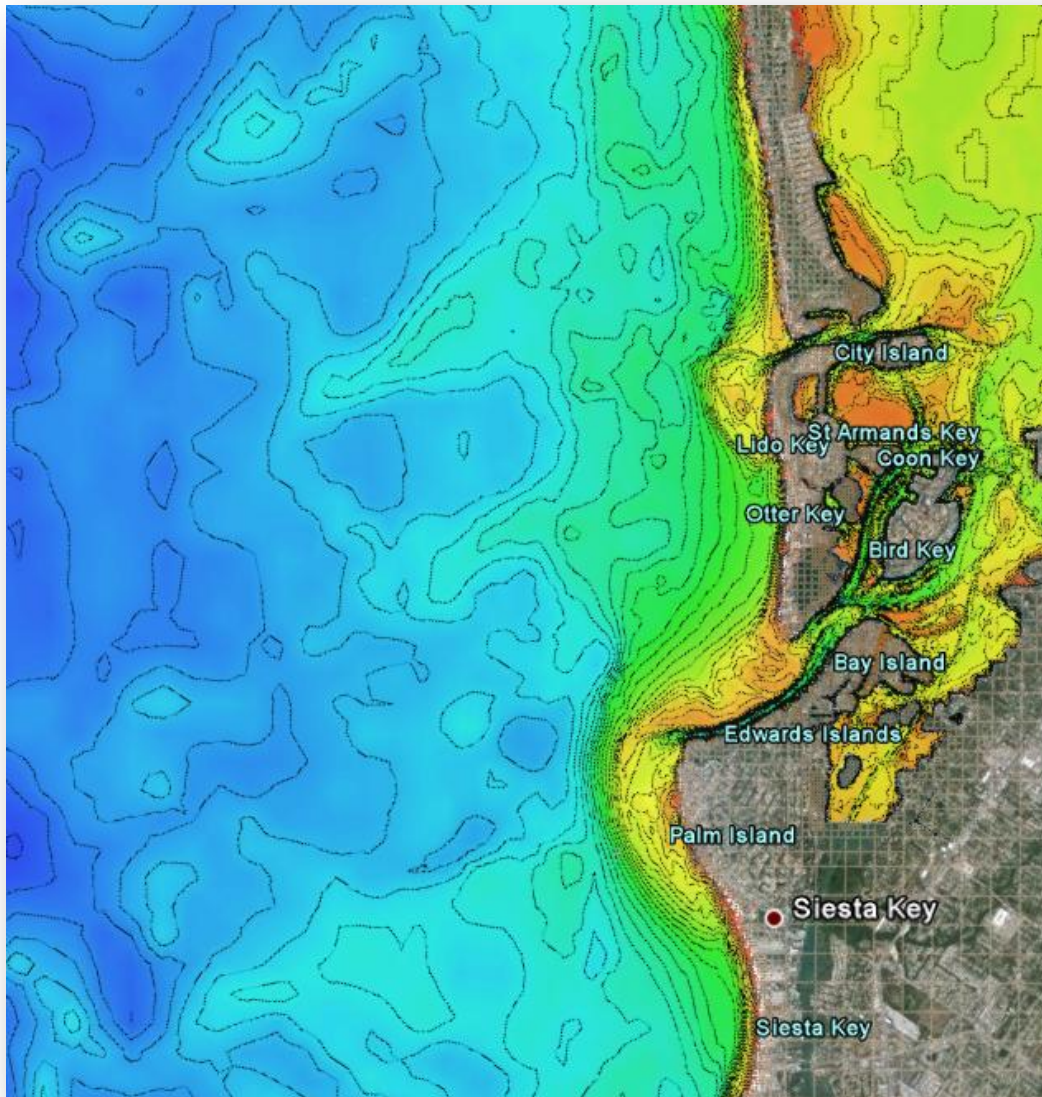


**Study of Big Sarasota Pass Sediment Mining Alternatives for
Sarasota County, Lido Key Federal Shore Protection Project**

Sarasota County, Florida

DRAFT 11 JUNE 2014



**US Army Corps
of Engineers**
Jacksonville District

Study of Big Sarasota Pass Sediment Mining Alternatives for Sarasota County, Lido Key Shore Protection Project

Sarasota County, Florida

Executive Summary

The USACE is requesting a State of Florida Water Quality Certification (WQC) from the Florida Department of Environmental Protection (FDEP) for the Lido Key Shore Protection Project (Lido Key SPP). USACE Jacksonville District performed a study which evaluates whether future excavation of the ebb shoal at Big Sarasota Pass (BSP) for use on Lido Key SPP, would significantly alter the ebb shoal morphology or local/regional sediment transport patterns in such a way that there would be adverse effects on adjacent beaches.

Included in this report is documentation of historical data as well as documentation of the methods and results from using the Coastal Modeling System (CMS) to examine potential change to the ebb shoal at Big Sarasota Pass for various ebb shoal mining scenarios to obtain sediment for the Shore Protection Project at Lido Key.

The volume and planform shape of the ebb shoal at BSP (~21MCY) has changed little since 1883. It was found from the analysis herein that it is possible to remove 1.3MCY of sediment from the ebb shoal without changing the planform area of the shoal. Further, it was determined that the project would be mining approximately 6% of the entire shoal volume. The mining volume is 56% of the “excess” sediment above the historical average of 21 MCY that has accreted over the past decade. The present volume of the ebb shoal of BSP is 23.3 MCY. After dredging, the volume would be approximately 22MCY.

It has been shown that the modifications of Lido Key in the 1920’s have lead to many of the present day issues including the accelerated erosion from the southern shoreline of Lido Key, channel pressure on the northern interior shoreline of Siesta Key, translation of the of the attachment point from the ebb shoal to the southeast along the shoreline of Siesta Key fronting the Gulf of Mexico, and ensuing erosion of the northwestern beaches of Siesta Key.

Results from the CMS model have shown that it is possible to mine the ebb shoal without affecting sediment transport pathways that deliver sediment to downdrift beaches (Siesta Key). A dredging configuration can be constructed that does not induce undesirable morphologic change at the ebb shoal, does not increase wave energy or affect navigation. Dredging configurations have been investigated that may potentially alleviate some of the negative impacts from the activities of the 1920’s through mid-century and relieve pressure from the main ebb channel on the interior north shoreline of Siesta Key, if desired. The dredging configuration ensures the sustainability of mining sediment from the ebb shoal, ensures that sediment transport pathways are not interrupted, and that sediment will continue to be bypassed to Siesta Key.

The historical sediment budget has been updated to include the potential effects of mining the ebb shoal and placing sediment on Lido Key. It has been found that sediment transport volumes to downdrift beaches will not be affected because additional sediment is brought into the system that had been immobile within the ebb shoal at Big Sarasota Pass. Expected annual bypassing rates for sediment are not decreased from the present rate.

Table of Contents

1.	OVERVIEW	15
1.1.	Introduction	15
1.2.	Historical Inlet Behavior	17
1.3.	John Ringling and the History of Lido Key	22
1.4.	Physical and Environmental Characteristics	25
1.5.	Big Sarasota Pass	25
1.5.1.	Bathymetric Analysis of Big Sarasota Pass: Ebb Shoal Volume and Planform ..	25
1.5.2.	Main ebb channel migration	39
1.5.3.	Ebb shoal Attachment Bar at Siesta Key History	42
2.	QUANTITATIVE ANALYSIS OF EXISTING DATA	45
2.1.	Sediment Budget	45
2.1.1.	Family of Solutions	49
3.	NUMERICAL MODELING	51
3.1.	CMS Model Description and Justification	51
3.1.1.	CMS Model Grid	51
3.2.	CMS Model Set-up and Structure	53
3.2.1.	Model Configuration Data	53
3.2.2.	Model Forcing Data	55
3.2.3.	Water Levels and Wave Forcing Local CMS-Flow CMS-Wave Grids	58
3.3.	Model Calibration	58
3.3.1.	Model Calibration Data	58
3.3.2.	Hydrodynamic Configuration and Parameter Selection	59
3.3.3.	Sediment Transport and Morphodynamic Parameter Selection	62
3.4.	Test of Model Skill	67
4.	ALTERNATIVE SELECTION	70
4.1.	Inlet Dredging Alternatives	70
4.2.	Model Results and Alternative Selection	73
4.3.	Selected Alternative Plans D2-C-B, D3*-C-B, D3**-B	74
4.3.1.	Alternative D2-C-B	74
4.3.2.	Alternative D3*-C-B	79
4.3.3.	Alternative D3**-B	83

4.4.	Sediment Transport Pathways and Sediment Fluxes	87
5.	ROLE OF GROINS AND BEACH NOURISHMENT ON THE SELECTED ALTERNATIVE	97
5.1.	Alternative D2-C-B with and without Groins / No Nourishment.....	98
5.2.	Alternative D2-C-B with and without Groins / With Nourishment	99
6.	ROLE OF SELECTED ALTERNATIVES ON FUTURE MORPHOLOGY	100
6.1.	Six-Month Runs.....	104
6.1.1.	Morphology Change for Alternatives	104
6.1.2.	Depth Comparisons among Alternatives and “No Action” Alternative.....	104
6.1.3.	Morphologic Comparisons among Alternatives	107
6.1.4.	Time Integrated Sediment Transport Pathways.....	109
6.2.	1.5 Year Runs	122
6.2.1.	Morphology Change within Alternatives.....	122
6.2.2.	Depth Comparisons among Alternatives.....	125
6.2.3.	Morphologic Comparisons among Alternatives	127
7.	UPDATED SEDIMENT BUDGETS - FUTURE ALTERNATIVES	129
7.1.	Future Without Nourishment.....	129
7.1.1.	Family of Solutions.....	130
7.2.	Future With-project D2-C-B.....	133
7.2.1.	Family of Solutions.....	133
7.3.	Future With-project D3*-C-B.....	136
7.3.1.	Family of Solutions.....	136
7.4.	Future With-project D3**-B	138
7.4.1.	Family of Solutions.....	139
8.	DISCUSSION	141
8.1.	Ebb Shoal Volume, Ebb Shoal Growth and Excavation Volume	141
8.2.	The Creation of Lido Key and the migration of the Main Ebb Channel	142
8.3.	Selected Alternatives	148
8.4.	Sediment Budgets.....	150
8.5.	Alternative Scenarios.....	150
9.	CONCLUSIONS	153
10.	REFERENCES	155

11.	APPENDIX A	157
11.1.	Alternative D3.....	157
11.2.	Alternative D2.....	160
11.3.	Alternative C	163
11.4.	Alternative B.....	166
11.5.	Alternative D1.....	169

Table of Figures

Figure 1: Sarasota County Area Map.....	18
Figure 2: Project Location.....	19
Figure 3: Changes in the GIWW and Long Key, Lido Key and Siesta Key.....	20
Figure 4: Changes in Land and Water Configuration from 1890 to 1990.....	21
Figure 5: Ringling Isles	22
Figure 6: Big Sarasota Pass and Lido Key 1920's	23
Figure 7: Big Sarasota Pass and Lido Key 2013.....	23
Figure 8: Lido Key and New Pass 1920's.....	24
Figure 9: Lido Key and New Pass 2013 (Google Earth).....	24
Figure 10: Big Sarasota Pass Bathymetry 1883 – Digital Depth in METERS, Drawn map depths in FEET and FATHOMS, offshore	27
Figure 11: Big Sarasota Pass Bathymetry 1953 - Digital Depth in METERS, Drawn map depths in FEET	28
Figure 12: New Pass and Big Sarasota Pass Ebb Shoals LIDAR 2004 – Depths in METERS.....	29
Figure 13: New Pass and Big Sarasota Pass Ebb Shoals LIDAR 2010 – Depth in METERS	29
Figure 14: New Pass and Big Sarasota Pass 2010-2004 LIDAR Elevation Difference (METERS) ...	29
Figure 15: Volume (MCY) of sediment using method by Walton and Adams, (1979) at Big Sarasota Pass, change in volume from 1955 to 2013	31
Figure 16: Bathymetry BSP 1883, 20-24MCY	32
Figure 17: Bathymetry BSP 1953; 19-21MCY	32
Figure 18: Bathymetry BSP 1991; 20.8MCY	32
Figure 19: Bathymetry BSP 2004; 20.3MCY	33
Figure 20: Bathymetry BSP 2006 20.7MCY.....	33
Figure 21: Bathymetry BSP 2010 23.3MCY.....	33
Figure 22: Bathymetry BSP 2013 23.3MCY.....	34
Figure 23: D BSP 2004-2013 3.02MCY.....	34
Figure 24: Ebb shoal volume - Walton Adams (1976); red circle is the volume of the ebb shoal at Big Sarasota Pass in 1955, and the red triangle is the ebb shoal volume in 2010. The sloped line is the equation that predicts equilibrium ebb shoal volume based upon the tidal prism	36
Figure 25: Cumulative Nourishment Volumes for Lido Key and Cumulative Ebb Shoal Growth .	37
Figure 26: Cumulative Beach Nourishment from Offshore Sources and Ebb Shoal Growth	38
Figure 27: Ebb Shoal Contours 1883, Red; 1991, Orange; 2010, Green.....	38
Figure 28: Ebb Shoal Contours: 1991, Orange; 2004, Red; 2006, Yellow; 2010, Green; 2013, Cyan	39
Figure 29: Migration of the Main Ebb Channel at Big Sarasota Pass since 1924 (IMP, CPE, 1992)	41
Figure 30: BSP in 1943	42
Figure 31: BSP Siesta 1969.....	42
Figure 32: BSP and Siesta Key in 2008.....	43
Figure 33: BSP and Siesta Key in 2009.....	43
Figure 34: BSP and Siesta Key in 2012.....	43

Figure 35: BSP Siesta 2013.....	43
Figure 36: Inter-year migration of the attachment point of the	44
Figure 37: Region where attachment point migrates	44
Figure 38: Sediment Budget from 1987 - 2006. From Coastal Tech, Coastal Engineering Consultants and the University of South Florida, 2008.....	46
Figure 39: Definition of variables for sediment budget (from CEM IV-6; USACE 2008).....	47
Figure 40: Existing 1987 - 2006 Sediment Budget Family of Solutions. The red shaded area represents the mean solution.	49
Figure 41: Finalized Sediment Budget Existing Condition 1987 - 2006	50
Figure 42: CMS Flow Mesh	52
Figure 43: CMS Grid Bathymetry (Depth in METERS).....	52
Figure 44: Sediment grain size in the vicinity of Big Sarasota Pass (Davis and Wang, 2004).....	55
Figure 45: D_{50} (mm) at Big Sarasota Pass, New Pass and Nearshore Region	55
Figure 46: South West FL Regional Mesh	56
Figure 47: South West FL Regional Grid Bathymetry (Depth in METERS).....	57
Figure 48: Water Surface Elevation Calibration for the	58
Figure 49 a&b: Measured vs Calculated Water Surface Elevations for BSP and NP.	60
Figure 50: Location map of D-ADCP surveyed cross-sections and transects	61
Figure 51: Measured vs. Calculated Current Magnitude BSP and NP	62
Figure 52: NOAA Historical Hurricane Tracks; Shaded region is within 65 nm from Lido Key. Hurricane Charley made landfall at Port Charlotte on August 13, 2004 at 20Z and was a Category 4 Hurricane with wind of 125 kts at the time; Hurricane Francis made passage closest to Lido Key as a Tropical Storm on September 5, 2004 at 18Z and September 6, 2004 at 0Z at 60 and 55 kts, respectively; Hurricane Jeanne made passage closest to Lido Key on September 26, 2004 as a Category 1 Hurricane at 12Z at 75 kts and as a Tropical Storm at 18Z at 55 kts.....	64
Figure 53: NOAA Historical Hurricane Tracks: Shaded area is within 200 nm from Lido Key. Hurricane Ivan made first passage on September 14, 2004 as a Category 4 Hurricane and made second passage on September 22, 2004 as a Tropical Depression.....	65
Figure 54: Offshore Wave Height, Direction and Period August, September 2004	66
Figure 55: Calculated temporal change Big Sarasota Pass May 2004 (Left) November 2004 (Right), Depths are in METERS	68
Figure 56: Calculated Significant Temporal Change ($> \pm 0.5$ m); May to November 2004. Warm Colors are Accretion, Cool Colors are Erosion, Depth Changes are in METERS	68
Figure 57: Comparison of Measured 2004 Bathymetry with Calculated 2004 Bathymetry for planform region of Accretion and Erosion	69
Figure 58: Modeled (left) and Measured (right) Morphologic Change Big Sarasota Pass and New Pass, 2004	70
Figure 59: Alternatives developed from the Inlet Management Plan (2008)	71
Figure 60: Alternative D2-C-B initial condition.....	75
Figure 61: “No Action” Alternative (left), Alternative D2-C-B (right) end state November 2004	76
Figure 62: Spatial difference in bathymetry between “No Action” Alternative and Alternative D2-C-B end state November 2004.....	78

Figure 63: Temporal evolution of the Ebb Shoal; May 2004 - November 2004 Alternative D2-C-B	78
Figure 64: Cumulative Wave Energy May 2004 - November 2004 Alternative D2-C-B/No Action	78
Figure 65: Alternative D3*-C-B initial condition.....	80
Figure 66: “No Action” Alternative (left), Alternative D3*-C-B (right) end state November 2004	81
Figure 67: Spatial difference in bathymetry between “No Action” Alternative and Alternative D3*-C-B end state November 2004.....	82
Figure 68: Temporal evolution of the Ebb Shoal; May 2004 - November 2004 Alternative D3*-C-B.....	82
Figure 69: Cumulative Wave Energy May 2004 - November 2004 Alternative D3*-C-B/No Action	82
Figure 70: Alternative D3**-B initial condition	84
Figure 71: “No Action” Alternative (left), Alternative D3**-B (right) end state November 2004	85
Figure 72: Spatial difference in bathymetry between “No Action” Alternative and Alternative D3**-B end state November 2004	86
Figure 73: Temporal evolution of the Ebb Shoal; May 2004 - November 2004 Alternative D3**-B	86
Figure 74: Cumulative Wave Energy May 2004 - November 2004 Alternative D3**-B/No Action	86
Figure 75: Sediment transport pathways for the 12 September 2004 3:00 am; No Action condition under southerly storm waves and a flooding current	89
Figure 76: Sediment transport pathways for the 12 September 2004 3:00 am; Alternative D2-C-B under southerly storm waves and a flooding current.....	89
Figure 77: Sediment transport pathways for the 12 September 2004 3:00 am; Alternative D3*-C-B under southerly storm waves and a flooding current.....	89
Figure 78: Sediment transport pathways for the 12 September 2004 3:00 am; Alternative D3**-B under southerly storm waves and a flooding current.....	89
Figure 79: Sediment transport pathways for the 11 September 2004 9:00 pm; No Action condition under southerly storm waves and an ebbing current.....	90
Figure 80: Sediment transport pathways for the 11 September 2004 9:00 pm; Alternative D2-C-B under southerly storm waves and an ebbing current.....	90
Figure 81: Sediment transport pathways for the 11 September 2004 9:00 pm; Alternative D3*-C-B under southerly storm waves and an ebbing current	90
Figure 82: Sediment transport pathways for the 11 September 2004 9:00 pm; Alternative D3**-B under southerly storm waves and an ebbing current.....	90
Figure 83: Sediment transport pathways for the 16 September 2004 4:30 pm; No Action condition under northwesterly storm waves and a flooding current.....	91
Figure 84: Sediment transport pathways for the 16 September 2004 4:30 pm; Alternative D2-C-B under northwesterly storm waves and a flooding current	91

Figure 85: Sediment transport pathways for the 16 September 2004 4:30 pm; Alternative D3*-C-B under northwesterly storm waves and a flooding current.....	91
Figure 86: Sediment transport pathways for the 16 September 2004 4:30 pm; Alternative D3**-B under northwesterly storm waves and a flooding current	91
Figure 87: Sediment transport pathways for the 16 September 2004 11:30 pm; No Action condition under northwesterly storm waves and an ebbing current	92
Figure 88: Sediment transport pathways for the 16 September 2004 11:30 pm; Alternative D2-C-B under northwesterly storm waves and an ebbing current.....	92
Figure 89: Sediment transport pathways for the 16 September 2004 11:30 pm; Alternative D3*-C-B under northwesterly storm waves and an ebbing current.....	92
Figure 90: Sediment transport pathways for the 16 September 2004 11:30 pm; Alternative D3**-B under northwesterly storm waves and an ebbing current.....	92
Figure 91: General Sediment Transport under FLOOD currents (BLUE) AND SOUTHERLY WAVES (BROWN).	94
Figure 92: General Sediment Transport under EBB currents (BLUE) AND SOUTHERLY WAVES (BROWN).	94
Figure 93: General Sediment Transport under FLOOD currents (BLUE arrows) AND NORTHWESTERLY WAVES (BROWN arrows).....	96
Figure 94: General sediment Transport under EBB currents (BLUE) AND NORTHWESTERLY WAVES (BROWN).....	96
Figure 95: Plan view of groins; Groin design is from the 2004 Feasibility Report, 2013 Shoreline at Lido Key	97
Figure 96: Groins without nourishment; Ending morphology difference for six month run 2004 = (groins were in place with no beach nourishment) – (no groins and no beach nourishment).....	99
Figure 97: Groins with nourishment; Ending morphology difference for six month run 2004 = (groins were in place with beach nourishment).....	100
Figure 98: Model grid bathymetry for the 2013 existing condition and the three selected alternatives.....	103
Figure 99: Morphology Change No Action	105
Figure 100: Morphology Change D2-C-B	105
Figure 101: Morphology Change D3*-C-B (note brown section of cut D3 was not dredged)	105
Figure 102: Morphology Change D3**-B	105
Figure 103: delta Depth D2-C-B vs NA.....	106
Figure 104: delta Depth D3*-C-B vs NA (note brown section of cut D3 was not dredged)	106
Figure 105: delta Depth: D3**-B vs. NA	106
Figure 106: delta Morph: D2-C-B vs. N.A.....	108
Figure 107: delta Morphology D3*-C-B vs. N.A.....	108
Figure 108: delta Morphology: D3**-B vs. NA	108
Figure 109: Integrated sediment transport concentration and transport vectors for the no action condition: May 2004 - November 2004 waves	110
Figure 110: Integrated sediment transport vectors final bathymetry “No Action” Alternative November 2004.....	110

Figure 111: Integrated sediment transport vectors final morphologic change “No Action” Alternative November 2004	110
Figure 112 : Integrated sediment transport concentration and transport vectors for alternative D2-C-B: May 2004 - November 2004 waves.....	111
Figure 113: Integrated transport vectors for alternative D2-C B: May 2004 - 2004 waves and final bathymetry	111
Figure 114: Integrated transport vectors for alternative D2-C B: May 2004 - 2004 waves and final morphologic change	111
Figure 115: Integrated sediment transport concentration and transport vectors for alternative D3*-C-B: May 2004 - November 2004 waves (tip at location)	113
Figure 116: Integrated transport vectors for alternative D3*-C-B: May 2004 - 2004 waves and final bathymetry (tip at location)	113
Figure 117: Integrated transport vectors for alternative D3*-C-B: May 2004 - 2004 waves and final morphologic change (tip at location)	113
Figure 118: Integrated sediment transport concentration and transport vectors for alternative D3**-B: May 2004 - November 2004 waves (tip at location)	114
Figure 119: Integrated transport vectors for alternative D3**-B: May 2004 - 2004 waves and final bathymetry (tip at location)	114
Figure 120: Integrated transport vectors for alternative D3**-B: May 2004 - 2004 waves and final morphologic change (tip at location)	114
Figure 121: Residual sediment transport magnitude in X-Direction (Yellow=East, Blue=West) and total transport vectors for the no action condition: May 2004 - November 2004 waves (tip at location).....	116
Figure 122: Residual sediment transport magnitude in Y-Direction (Yellow=North, Blue=South) and total transport vectors for the no action condition: May 2004 - November 2004 waves (tip at location).....	116
Figure 123 Residual sediment transport magnitude in X-Direction (Yellow=East, Blue=West) and total transport vectors for the D2-C-B Alternative: May 2004 - November 2004 waves (tip at location).....	117
Figure 124: Residual sediment transport magnitude in Y-Direction (Yellow=North, Blue=South) and total transport vectors for the D2-C-B Alternative: May 2004 - November 2004 waves (tip at location).....	117
Figure 125 Residual sediment transport magnitude in X-Direction (Yellow=East, Blue=West) and total transport vectors for the D3*-C-B Alternative: May 2004 - November 2004 waves (tip at location).....	118
Figure 126: Residual sediment transport magnitude in Y-Direction (Yellow=North, Blue=South) and total transport vectors for the D3*-C-B Alternative: May 2004 - November 2004 waves (tip at location).....	118
Figure 127 Residual sediment transport magnitude in X-Direction (Yellow=East, Blue=West) and total transport vectors for the D3**-B Alternative: May 2004 - November 2004 waves (tip at location).....	119

Figure 128: Residual sediment transport magnitude in Y-Direction (Yellow=North, Blue=South) and total transport vectors for the D3**-B Alternative: May 2004 - November 2004 waves (tip at location).....	119
Figure 129: Difference in Morphology between D2-C-B and “No Action” Alternative, and difference between total transport vectors for the D2-C-B Alternative: May 2004 - November 2004 waves (tip at location)	120
Figure 130: Difference in Morphology between D3*-C-B and “No Action” Alternative, and difference between total transport vectors for the D3*-C-B Alternative: May 2004 - November 2004 waves (tip at location)	120
Figure 131: Difference in Morphology between D3**-B and “No Action” Alternative, and difference between total transport vectors for the D3**-B Alternative: May 2004 - November 2004 waves (tip at location)	120
Figure 132: Morphology Change No Action	123
Figure 133: Morphology Change D2-C-B	123
Figure 134: Morphology Change D3*-C B	124
Figure 135: Morphology Change D3**-B	124
Figure 136: delta Depth D2-C-B vs NA.....	126
Figure 137: delta Depth D3*-C-B vs NA.....	126
Figure 138: delta Depth: D3**-B vs NA.....	126
Figure 139: delta Morphology: D2-C-B vs. N.A.....	128
Figure 140: delta Morphology D3*-C-B vs. N.A.....	128
Figure 141: delta Morphology: D3**-B vs. N.A.	128
Figure 142: Future Sediment Budget No Action and No Continued Nourishment from Offshore; Narrowed Family of Solutions; Red dot indicates Mean Solution	131
Figure 143: Finalized Sediment Budget Future Condition, “No Action” Alternative and No Offshore Inputs.....	132
Figure 144: Future Sediment Budget Alternative D2-C-B; Narrowed Family of Solutions; Red dot indicates Mean Solution	134
Figure 145: Solutions for Equations in Figure 6 from the Bodge Method (CEM IV-6; USACE 2008); Finalized Sediment Budget Future Condition, Alternative D2-C-B.....	135
Figure 146: Future Sediment Budget Alternative D3*-C-B; Narrowed Family of Solutions; Red dot indicates Mean Solution	137
Figure 147: Solutions for Equations in Figure 6 from the Bodge Method (CEM IV-6; USACE 2008); Finalized Sediment Budget Future Condition, Alternative D3-C-B.....	138
Figure 148: Future Sediment Budget Alternative D3*-C-B; Narrowed Family of Solutions; Red dot indicates Mean Solution	139
Figure 149: Solutions for Equations in Figure 6 from the Bodge Method (CEM IV-6; USACE 2008); Finalized Sediment Budget Future Condition, Alternative D3**-B	140
Figure 150: Volume of sediment using method by Walton and Adams (1979) at Big Sarasota Pass, change in volume from 1955 to 2013. Grey dotted line represents the volume to be removed from the ebb shoal by the Lido Key Shore Protection Project.....	141

Figure 151: Ebb Shoal Growth in the past decade; 1.3 MCY reduction leaves a surplus of sediment.....	142
Figure 152: Integrated sediment transport concentration and transport vectors for 1883 bathymetry	144
Figure 153: Integrated sediment transport vectors final bathymetry for 1883 bathymetry	144
Figure 154: Integrated sediment transport vectors final morphologic change for 1883 bathymetry	144
Figure 155: Integrated sediment transport concentration and transport vectors for 2004 bathymetry	145
Figure 156: Integrated sediment transport vectors final bathymetry for 2004 bathymetry	145
Figure 157: Integrated sediment transport vectors final morphologic change for 2004 bathymetry	145
Figure 158: Difference in morphology and difference in total transport vectors between 1883 and 2004	146
Figure 159: Shoreline change (from 1992 IMP CPE).....	147
Figure 160: “No Action” Alternative (left), Alternative D3 (right); end state November 2004..	158
Figure 161: Spatial difference in bathymetry between “No Action” Alternative and Alternative D3 end state November 2004	159
Figure 162: Temporal evolution of the Ebb Shoal; May 2004 - November 2004 Alternative D3	159
Figure 163: Cumulative Wave Energy May 2004 - November 2004 Alternative D3*-C-B	159
Figure 164: “No Action” Alternative (left), Alternative D2 (right); end state November 2004..	161
Figure 165: Spatial difference in bathymetry between “No Action” Alternative and Alternative D2 end state November 2004	162
Figure 166: Temporal evolution of the Ebb Shoal; May 2004 - November 2004 Alternative D2	162
Figure 167: Cumulative Wave Energy May 2004 - November 2004 Alternative B+C+D2	162
Figure 168: “No Action” Alternative (left), Alternative C (right); end state November 2004	164
Figure 169: Spatial difference in bathymetry between “No Action” Alternative and Alternative C end state November 2004.....	165
Figure 170: Temporal evolution of the Ebb Shoal; May 2004 - November 2004 Alternative C.	165
Figure 171: Cumulative Wave Energy May 2004 - November 2004 Alternative C	165
Figure 172: “No Action” Alternative (left), Alternative B (right); end state November 2004	167
Figure 173: Spatial difference in bathymetry between “No Action” Alternative and Alternative B end state November 2004.....	168
Figure 174: Temporal evolution of the Ebb Shoal; May 2004 - November 2004 Alternative B.	168
Figure 175: Cumulative Wave Energy May 2004 - November 2004 Alternative B	168
Figure 176: “No Action” Alternative (left), Alternative D1 (right); end state November 2004..	170
Figure 177: Spatial difference in bathymetry between “No Action” Alternative and Alternative C end state November 2004.....	171
Figure 178: Temporal evolution of the Ebb Shoal; May 2004 - November 2004 Alternative C...	171
Figure 179: Cumulative Wave Energy May 2004 - November 2004 Alternativ.....	171

Table of Tables

Table 1: Big Sarasota Pass Ebb Shoal Survey History	26
Table 2: Ebb Shoal Volumes	30
Table 3: Nourishment History Lido Key	36
Table 4: Nourishment History: Longboat and Lido Keys from Offshore Sources	37
Table 5: CMS Model Parameters	54
Table 6: Sediment transport and morphology parameters in the CMS.	63
Table 7: Description of Model Alternatives.....	72
Table 8: Time periods for initial and end conditions of each model run	72
Table 9: Alternative Run Summaries	74
Table 10. Modeling Matrix for CMS runs with Groins Summary of Model Results	98
Table 11: Description of Model Alternatives.....	101
Table 12: Time periods for initial and end conditions of each model run	102
Table 13: Volume losses and Gains on Lido Key and Big Sarasota Pass Ebb Shoal (THOUSANDS OF CUBIC YARDS)	121
Table 14: Alternatives Risks and Benefits.....	151

1. OVERVIEW

1.1. Introduction

USACE Jacksonville District performed a study which evaluates whether excavation of the ebb shoal at Big Sarasota Pass will significantly alter the ebb shoal morphology or local/regional sediment transport patterns in such a way that there would be adverse effects on adjacent beaches.

Engineering analyses are conducted to assess whether excavations of the ebb shoal at Big Sarasota Pass will result in a significant adverse impact to the coastal littoral system and the adjacent beaches. Analysis of existing data alone cannot not be used to infer whether additional, future excavations of the ebb shoal alone will (or will not) result in a significant adverse impact. The analyses were conducted in the following manner to further the current understanding of the inlet processes at Big Sarasota Pass, to further understand how the present condition of the inlet and beaches of Lido and Siesta Keys are related to historical change and to predict expected change in the inlet-complex morphology and adjacent beach volumes due to ebb shoal mining and the proposed Shore Protection Project at Lido Key.

Methodology Workflow and Report Layout is as follows:

i. REPORT SECTIONS 1 & 2

Determine those processes in the inlet and adjacent shorelines that have been changed due to anthropogenic manipulation of the environment in the early 20th Century.

- a. Conduct a Historic Behavior Study to determine those processes which have been perturbed by development of the region.
- b. Examine the Volume, Planform Area and Stability of the Ebb shoal in response to anthropogenic perturbation
- c. Construct an Existing Sediment Budget

Result: Move forward with a better understanding of the vulnerability and resilience of the ebb shoal system, the underlying historical processes that cause erosion at Lido and Siesta Key, and determine a baseline from which change due to the Proposed Project can be measured.

ii. REPORT SECTIONS 3 & 4

Determine acceptable ebb shoal mining scenarios based upon measured change as a baseline.

- a. Control: Measured May – November 2004 bathymetric change is the baseline from which to evaluate morphologic change due to ebb shoal mining.
- b. Alternative: CMS modeling of 2004 morphology and 2004 environmental forcing to numerically simulate ebb shoal morphologic change due to mining of the ebb shoal.
 - i. Screening Criteria:
 - 1. *Significant morphologic change of ebb shoal features which could indicate degraded function of the inlet complex*
 - 2. *Increased wave energy at the shoreline*
 - 3. *Increased shoaling of the main navigation channel*
 - ii. Determine tidally driven and wave driven sediment transport pathways for existing conditions and for mining alternatives

Result: Select ebb shoal mining scenario based upon rejection of the three screening criteria and upon integrity of sediment transport pathways.

iii. **REPORT SECTION 5**

Determine the effect of the installation of Groins at the South end of Lido Key

- a. Test Matrix:
 - i. Ebb Shoal Mining Alternative; No Groins; No Nourishment
 - ii. Ebb Shoal Mining Alternative; Groins; No Nourishment
 - iii. Ebb Shoal Mining Alternative; Groins; Nourishment
 - iv. Ebb Shoal Mining Alternative; No Groins; Nourishment

Result: Verify that the installation of groins do not have adverse effects on the ebb shoal or downdrift beaches.

iv. **REPORT SECTION 6**

Determine the effect of the Selected Ebb Shoal Mining Alternative, Nourishment Template and Groin installation on *Future Morphology*

- a. Six-Month Runs
 - i. Control: 2013 Bathymetry; Nourishment Template; Groins; No Cuts in the Ebb Shoal
 - ii. Alternative: 2013 Bathymetry; Nourishment Template; Groins; Selected Mining Alternative for the Ebb Shoal
 - iii. Environmental Forcing: Waves and Water Levels from May to November 2004
- b. 1.5 year Runs
 - i. Control: 2013 Bathymetry; Nourishment Template; Groins; No Cuts in the Ebb Shoal
 - ii. Alternative: 2013 Bathymetry; Nourishment Template; Groins; Selected Mining Alternative for the Ebb Shoal

- iii. Environmental Forcing: Waves and Water Levels from January 2005 to June 2006

Result: Verify that the selected mining alternative *in conjunction with the nourishment template and installation of groins* do not have adverse effects on the ebb shoal or downdrift beaches using the most recent bathymetric measurements available.

Result: Calculate the future expected volume change at Lido Key and the Ebb Shoal to Construct Future Sediment Budgets.

v. **REPORT SECTION 7**

Determine the effect of the Selected Ebb Shoal Mining Alternative, Nourishment Template and Groin installation on *Future Sediment Budgets*

- a. Use calculated volume change for Future Expected Volume Change for Lido Key and for the Ebb Shoal/Inlet Complex at Big Sarasota Pass to construct a sediment budget
 - i. Future without-project at Lido Key
 - ii. Future with Selected Ebb Shoal Mining Alternative, Nourishment Template, Groin Installation

Result: Verify that the selected mining alternative *in conjunction with the nourishment template and installation of groins* do not impound sediment from and decrease bypassing to downdrift beaches.

1.2. Historical Inlet Behavior

Big Sarasota Pass has existed since the earliest available maps of the area; however, Lido Key and much of the GIWW have experienced considerable change over the last century (Davis and Wang, 2004). The behavior and history of Big Sarasota Pass is well documented; the reader is directed to studies conducted by Truitt, 1992; Antonini, 1993; Davis and Wang, 2004; Davis, Wang and Beck, 2007, and Wang, Beck and Davis, 2007. All authors point toward both natural and anthropogenic factors playing a significant role in producing the present morphodynamic conditions at Big Sarasota Pass. To illustrate this effect, anthropogenic changes to the Sarasota Bay system and the Keys are noted in Figure 3 and Figure 4.

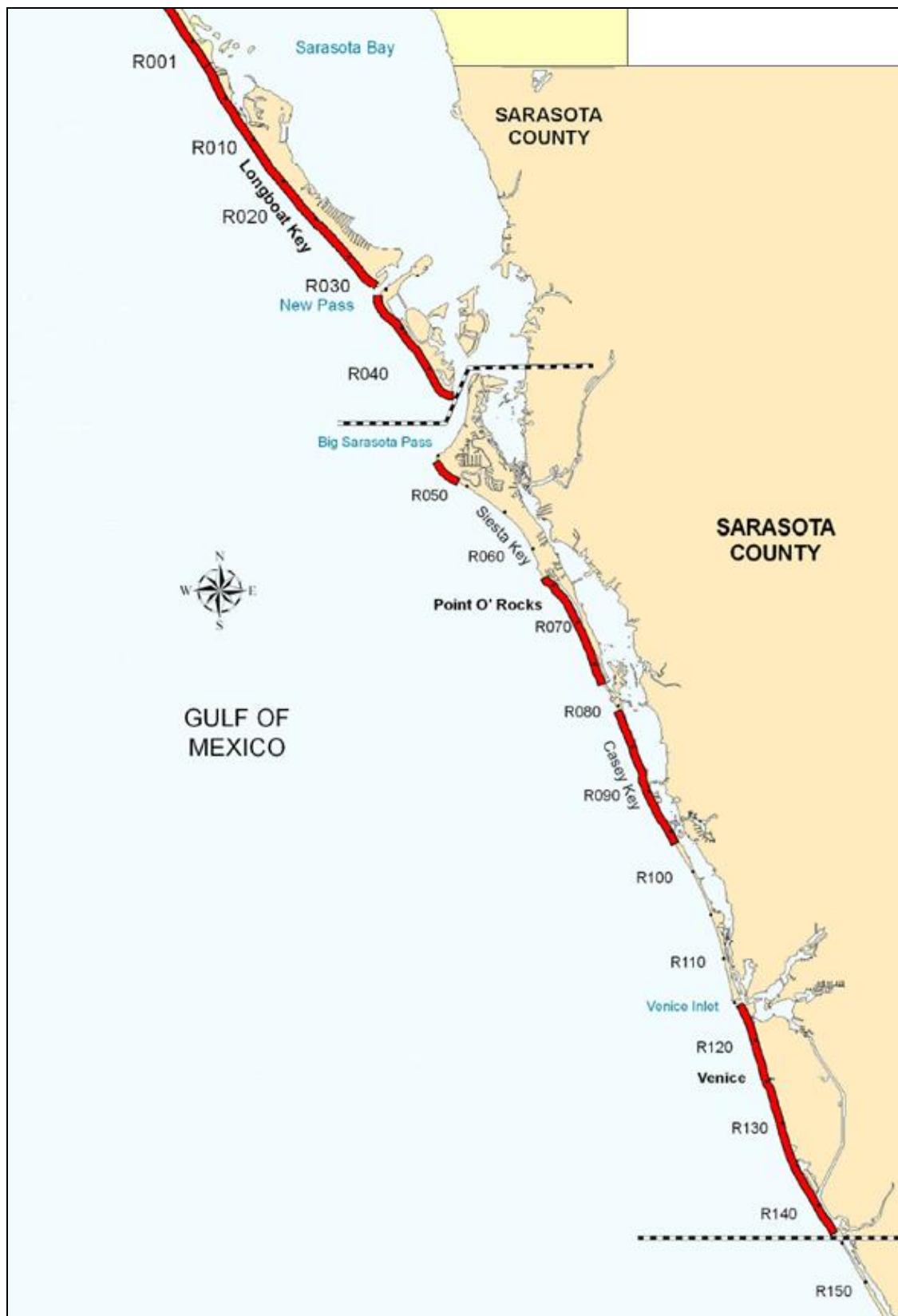
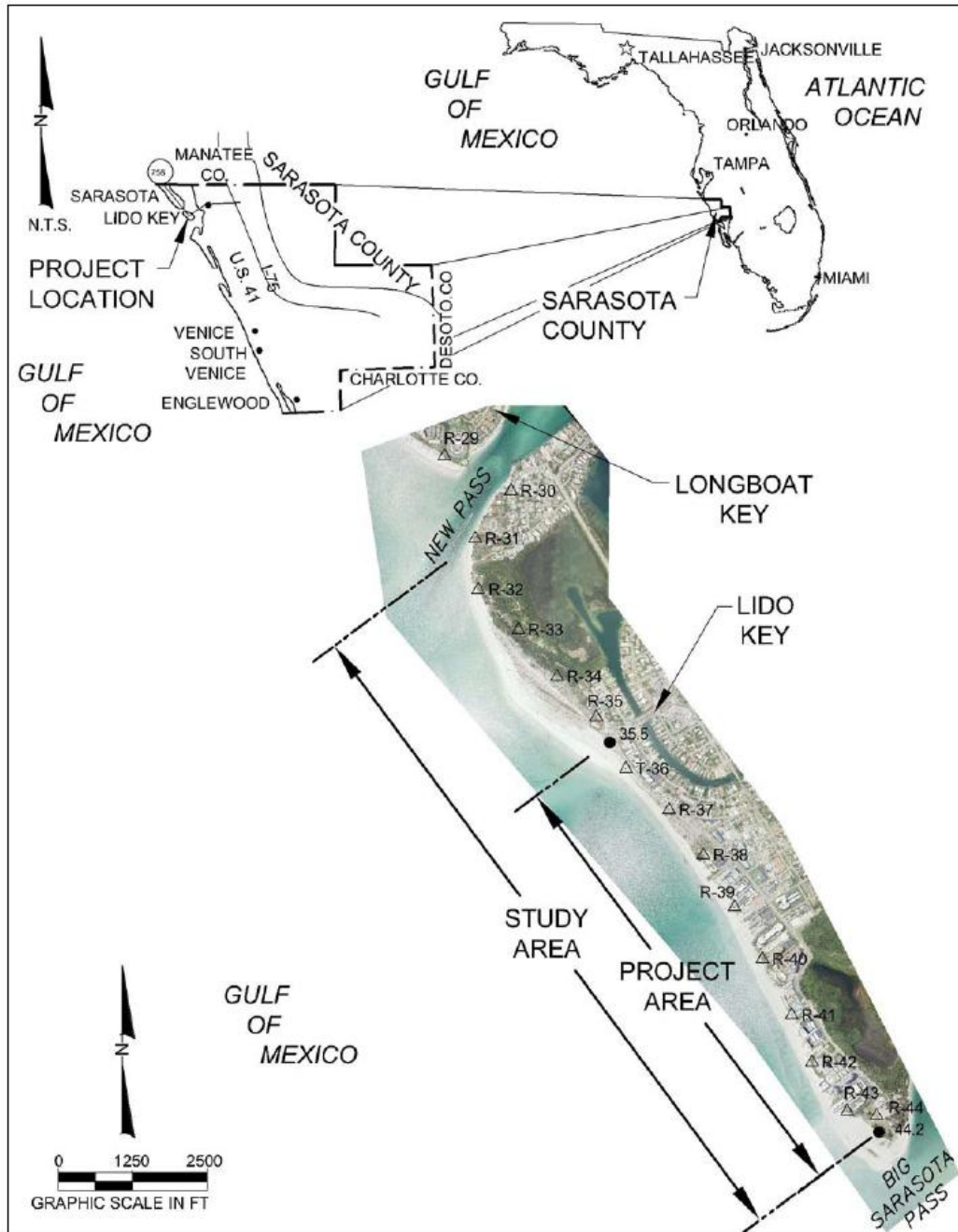


Figure 1: Sarasota County Area Map



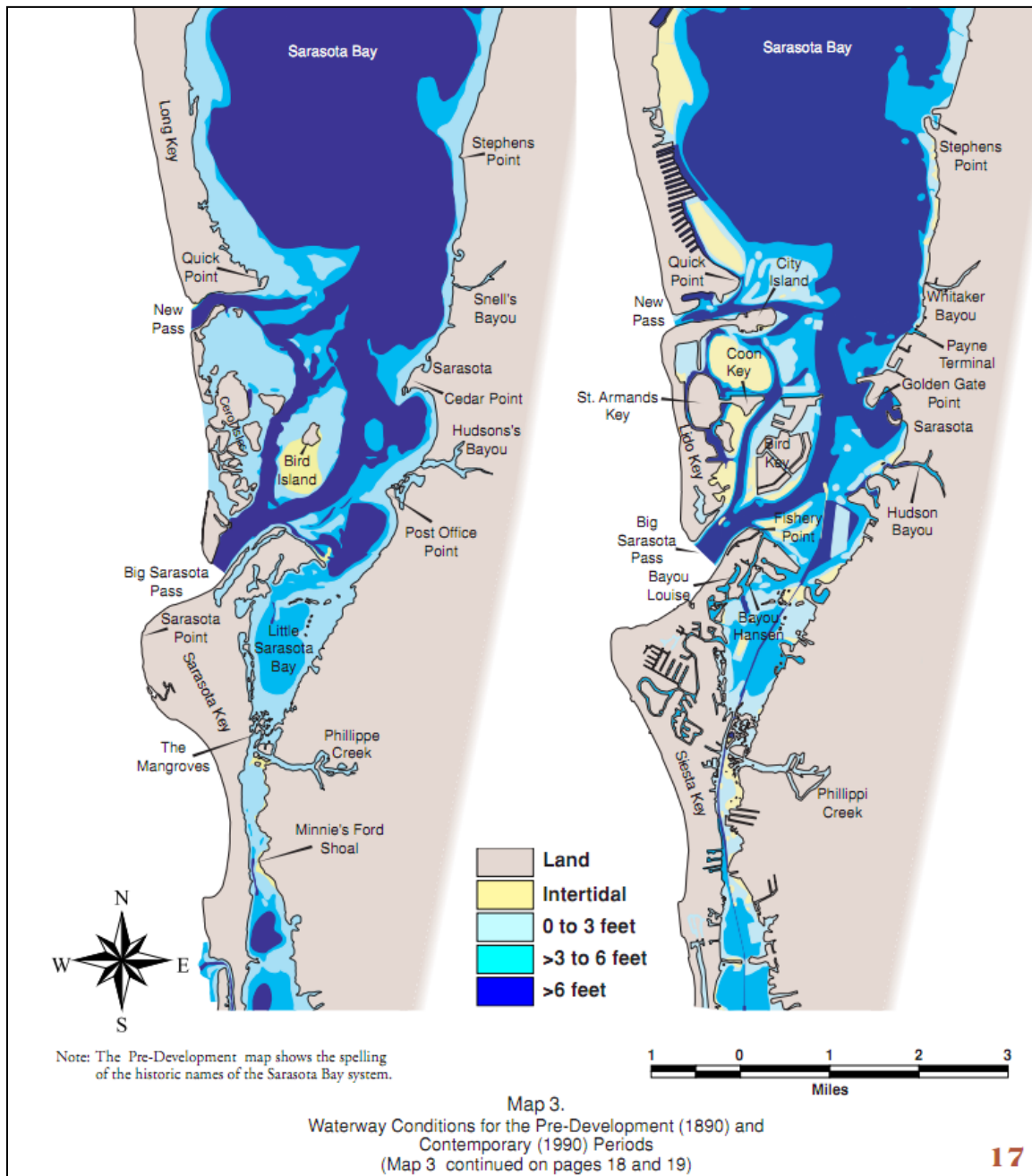
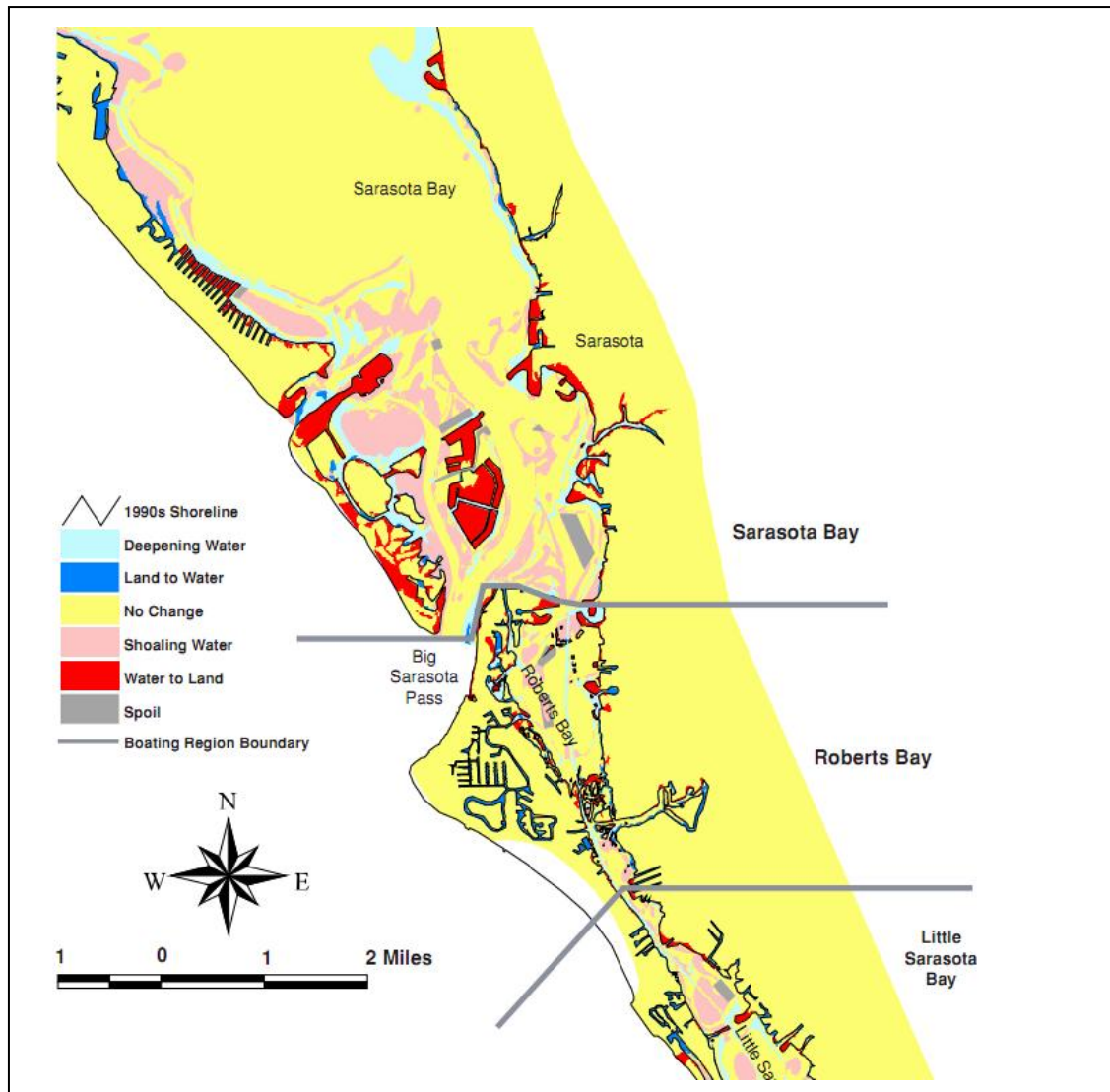


Figure 3: Changes in the GIWW and Long Key, Lido Key and Siesta Key from 1890 to 1990. (Antonini, 1993)



**Figure 4: Changes in Land and Water Configuration from 1890 to 1990.
Note especially the infilling of Lido Key. Antonini, 1993)**

1.3. John Ringling and the History of Lido Key

A discussion of the Lido Key Shore Protection Project and the study and analysis of the mining of sediment from Big Sarasota Pass would not be complete if the history of Lido Key was not understood. Neither Lido Key nor St. Armands Key existed 100 years ago and were instead a grouping of small islands called the Cerol Isles (Figure 5 and Figure 6).

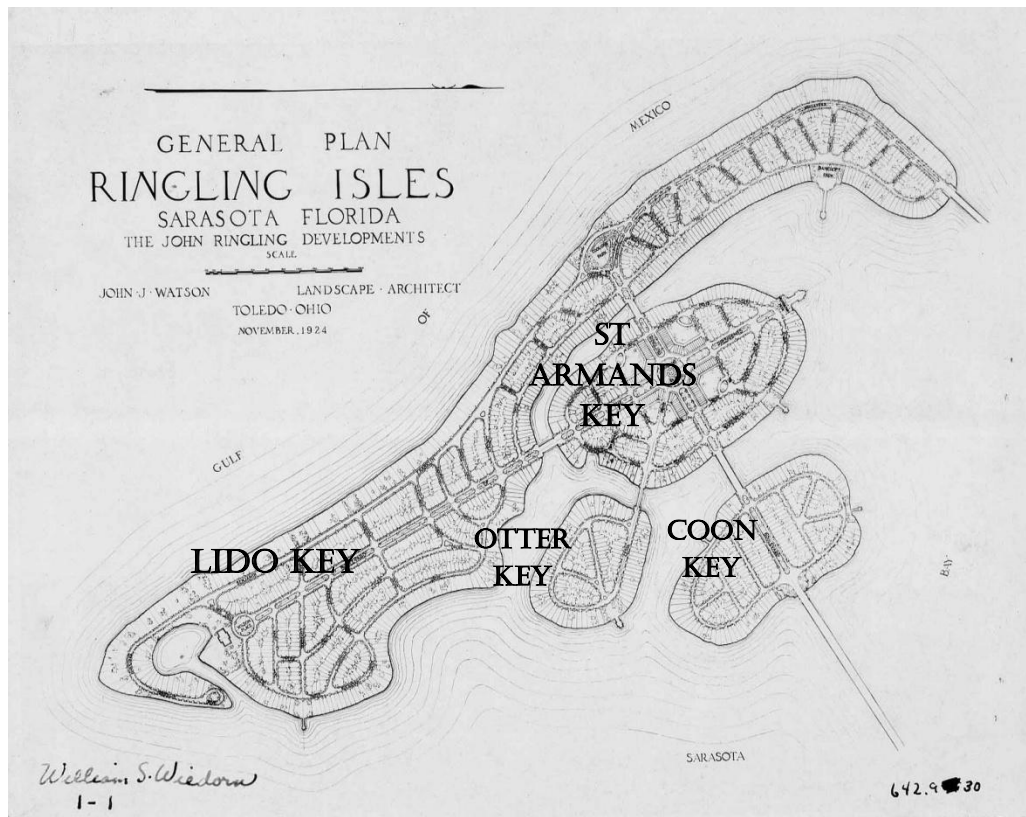


Figure 5: Ringling Isles

During the 1920's, the shallows separating the Cerol Isles were filled by Mr. Ringling, and the new island became Lido Key. In 1925, a causeway was built from the mainland. Ringling and partner Owen Burns dredged channels and filled land as part of the proposed Ringling Isles development (Figure 5). Bird Key was developed in the 1960's where five miles of canals were dredged. Today, Otter Key is the only island that remains undeveloped (Figure 7).



Figure 6: Big Sarasota Pass and Lido Key 1920's



**Figure 7: Big Sarasota Pass and Lido Key 2013
(Google Earth)**

This oblique aerial shows Big Sarasota Pass and Lido Key in the late-1920's and 2013, respectively (Figure 6 and Figure 7). Bird Key was originally only region (a). Ringling dredged and filled an extension from Bird Key (b) to connect the causeway (region c) that came from the mainland. Coon Key (d) and Lido Key (e) were still not yet extensively developed. The dredged channel that provided access to Bird Key is denoted by (f) and area (g) was habitat for sea grass. Big Sarasota Pass (h) is in the background.



Figure 8: Lido Key and New Pass 1920's



Figure 9: Lido Key and New Pass 2013 (Google Earth)

Otter Key, St. Armands and Lido Key are shown here from the 1920's and 2013, respectively (Figure 8 and Figure 9). Note the fire on St. Armands Key (a) where land is being cleared. New Pass (b) has been dredged and the material was sidecast from the dredge to form City Island (c). The causeway (d) connecting Lido Key, St. Armands Key and Bird Key to the mainland was created from dredged material from the north side of St. Armands Key. Here, the dredge is at Otter Key (e). The entire area between Otter Key and Lido Key (f) was dredged to create fill for development.

1.4. Physical and Environmental Characteristics

The reader is referred to Sarasota County, Florida Hurricane and Storm Damage Reduction Project: Lido Key, Feasibility report with environmental assessment, (USACE, 2002, 2004), for a thorough analysis and description of the physical and environmental characteristics of Sarasota County in general and Big Sarasota Pass in particular. Included in the study are environmental forcing conditions due to wind and tides, currents, meteorological fronts, waves, shoreline change, volume change, inlet effects and littoral transport. In addition, sections also discuss sediment characteristics and existing shoreline protective structures.

The reader is also referred to Chapter 2 of the Sarasota County Comprehensive Inlet Management Program Big Pass and New Pass Management Alternatives, (2008) authored by Coastal Technology Corp., University of South Florida, Coastal Engineering Consultants, Inc. with input from the USACE Jacksonville District, for an analysis of collected data including bathymetric and topographic surveys, sediment investigation and composition for both New and Sarasota Pass, as well as the collection and analysis of current velocity and water level data at both Passes.

The reader is also referred to Lido Key Beach Renourishment Project New Pass Borrow Area Modeling Study City of Sarasota, Florida, authored by Coastal Planning & Engineering, Inc. for analysis of additional current velocities, wave climate and offshore water levels in the vicinity of Lido Key.

1.5. Big Sarasota Pass

1.5.1. Bathymetric Analysis of Big Sarasota Pass: Ebb Shoal Volume and Planform

The morphological features of Big Sarasota Pass were examined both historically and in recent times. Charts of Big Sarasota Pass from 1883 and 1953 were digitized in SMS (Figure 10 and Figure 11) to show the historic features of Big Sarasota Pass. LIDAR bathymetry from May 2004, (Figure 12) was examined to identify the major features of the region in recent times. The main channel, with typical depths between 6 and 7 meters (19.6 – 23 ft.) and depths of up to 8.0 m (26.2 ft.), runs between the ebb shoal and Siesta Key. The ebb shoal, between 0 and 2.0 m (6.56 ft.) depth, has one larger flood channel about mid-way along its length and 3 or 4 smaller flood channels adjacent to Lido Key. Bypassing at the southern end of the ebb shoal to Siesta Key is also evident. LIDAR bathymetry from 2010 (Figure 13) illustrates very similar morphological features but the ebb shoal has less defined flood channels and extends further west and south than it did in 2004 (Figure 12). Table 1 lists recent ebb shoal surveys obtained with LIDAR and by multi-beam survey. The present analysis included volume change

calculations between surveys that were made within the SMS framework. Hydrographic survey points were interpolated to create a raster surface of the study area using linear interpolation. The area elevation changes were calculated by taking the difference between rasters (Figure 14) to determine the elevation change between surveys.

Table 1: Big Sarasota Pass Ebb Shoal Survey History

<i>Description</i>	Dates
LIDAR – JALBTCX / USACE Survey	
2004 Pre-Storm - LIDAR	May 2004
2004 Post-Storm – LIDAR	November 2004
2006 – LIDAR	May 2006
2010 – LIDAR	July 2010
2013 – boat survey	August 2013

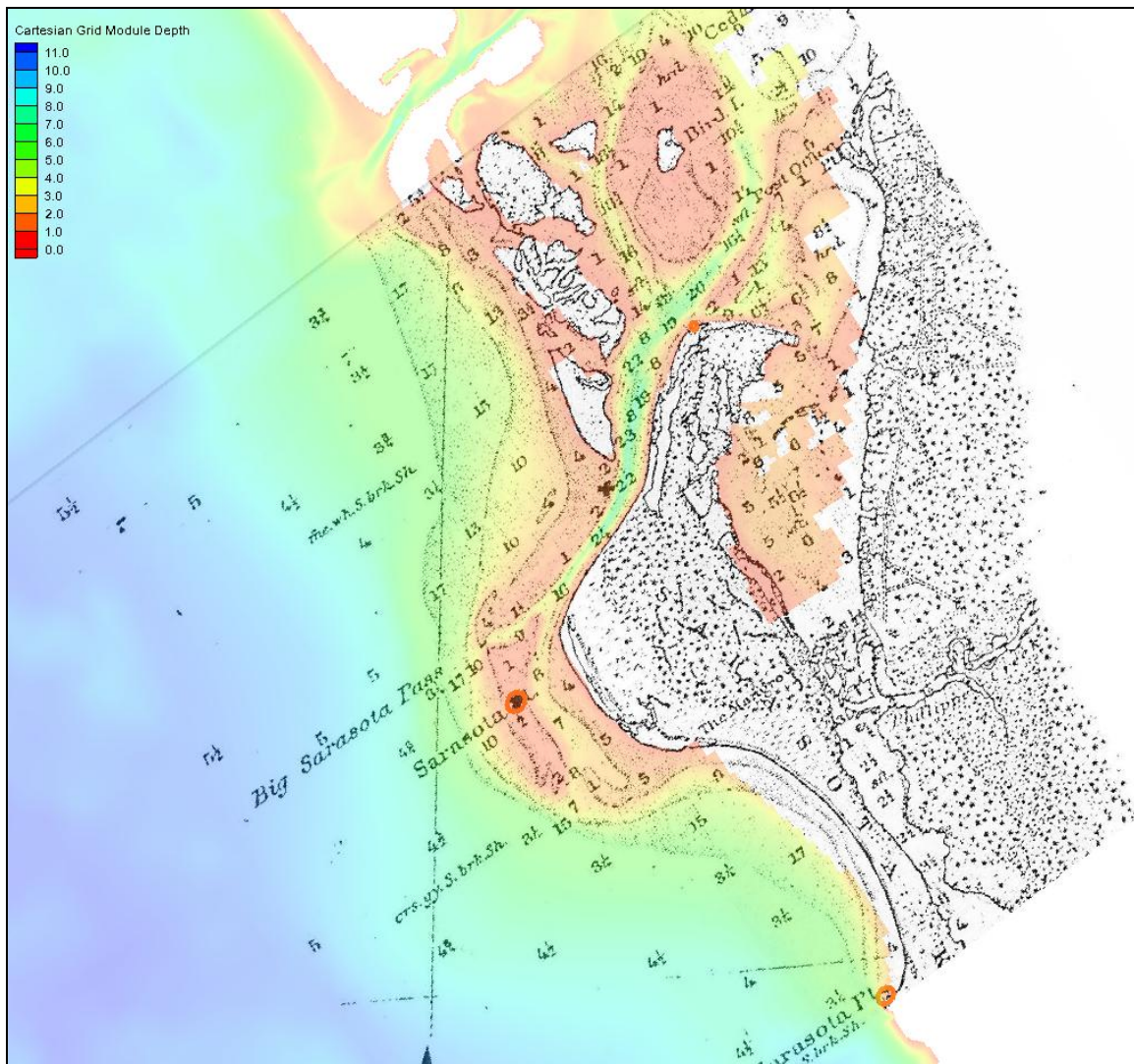


Figure 10: Big Sarasota Pass Bathymetry 1883 – Digital Depth in METERS, Drawn map depths in FEET and FATHOMS, offshore

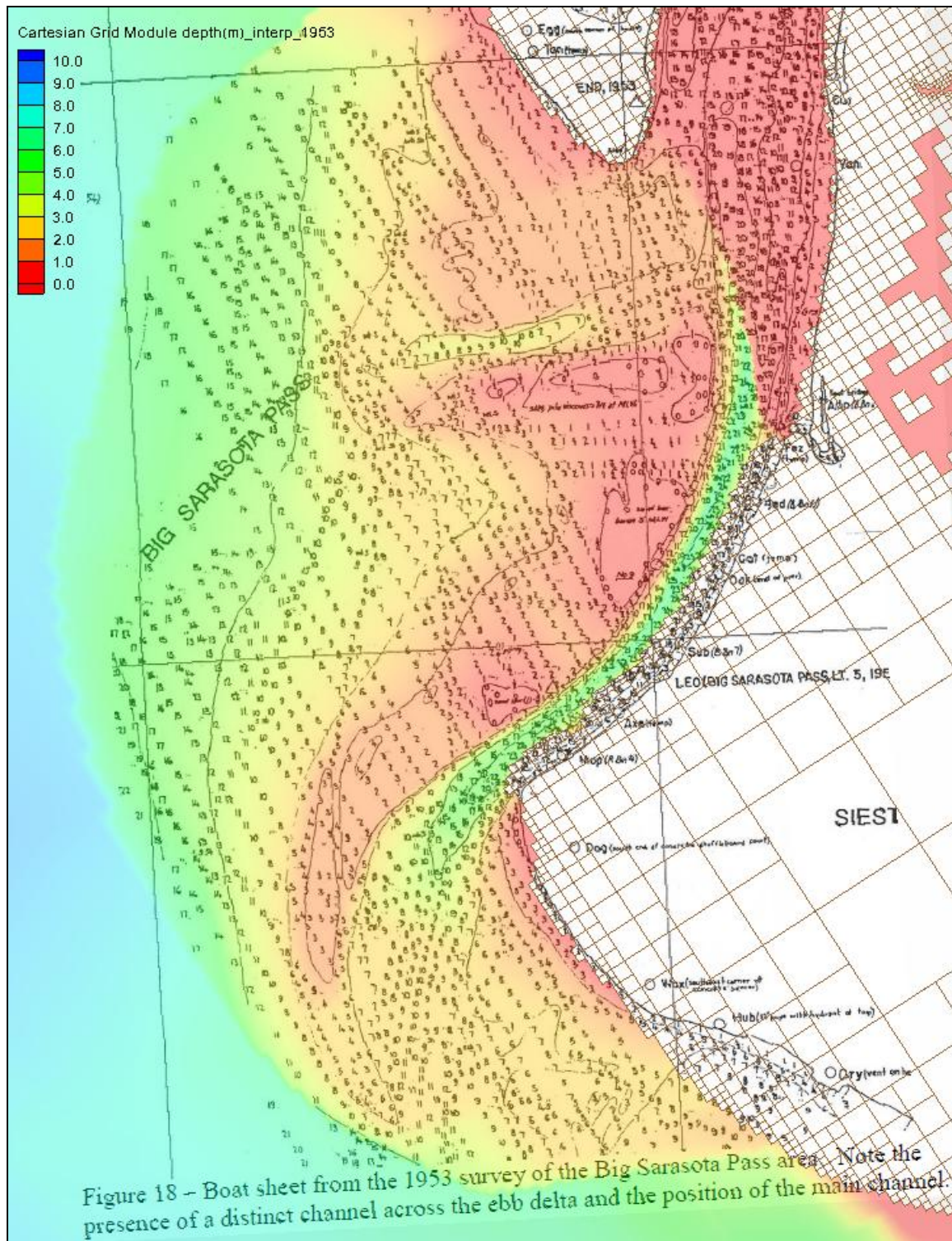


Figure 11: Big Sarasota Pass Bathymetry 1953 - Digital Depth in METERS, Drawn map depths in FEET

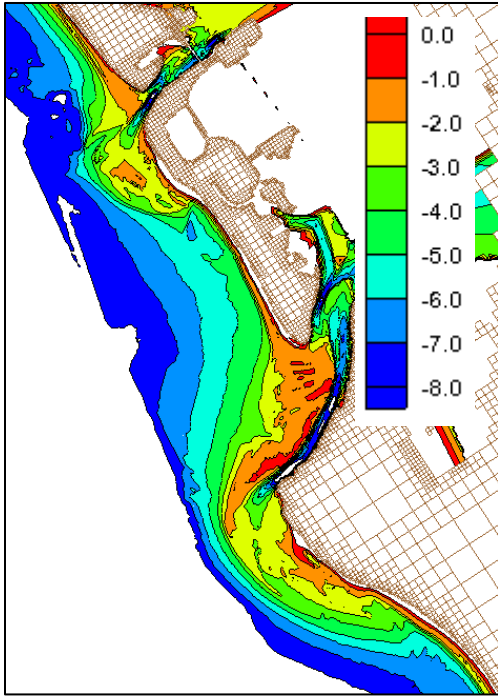


Figure 12: New Pass and Big Sarasota Pass Ebb Shoals LIDAR 2004 – Depths in METERS

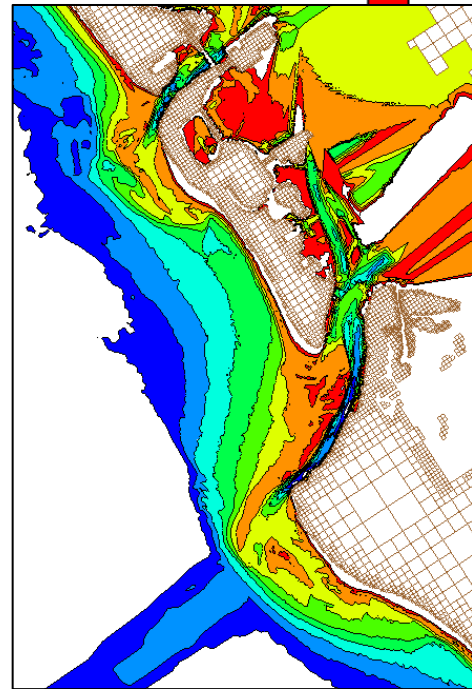


Figure 13: New Pass and Big Sarasota Pass Ebb Shoals LIDAR 2010 – Depth in METERS

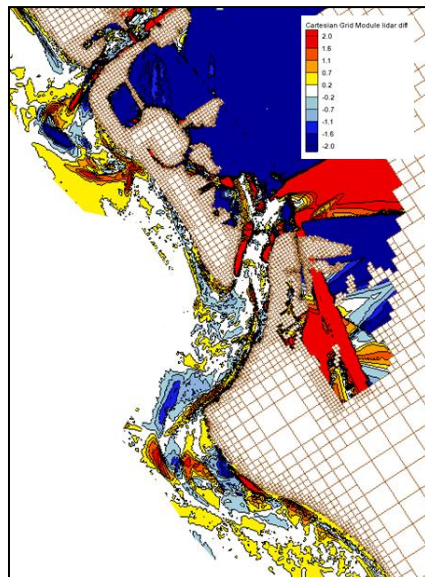


Figure 14: New Pass and Big Sarasota Pass 2010-2004 LIDAR Elevation Difference (METERS)

contains the ebb shoal volume calculated using the method described by Walton and Adams (1976). The ebb shoal volume is calculated by bisecting the measured bathymetry by a plane that contains a beach, only. The bisecting plane was constructed by using beach profiles in Lido Key and in Sarasota Key. Volumes were also calculated by bisecting the measured bathymetry with a plane at the 18 ft depth contour as shown in the lower right hand corner of the volume change maps. The volumes and change in volume using the Walton and Adams method for Big Sarasota Pass Ebb Shoal are shown in Figure 15 and in Figures 16-23. Given the error and uncertainty associated with depths from the 1883 and 1953 surveys, the depths were assumed to be +/- 1 foot, and volumes were reported given this assumed error. The long-term, yearly-weighted average volume of the ebb shoal is 21 MCY. The ebb shoal grew approximately 2.3 MCY between 2004 and 2013. The 2013 survey did not capture the attachment point and the southeasterly growth of the ebb shoal, so interpretation of these results is limited because the southeastern portion of the shoal was not measured. The yearly accretional *average* between 1991 and 2013 is 113,000 cy/yr.

Table 2: Ebb Shoal Volumes

<i>Year</i>	<i>Calculated Volume</i>	ΔV	$\Delta V/yr$
	CY	CY	CY/yr
1883	20 M – 24 M	na	na
Mar-53	19 M – 21 M	na	na
May-91	20,825,713*	2,125,713	59,048
May-04	20,293,508	-532,205	-40,939
May-06	20,713,622	420,114	210,057
Jul-10	23,314,351	2,600,729	650,182
Aug-13	23,317,189	2,838	1,419

*CPE IMP (1992)

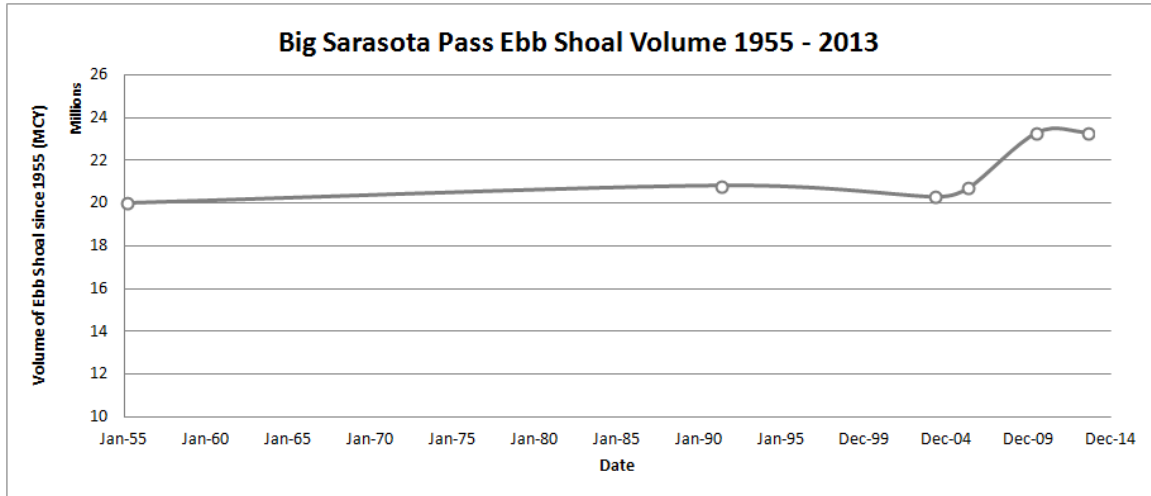


Figure 15: Volume (MCY) of sediment using method by Walton and Adams, (1979) at Big Sarasota Pass, change in volume from 1955 to 2013

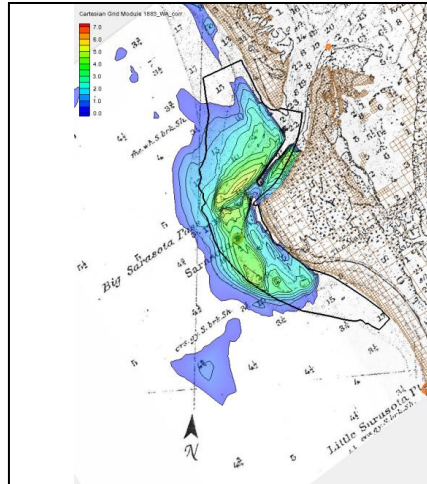


Figure 16: Bathymetry BSP 1883, 20-24MCY

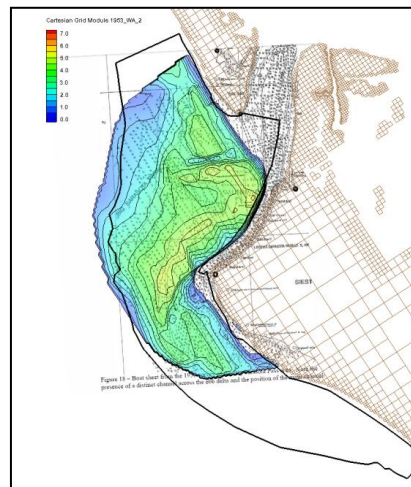


Figure 17: Bathymetry BSP 1953; 19-21MCY

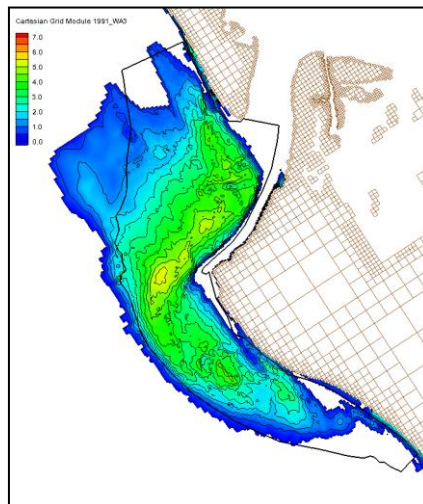


Figure 18: Bathymetry BSP 1991; 20.8MCY

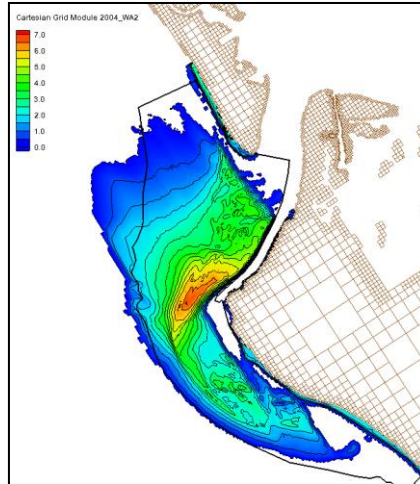


Figure 19: Bathymetry BSP 2004; 20.3MCY

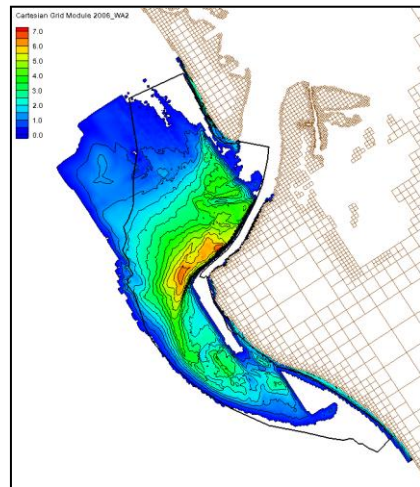


Figure 20: Bathymetry BSP 2006 20.7MCY

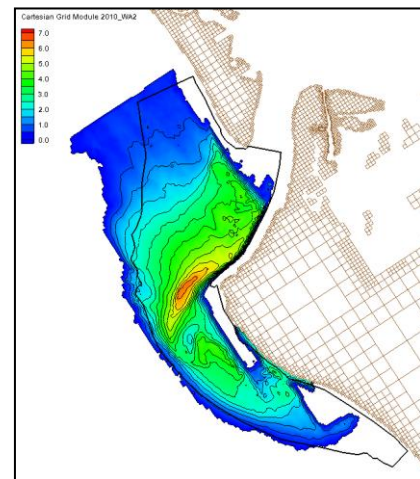


Figure 21: Bathymetry BSP 2010 23.3MCY

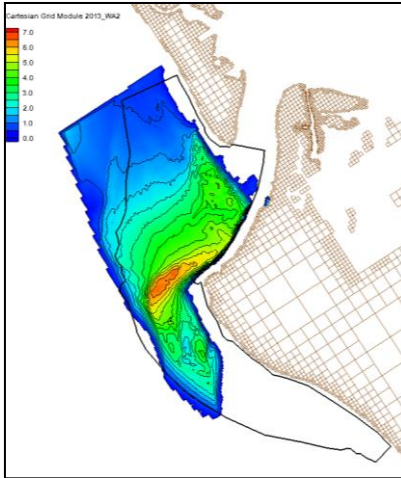


Figure 22: Bathymetry BSP 2013 23.3MCY

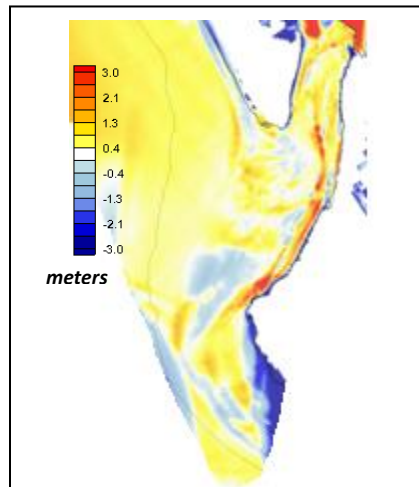


Figure 23: D BSP 2004-2013 3.02MCY

As discussed previously, the volume of the ebb shoal was calculated using the Walton Adams method. In addition, using the data collected and published by Walton and Adams (1976). It can be seen in Figure 24 that the total volume of the ebb shoal at Big Sarasota Pass (BSP) is much larger than what would be predicted both for Atlantic and for Gulf Coast inlets. Back in 1955 and even extending back to 1883 (Figure 10 and Figure 11), the ebb shoal at BSP has been large (~20 MCY) (Figure 24). From the data collected and published by Walton and Adams (1976) and re-analyzed by Kraus (2009), the relationship between equilibrium shoal volume and tidal prism as:

$$VE = CE * P^{1.1673} \quad (1)$$

where V_E is the ebb-shoal volume in m^3 , $C_E = 2.121 \times 10^{-2}$, and P is the tidal prism in m^3 . The solution of Equation 1 for Big Sarasota Pass would be equilibrium volume would be approximately 6 MCY. Today the ebb shoal volume remains >20 MCY.

Over the past decade, the ebb shoal has grown approximately 3 MCY since 2004 (see Table 2 and Figure 23). SAJ examined the nourishment history of Lido Key as well as the input of sediment from offshore sources to determine if there is an apparent correlation between nourishment volume and ebb shoal growth (Figure 23).

The growth of the ebb shoal and the nourishment volumes from Lido Key show that the ebb shoal is accreting at a greater volume than that which was placed on Lido Key (Figure 25) and nourishment volumes at Lido Key alone cannot explain the growth of the ebb shoal.

SAJ also examined the growth of the ebb shoal on the basis of the volumes placed on Longboat Key and Lido Key from offshore sources (Figure 26). The ebb shoal has grown by 50% of the volume placed. This does not mean that the sediment in the ebb shoal are exactly those sediments that had been placed; however, it does appear that the placement of offshore sediment has contributed to the growth of the ebb shoal in the previous decade.

The 1 m (3.28 ft.) contour from the ebb shoal volume calculations using the Walton and Adams method (Table 2) was used to map the planform extent of the ebb shoal from 1883 to 2010. Figure 27 and Figure 28 show that Big Sarasota Pass has always maintained the same orientation and similar morphology for the past 100 years, which has also been found by Davis and Wang (2004).

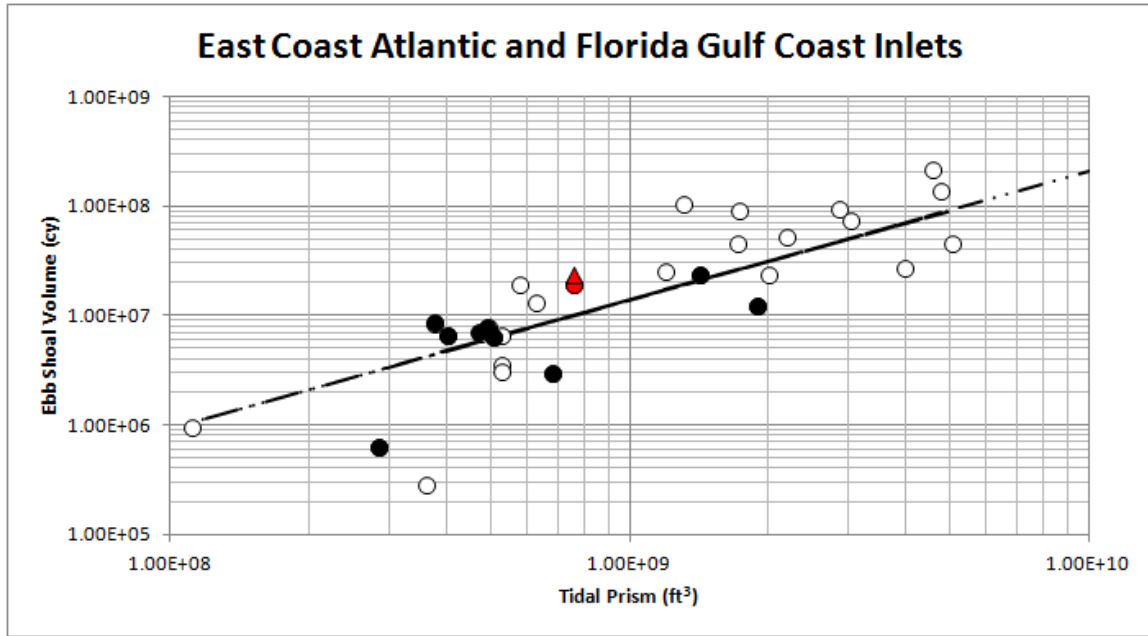


Figure 24: Ebb shoal volume - Walton Adams (1976); red circle is the volume of the ebb shoal at Big Sarasota Pass in 1955, and the red triangle is the ebb shoal volume in 2010. The sloped line is the equation that predicts equilibrium ebb shoal volume based upon the tidal prism

In the past decade, however, (see Table 2 and Figs 16-23) the ebb shoal has grown approximately 3 MCY since 2004. SAJ examined the nourishment history of Lido Key as well as the input of sediment from offshore sources (Table 3 and Table 4) to determine if there is an apparent correlation between nourishment volume and ebb shoal growth.

Table 3: Nourishment History Lido Key

Nourishment History Lido Key			
Date	CY Nourishment	Cumulative CY	Source
Feb-91	137,500	137,500	New Pass
Sep-97	163,000	300,500	New Pass
May-98	285,000	585,500	Offshore
Apr-01	360,000	945,500	Offshore
Feb-03	125,000	1,430,500	New Pass
Apr-09	464,176	1,894,676	New Pass

Table 4: Nourishment History: Longboat and Lido Keys from Offshore Sources

Nourishment History: Longboat and Lido Keys from Offshore Sources			
Date	CY Nourishment	Cumulative CY	Source
Aug-93	2,329,000	2,329,000	Longboat Key (800,000 of 3,219,000 from New Pass)
Feb-97	891,000	3,220,000	Longboat Key from Offshore
May-98	285,000	3,505,000	Lido Key from Offshore
Apr-01	360,000	3,865,000	Lido Key Interim Nourishment from Offshore
May-01	105,000	3,970,000	Longboat Key from Offshore
Jul-06	1,388,000	5,358,000	Longboat Key from Offshore

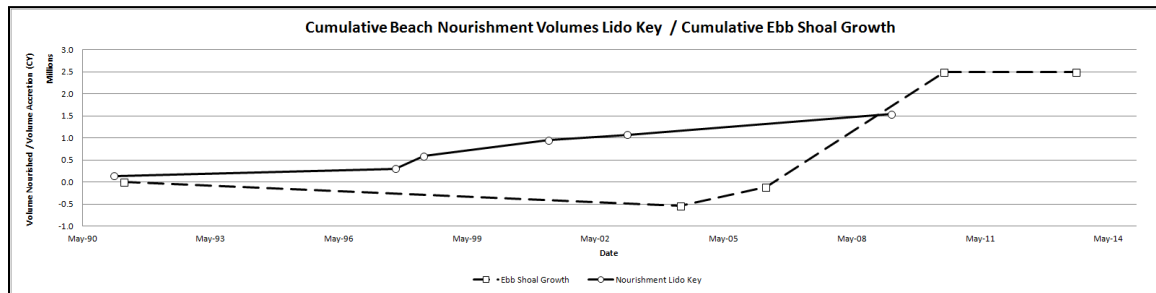


Figure 25: Cumulative Nourishment Volumes for Lido Key and Cumulative Ebb Shoal Growth

SAJ also examined the growth of the ebb shoal on the basis of the volumes placed on Longboat Key and Lido Key from offshore sources (Figure 26). The ebb shoal has grown at 50% of the volume placed. This does not mean that the sediment in the ebb shoal are exactly those sediments that had been placed, however it does appear that the placement of offshore sediment has contributed to the growth of the ebb shoal in the previous decade.

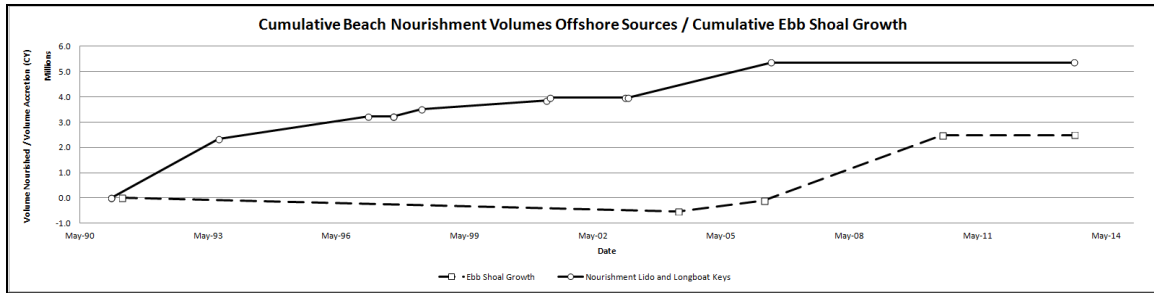


Figure 26: Cumulative Beach Nourishment from Offshore Sources and Ebb Shoal Growth

The 1 m (3.28 ft.) contour from the ebb shoal volume calculations using the Walton and Adams method was used to map the planform extent of the ebb shoal from 1883 to 2010 (Figure 27 and Figure 28). Here it can be seen that Big Sarasota Pass has always maintained the same orientation and similar morphology for the past 100 years which has also been found by Davis and Wang (2004).



Figure 27: Ebb Shoal Contours 1883, Red; 1991, Orange; 2010, Green



Figure 28: Ebb Shoal Contours: 1991, Orange; 2004, Red; 2006, Yellow; 2010, Green; 2013, Cyan

1.5.2. Main ebb channel migration

Big Sarasota Pass has always maintained the same orientation and similar morphology for the past 100 years; however, dredging in the 1920's through the 1950's in the GIWW have caused significant changes in the orientation of the south lobe of the inlet complex (Davis and Wang, 2004). Re-examining Table 2 and the extent of the ebb shoal from the Walton Adams method (Figure 27 and Figure 28 the volume (on the order of 20 MCY) and the planform extent of the ebb shoal has not changed appreciably over the past century (to be discussed in the following Section). What has changed extensively is the location of the main ebb channel location within the shoal (Figure 29).

In 1943, the main ebb channel of Big Sarasota Pass ran along the northern shoreline of Siesta Key, and the ebb shoal was more symmetrical than it has been since that time, with the attachment point directly at “Sarasota Point” (Figure 30).

The inlet management plan prepared by CPE (1992) also provides long-term history of Big Sarasota Pass and also notes that as early as 1952; the southern channel bank of Big Sarasota Pass was being hardened due to the construction of revetments along the embankment. The construction also added to the increase in local tidal currents and further defined the channel. The Interim Report on Lido Key (USACE, 1962) stated that the inlet channel of Big Sarasota Pass has steadily migrated southward for years and that the channel has cut into the south bank of the inlet severely along Siesta Key. In addition, the material eroded from Lido Key and deposition of material from littoral drift has resulted in a rather large shoal that reinforces the location of the inlet channel against the south bank of the inlet. The report notes that a swash channel occasionally breaks through to the north of the main channel, but does not remain open for a time period that would provide relief to the south bank. By 1969, the south tip of Lido Key and “Sarasota Point” at Siesta Key has started eroding. Although southward bypassing is still apparent in 1969, the attachment point has moved well to the south, which has most likely exacerbated the erosion of “Sarasota Point” (Wang et. al, 2007) (Figure 31).

Previous reports (USACE, 1962, Antonini, 1993; Davis and Wang, 2004; IMP, 2008) all indicate that the change in tidal currents, as a function of the infilling of the Cerol Islands in the 1920’s, dredging of the GIWW, hardening of the southern channel bank of Big Sarasota Pass, and the increase in alongshore sediment transport in conjunction with the creation of Lido Key, has contributed to the southerly migration and confinement of the main inlet channel against the northern shoreline of Siesta Key.

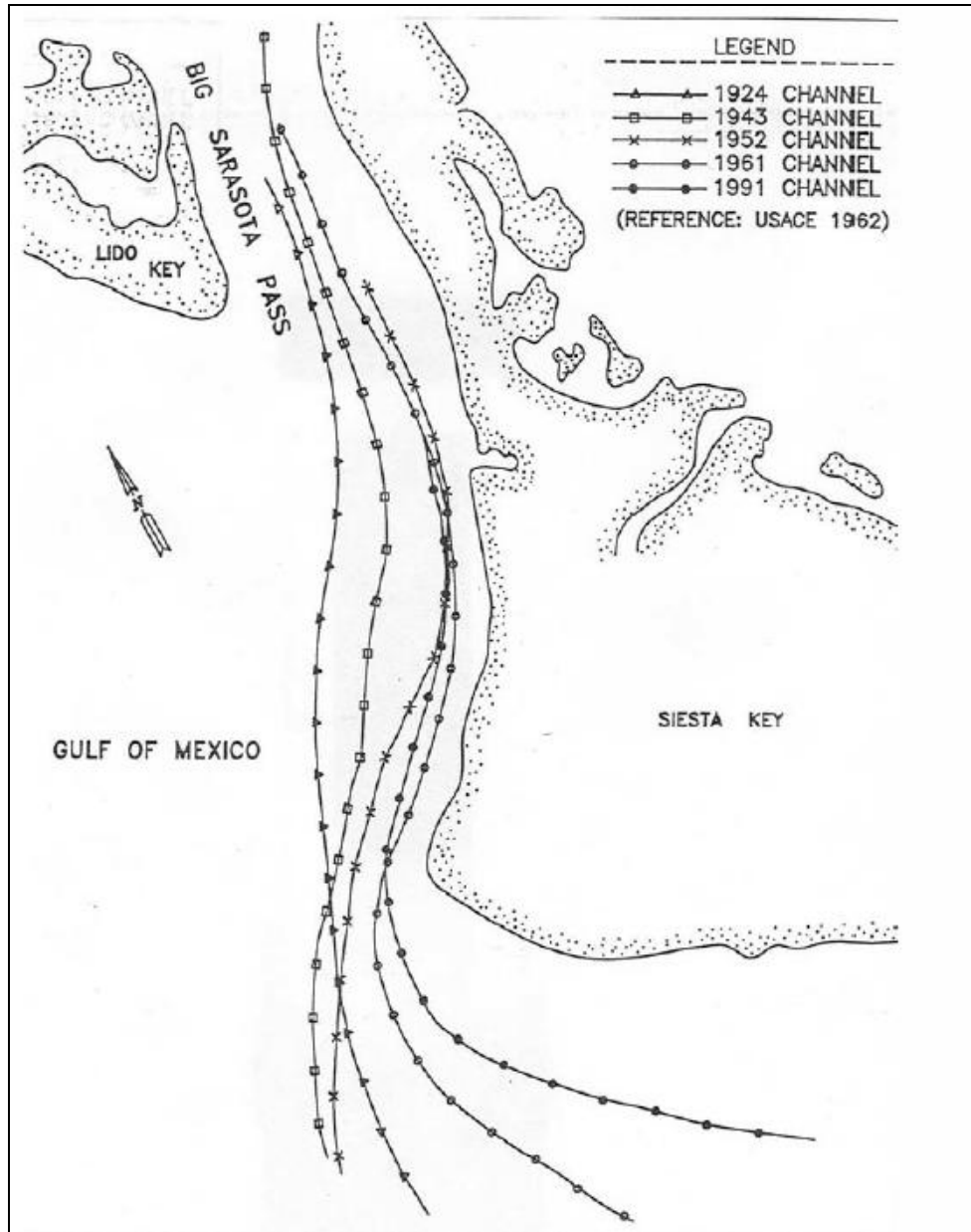


**Figure 29: Migration of the Main Ebb Channel at Big Sarasota Pass since 1924
(IMP, CPE, 1992)**



Figure 30: BSP in 1943



Figure 31: BSP Siesta 1969

1.5.3. Ebb shoal Attachment Bar at Siesta Key History

As discussed above, the channel through Big Sarasota Pass had migrated to the south and was beginning to be pinned against the northern shoreline of Siesta Key by the early 1950's. At the same time, the attachment point of the ebb shoal was migrating to the south as well, and the northern beaches of Siesta Key which face the Gulf of Mexico began to erode due to the lack of sediment supply. With the acquisition of more aerial photography, especially in recent years, it can be seen that the attachment point “wobbles” among locations along an approximate one-mile length of shoreline along Siesta Key. For the time periods where photography exists that capture the attachment point, it can be seen that the attachment point has meandered along a 1-mile stretch of shoreline from 1976 to the present. Figure 32 - Figure 35 clearly show the swash bars that move across shore to build the shoreline of Siesta Key at the attachment point for the ebb shoal. In 2012 and 2013, the attachment had migrated to the northwest from the earlier period in 2008 and 2009. An examination of a time history of aerial photographs show the meander of the attachment point and has been documented previously (Wang et al., 2007) (Figure 36, Figure 37). During all of this time, the attachment point has never returned “Sarasota Point”, where it had been in 1943 (Figure 30).

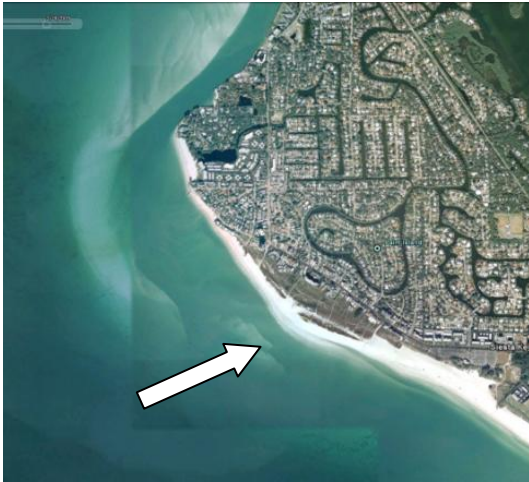


Figure 32: BSP and Siesta Key in 2008



Figure 34: BSP and Siesta Key in 2012



Figure 33: BSP and Siesta Key in 2009

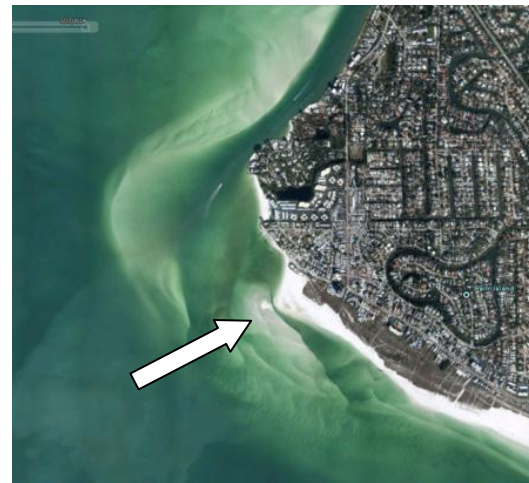


Figure 35: BSP Siesta 2013

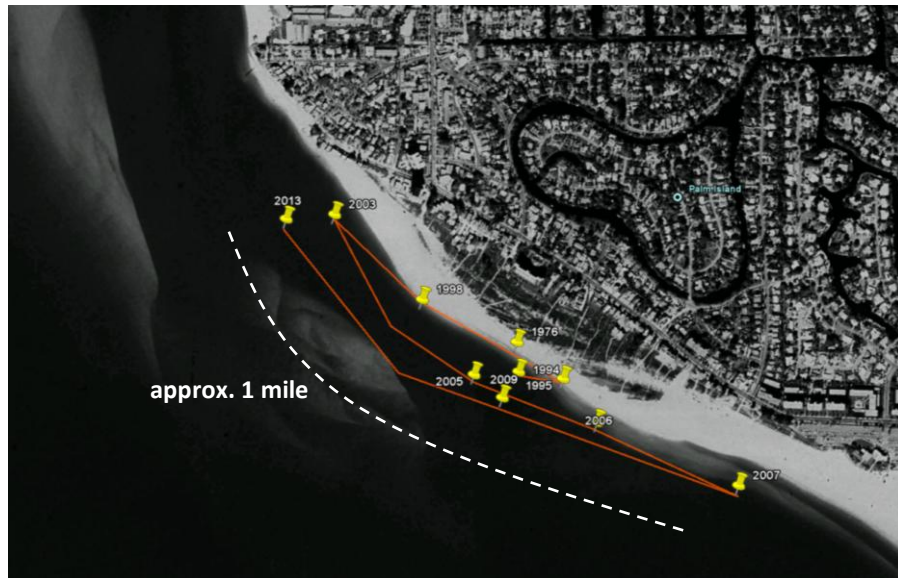


Figure 36: Inter-year migration of the attachment point of the Big Sarasota Pass Ebb Shoal

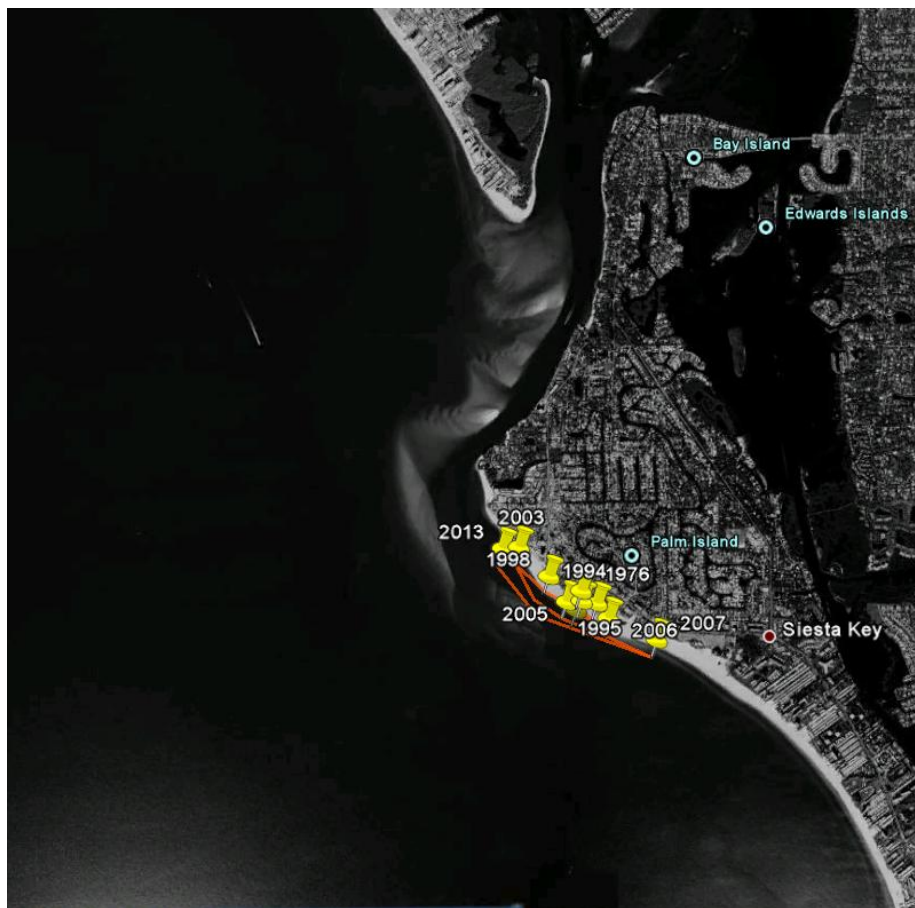


Figure 37: Region where attachment point migrates

2. QUANTITATIVE ANALYSIS OF EXISTING DATA

The Sarasota County Comprehensive Inlet Management Program Big Pass and New Pass Management Alternatives, (2008) authored by Coastal Technology Corp., University of South Florida, Coastal Engineering Consultants, Inc. with input from the USACE Jacksonville District, contains a thorough, peer-reviewed, quantitative analysis of existing data for Lido Key, Big Sarasota Pass and Siesta Key and will not be reproduced here. The reader is referred to Chapter 3, “Erosion Analysis, Morphology and Sediment Budget” for an analysis of beach profile change, historical morphological assessment and summary of Big Sarasota Pass Morphodynamics (see esp. Wang, Beck and Davis, 2007) as well as the development of a Conceptual Sediment Budget.

2.1. Sediment Budget

The Sarasota County Comprehensive Inlet Management Program Big Pass and New Pass Management Alternatives, (2008) authored by Coastal Technology Corp., University of South Florida, Coastal Engineering Consultants, Inc. with input from the USACE Jacksonville District, contains a thorough, peer-reviewed sediment budget for New Pass, Lido Key, Big Sarasota Pass and Siesta Key (Figure 38).

The sediment 1987 - 2006 sediment budget produced in the 2008 report served as the reference historical sediment budget from which would be examined:

- 1) The gross transport into and out of Big Sarasota Pass and adjacent shorelines
- 2) Any changes that may occur to both gross and net transport at Big Sarasota Pass and adjacent shorelines due to future modification in sediment management strategy including nourishment of Lido Key from sediments mined at Big Sarasota Pass.

To further refine the 1987 to 2006 sediment budget, the Bodge Method (Bodge 1993; Coastal Engineering Manual Part V-6) was applied. This method uses the volumetric change rate of the inlet and ebb shoal complex and the updrift and downdrift beaches as calculated from the profile data, and evaluates these against a range in viable net and gross transport rates for the region. The method also assigns a likely range in values for bypassing, inlet-induced erosion, and impoundment at jetties (if any) for both updrift and downdrift beaches. The resulting calculations that balance the known volumetric changes represent a “Family of Solutions” that each represent a viable budget. These results can be narrowed to better represent the more likely conditions during the period of the budget.

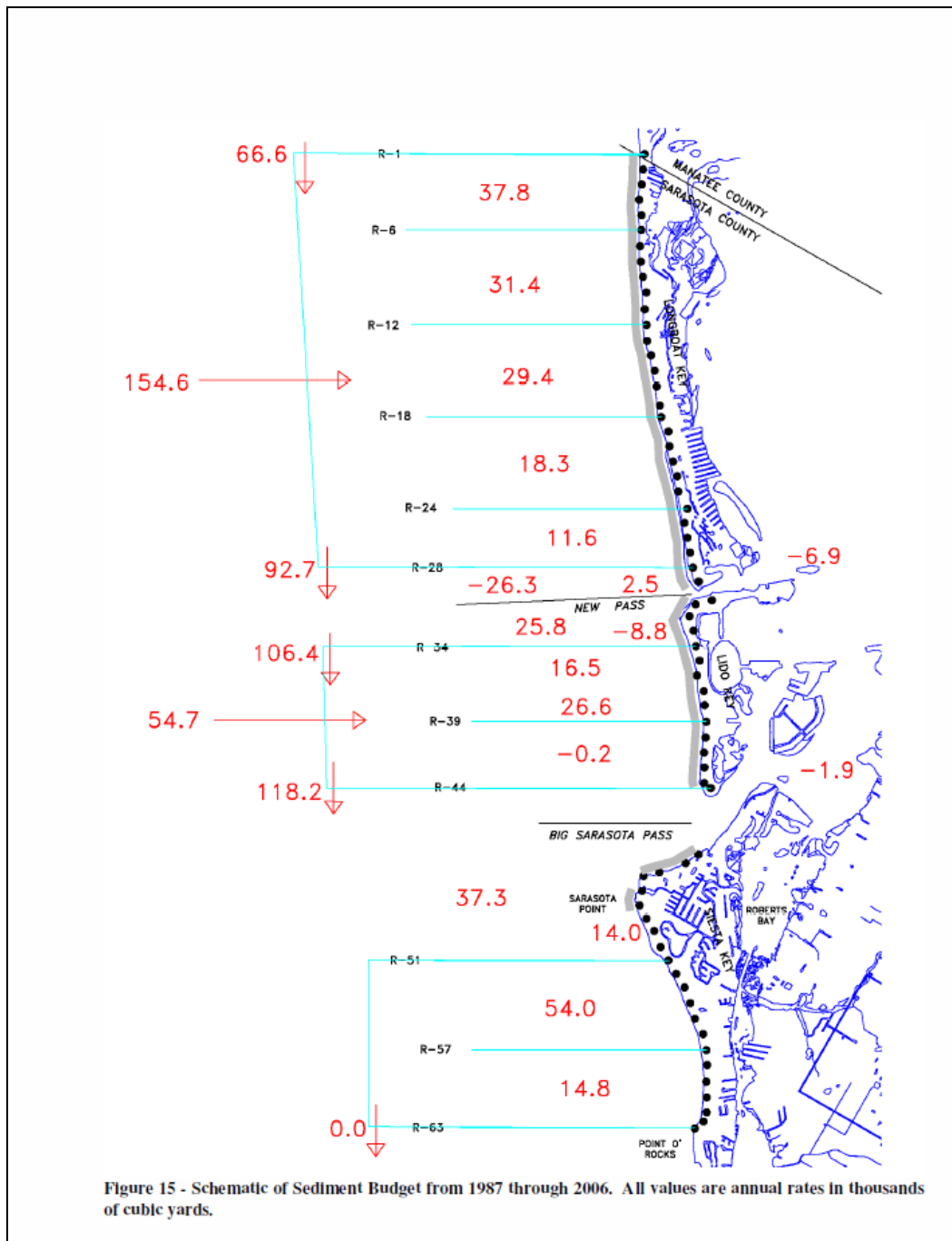


Figure 38: Sediment Budget from 1987 - 2006. From Coastal Tech, Coastal Engineering Consultants and the University of South Florida, 2008

The Comprehensive Inlet Management Program report (2008) states that Big Sarasota Pass accretes at a rate of approximately 37,300 cy/yr, Lido Key accretes by 42,900 cy/yr due to an annualized rate of nourishment of 54,700 cy/yr from a combination of New Pass and offshore sources, and finally, Siesta Key accretes by 82,800 cy/yr. Overall, Sarasota County is an accretional system provided that a continual supply of sediment can be placed on Lido Key. What is not addressed in the sediment budget in the Comprehensive Inlet Management Program report (2008) is the gross transport in the system and a description of the volume contribution to Big Sarasota Pass by both Lido and Siesta Keys.

The system of equations developed for the sediment budget applies values for left and right beaches from the perspective of a seaward-looking observer (Figure 39).

The equations solved are as follows (Bodge 1993):

$$\Delta V_L = L_1 - p_2 L_2 - m_1 R_1 \quad (1)$$

$$\Delta V_{shoal} = R_1 - p_1 R_1 + m_1 R_1 - L_2 + p_2 L_2 - m_2 L_2 \quad (2)$$

$$\Delta V_R = -R_2 + p_1 R_1 + m_2 L_2 \quad (3)$$

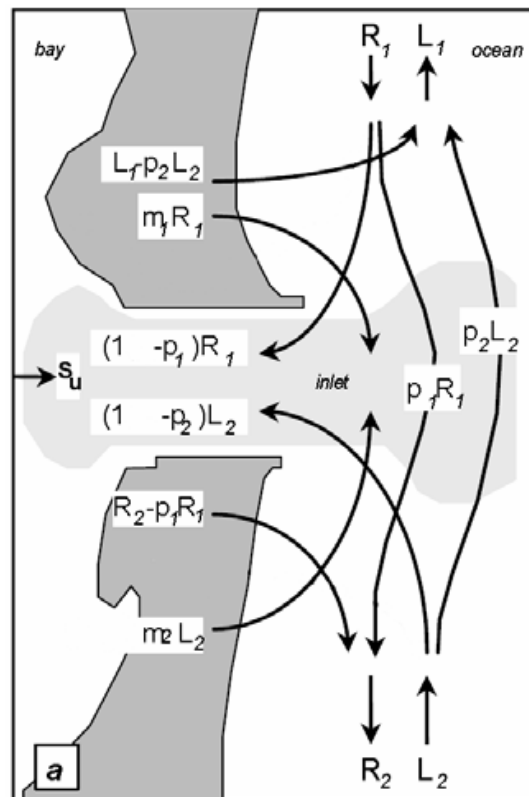


Figure 39: Definition of variables for sediment budget (from CEM IV-6; USACE 2008)

Values applied in the 1987 – 2006 calculation were as follows:

Volume change rate of inlet shoal system =

$$\Delta V_{shoal}=37,300 \text{ cy/yr}$$

Volume change rate to the left (SOUTH) shoreline =

$$\Delta V_L=82,800 \text{ cy/yr}$$

Volume change rate to the right (NORTH) shoreline =

$$\Delta V^R=42,900 \text{ cy/yr}$$

To develop the Family of Solutions, the parameters $p1$, $p2$, $m1$, and $m2$ ranged from 0 to 1:

$p1$, $p2$ = fraction of incident transport (R or L) naturally bypassed across the inlet ($p1$ = from the left, $p2$ = from the right; 0.0 = no bypassing; 1.0 = perfect bypassing);

$m1$ = local inlet-induced transport from the left shoreline into the inlet (expressed as a fraction or multiple of the right-directed incident transport, $R1$)

$m2$ = local inlet-induced transport from the right shoreline into the inlet (expressed as a fraction or multiple of the left-directed incident transport, $L2$);

A range of right-directed and left-directed transport rates were applied:

R , L = rightward- and leftward-directed incident transport values at the study area's boundaries, based upon a range of gross transport rates published by Davis et al (2008) and from Figure 14 of the 2008 Inlet Management Program study.

$$R1=R2=0 \text{ to } 50,000 \text{ cy/yr}$$

$$L1= -1 * R1$$

$$L2=0 \text{ to } -200,000 \text{ cy/yr}$$

$$R1+ L2= -106,000 \text{ cy/yr}$$

Solutions to Equations 1 – 3 were forced to be ± 1000 cy of the measured values for ΔV_{shoal} , ΔV_L and ΔV_R . A Matlab code was applied with the values as discussed above and 300,000 solutions were calculated.

2.1.1. Family of Solutions

To narrow the solutions, a family of solutions was created using knowledge of the region. First, it was specified that net transport into the system is 106,000 cy/yr based upon the sediment budget developed from the Inlet Management Program (2008). It is also assumed that shoaling into Big Sarasota Pass from Lido Key is greater than shoaling from Siesta Key. Further, it is assumed that bypassing from Lido Key is greater than 53,000 cy/yr, which again is based upon the sediment budget developed from the Inlet Management Program (2008). Finally, it was assumed, due to the significant amount of net transport from the north, that shoaling from Siesta Key is less than 20% of the total sediment volume entering the ebb shoal each year. The narrowed family of solutions is shown in Figure 40. The mean for each calculated parameter was used to verify the method developed by Bodge (1993) that is cited in the CEM (USACE, 2008).

The resulting Family of Solutions is shown in Figure 40.

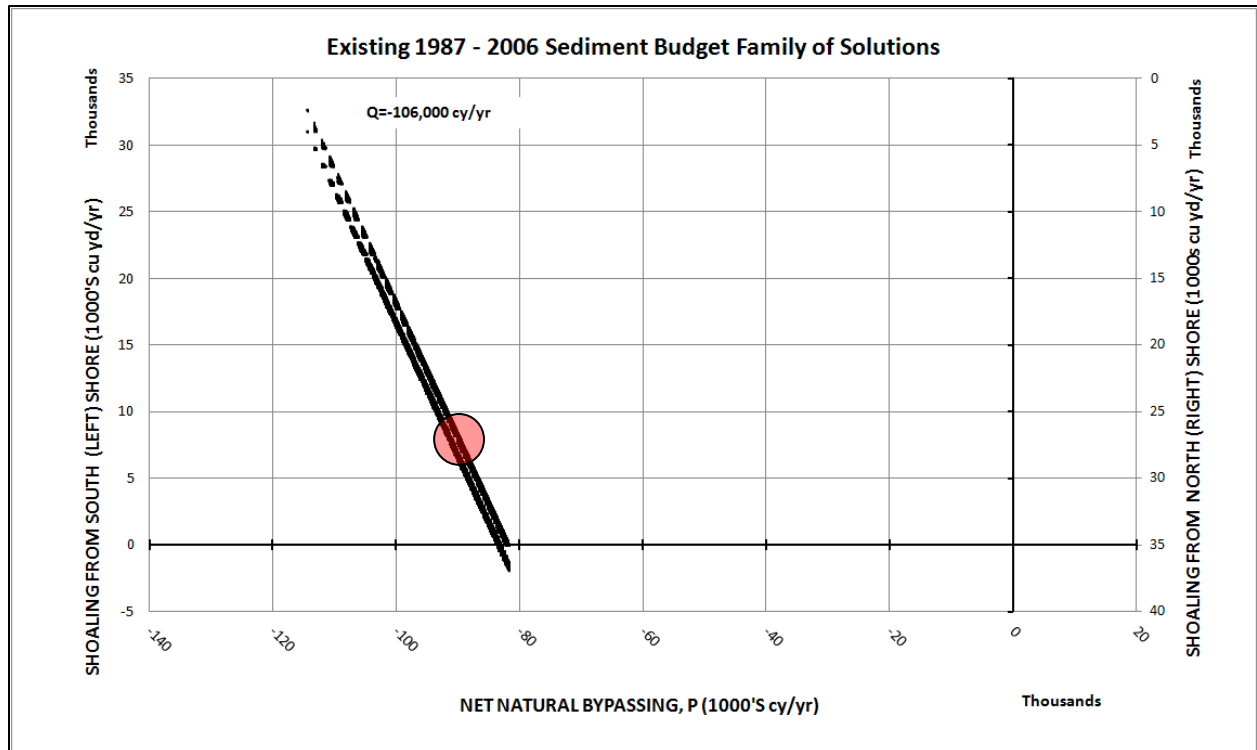


Figure 40: Existing 1987 - 2006 Sediment Budget Family of Solutions. The red shaded area represents the mean solution.

The mean solution, shown in Figure 40, solves the Equations shown in Figure 39 from the Bodge Method. This mean solution has a net longshore sand transport at the northern boundary of the study area of 106,000 cy/yr, with approximately 90,000 cy/yr bypassing the inlet toward the south. Shoaling from the north into the inlet complex was ~ 29,000 cy/yr (15,160 + 13,462 cy/yr), and shoaling from the south into the inlet was ~8,000 cy/yr (4,088 + 4,373 cy/yr). At the southern boundary of the study area at Point of Rocks, the net longshore sand transport was to the south at 0 cy/yr.

These values were combined into Figure 41 to show transport into the inlet complex at Big Sarasota Pass from Lido Key and from Siesta Key, which are approximately 27,000 cy/yr and 8,500 cy/yr, respectively. Bypassing around Big Sarasota Pass to Siesta Key is approximately 90,000 cy/yr.

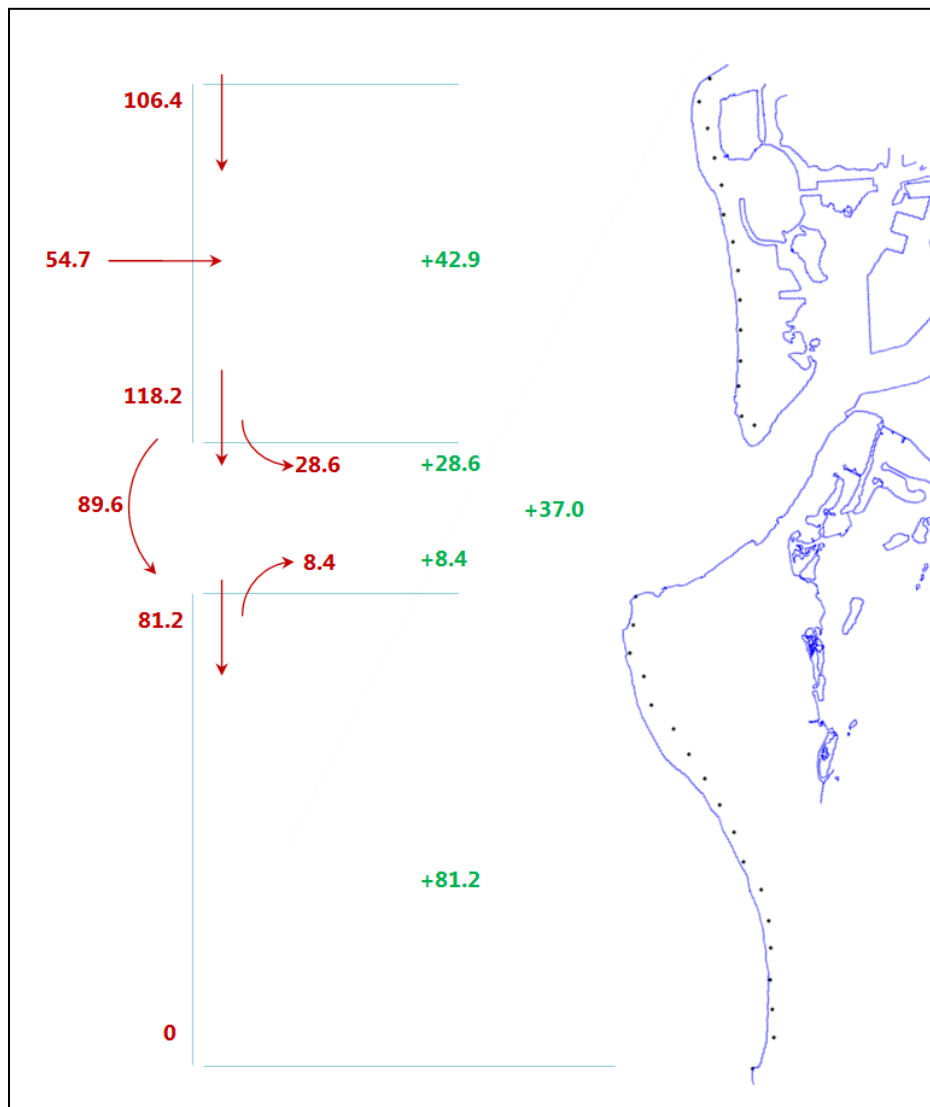


Figure 41: Finalized Sediment Budget Existing Condition 1987 - 2006

3. NUMERICAL MODELING

3.1. CMS Model Description and Justification

The COASTAL MODELING SYSTEM, VERSION 4 (CMS), a process-based morphology-change model, was selected to model the effect of each alternative on the coastal system. The CMS provides modeling outputs that will be used to determine: 1) response and evolution of inlet and ebb shoal morphology as a function of mining of the ebb shoal for sediments, 2) changes to the wave climate due to changes in the ebb shoal morphology, 3) response of the main ebb tide channel due to evolution of the inlet morphology 4) changes in sediment transport pathways that link the beach to the ebb shoal to adjacent beaches.

The CMS is a product of the Coastal Inlets Research Program (CIRP – <http://cirp.usace.army.mil>) conducted at the US Army Engineer Research and Development Center and is composed of two coupled models, CMS-Flow (Buttolph et al. 2006; Wu et al. 2010) and CMS-Wave (Lin et al. 2008). CMS-Flow is a finite-volume, depth-averaged model that can calculate water surface elevation, flow velocity, sediment transport (Camenen and Larson 2007), and morphology change. In the Coastal Modeling System, CMS-Flow is coupled with CMS-Wave which calculates spectral wave propagation including refraction, diffraction, reflection, shoaling, and breaking, and also provides wave information for the sediment transport formulas. This model was chosen for this study because of its capability to reproduce nearshore sediment dynamics at tidal inlets. The use of the CMS to accurately calculate sediment transport and morphologic evolution at inlets is advantageous over other morphological models because the CMS was specifically developed to represent inlet processes.

3.1.1. CMS Model Grid

A CMS-Flow and sand transport model grid was developed for representing New Pass and Big Sarasota Pass (Figure 42 and Table 5). The CMS-Flow grid extends approximately 12 km (7.5 mi) offshore from the throat of Big Sarasota Pass and approximately 10 km (6.2 mi) to both the north and south of the inlet. The CMS-Wave grid had the same alongshore and offshore extent as the CMS-flow grid (Figure 43). The offshore boundary was set to the offshore location at the contour depth of the wave forcing. Therefore, the resultant two grids cover the same alongshore distance of 20 km (12.4 mi) and a cross-shore distance extending from the land seaward to the ocean boundary of 12 km (7.5 mi). The finest resolution of the model grid cells were set to 12.5 m (41.0 ft.) in the inlet throat, and 25 m (82 ft.) in the main bay channels, ebb-tidal delta and nearshore. Maximum cells

sizes in the bay reached 120 m (393 ft.) over large open bay expanses, and to 400 m (1312 ft.) along the offshore boundary. The CMS-Flow grid had 71,064 cells and the CMS-Wave grid had 33,120 cells.

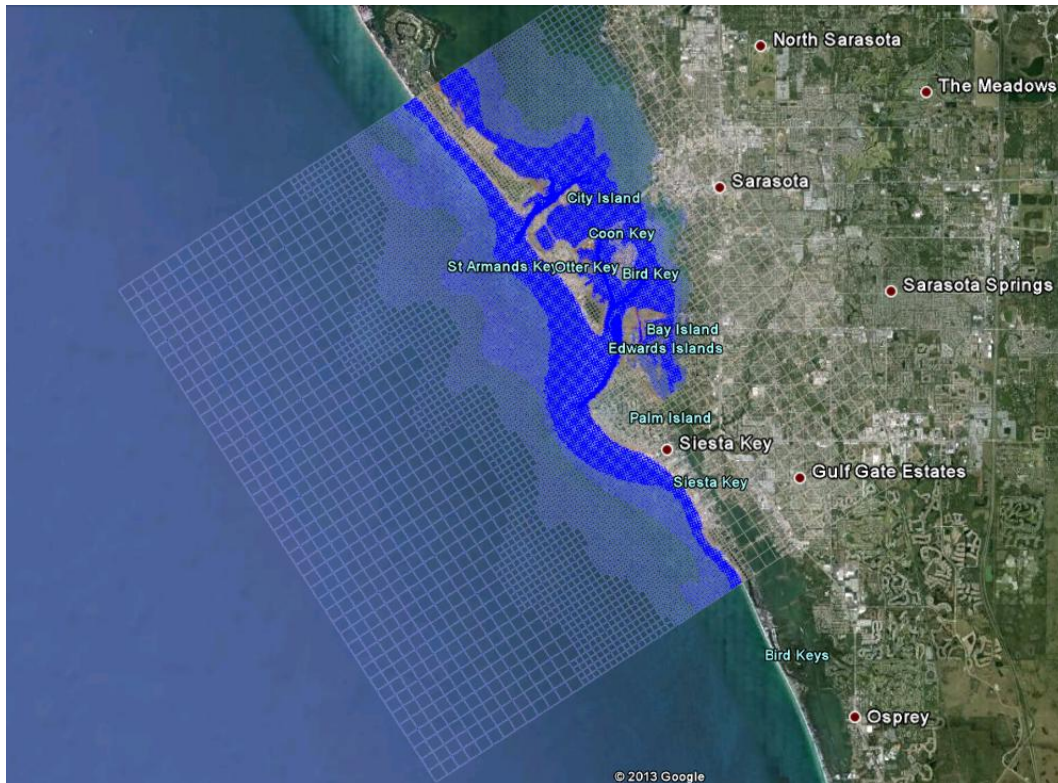


Figure 42: CMS Flow Mesh

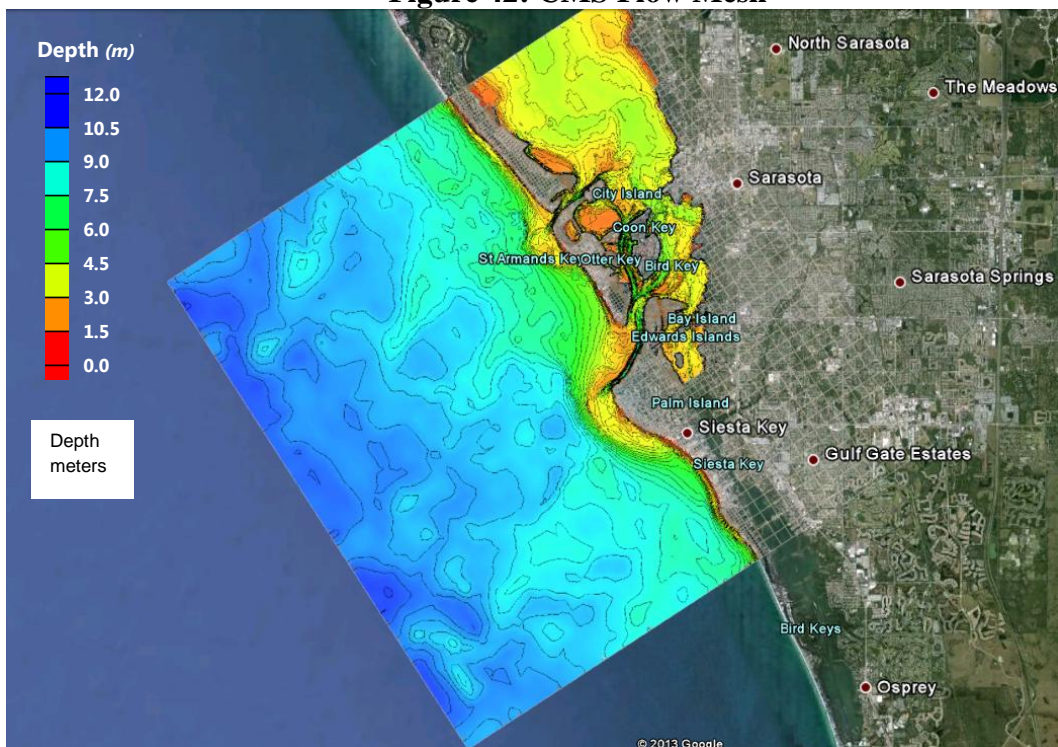


Figure 43: CMS Grid Bathymetry (Depth in METERS)

Each CMS grid was forced along the ocean boundary. CMS-Wave propagates spectral waves from the offshore ocean boundary toward land. The forcing in the CMS-Flow grid for this project was a water-surface elevation calculated in the South West Florida (SWFL) Regional CMS Model at the offshore ocean and inshore bay boundaries. Winds were not included in the local grid because they do not generate significant currents or waves in the bay due to limited fetch of the local CMS grid. The model grid is not long or wide enough to generate wind waves of significant energy, or to generate currents of substantial velocity. For CMS-Wave, wind stresses were already incorporated in the generation of the hindcast nearshore waves and therefore were not included in the offshore forcing of the wave model.

There is shared, or coupled, forcing that is generated in each model and subsequently passed between both models. Radiation stresses and water levels, which include wave setup, are passed from CMS-Wave to CMS-Flow. CMS-Flow interpolates these input data from a present and future wave simulation over a certain time interval (or steering interval) and then calculates the hydrodynamics and sediment transport over that period of time utilizing the interpolated values. At the end of the steering interval, CMS-Flow passes water levels and current velocities back to the wave model for the next CMS-Wave simulation. Morphology is updated on a larger timescale, every 3 hours, to record updated bed topography.

3.2. CMS Model Set-up and Structure

3.2.1. Model Configuration Data

3.2.1.1. Bathymetry & Shoreline

The model domain for the flow CMS model covered a local scale of approximately Bathymetry representing the bay, entrance channel, and ocean were assembled from several sources including LIDAR (USACE, JALBTCX), beach profile surveys FDEP Historical Shoreline Database (<http://www.dep.state.fl.us/beaches/data/his-shore.htm#ProfileData>) and the Coastal Relief Model (CRM) (<http://www.ngdc.noaa.gov/mgg/coastal/crm.html>) (NOAA, NGDC) for calibration, model skill and *initial* alternative analyses. All LIDAR data were obtained at the vertical datum of NAVD 88 in meters. The CRM is obtained at the vertical datum MSL. These data were converted to the same horizontal and vertical datum used in the model using software provided by the Surface-water Modeling System, through which the CMS is operated. The final horizontal datum for all bathymetry was Florida WEST State Plane (NAD83)

in meters, and the vertical datum was NAVD 88. When necessary, vertical data were shifted using NOAA Tide Gauge 8726803 at Sarasota, FL and NOAA Tide Gauge 8726089 at Longboat Key, FL (Figure 43 and Figure 44). Bathymetry from the most recent ebb shoal survey (August 2013), beach surveys (August 2013), 2010 LIDAR (July 2010) and the Coastal Relief Model (CRM) were used for the final alternative analysis and are described in *Section 6*.

3.2.1.2. Sediment and Bottom Friction Characteristics

Median sediment grain sizes, D_{50} , were incorporated in the CMS where data existed and included the beach, nearshore, and ebb-tidal delta. Sediment grain size data presented in a study of Big Sarasota Pass and New Pass by Davis and Wang (2004) and a study by Kowalski (1995) were used as a baseline to delineate general D_{50} values (Figure 45). Median grain size across the model domain was generated by nearest neighbor interpolation using measured data (Figure 44). Although no record exists of sediment grain sizes for the inlet throat, discussions with University of South Florida and ERDC geologists confirm that the channel thalweg is somewhat armored with large shell fragments (typical of Florida tidal inlets) (Beck, pers. comm.). Bottom friction was specified for CMS-Flow and CMS-Wave using Manning's n and Darcy Weisbach bottom friction, respectively.

Table 5: CMS Model Parameters

	<i>Offshore/Nearshore</i>	<i>Bay</i>	<i>Channel</i>
D_{50} (mm) (median grain diameter)	0.15 – 0.2	0.15 – 5.0	0.2 – 8.0
Manning's n (bottom friction – CMS-Flow)	0.025	0.025	0.025
C_f (Darcy Weisbach bottom friction – CMS-Wave)	0.005	0.005	0.005



Figure 44: Sediment grain size in the vicinity of Big Sarasota Pass (Davis and Wang, 2004)

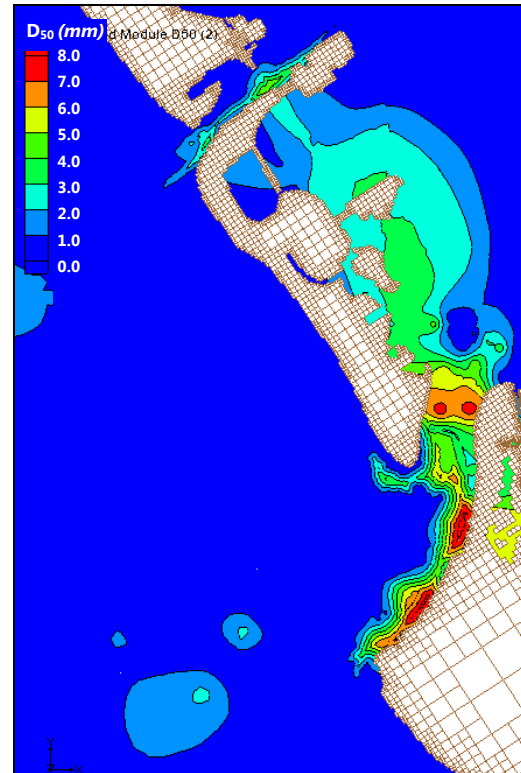


Figure 45: D_{50} (mm) at Big Sarasota Pass, New Pass and Nearshore Region

3.2.2. Model Forcing Data

3.2.2.1. Water Levels SWFL Regional Grid

A SWFL Regional CMS model grid was developed representing the South West Florida coast for the purpose of extracting water levels for the local CMS-Flow and CMS-Wave grids (Figure 46 and Figure 47). The cross-shore distance of the SWFL Regional CMS grid was approximately 40 km from the throat of Big Sarasota Pass and extended approximately 86 km in the alongshore, from Treasure Island to South Venice Inlet and including all of Tampa Bay. The offshore boundary of the SWFL Regional CMS model was forced along the ocean boundary with 6-minute measured water levels from NOAA Stations 8726724 Clearwater Beach, FL and 8725110 Naples, FL. The finest resolution of the model grid cells were set to 12.5 m (41.5 ft) in the inlet throat, and 25 m (82 ft.) in the main bay channels, ebb-tidal delta and nearshore. Maximum cells sizes in the bay reached 120 m (393 ft.) over large open bay expanses, and to 800 m (2624 ft) along the offshore boundary. The CMS-Regional-Flow grid had 132,265 cells and calculated water surface elevation and velocities, only.

The modeled time period was from 24 February to 31 March 2006. The model run was set for a ramp period, or spin-up period, of 6 hours which is typical for implicit model runs. The hydrodynamic time-step was set to 600 seconds (10 minutes) to ensure capturing the tidal curve.

The SWFL Regional CMS model was calibrated to water levels measured in New Pass and Big Sarasota Pass by University of South Florida. These data are discussed in 3.3.2.1.1. Figure 48 shows a comparison between the measured and calculated water levels at the two bay gauges. The correlation coefficient, or R^2 -values, between measurements and calculated values are 86% for Big Sarasota Pass, and 85% for New Pass.

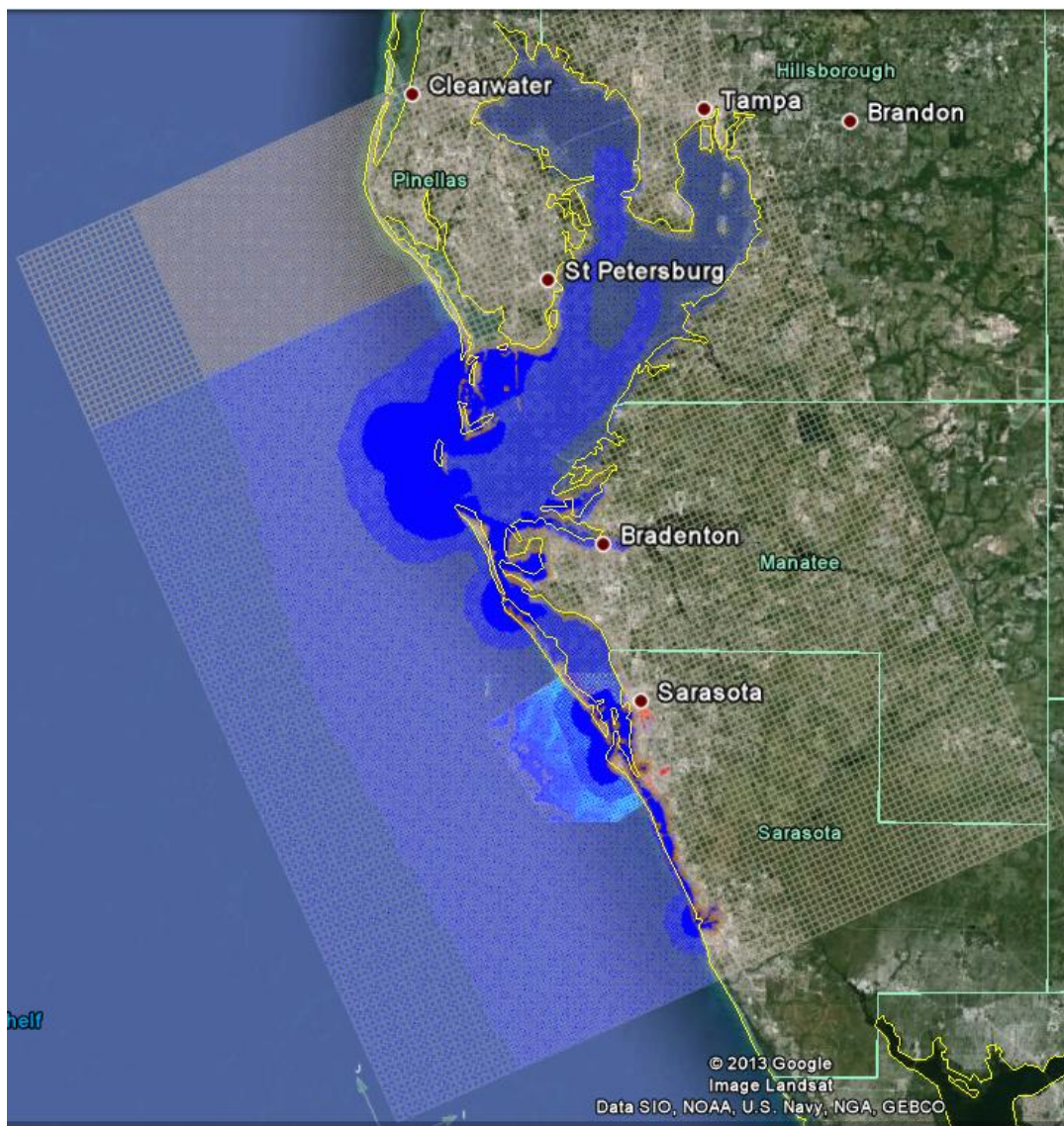


Figure 46: South West FL Regional Mesh

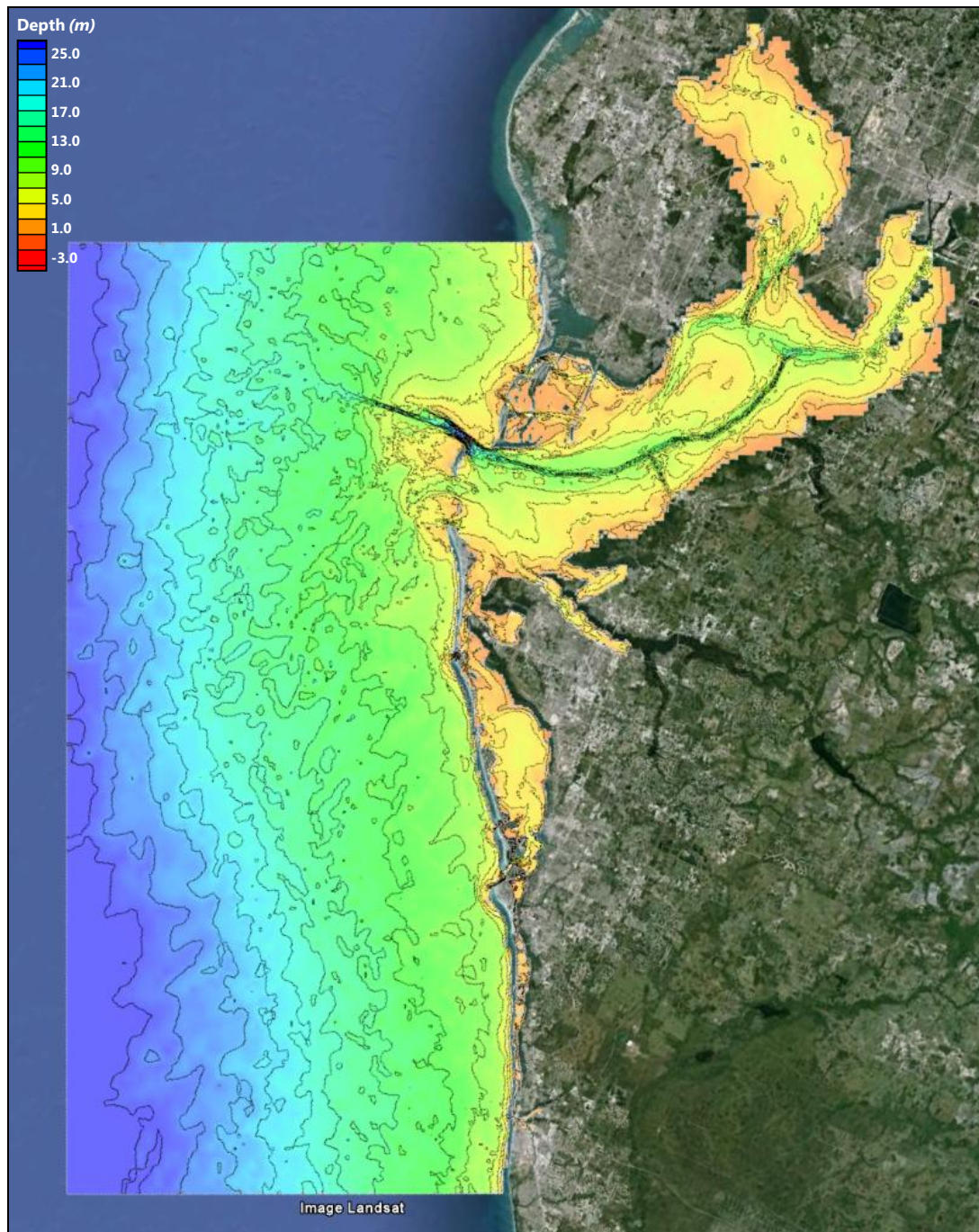


Figure 47: South West FL Regional Grid Bathymetry (Depth in METERS)

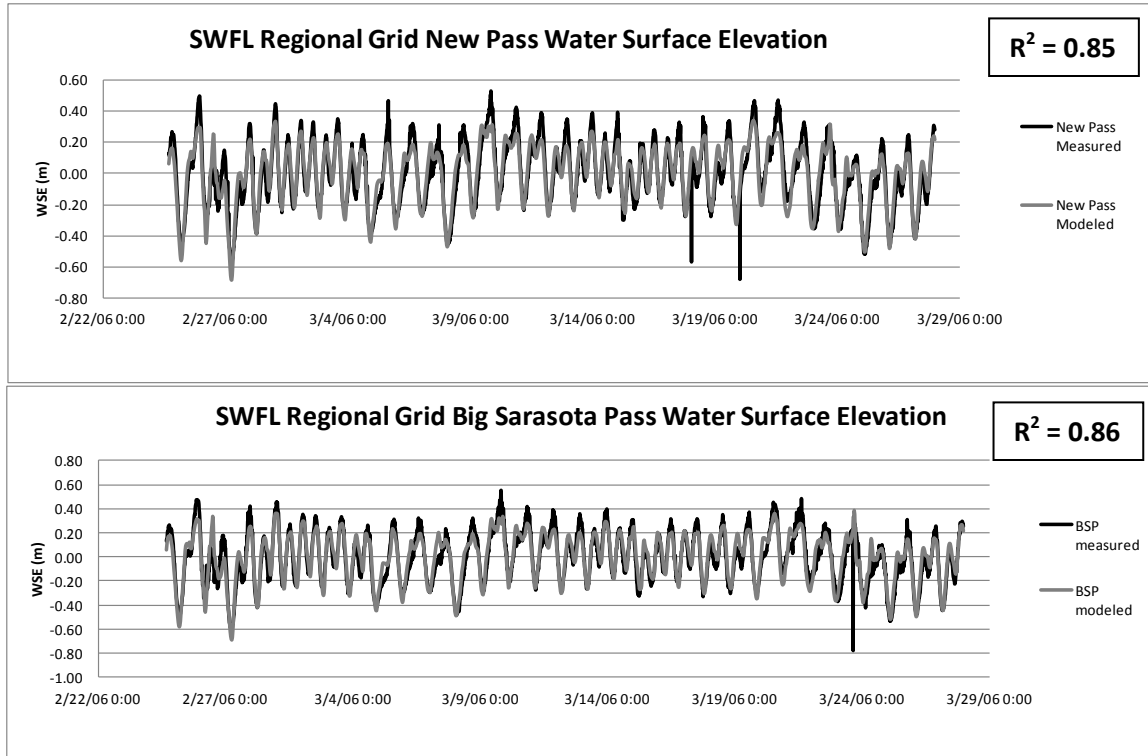


Figure 48: Water Surface Elevation Calibration for the SWFL Regional CMS Model

3.2.3. Water Levels and Wave Forcing Local CMS-Flow CMS-Wave Grids

Model forcing data for the CMS-Flow and CMS-Wave grid includes water level forcing from the SWFL CMS Regional Grid and waves from the Wave Watch III (Tolman, 2009) wave hindcast model. Water levels from the SWFL CMS Regional Grid were extracted along the open boundary of the CMS-Flow Local Grid (Figure 42). Wave forcing was extracted from the Wave Watch III hindcast and was supplied to the CMS-Wave Local Grid (Figure 43). The wave hindcast station lies directly offshore of the open ocean boundary of the CMS-Wave Grid, outside of the influence of nearshore perturbations such as the ebb-tidal delta. Due to numerous shore-oblique shoals existent along this stretch of coast, a centrally located wave station was chosen along the 25-m (82 ft.) water depth contour (Figure 43).

3.3. Model Calibration

3.3.1. Model Calibration Data

Calibration of the CMS for Big Sarasota Pass and New Pass was completed in two parts: first, through comparison of measured and calculated hydrodynamics, and secondly through comparison of morphologic end-states. The model was forced at the offshore boundary with extracted water levels from the Regional Grid and waves from the WWIII Model. Hydrodynamics were calibrated by

comparing model results with measurements of water level and currents collected from 24 February to 31 March 2006 by University of South Florida. The bathymetry used in the model grid was from the CRM (NOAA), Beach Profile Surveys (FDEP Database) and LIDAR collected in May 2006, which was quality checked by the USACE JALBTCX and NOAA CSC.

Measured morphology change was used to test model skill from LIDAR surveys conducted in May and November 2004. The measured morphologic change was used in comparison with calculated morphology change.

3.3.2. Hydrodynamic Configuration and Parameter Selection

3.3.2.1. Calibration to Hydrodynamics

Ocean water levels and wave hindcast were used to drive CMS-Flow at the ocean boundary. Calculations of water level and current with the coupled CMS are compared here to measurements made within the modeled domain. The modeled time period from 24 February to 31 March 2006 served as the primary calibration period. The model run was set for a ramp period, or spin-up period, of 12 hours which is more than typically needed for implicit model runs. The hydrodynamic time-step was set to 600 seconds (10 minutes), which is reasonable for an implicit model, but not set too high to deviate from capturing the tidal curve.

The model was calibrated to measured water levels and current velocities in the throat of both inlets (Wang et al., 2007).

The final adjustments made to the CMS grid and modeling parameters were completed during the calibration of hydrodynamics. Manning's n and sediment D50 values are the only spatially variable parameters, and are collocated on the grid. Manning's n was modified along locations of bridges. Manning's n was set at 0.025 which is typical for coastal inlet regions, but was increased to 0.06 in the vicinity of the bridge at New Pass. Other parameters included in the CMS were flooding and drying, eddy viscosity due to currents and wave breaking, and sediment transport and morphology parameters. Flooding and drying and eddy viscosity were set to default values; however, the eddy-viscosity model used was the mixing length scheme rather than other simplified formula. CMS-Wave model parameters included a Darcy-Weisbach bottom friction value (C_f), which was set to the default spatially constant value of 0.005, a typical value applied in coastal inlet studies.

3.3.2.1.1. Water Levels

Modeled water levels for the calibration time period were compared with water levels measured by USF (Wang et al., 2007) in Big Sarasota Pass and New Pass. Figure 49 a and b show a comparison between the measured and calculated water levels at the two bay gauges. The correlation coefficient, or R^2 -values, between measured and calculated water surface elevations are 90% for Big Sarasota Pass, and 90% for the New Pass.

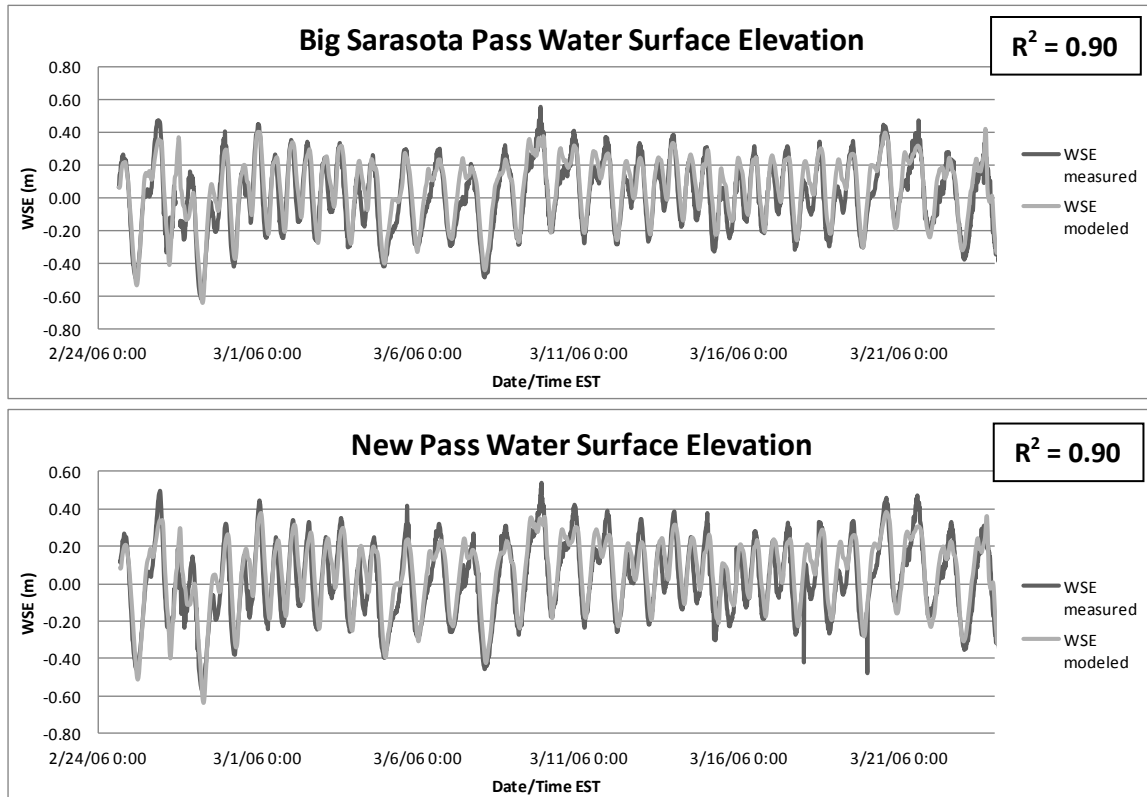


Figure 49 a&b: Measured vs Calculated Water Surface Elevations for BSP and NP.

3.3.2.1.2. Currents

Hydrodynamics were further calibrated to current measurements collected by University of South Florida (Wang et al., 2007). The measurements compared here include depth-averaged currents across inlet throat of Big Sarasota Pass and New Pass. The locations of the D-ADCP's are illustrated in Figure 50.



**Figure 50: Location map of D-ADCP surveyed cross-sections and transects
(Wang et al., 2007)**

Comparisons of the measured, depth-averaged currents are given in Figure 51. Inlet throat cross-section measurements show good correlation with the calculated model results. The correlation coefficient, or R^2 -values, between measured and calculated along-channel current velocities are 87% for Big Sarasota Pass, and 84% for the New Pass.

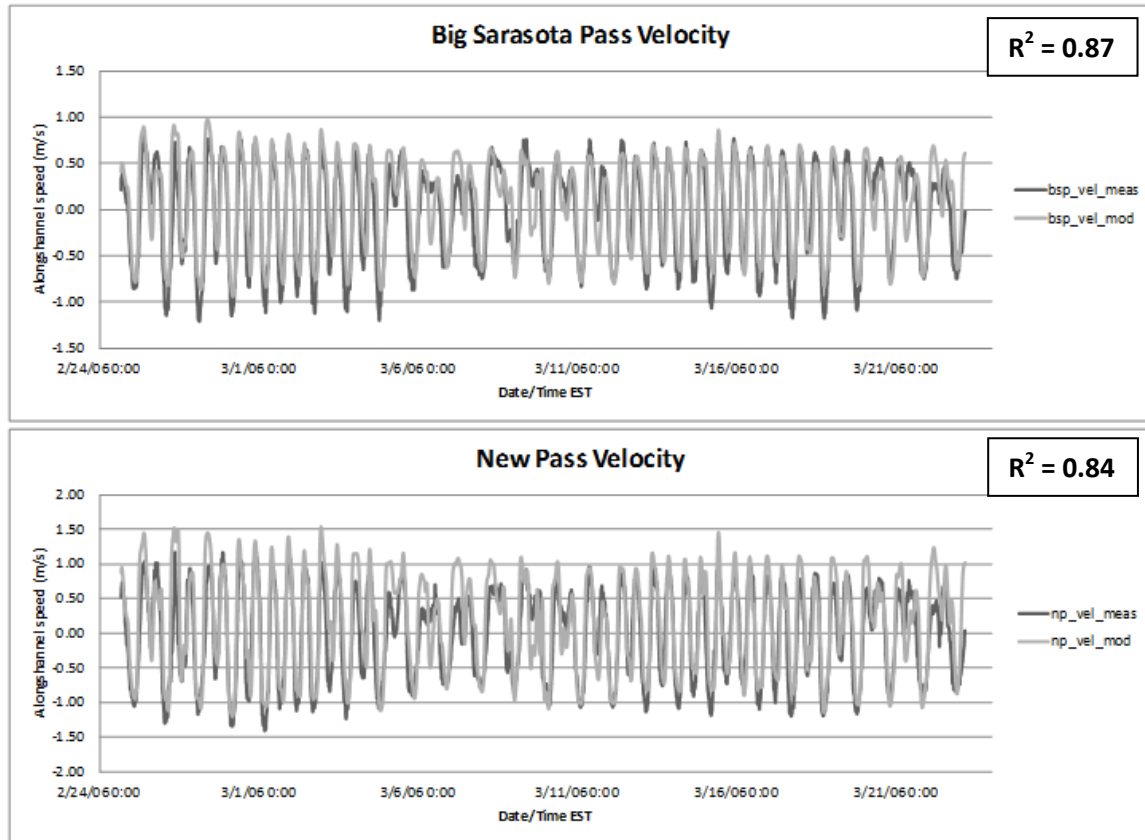


Figure 51: Measured vs. Calculated Current Magnitude BSP and NP

3.3.3. Sediment Transport and Morphodynamic Parameter Selection

There are three sediment transport models available in the CMS: a sediment mass balance model, an equilibrium advection diffusion model, and non-equilibrium advection-diffusion model. The Non-equilibrium Transport (NET) model, which is based on a total load advection-diffusion approach, was selected to calculate sediment transport rates in CMS-Flow. The Watanabe transport formula (Watanabe, 1987) was selected as the governing empirical formulas to calculate bedload and suspended load within CMS-Flow for combined waves (breaking and non-breaking) and current. Bed change is calculated over the same sediment transport time step, which was 900 seconds (15 minutes), and updated in both the wave and flow models. Bed change was updated in the wave model on the steering interval of 3 hours.

Apart from the spatially variable parameters calibrated in the hydrodynamic calibration, sediment transport and morphology default parameters are listed in Table 6. Calibration of sediment transport is described below as an attempt to reproduce both measured transport estimates for the area and measured morphology change with long-term morphologic simulations.

Table 6: Sediment transport and morphology parameters in the CMS.

<i>Parameter</i>	<i>Model Default Value</i>	<i>Model Value Used</i>
Formulation	Advection-Diffusion	Advection-Diffusion
Use Non-equilibrium Transport	Yes	Yes
Sediment Transport Formula	Lund-CIRP	Watanabe
Sediment Density	2650	2650
Watanabe Transport Factor	na	0.5
Bed Load Scaling Factor	1.0	1.0
Suspended Load Scaling Factor	1.0	1.0
Sediment porosity	0.4	0.4
Bed Slope Coefficient	1.0	0.1
Morphologic Acceleration Factor	1.0	1.0
Total Load Adaptation Length Method	Constant	Constant
Adaptation Length	10	10

3.3.3.1. Calibration to Morphology

Model calibration is discussed here as the comparison of measured and calculated sediment transport and morphology change between the time period extending from the May 2004 LIDAR data set to the November 2004 LIDAR data set. In September 2004, Hurricanes Charley, Frances, and Jeanne passed within 65 nautical miles to the study area (Figure 52). Hurricane Ivan passed within 300 nm of the area (Figure 53). Hurricanes

Frances, Ivan and Jeanne produced waves greater than 12 feet offshore of Big Sarasota Pass (Figure 54). Calibration of sediment transport to capture measured trends in transport rates requires modifications to the sediment transport formula, the bed slope coefficient, and the bed load and suspended load scaling factors.

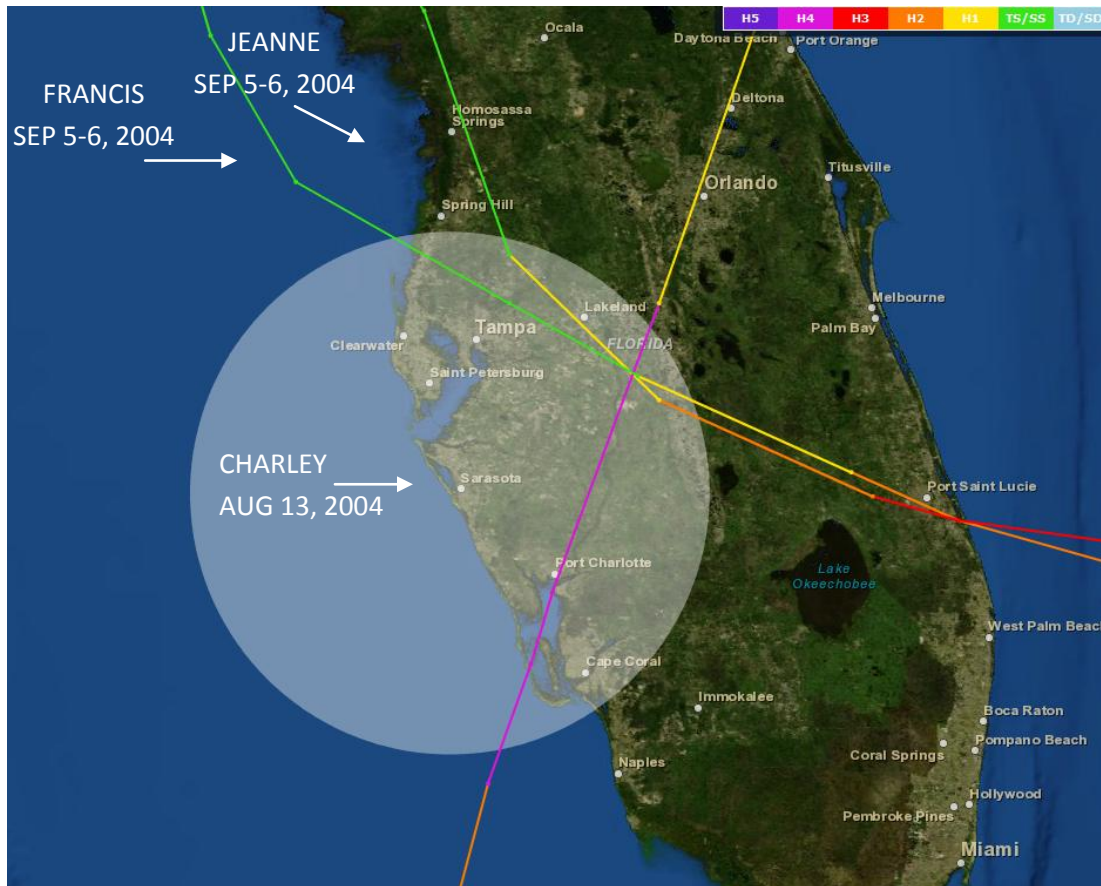


Figure 52: NOAA Historical Hurricane Tracks; Shaded region is within 65 nm from Lido Key. Hurricane Charley made landfall at Port Charlotte on August 13, 2004 at 20Z and was a Category 4 Hurricane with wind of 125 kts at the time; Hurricane Francis made passage closest to Lido Key as a Tropical Storm on September 5, 2004 at 18Z and September 6, 2004 at 0Z at 60 and 55 kts, respectively; Hurricane Jeanne made passage closest to Lido Key on September 26, 2004 as a Category 1 Hurricane at 12Z at 75 kts and as a Tropical Storm at 18Z at 55 kts

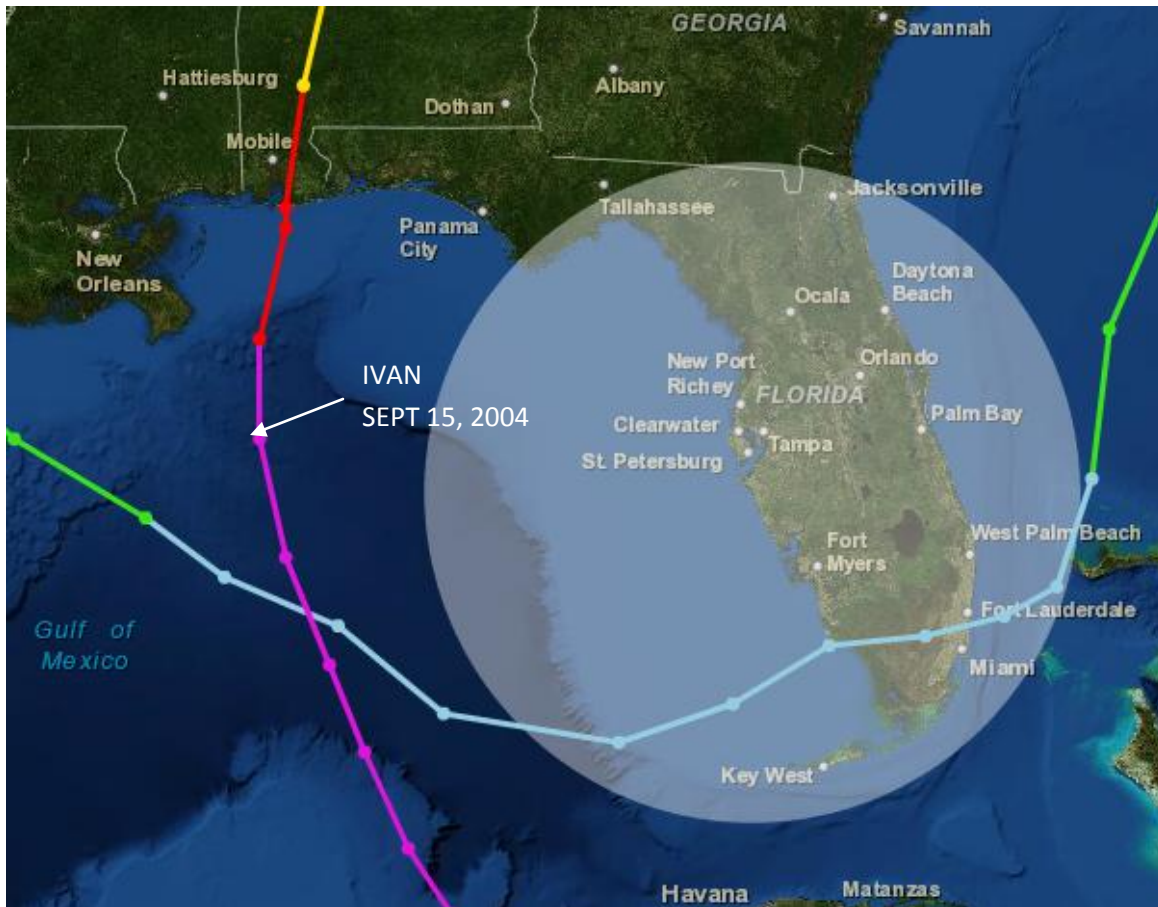


Figure 53: NOAA Historical Hurricane Tracks: Shaded area is within 200 nm from Lido Key. Hurricane Ivan made first passage on September 14, 2004 as a Category 4 Hurricane and made second passage on September 22, 2004 as a Tropical Depression

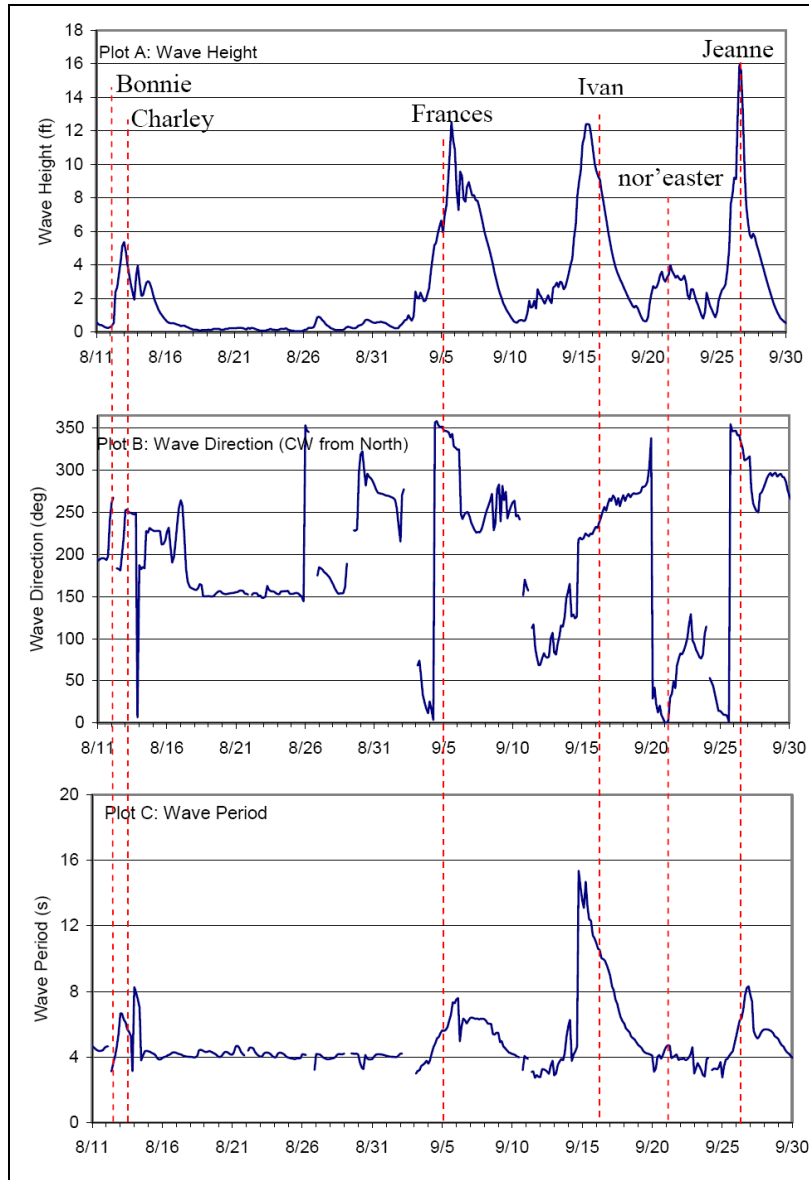


Figure 54: Offshore Wave Height, Direction and Period August, September 2004

The Watanabe sediment transport formula was chosen for the BSP and NP application because of its good representation of morphology change over both ebb shoals. The bed slope coefficient was set to 0.1 for closer representation to the morphology of channel slopes at both Passes. The default CMS suspended load and bed load sediment transport scaling factors were not modified.

The Non-equilibrium Transport (NET) method controls the capacity of sediment transport through scaling factors such as adaptation lengths or times, generally dependent upon length-scales of morphologic features such as bed-forms or timescales of sediment movement. As a total load formulation is

used with the NET, the Adaptation Length must be modified to calibrate to morphology. The Adaptation Length is a length scaling factor that is typically based on localized bed-forms. The smaller the Adaptation Length, the closer the model is to Equilibrium Transport which results in greater rates of transport that is more localized. Adaptation Lengths tested included 1, 5, and 10 meters (32.8 ft.). An Adaptation Length of 10 meters (32.8 ft.) was selected for the entire domain of the final calculations because of the realistic patterns and trends observed in the calculations as compared to the measurements.

3.4. Test of Model Skill

Figure 55 and Figure 56 shows the calculated temporal change of Big Sarasota Pass from May to November 2004. As the non-uniform sediment transport sorts sediments over the domain, there is general deflation of the updrift shoal and the main channel infills with sediment that had originated on the shoal. There is erosion of the most northerly flood marginal channel at the southern tip of Lido Key and increased definition (erosion) of the flood marginal channels across the updrift shoal. There is slight accretion of the distal lobe of the ebb shoal, as the entire ebb shoal exhibits “clockwise rotation”, from deflation of the updrift lobe, infilling of the channel and accretion of the distal lobe. This pattern of sediment redistribution is observed in the measured morphologic change from LIDAR data (Figure 14).

Here, ebb shoal attributes (Figure 14), including the main ebb channel and offshore shoals, were well represented in the model. The processes that control erosion and deposition over much of the ebb shoal were the focus of the calibration. The CMS successfully reproduced sedimentation patterns and quantities within the area of focus.

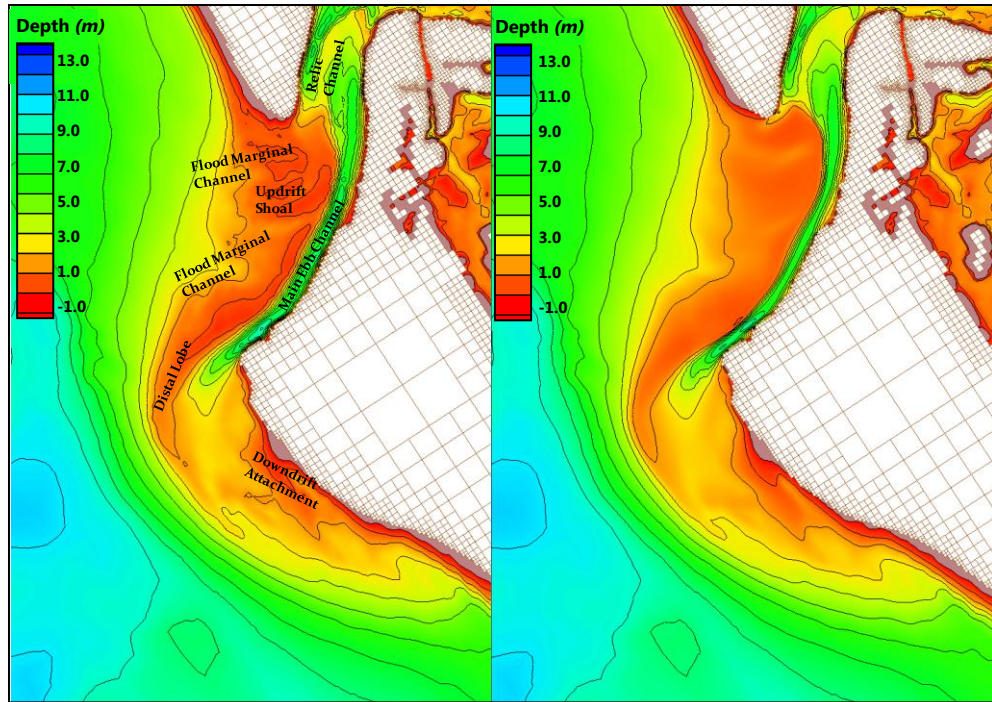


Figure 55: Calculated temporal change Big Sarasota Pass May 2004 (Left) November 2004 (Right), Depths are in METERS

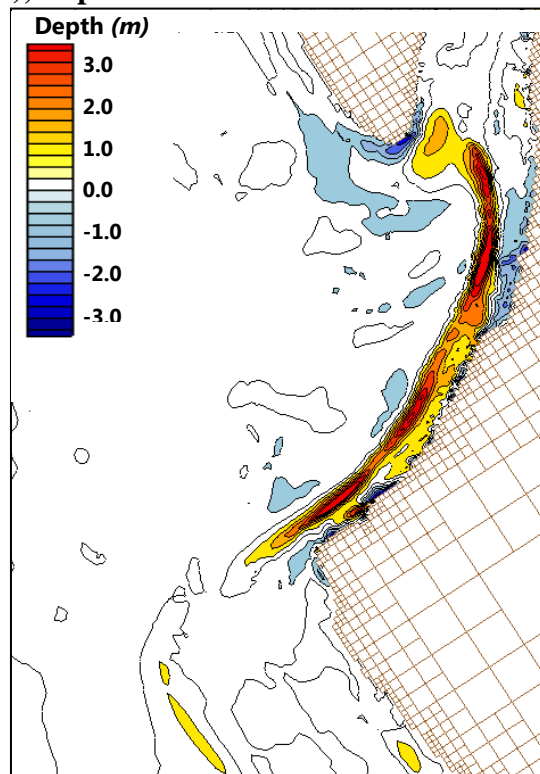


Figure 56: Calculated Significant Temporal Change ($> \pm 0.5$ m); May to November 2004. Warm Colors are Accretion, Cool Colors are Erosion, Depth Changes are in METERS

Model skill was tested through a comparison of the calculated morphology change and measured morphology change for the six-month simulation from May 2004 to November 2004. Figure 57 is a visual correlation of the measured and calculated *regions* of accretion and erosion from May to November 2004. Morphology change, illustrated in Figure 58 where warm colors represent accretion (deposition) and cool colors represent erosion, captures the overall morphologic change of the shoal features including the channel infilling, ebb shoal platform deflation and migration of sediments to the attachment point of downdrift beaches.

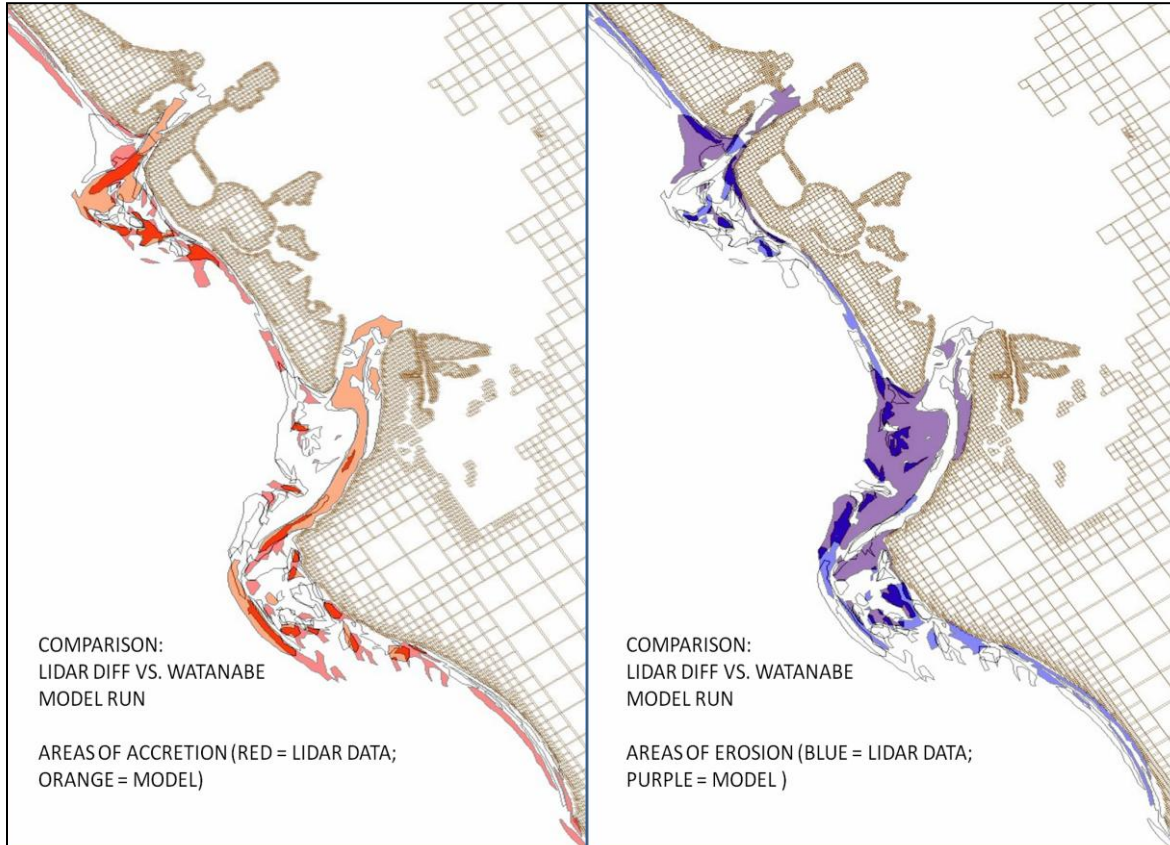


Figure 57: Comparison of Measured 2004 Bathymetry with Calculated 2004 Bathymetry for planform region of Accretion and Erosion

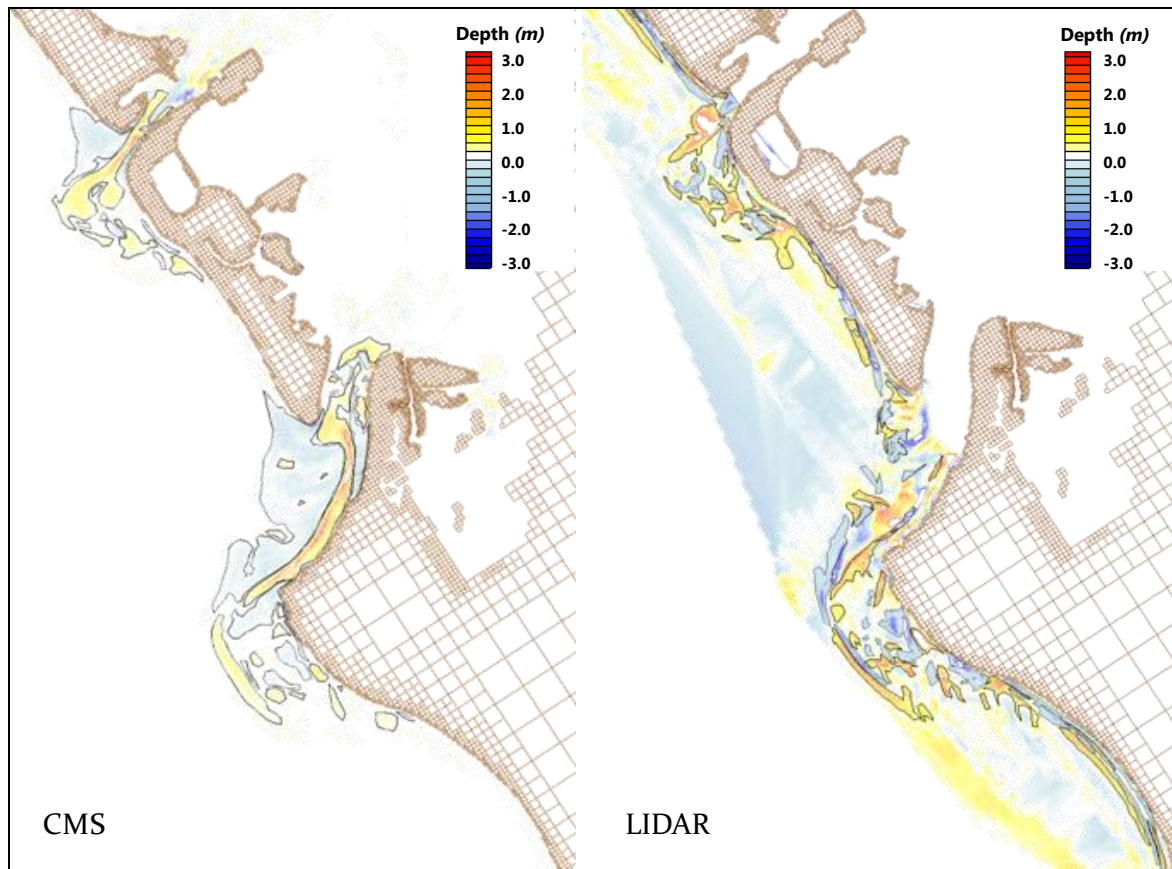


Figure 58: Modeled (left) and Measured (right) Morphologic Change Big Sarasota Pass and New Pass, 2004

4. ALTERNATIVE SELECTION

4.1. Inlet Dredging Alternatives

For this study, SAJ used the inlet dredging alternatives outlined in the Sarasota County Comprehensive Inlet Management Program Big Pass and New Pass Management Alternatives, (2008) authored by Coastal Technology Corp., University of South Florida, Coastal Engineering Consultants, Inc. with input from the USACE Jacksonville District, (Figure 59) to determine the most appropriate ebb shoal mining design for sediment for the Lido Key Shore Protection Plan. Alternatives were either analyzed further or were removed from consideration for the project based upon three criteria:

- 1) Significant morphologic change of ebb shoal features, which could indicate degraded function of the inlet complex**
- 2) Increased wave energy at the shoreline**
- 3) Increased shoaling of the main channel**

For each alternative, morphologic change was compared to known change for the 2004 “no mining” condition.

Preliminary screening analysis answered the question: Had BSP been mined for sediment in 2004, and Hurricanes Charley, Frances, Ivan and Jeanne made close passages the region, what would have been the morphologic change, wave energy and shoaling of the navigation channel?

Ten alternatives were tested, B, C, D1, D2, D3, D3* and combinations D1-C-B, D2-C-B, D3*-C-B, D3**-B (Table 7). The 2004 existing and 2004 mined condition for each alternative were modeled over the same time period with the same waves containing the extreme wave events of 2004 so that ending morphologic states could be compared. Table 8 describes the bathymetric datasets and the wave datasets used.

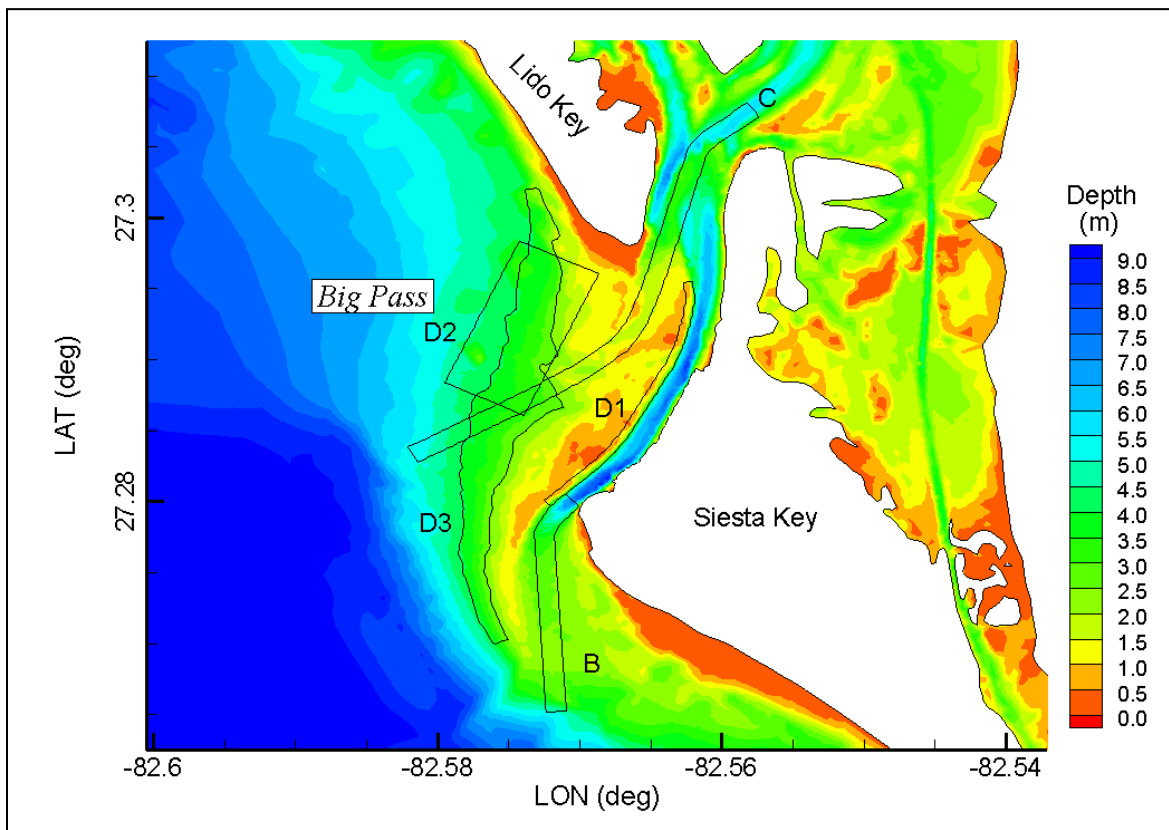


Figure 59: Alternatives developed from the Inlet Management Plan (2008)

Table 7: Description of Model Alternatives

<i>Alt</i>	<i>Description</i>	<i>Cut Depth (ft MLW)</i>
A	No Action / No Dredging	0
B	Existing Channel : Dredge Southwestern Portion	12
C	Ebb Shoal: Dredging of Ephemeral Flood Channel	12
D1	Ebb Shoal: Emergent Shoal	10
D2	Ebb Shoal: Rectangular Geometry	12
D3	Ebb Shoal: Contour Dredging	16
D3*	Ebb Shoal: Contour Dredging north of Alt C, only	12
D1-C-B	Emergent Shoal, Extension Existing Channel, Ephemeral Channel	10,12
D2-C-B	Rectangular Geom, Extension Existing Channel, Ephemeral Channel	12
D3*-C-B	Contour Dredging, Extension Existing Channel, Ephemeral Channel	12
D3**-B	Contour Dredging to 14', Extension Existing Channel	14,12

Table 8: Time periods for initial and end conditions of each model run

<i>Initial Condition Bathymetry/Topography (2004)</i>			<i>End Condition Bathymetry/Topography (2004)</i>		
2004 Existing	2004 Alternatives	WWIII Waves	2004 Existing	2004 Alternatives	WWIII Waves
Measured Ebb Shoal Bathymetry, 4 May 2004	Modified Ebb Shoal Bathymetry, 4 May 2004	4 May 2004	Calculated Ebb Shoal Bathymetry, 4 Nov 2004	Calculated Ebb Shoal Bathymetry, 4 Nov 2004	4 Nov 2004

Initial model runs used for the screening analysis examined changes in the dredging template within ebb shoal, only. No beach nourishment volumes have been placed in the model, which, as will be demonstrated later, mitigate for erosion of Lido Key.

4.2. Model Results and Alternative Selection

All model results are presented in Table 12 and details presented in Appendix A for comparison as well as decision criterion for keeping or rejecting the alternative. First, SAJ needed to calculate the volume that would be removed. This was done by differencing the non-dredged and dredged rasters. Column 2 of Table 12 indicates how many CY would be removed from the dredge cut for potential use by the Lido Key SPP. The volume required is 1.3 MCY. Column 3, the column titled, “Required Volume” indicates if the amount that maybe removed during dredging is greater than (YES) or less than (NO) 1.3 MCY. If the answer is NO, then the required volume does not exist. The last three columns of the table were based upon the three criteria:

- 1) Significant morphologic change of ebb shoal features which could indicate degraded function of the inlet complex**
- 2) Increased wave energy at the shoreline**
- 3) Increased shoaling of the main navigation channel**

None of the alternatives tested caused significant morphologic change in the ebb shoal. Run D3 did increase wave energy in the vicinity of Siesta Key, and Run D1 had the potential to infill the navigation channel. Alternatives D2, D1, C and B were removed from consideration as “Stand-Alone” alternatives because they did not yield the amount of sediment required for the project. Alternative D3 was removed from consideration as an alternative based upon the fact that this alternative increased wave energy off the coast of Siesta Key. Alternative D1-C-B was removed from consideration as there was risk to the navigation channel during construction.

The remaining alternatives, D3*-C-B, D2-C-B, and D3**-B were retained as viable alternatives for the Project.

Table 9: Alternative Run Summaries

<i>End Condition Bathymetry/Topography (November 2004)</i>					
Alternative	CY removed	Required Volume	Significant Morphologic Change	Increased Cumulative Wave Energy	Navigation Channel Infilling
D3	2.7 MCY	YES	NO	YES	NO
D2	680 KCY	NO	NO	NO	NO
D1	358 KCY	NO	NO	NO	NO
C	797 KCY	NO	NO	NO	NO
B	250 KCY	NO	NO	NO	NO
D3*-C-B (modified)	1.45 MCY	YES	NO	NO	NO
D2-B	1.7 MCY	YES	NO	NO	NO
D1-C-B	1.33 MCY	YES	NO	NO	POTENTIAL DURING CONSTRUCTION
D3**-B	1.38 MCY	YES	NO	NO	NO

4.3. Selected Alternative Plans D2-C-B, D3*-C-B, D3**-B

4.3.1. Alternative D2-C-B

Alternative D2-C-B would mine 1.7 million cubic yards from Big Sarasota Pass. The initial bathymetry is shown in Figure 60 showing the rectangular cut at the northeast portion of the shoal, the cut through the ephemeral channel that occasionally appears in the ebb shoal and the extension of the navigation channel through the south western part of the ebb shoal. Figure 61 shows the bathymetry and ebb shoal morphology at the end of the six month model run from May 4, 2004 to November 4, 2004. Examination of the ending morphology shows that for the “No Action” case (Figure 61, left) as previously described in Section 3.4, the general deflation of the updrift shoal as the main channel infills with sediment that had originated on the shoal. There is erosion of the most northerly flood

marginal channel at the southern tip of Lido Key and increased definition (erosion) of the flood marginal channels across the updrift shoal.

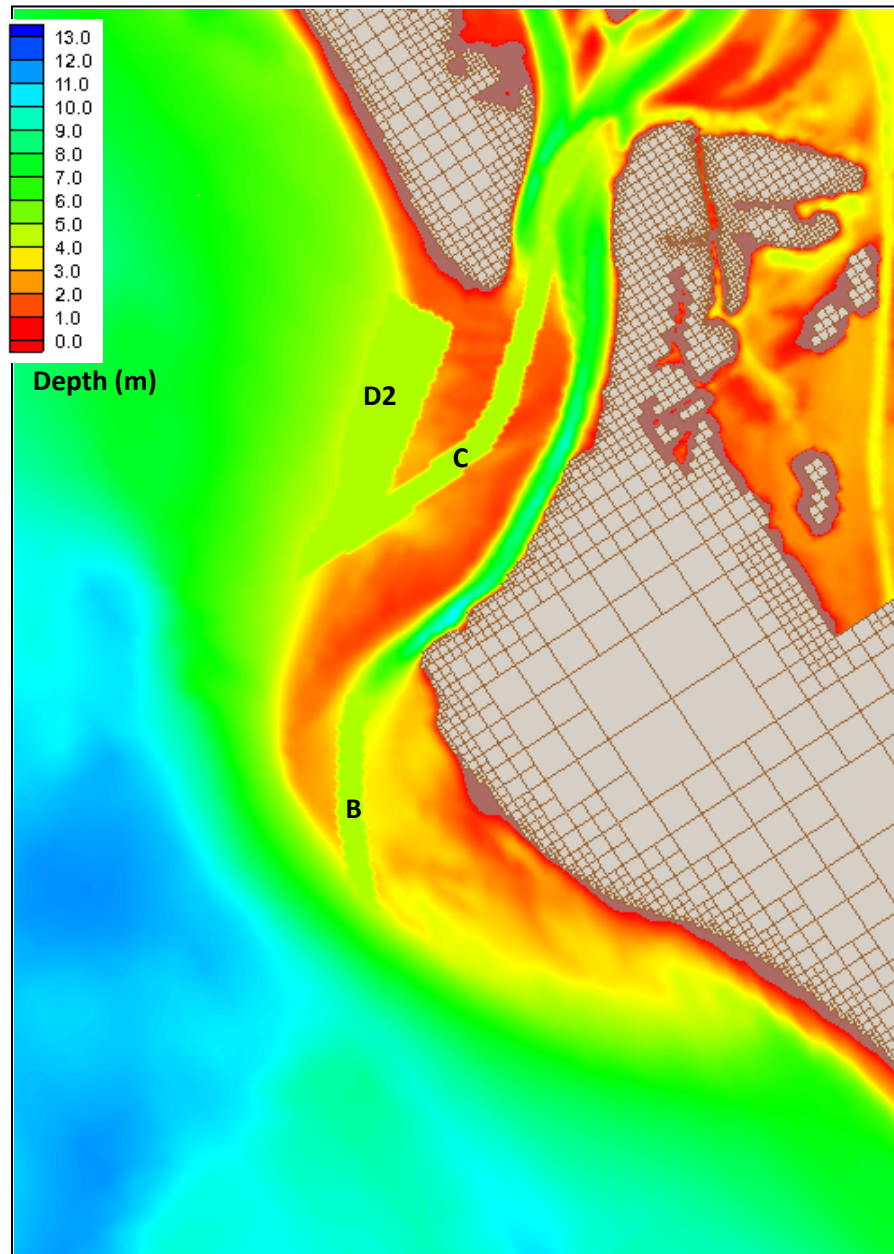


Figure 60: Alternative D2-C-B initial condition

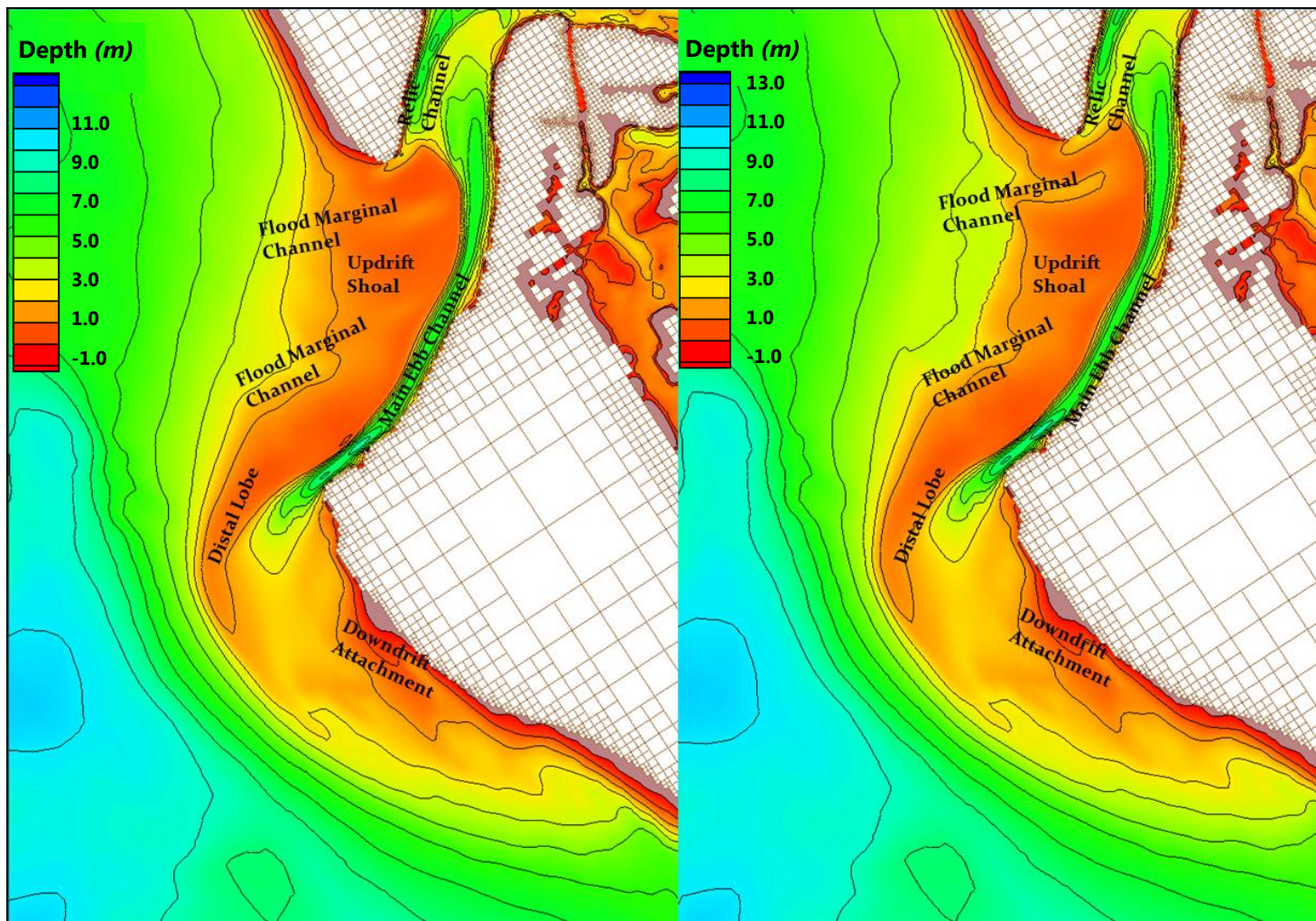


Figure 61: “No Action” Alternative (left), Alternative D2-C-B (right) end state November 2004

Examination of the ending morphology for Alternative D2-C-B (Figure 61, right) shows the infilling of Cut C, which is the cut through the ephemeral channel in the ebb shoal. It also shows the relative stability of Cut B at the terminus of the navigation channel. The downdrift attachment point at Siesta Key is unchanged. The greatest difference between the two cases is at the location of cut D2. There is some infilling at its most northeasterly corner, but less than 4% of the total volume removed.

Figure 62 and Figure 63 show differences both vertically and temporally between the “No Action” Alternative and Alternative D2-C-B, directly. In Figure 62, the most significant changes spatially between both alternatives are the dredge sites themselves. The residual depression in bathymetry at cuts D2, C and B can be readily seen which are approximately 1 ft to 12 ft deeper than the “No Action” Alternative. There is slight erosion present at the southeastern portion of Lido Key and slight accretion on the most northwestern portion of Siesta Key. In Figure 63, the temporal change from May to November 4, 2004 can be seen for Alternative D2-C-B. Here infilling in Cut C and in the navigation channel are readily observed. Infilling of the navigation channel occurs in the “No Action” Alternative (Figure 56), therefore there is no difference in bathymetry at the location of the navigation channel when comparing the “No Action” Alternative with Alternative D2-C-B (Figure 62). The volume of sediment in the Ebb Shoal of Big Sarasota Pass and northwesterly wave attack causes the infilling and southeasterly migration of the navigation channel. The project may offer some relief from this behavior and will be discussed in the Discussion Section.

Also calculated from the model results was the normalized cumulative wave energy throughout the model grid Figure 64. To understand this figure, one must imagine standing on the shoreline, or being anchored at one location in a vessel for the entire six-month model run. At the conclusion of the model run, depending on the observer’s location, the question, “How much more wave energy did this location receive given that the project has been built relative to the wave energy that this location would receive without the project?” can be answered. For example, if the observer is at the most northwest point of Siesta Key, that answer would be approximately 1.1 times more energy, or 10% more wave energy. If the observer is anchored on the northwest portion of the ebb shoal, the answer would be approximately 1.6 times more energy, or 60% more wave energy. This result is due to the fact that cut D2 allows more wave energy to the northwestern portion of the shoal, directly to the east of the cut. The increased depth of cut D2 decreases friction at that location, which in turn does not allow for wave attenuation as waves traverse the mining site.

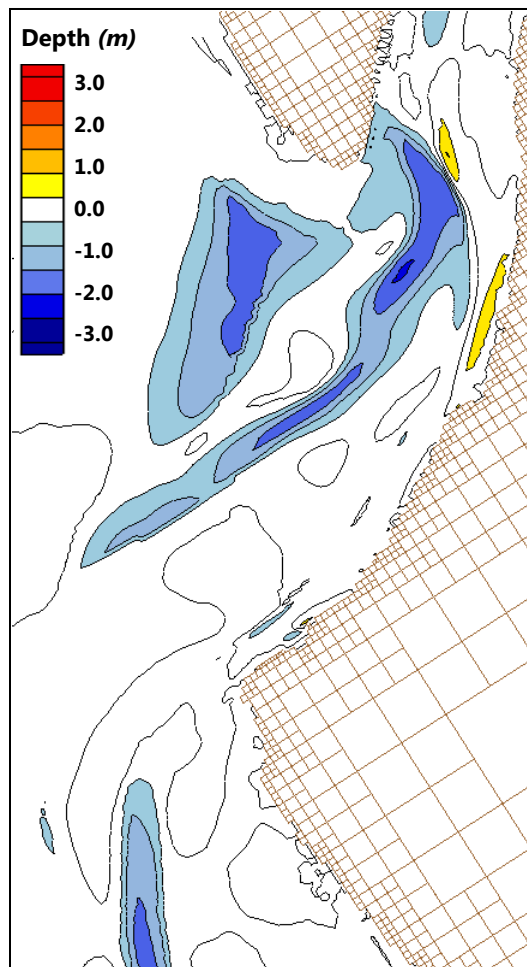


Figure 62: Spatial difference in bathymetry between “No Action” Alternative and Alternative D2-C-B end state November 2004

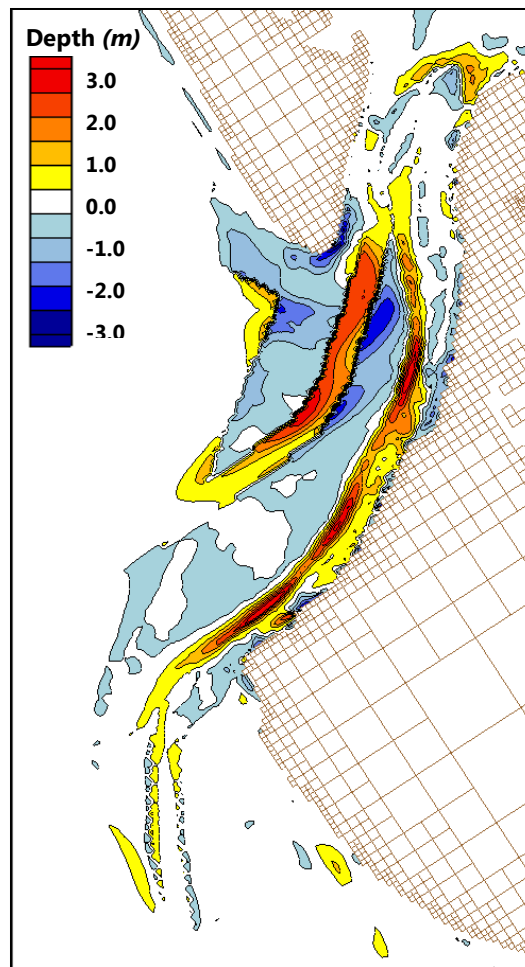


Figure 63: Temporal evolution of the Ebb Shoal; May 2004 - November 2004 Alternative D2-C-B

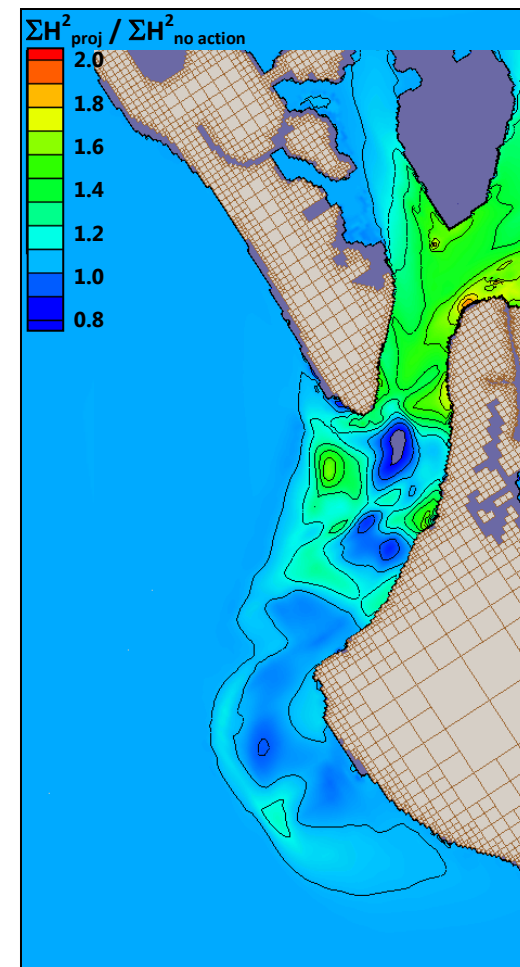


Figure 64: Cumulative Wave Energy May 2004 - November 2004 Alternative D2-C-B/No Action

4.3.2. Alternative D3*-C-B

Alternative D3*-C-B (Alt D3 was modified to 12 ft depth MLW and extends no further south than channel C) would mine 1.45 million cubic yards from Big Sarasota Pass. The initial bathymetry in Figure 65 shows the contour cut at the northeast portion of the shoal, the cut through the ephemeral channel that occasionally appears in the ebb shoal and the extension of the navigation channel through the southwestern part of the ebb shoal. Figure 66 shows the bathymetry and ebb shoal morphology at the end of the six month model run from May 4, 2004 to November 4, 2004. Examination of the ending morphology shows that for the “No Action” case (Figure 66, left) as previously described in Section 3.4, the updrift shoal generally deflates as the main channel infills with sediment that had originated on the shoal. There is erosion of the most northerly flood marginal channel at the southern tip of Lido Key and increased definition (erosion) of the flood marginal channels across the updrift shoal.

It also shows the relative stability of Cut B at the terminus of the navigation channel. The downdrift attachment point at Siesta Key is unchanged. The greatest difference between the two cases is at the location of cut D3*.

Figure 67 and above Figure 68 show differences both vertically and temporally between the “No Action” Alternative and alternative D3*-C-B, directly. In Figure 67, the most significant changes spatially between both alternatives are the dredge sites themselves. The residual depression in bathymetry at cuts D3*, C and B can be readily seen which are approximately 1 ft to 12 ft deeper than the “No Action” Alternative. There is slight erosion present at the southeastern portion of Lido Key and slight accretion on the most northwestern portion of Siesta Key. In Figure 68, the temporal change from May to November 4, 2004 can be seen for Alternative D3*-C-B. Here infilling in Cut C and in the navigation channel are readily observed. Again, it is important to recall that infilling of the navigation channel occurs in the “No Action” Alternative as seen in Figure 56. Here, as demonstrated by Figure 67, there is no difference in bathymetry at the location of the navigation channel when comparing the “No Action” Alternative with alternative D2-C-B. The volume of sediment in the Ebb Shoal of Big Sarasota Pass and northwesterly wave attack causes the infilling and southeasterly migration of the navigation channel. The project may offer some relief from this behavior and will be discussed in Discussion Section.

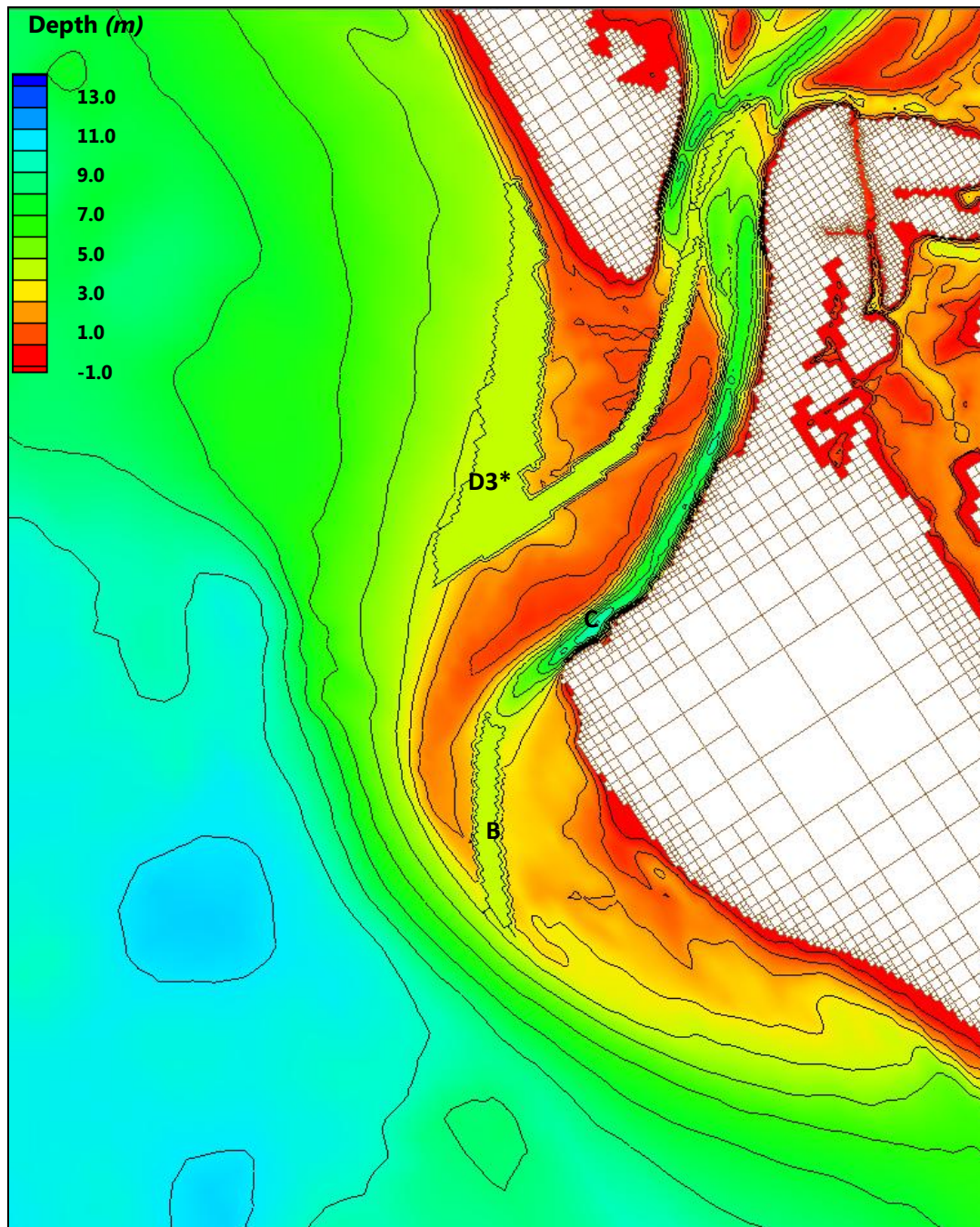


Figure 65: Alternative D3*-C-B initial condition

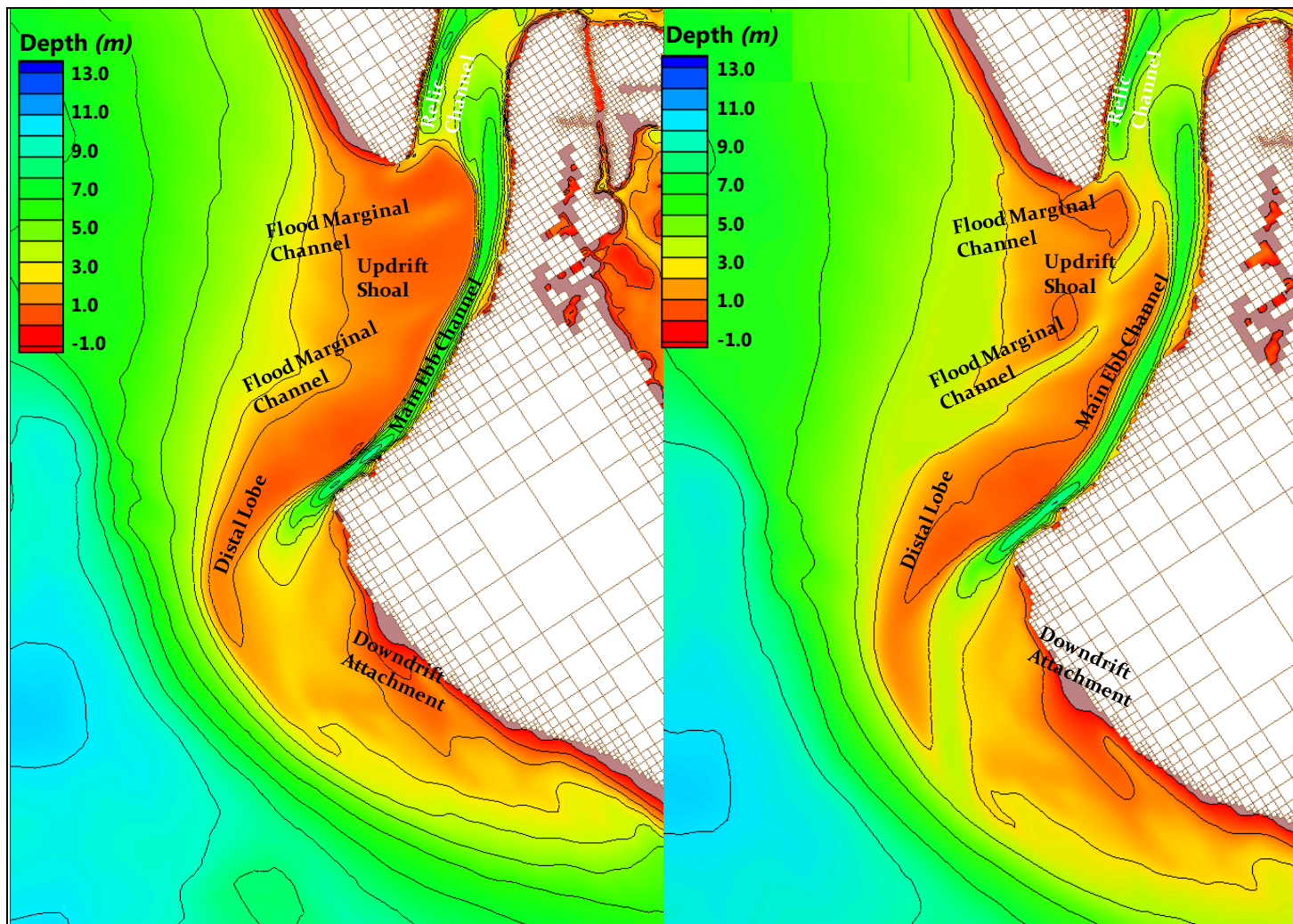


Figure 66: “No Action” Alternative (left), Alternative D3*-C-B (right) end state November 2004

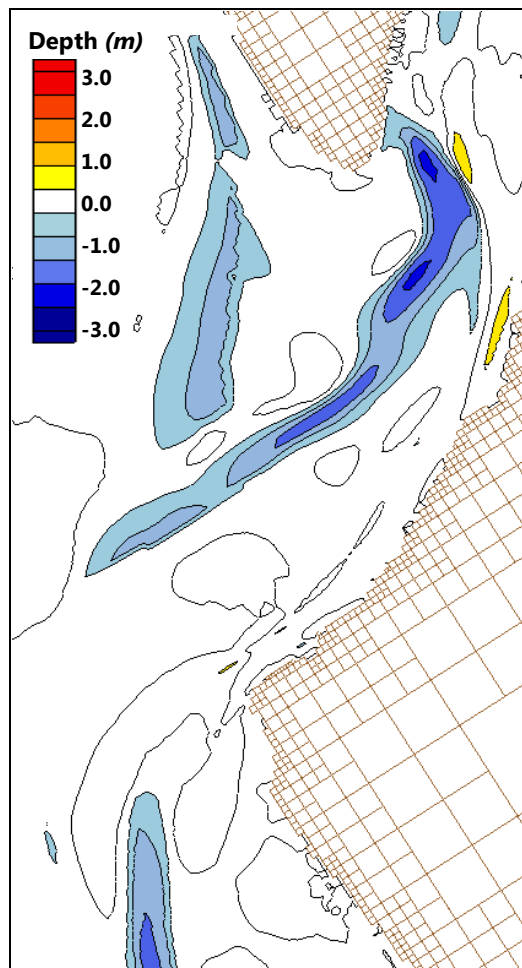


Figure 67: Spatial difference in bathymetry between “No Action” Alternative and Alternative D3*-C-B end state November 2004

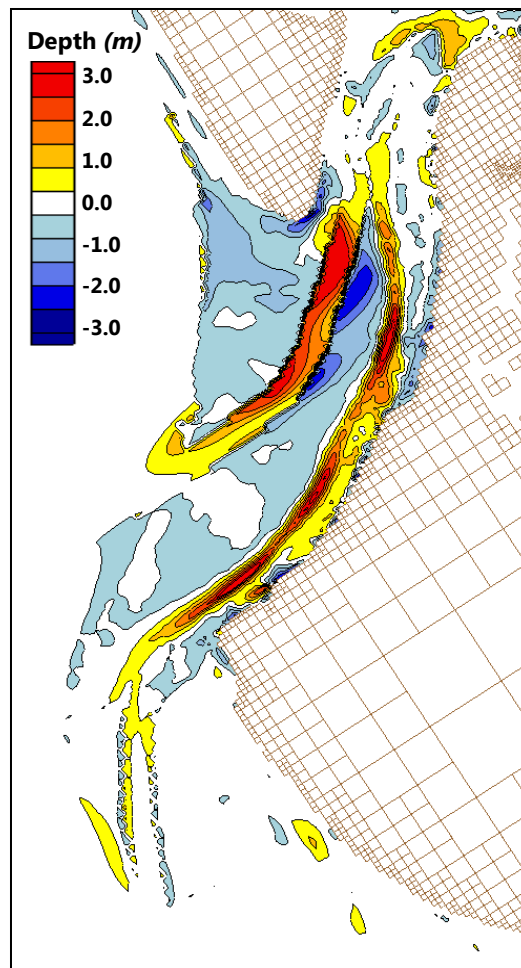


Figure 68: Temporal evolution of the Ebb Shoal; May 2004 - November 2004 Alternative D3*-C-B

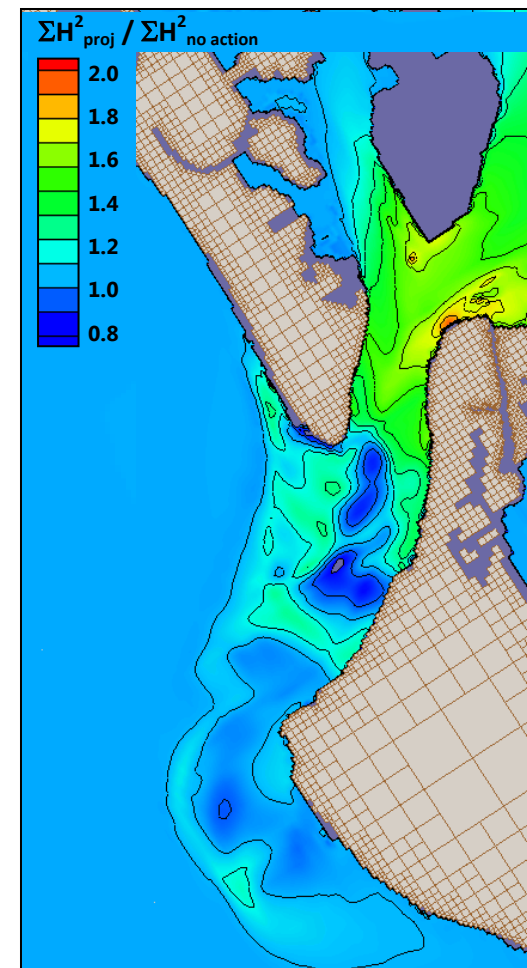


Figure 69: Cumulative Wave Energy May 2004 - November 2004 Alternative D3*-C-B/No Action

Also calculated from the model results was the normalized cumulative wave energy throughout the model grid Figure 69. For this case, if the observer is at the most northwest point of Siesta Key, that answer would be less than 1.1 times more energy, or < 10% more wave energy. If the observer is anchored on the northwest portion of the ebb shoal, the answer would be approximately 1.5 times more energy, or 50% more wave energy. This result is due to the fact that cut D3* allows more wave energy to the northwestern portion of the shoal, directly to the east of the cut.

4.3.3. Alternative D3-B**

Alternative D3*-B (Alt D3 was modified to 14 ft depth MLW and extends no further south than channel C) would mine 1.38 million cubic yards from Big Sarasota Pass. The initial bathymetry is in Figure 70 showing the contour cut at the northeast portion of the shoal and the extension of the navigation channel through the south western part of the ebb shoal. Figure 71 shows the bathymetry and ebb shoal morphology at the end of the six month model run from May 4, 2004 to November 4, 2004. Examination of the ending morphology shows that for the “No Action” case (Figure 71, left) as previously described in Section 3.4, the updrift shoal generally deflates as the main channel infills with sediment that had originated on the shoal. There is erosion of the most northerly flood marginal channel at the southern tip of Lido Key and increased definition (erosion) of the flood marginal channels across the updrift shoal.

Examination of the ending morphology for Alternative D3**-B (Figure 71, right) shows the relative stability of Cut B at the terminus of the navigation channel. The downdrift attachment point at Siesta Key is unchanged. The greatest difference between the two cases is at the location of cut D3**.

Figure 72 and above Figure 73 show differences both spatially and temporally between the “No Action” Alternative and Alternative D3**-B, directly. In Figure 72, the most significant changes vertically between both alternatives are the dredge sites themselves. The residual depression in bathymetry at cuts D3** and B can be readily seen which are approximately 1 ft to 14 ft deeper than the “No Action” Alternative. There is slight erosion present at the southeastern portion of Lido Key and slight accretion on the most northwestern portion of Siesta Key. In Figure 73, the temporal change from May to November 4, 2004 can be seen for Alternative D3**-B. Here infilling in the navigation channel is readily observed. Again, it is important to recall that infilling of the navigation channel occurs in the “No Action” Alternative as seen in Figure 56. There is no appreciable increase in wave energy due to the project (Figure 74). Here, as demonstrated by Figure 72, the difference in bathymetry at the location of the navigation channel

between the “No Action” Alternative and Alternative D3**-B is not significant and is less than 3 ft.

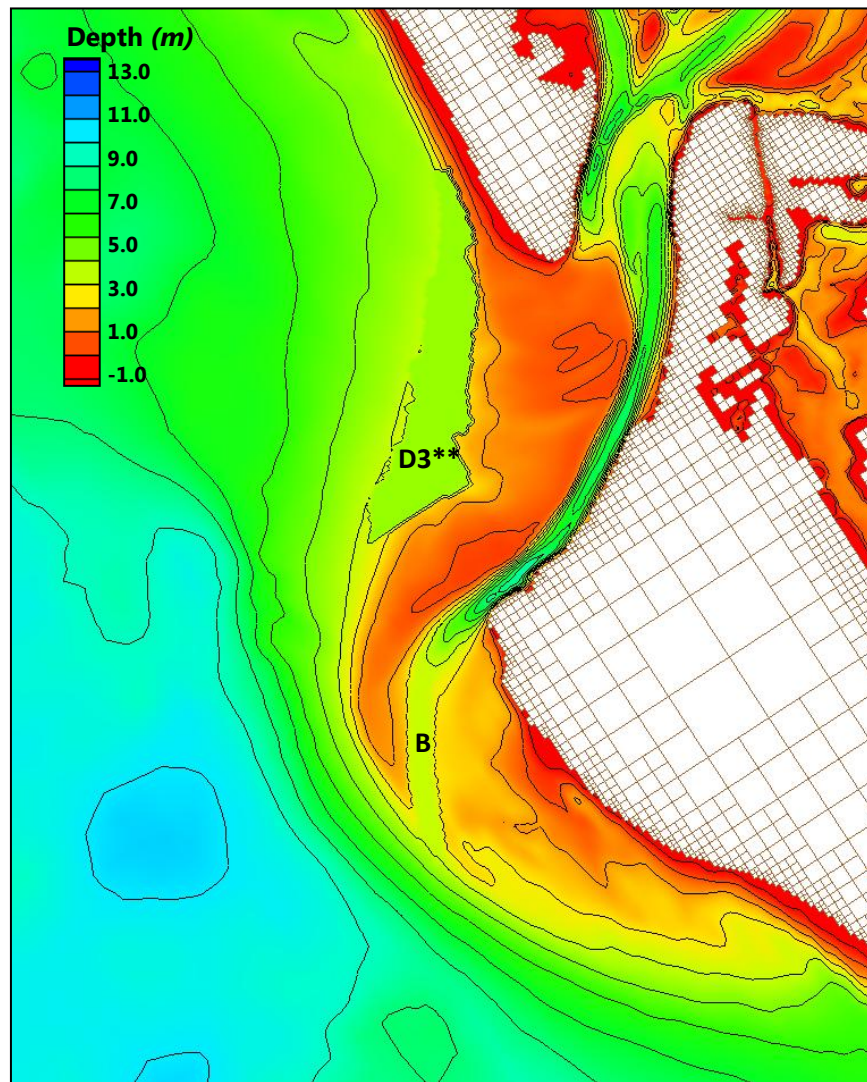


Figure 70: Alternative D3-B initial condition**

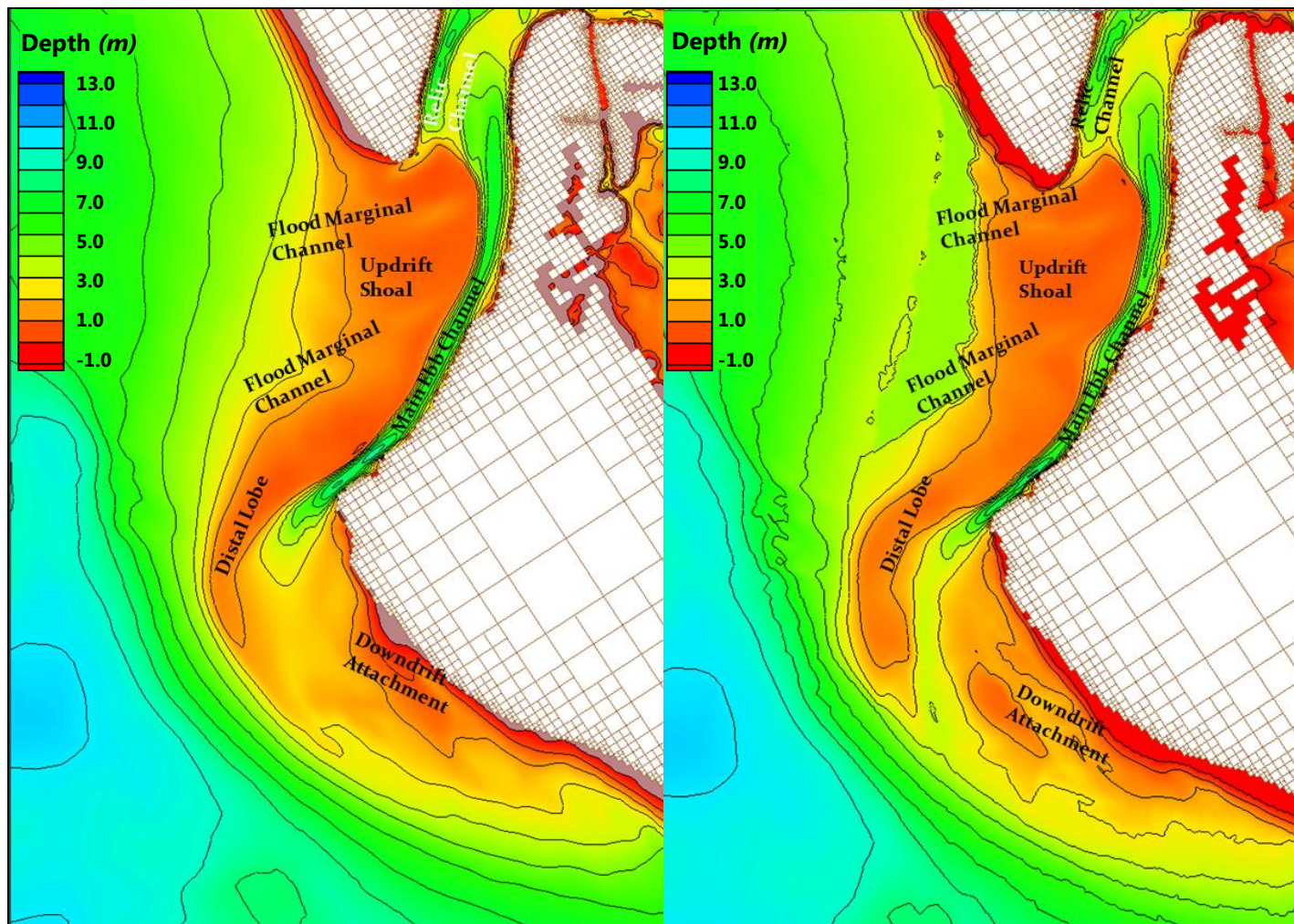


Figure 71: “No Action” Alternative (left), Alternative D3**-B (right) end state November 2004

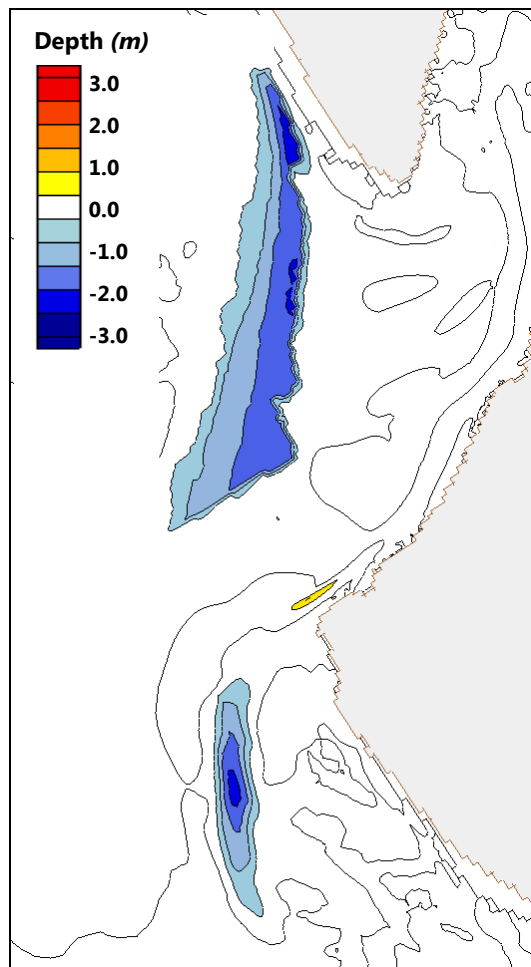


Figure 72: Spatial difference in bathymetry between "No Action" Alternative and Alternative D3-B end state November 2004**

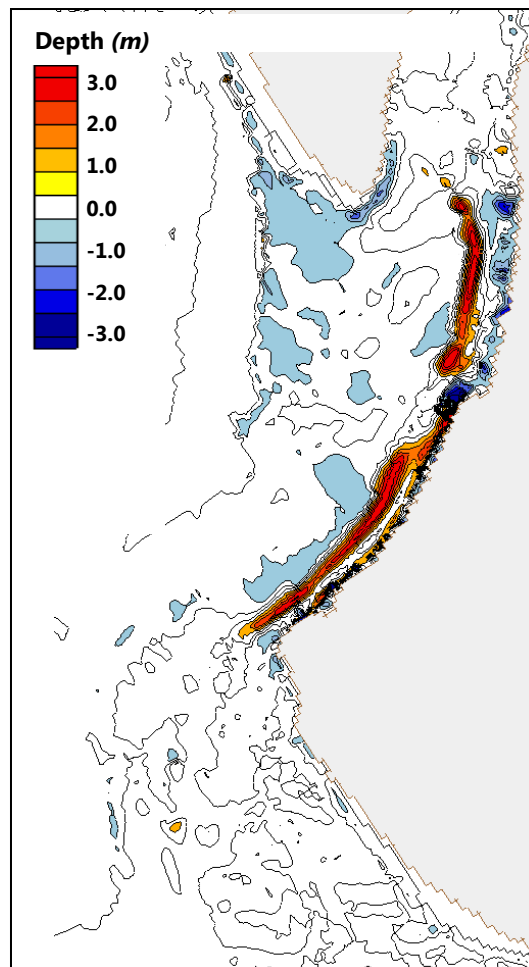


Figure 73: Temporal evolution of the Ebb Shoal; May 2004 - November 2004 Alternative D3-B**

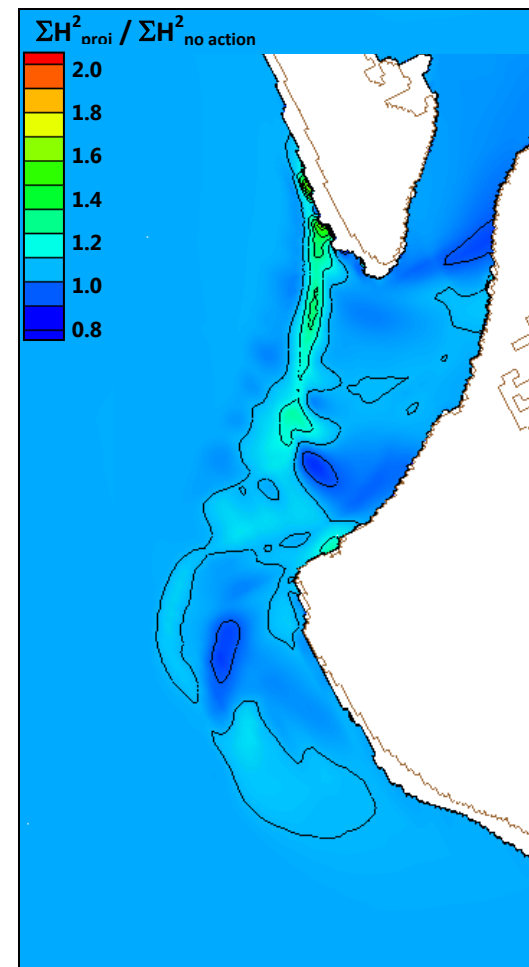


Figure 74: Cumulative Wave Energy May 2004 - November 2004 Alternative D3-B/No Action**

4.4. Sediment Transport Pathways and Sediment Fluxes

Sediment pathways are examined here to compare transport pathways among the “No Action” Alternative, Alternative D2-C-B, Alternative D3*-C-B, and Alternative D3***-B. Four typical cases were compared. First, sediment transport (sediment concentration and transport vectors) was examined under southerly storm waves and a flooding current (Figure 75, Figure 76, Figure 77, Figure 78). Second, sediment transport was examined under southerly storm waves and an ebbing current (Figure 79, Figure 80, Figure 81, Figure 82). Transport was also examined under northwesterly storm waves and flooding current (Figure 83, Figure 84, Figure 85, Figure 86) and ebbing current (Figure 87, Figure 88, Figure 89, Figure 90), respectively. Both ebbing and flooding conditions are illustrated in order to show the very different sediment transport pathways under the ambient tidal conditions. The color intensity in each image illustrates the quantity of sediment suspended in the water column. The black vectors in each figure illustrate the direction of transport. Color is not directly related to pathway location, only to areas of increased sediment concentration in the water column. It was observed in Figure 75 - Figure 90 that Alternatives D2-C-B, D3*-C-B and D3***-B had no appreciable differences in sediment transport pathways from the “No Action” Alternative as detailed by both similar (if not exactly the same) sediment concentrations and transport vectors among the cases examined. The biggest difference in transport magnitude is in the vicinity of Cut C for templates D2-C-B and D3*-C-B, however due to the ephemeral channels that exist in this region throughout the history of observations of the ebb shoal (Wang and Beck, 2007) it would be expected that mining the ebb shoal for either of those two templates would not obstruct the function of the ebb shoal to bypass sediments.

Transport over the northern lobe, or updrift platform, of the ebb shoal is active under ebbing and flooding conditions, as well as north and south directed waves. Wave direction does not have as great an effect on transport direction as do tidal currents over the north lobe. This is especially true under higher energy waves that tend to refract over the ebb shoal to very acute angles or shore normal (typically -30 to 30 degrees from shore normal). However, there is a distinct difference in transport direction under ebb versus flood currents. The CMS reproduces wave-wave and wave-current interactions, and Figure 75 through Figure 90 which clearly illustrate a shift in transport direction from updrift and offshore during ebbing conditions, to landward and inlet-directed transport during flooding conditions. As the ebb jet exits through the main ebb channel and over the updrift part of the shoal, the tidal current laden with sediment induces a force on the wave-generated currents that would normally be directed landward. This redirected transport tends to orient east-west, facilitating sediment to be transported to the outer shield of the ebb shoal. Under each condition given in the figures below, transport over the updrift platform is very similar in aerial extent and magnitude with the exception of Cut C as described

previously. Most of the ebb-directed flow in the ebb jet moves transport toward the location of Cuts D2 and D3*, or in the case of the “No Action” Alternative, toward the offshore outer lobe of the ebb shoal.

Under ebbing tidal currents, transport over the southern lobe, or downdrift platform, has very similar patterns and intensity within the navigation channel for all conditions (Figure 79 - Figure 82 and Figure 87 - Figure 90). There are great differences in transport over the southern ebb shoal lobe, or downdrift platform, under flooding currents (Figure 75 - Figure 78 and Figure 83 -Figure 86). Here, the wave-generated currents clearly dominate transport direction. Under southerly waves, for the flood tide, transport is to the northeast over the southern lobe and along the shoreline of Siesta Key (Figure 75 - Figure 78), however, under northerly waves, the transport direction over the southern lobe is toward the southeast, essentially against tidally driven flood currents both over the south lobe and along the shoreline of Siesta Key (Figure 83 - Figure 86). Despite Cut B in the region, there are no appreciable differences in sediment transport magnitude and direction in the vicinity of the southern lobe and along the shoreline of Siesta Key.

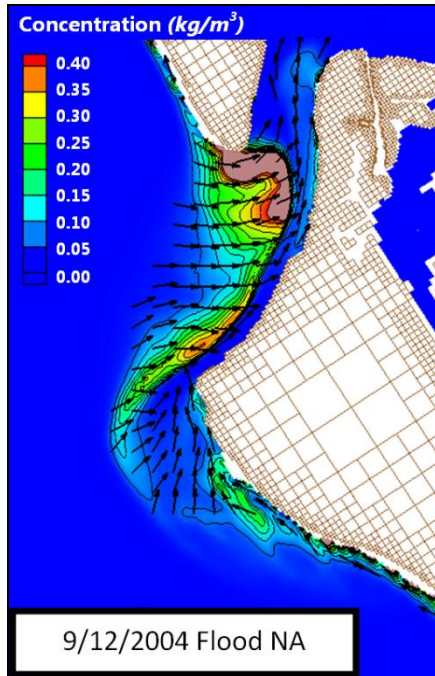


Figure 75: Sediment transport pathways for the 12 September 2004 3:00 am; No Action condition under southerly storm waves and a flooding current

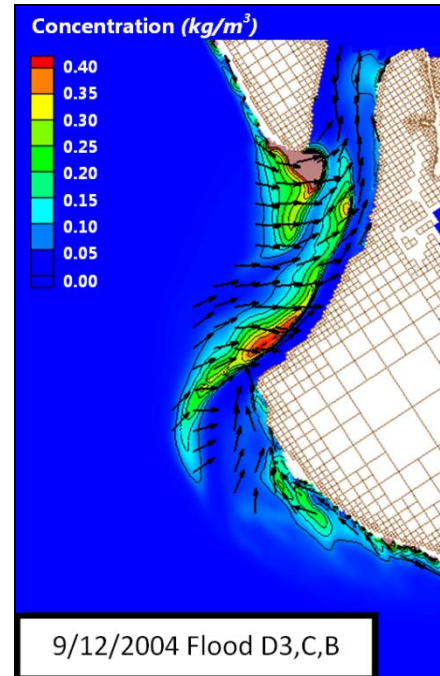


Figure 77: Sediment transport pathways for the 12 September 2004 3:00 am; Alternative D3*-C-B under southerly storm waves and a flooding current

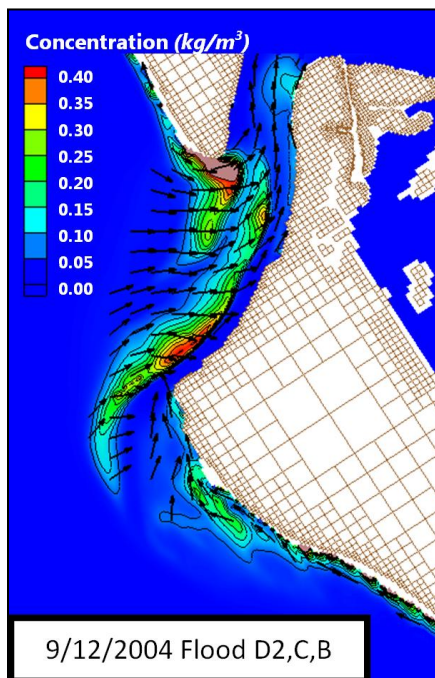


Figure 76: Sediment transport pathways for the 12 September 2004 3:00 am; Alternative D2-C-B under southerly storm waves and a flooding current

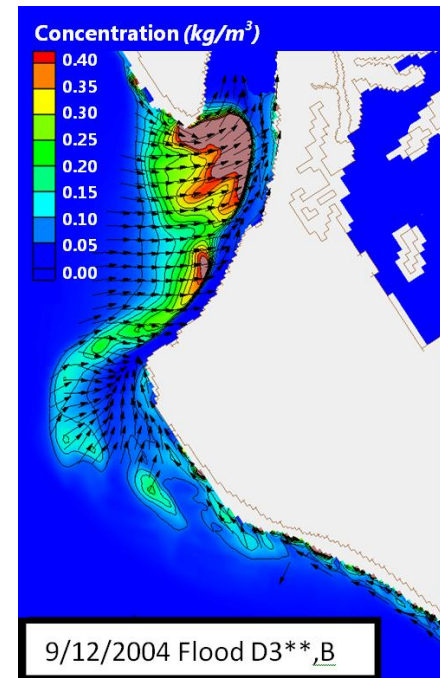


Figure 78: Sediment transport pathways for the 12 September 2004 3:00 am; Alternative D3**-B under southerly storm waves and a flooding current

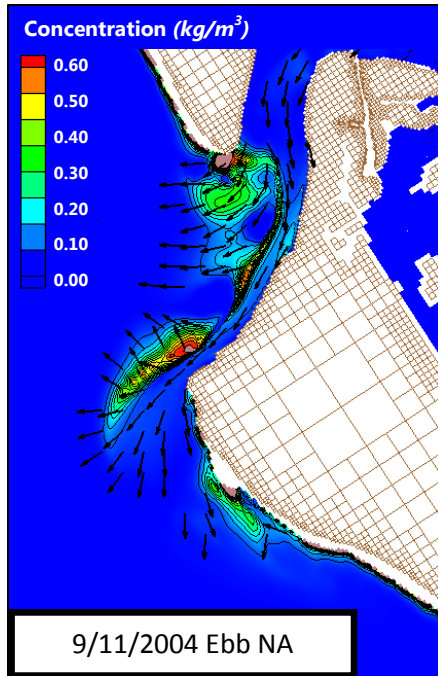


Figure 79: Sediment transport pathways for the 11 September 2004 9:00 pm; No Action condition under southerly storm waves and an ebbing current

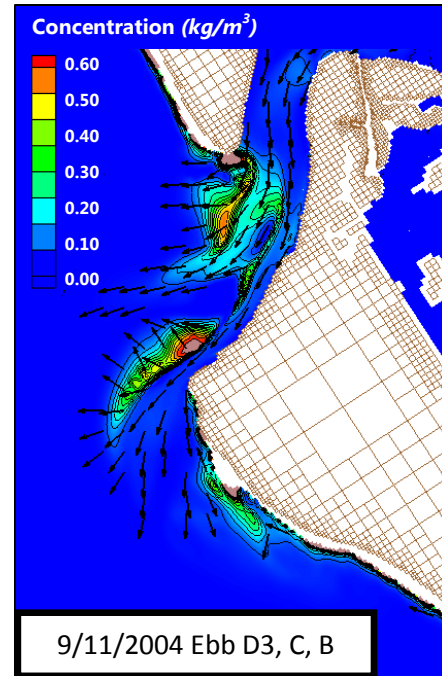


Figure 81: Sediment transport pathways for the 11 September 2004 9:00 pm; Alternative D3*-C-B under southerly storm waves and an ebbing current

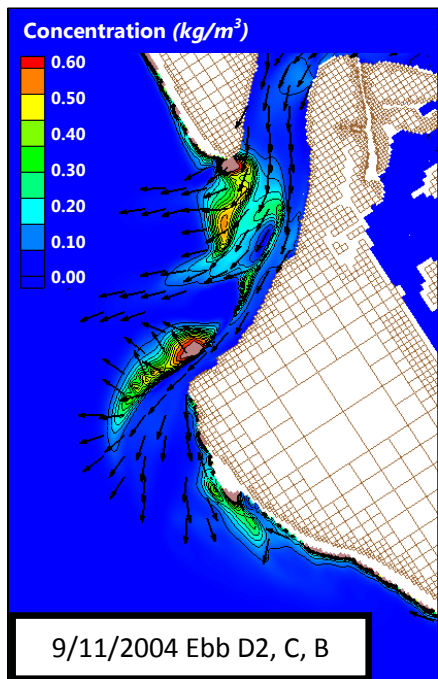


Figure 80: Sediment transport pathways for the 11 September 2004 9:00 pm; Alternative D2-C-B under southerly storm waves and an ebbing current

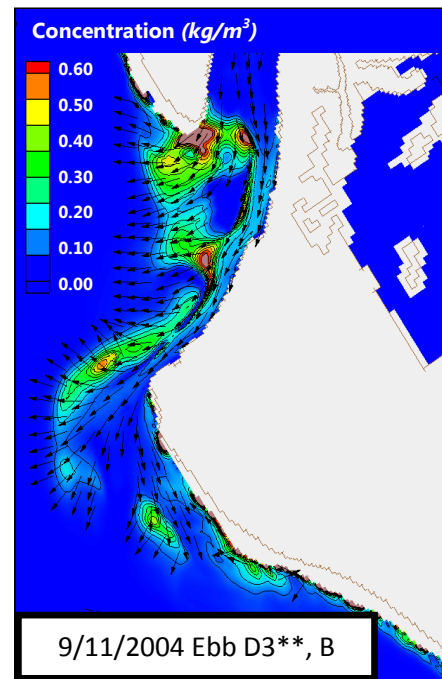


Figure 82: Sediment transport pathways for the 11 September 2004 9:00 pm; Alternative D3**-B under southerly storm waves and an ebbing current

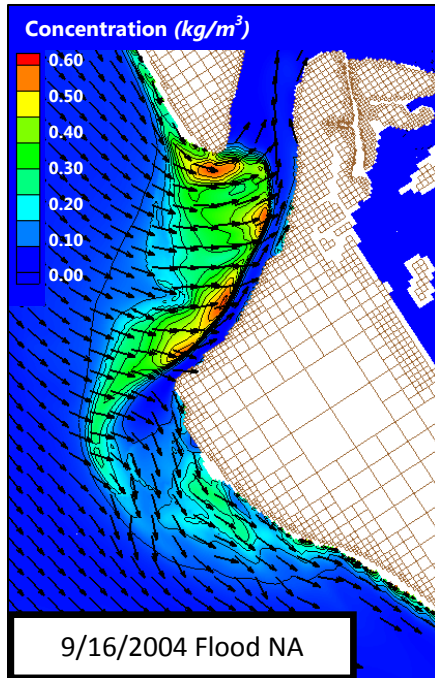


Figure 83: Sediment transport pathways for the 16 September 2004 4:30 pm; No Action condition under northwesterly storm waves and a flooding current

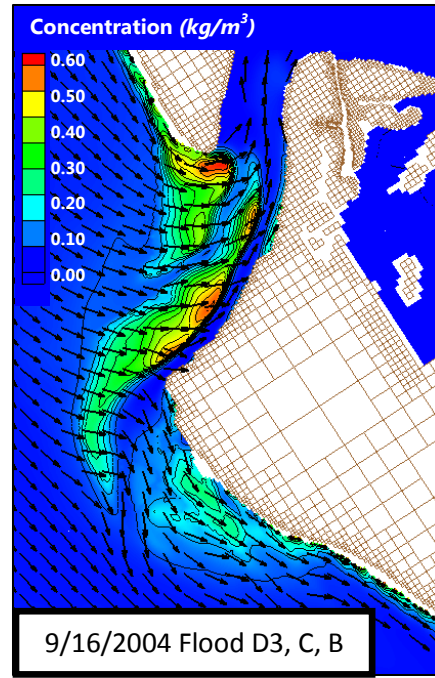


Figure 85: Sediment transport pathways for the 16 September 2004 4:30 pm; Alternative D3*-C-B under northwesterly storm waves and a flooding current

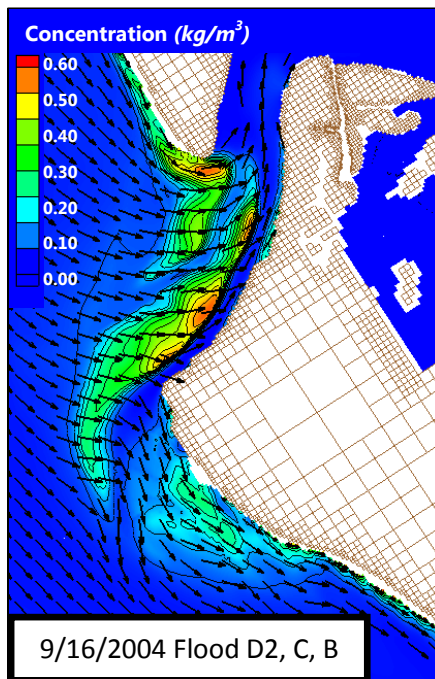


Figure 84: Sediment transport pathways for the 16 September 2004 4:30 pm; Alternative D2-C-B under northwesterly storm waves and a flooding current

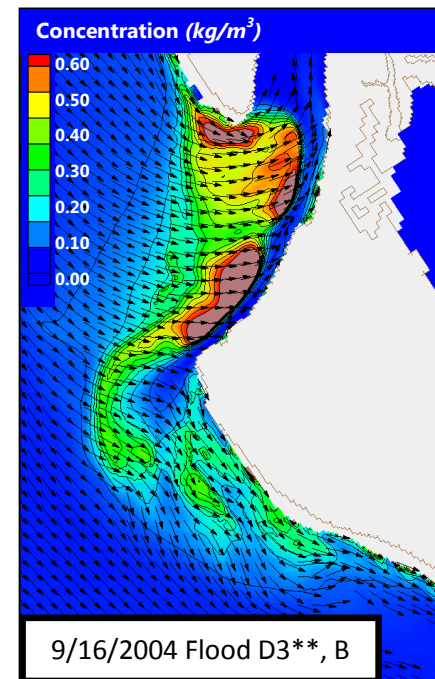


Figure 86: Sediment transport pathways for the 16 September 2004 4:30 pm; Alternative D3**-B under northwesterly storm waves and a flooding current

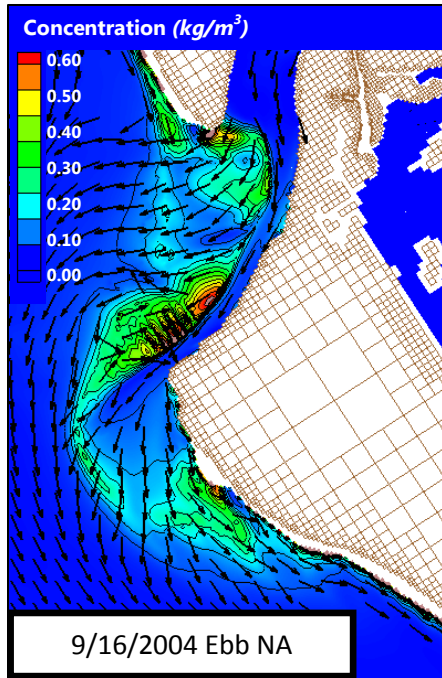


Figure 87: Sediment transport pathways for the 16 September 2004 11:30 pm; No Action condition under northwesterly storm waves and an ebbing current

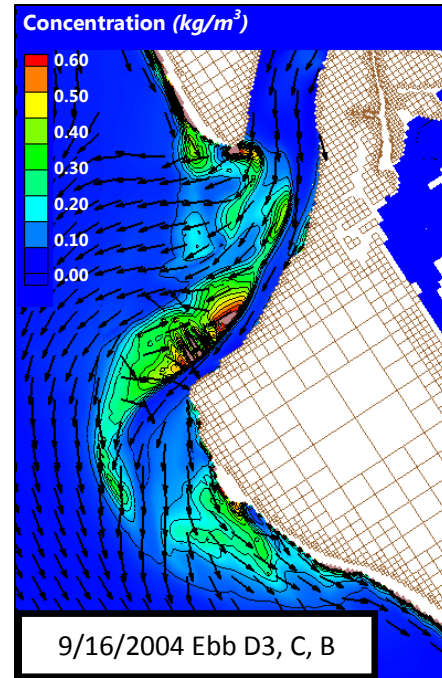


Figure 89: Sediment transport pathways for the 16 September 2004 11:30 pm; Alternative D3*-C-B under northwesterly storm waves and an ebbing current

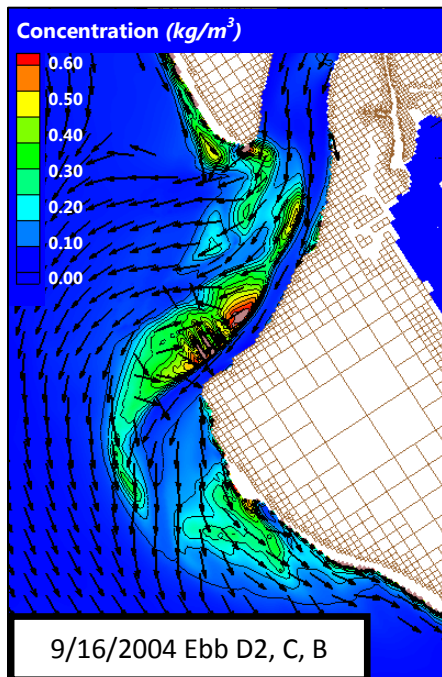


Figure 88: Sediment transport pathways for the 16 September 2004 11:30 pm; Alternative D2-C-B under northwesterly storm waves and an ebbing current

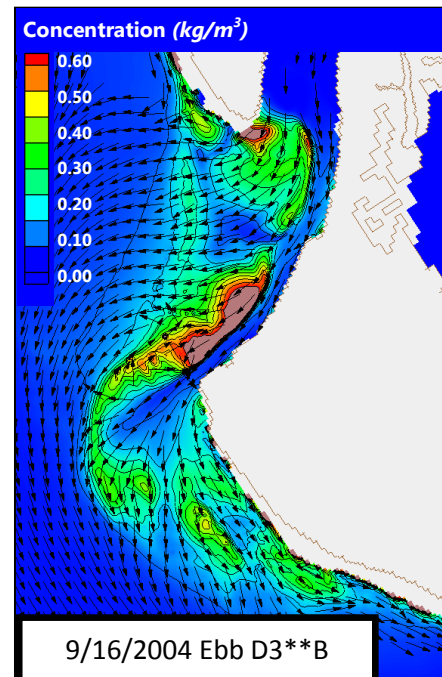


Figure 90: Sediment transport pathways for the 16 September 2004 11:30 pm; Alternative D3**-B under northwesterly storm waves and an ebbing current

These results were generalized into transport scenarios described in Figure 91, Figure 92, Figure 93, and Figure 94. Note that tidally-dominated transport is denoted by blue vectors and wave-dominated transport is denoted by brown vectors. The general pathways of current-induced sediment transport are essentially the same for all alternatives. The suspended sediment concentration is reduced in the vicinity of Cut C because the depth has increased, however this Cut does not affect the capacity for the ebb shoal to bypass sediment. For wave dominated pathways, transport is the same for all alternatives except for a reduction in sediment concentration for Cut B, at the terminus of the navigation channel.

Under southerly wave conditions (Figure 91, and Figure 92) the sediment transport pathways are as follows. During flood tide, sediments are transported by tidal currents to the east – northeast over the north (updrift) lobe, in the main ebb channel, in the flood marginal channel at the southern end of Lido Key, and through Cut C for Alternatives D2-C-B and D3*-C-B toward Sarasota Bay. Sediments are also transported by wave-dominated processes over the southern (downdrift) lobe toward the north at all phases of the tide. Under flooding currents, sediments are transported to the northeast over the outer shield and the southern lobe into the navigation channel and toward the northwest along Siesta Key. Under ebbing currents, sediments are transported to Cuts D2 and D3* as well as to the southern (downdrift) lobe by tidal currents and they are then rearranged by wave dominated forcing. Again, sediments are transported into the navigation channel and toward the northwest along Siesta Key. Sediments are also transported by wave-dominated forcing over the southern lobe, toward the northwest into Cuts D2 and D3*.

Under northerly wave conditions (Figure 93, and Figure 94) the sediment transport pathways are as follows. During flood tide, sediments are transported by tidal currents to the east – northeast over the north (updrift) lobe, in the main ebb channel, in the flood marginal channel at the southern end of Lido Key, and through Cut C for Alternatives D2-C-B and D3*-C-B toward Sarasota Bay. Sediments are also transported by wave-dominated processes over the southern (downdrift) lobe toward the southeast at all phases of the tide. Under flooding tidal currents, sediments are transported by wave-dominated forcing to the southeast over the outer shield and the southern lobe into the navigation channel and toward the north-west along Siesta Key. Under ebbing currents, sediments are transported to Cuts D2 and D3* as well as to the southern (downdrift) lobe by tidal currents and they are then rearranged by wave dominated forcing. Sediments are transported over the northern lobe into the most seaward portion of the navigation channel, where they are swept to the southern lobe and outer shield by ebbing tidal currents. Wave forcing continues to push sediment toward the outer-shield of the southern lobe and toward the southeast along Siesta Key.

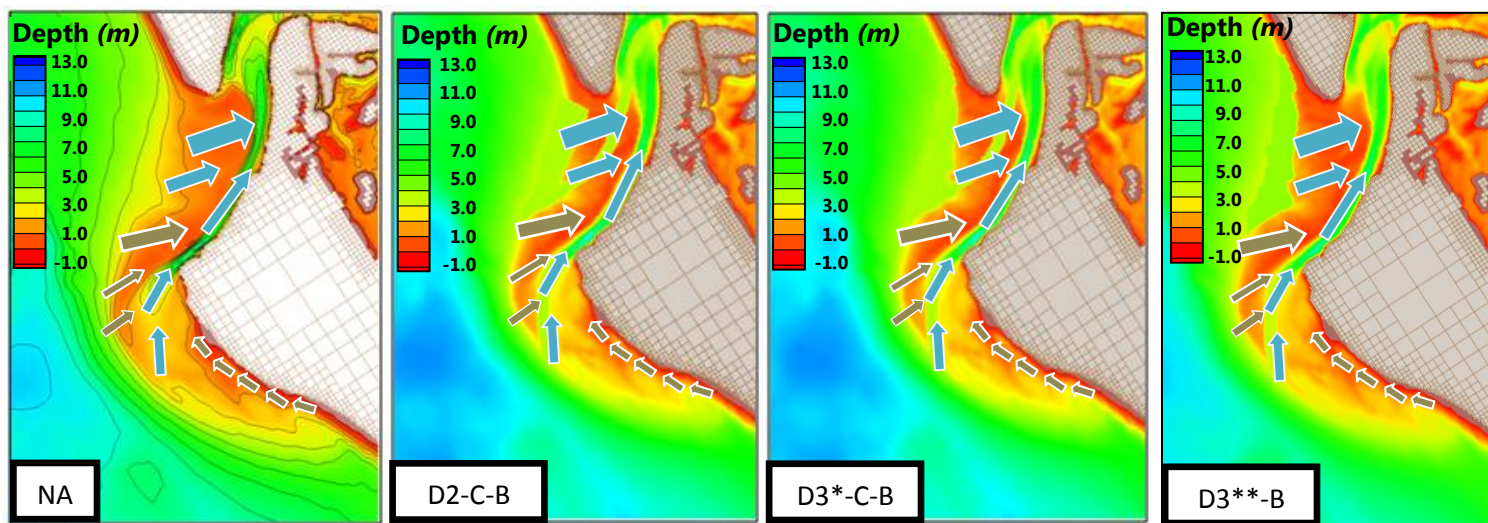


Figure 91: General Sediment Transport under FLOOD currents (BLUE) AND SOUTHERLY WAVES (BROWN).

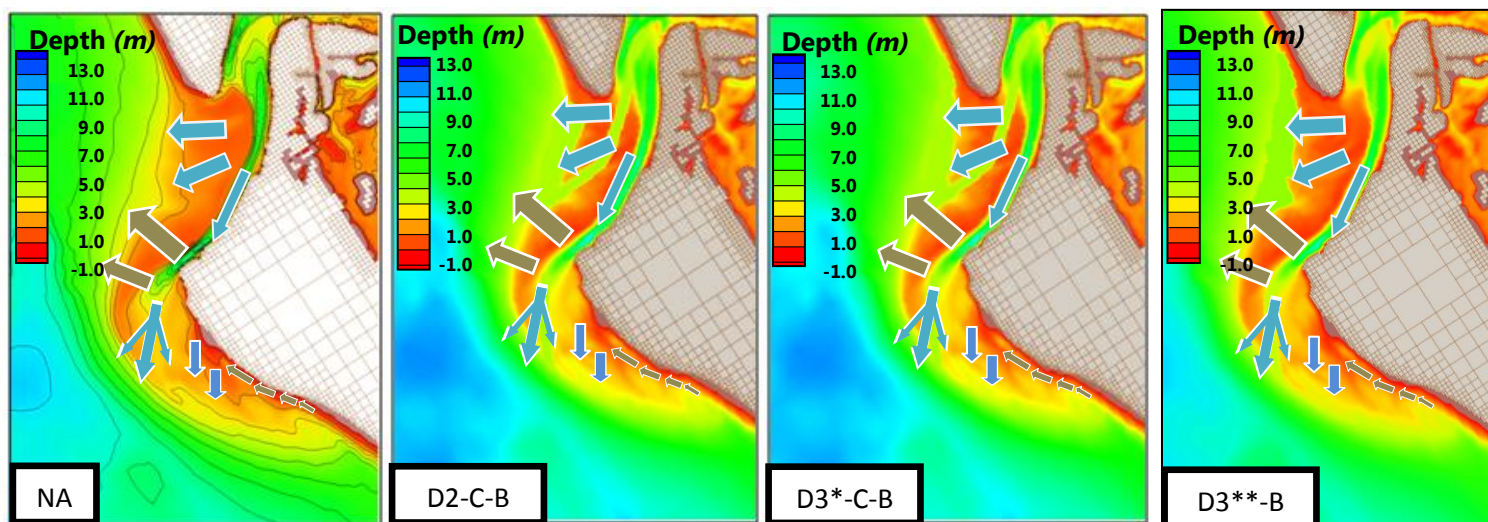


Figure 92: General Sediment Transport under EBB currents (BLUE) AND SOUTHERLY WAVES (BROWN).

In general, sediments are moved across the northern (updrift) lobe dominated by tidal currents. They move, through Cut C and through the ephemeral channels or through Cut B (under northerly waves, only), bringing sediments into the navigation channel on flood tide. On the ebb tide, sediments are moved seaward through the main ebb channel (navigation channel) and through Cut B by tidally driven currents out onto the southern (downdrift) lobe and to outer shield. On the southern lobe and along Siesta Key, sediment transport is dominated by wave forcing whereby sediments are worked upon and rearranged under this forcing. Under southerly waves, transport due to wave forcing is to the north under all phases of the tide. After sediments are moved onto the southern lobe by tidally-driven currents, they are moved by southerly wave action back into the navigation channel on the following flood tide, and they are moved offshore and into Cuts D2 and D3* over the next ebb tide. At all times, wave dominated forcing transports sediment to the northwest along Siesta Key, completely uninfluenced by tidal currents. Under northerly waves, sediments are always moved to the south-east over the south lobe and along the shoreline of Siesta Key, except for the most outer portion of the ebb shoal, when sediments are continued to be pushed onto the outer shield by northerly waves under an ebbing tide.

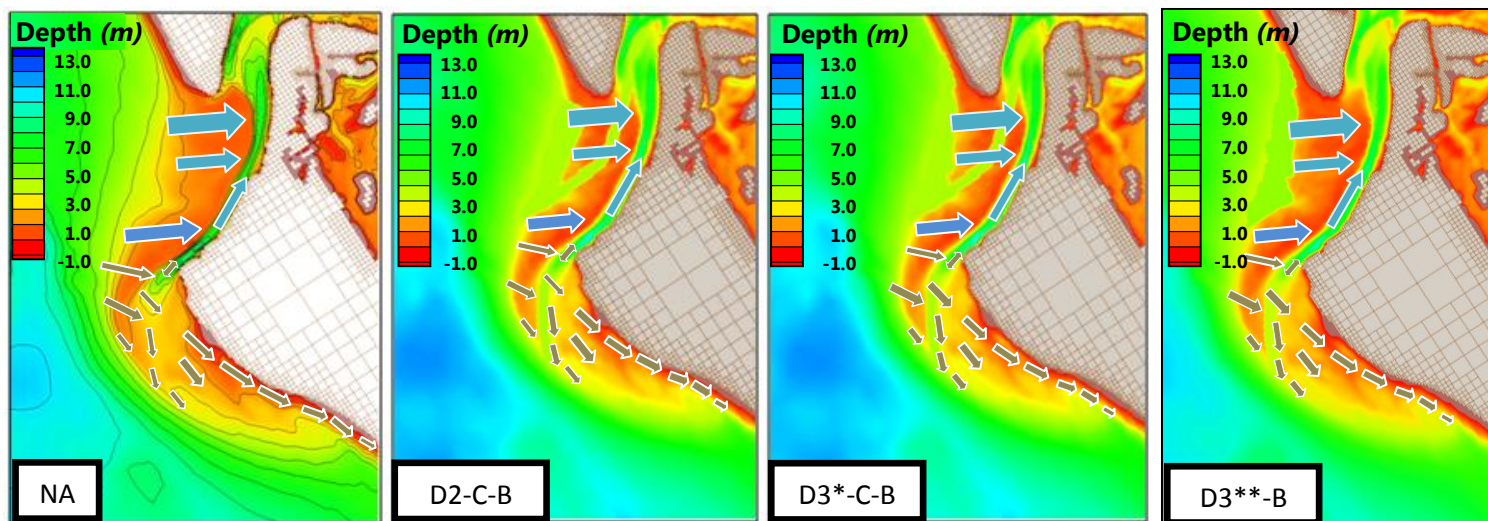


Figure 93: General Sediment Transport under FLOOD currents (BLUE arrows) AND NORTHWESTERLY WAVES (BROWN arrows).

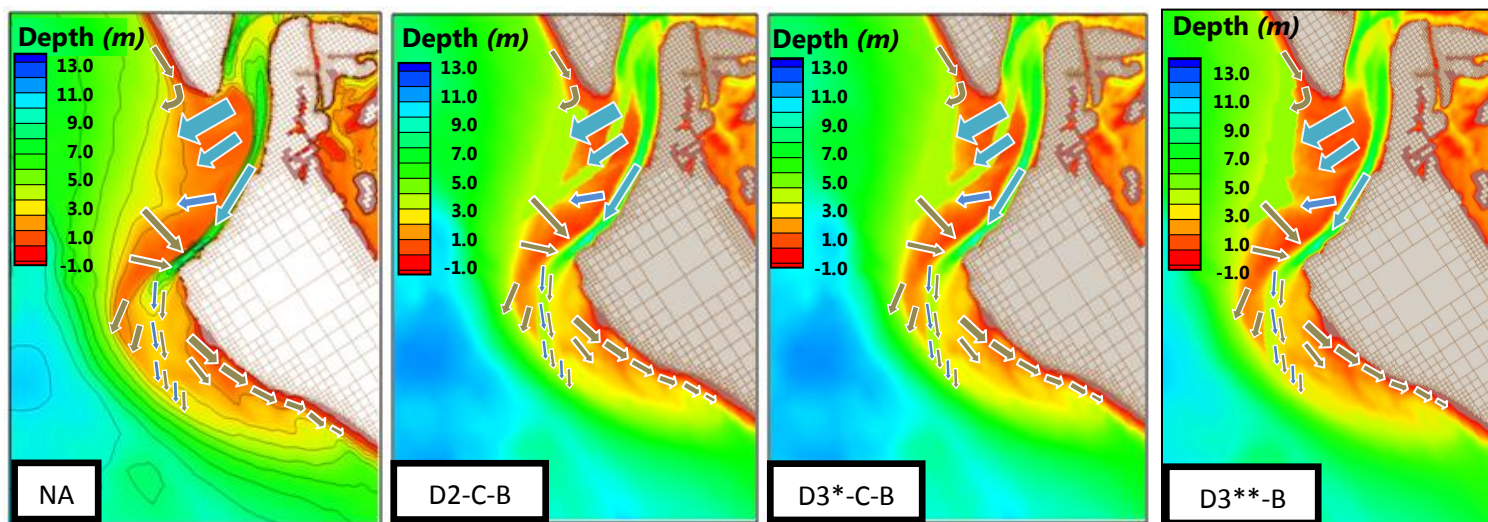


Figure 94: General sediment Transport under EBB currents (BLUE) AND NORTHWESTERLY WAVES (BROWN).

5. ROLE OF GROINS AND BEACH NOURISHMENT ON THE SELECTED ALTERNATIVE

Three additional CMS model runs were made with the groin design from the 2004 USACE Feasibility Report to determine the role of groins and beach nourishment on the selected alternative. The groins layout is presented in Figure 96 using the design from the 2004 Feasibility Report and the 2013 shoreline.

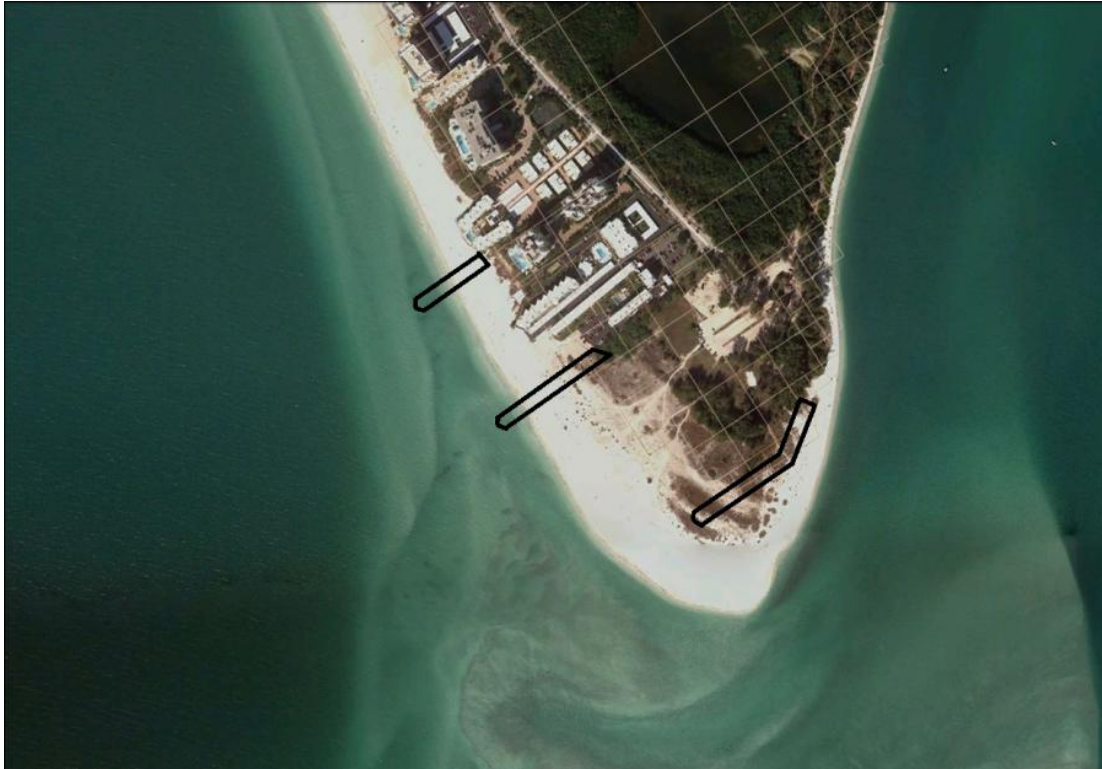


Figure 95: Plan view of groins; Groin design is from the 2004 Feasibility Report, 2013 Shoreline at Lido Key

The GENESIS numerical model was used to verify the groin design and is presented in Appendix B. The model was run for the most conservative alternative, defined as the alternative that would affect most change in the region. The model was run for Alternative D2-C-B which is the alternative for which the most morphologic change is expected due to the close proximity of the borrow sites to the project region. The model was run with and without the design nourishment project to see the effect of the groins both on the nourishment project and on the ebb shoal and sediment transport. The CMS Modeling Matrix is presented in Table 10.

Table 10. Modeling Matrix for CMS runs with Groins Summary of Model Results

Scenario	Initial Bathymetry	Waves
D2+C+B, alone No Groins No Nourishment	2004 with cut D2+C+B	WWIII May – Nov 2004
D2+C+B, Groins No Nourishment	2004 with cut D2+C+B	WWIII May – Nov 2004
D2+C+B, Groins Nourishment	2004 with cut D2+C+B with nourishment design template	WWIII May – Nov 2004
D2+C+B, No Groins Nourishment	2004 with cut D2+C+B with nourishment design template	WWIII May – Nov 2004

5.1. Alternative D2-C-B with and without Groins / No Nourishment

The model was run with groins and without the beach nourishment present. This run was compared with that from Section 4.3.1 for Alternative D2-C-B without groins and without nourishment (Figure 96). Figure 96 shows the difference in morphology, where warm colors denote a decrease in erosion and increase in accretion, and cool colors denote an increase in erosion and decrease in accretion. Here, the ending morphologic difference for six month run from May 2004 to November 2004 was compared. If the groins are in place with no nourishment, there would be a greater amount of sediment accreting in the vicinity of the groin field, especially in the region fronting the condominiums relative to the case where no groins. However, if there is no beach nourishment, the accretion in this region is at the expense of the most southerly part of Lido Key, where accretion is decreased and erosion is increased, which is an undesirable effect.

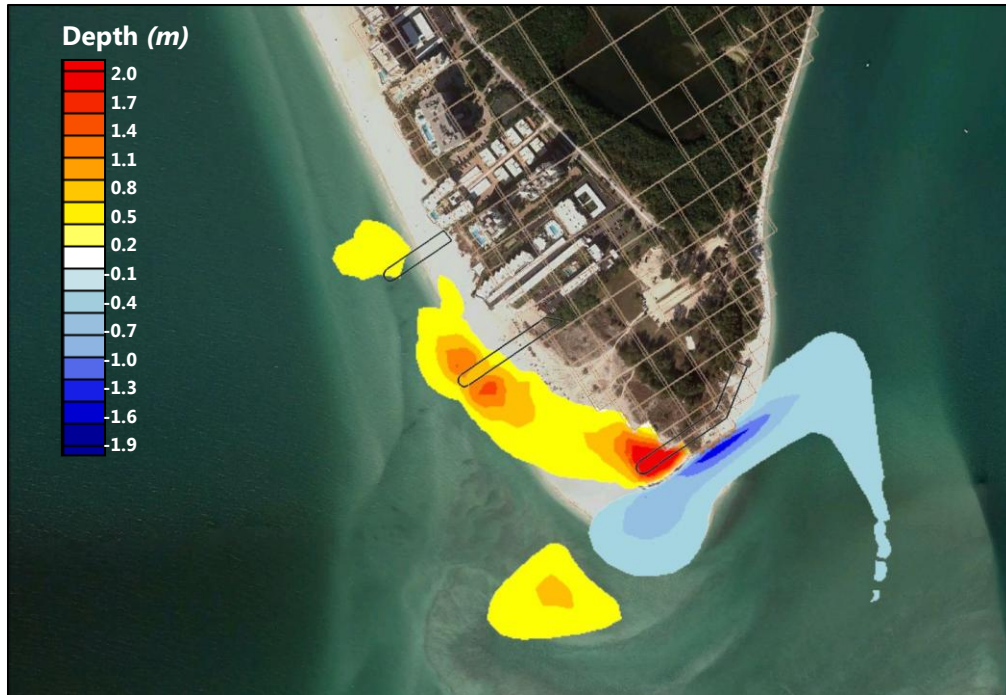


Figure 96: Groins without nourishment; Ending morphology difference for six month run 2004 = (groins were in place with no beach nourishment) – (no groins and no beach nourishment)

5.2. Alternative D2-C-B with and without Groins / With Nourishment

The model was run in the same manner as the case described in Section 4.3.1, but with the beach nourishment, with and without groins. Figure 97 shows the difference in morphology, where warm colors denote a decrease in erosion and increase in accretion, and cool colors denote an increase in erosion and decrease in accretion. Here, the ending morphologic difference for six month run from May 2004 to November 2004 was compared. It is shown here that if the groins are in place with nourishment, there would be a greater amount of sediment accreting in the vicinity of the groin field, especially in the region fronting the condominiums relative to the case without groins. Most important, if the nourishment project is in place, the most southerly part of Lido Key is stable, neither increasing in accretion, nor erosion as long as the nourishment design template is maintained.



Figure 97: Groins with nourishment; Ending morphology difference for six month run 2004 = (groins were in place with beach nourishment) – (no groins with beach nourishment)

6. ROLE OF SELECTED ALTERNATIVES ON FUTURE MORPHOLOGY

CMS was used to assess whether excavation of the ebb shoal would significantly change the entire ebb shoal bathymetry, not just the borrow area excavation alone, by reducing its depth either through deflation or collapse, and/or would reduce its planform such that it would result in a significant adverse impact to the coastal littoral system and adjacent beaches.

SAJ sought to examine how the ebb shoal morphology would evolve from its 2013 condition under both the storm condition of 2004 and under a 1.5 wave condition from 2005 – mid-2006. Alternative cases were run as well as the “No Action” Alternative (no ebb shoal mining) to examine change in ebb shoal morphology and evolution from the “No Action” Alternative. For all model runs, the beach nourishment project and groin fields were included in the model.

To determine the role of additional excavations of the ebb shoal on future morphology, CMS was run with the selected plans D2-B-C, D3*-B-C and D3**-B with nourishment and groins present and using the most recent survey bathymetry from 2013. Table 11 details the Model Alternatives and Table 12 describes the bathymetric datasets and the wave dataset used. Bathymetry used included the most recent ebb shoal survey (August 2013), beach surveys (August 2013), July 2010 Lidar and the Coastal Relief Model (CRM). These alternatives were modeled over the same time period with the same waves as those used in the model skill and above section on the 2004 analysis. In addition, they were run for a multi-year time period spanning from Jan 1, 2005 to June 1, 2006. The 2004 wave dataset was used for consistency in wave input for comparison of volume change and sediment transport pathways to other results. Figure 98 illustrates the existing bathymetry as well as that for the three selected alternatives plans D2-B-C, D3*-B-C, and D3**-B.

Table 11: Description of Model Alternatives

<i>Alt</i>	<i>Groins Present</i>	<i>Nourishment Present</i>	<i>Description</i>	<i>Cut Depth (ft MLW)</i>
A	YES	YES	No Action	0
D2-C-B	YES	YES	Rectangular Geometry, Extension Existing Channel, Ephemeral Channel	12
D3*-C-B	YES	YES	Contour Dredge, Extension Existing Channel, Ephemeral Channel	12
D3**-B	YES	YES	Contour Dredge, Extension Existing Channel	14

Table 12: Time periods for initial and end conditions of each model run

<i>Initial Condition Bathymetry/Topography (2013) Wave Forcing</i>					
2013 Existing	Selected Alternative 1.7 MCY Removed	Selected Alternative 1.48 MCY Removed	Selected Alternative 1.37 MCY Removed	Wave Forcing (WWIII) 6 month run	Wave Forcing (WWIII) 1.5 year run
2013 Ebb Shoal Bathymetry + 2013 Beach Profile Survey + 2010 Lidar + CRM	Modified 2013 Ebb Shoal Bathymetry + 2013 Beach Profile Survey + 2010 Lidar + CRM	Modified 2013 Ebb Shoal Bathymetry +2013 Beach Profile Survey + 2010 Lidar + CRM	Modified 2013 Ebb Shoal Bathymetry +2013 Beach Profile Survey + 2010 Lidar + CRM	5 May 2004 – 4 November 2004	1 Jan 2005 – 1 June 2006
N.A.	D2+B+C	D3*+B+C	D3**+B	WWIII	WWIII

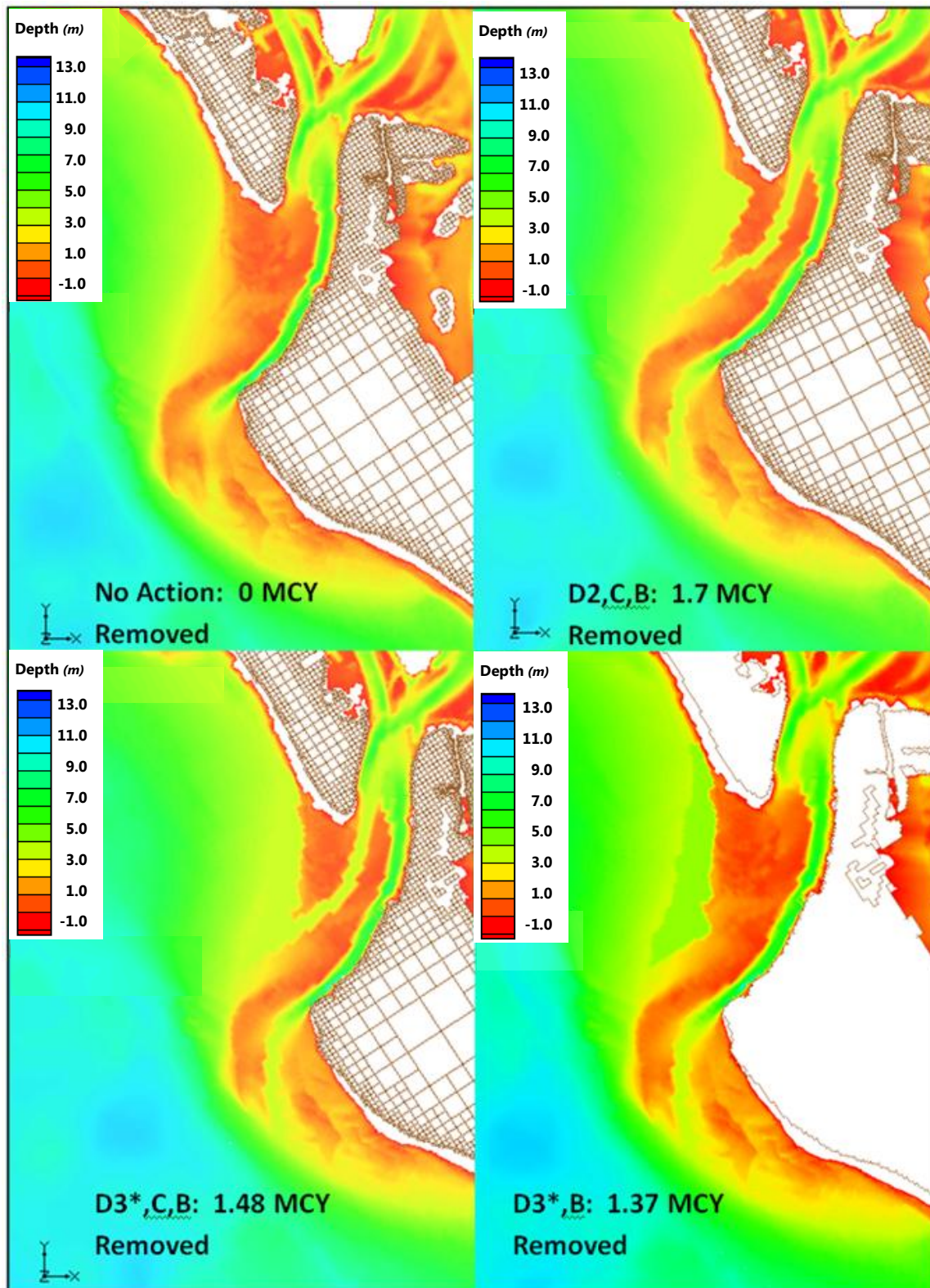


Figure 98: Model grid bathymetry for the 2013 existing condition and the three selected alternatives

6.1. Six-Month Runs

6.1.1. Morphology Change for Alternatives

Figure 99 through Figure 101 show the change in morphology for all of the alternatives after having run the model with the 2013 bathymetry. Figure 99 shows the morphologic change for the “No Action” Alternative at the end of the six-month run from May 2004 through November 2004. The results are very similar to those run with 2004 bathymetry in Figure 56. There is slight deflation of the northern lobe as wave energy transports sediment into the main navigation channel. Figure 100 shows the morphologic change for the D2-C-B Alternative over the same time period. Here as expected there is significant accretion in Cut C and in the main navigation channel. There is modest accretion in Cut D2 and less than 3 ft deflation of the north lobe from the most northeastern part of Cut D2, across the north lobe to the main navigation channel. Figure 101 shows the morphologic change for the D3*-C-B Alternative. Again, there is significant accretion in Cut C and in the main navigation channel. There is little to no appreciable accretion in Cut D3* and less than 3 ft deflation of the north lobe to the main navigation channel. Figure 102 shows the morphologic change for the D3***-B Alternative.

For this alternative, the morphologic change is very similar to the “No Action” Alternative.

6.1.2. Depth Comparisons among Alternatives and “No Action” Alternative

Alternatives were compared by depth to understand how the bathymetry has changed due to ebb shoal mining relative to the “no action” condition. For Alternative D2-C-B (Figure 103), the regions in Cut D2, C and B are deeper due to the dredging activity itself. From Figure 100 it was shown that there has been appreciable accretion in Cut C and some accretion in Cut D2, however, the volume of sediment deposited into these regions did not bring the bed elevation up to pre-mining conditions over the six-month time period. We find the same for Alternative D3*-C-B (Figure 104) in which the greatest differences between the “No Action” Alternative and Alternative D3*-C-B are the dredging sites themselves. For both Alternatives (D2-C-B and D3*-C-B) the region of the navigation channel adjacent to the most seaward extent of Siesta Key is relatively deeper than the “No Action” Alternative. Alternative D3***-B is compared against the “No Action” Alternative in Figure 105. Here there are very little differences aside from the dredge cuts themselves. There is modest shoaling in Cut B and slight erosion westward of Cut B.

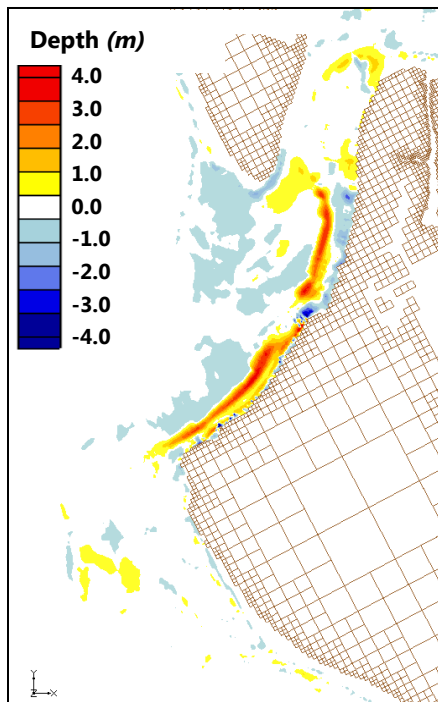


Figure 99: Morphology Change No Action

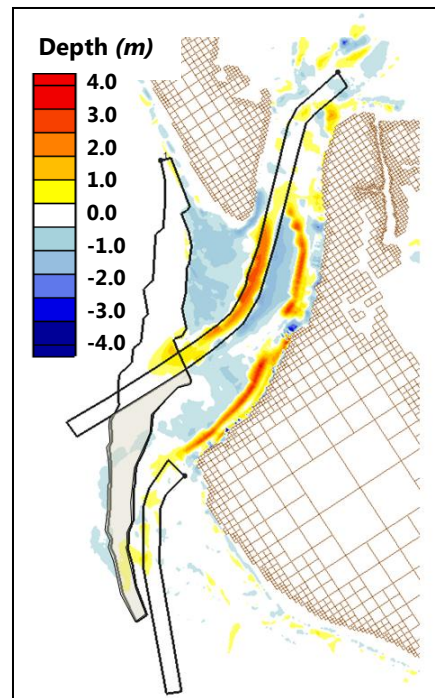


Figure 101: Morphology Change D3*-C-B (note brown section of cut D3 was not dredged)

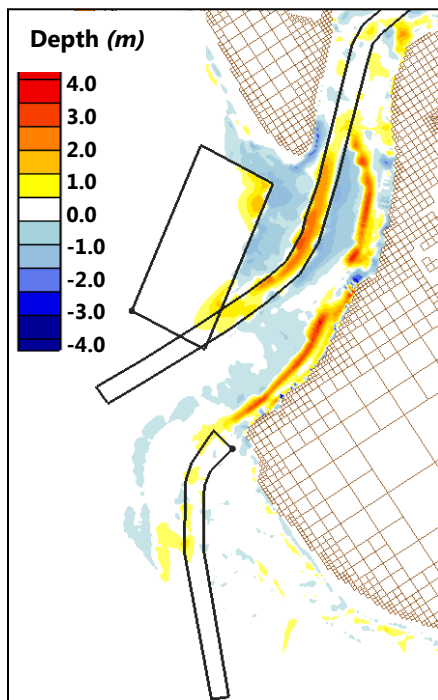


Figure 100: Morphology Change D2-C-B

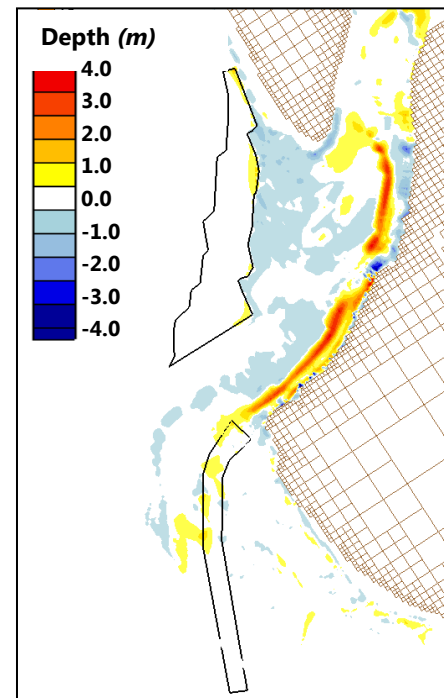


Figure 102: Morphology Change D3-B**

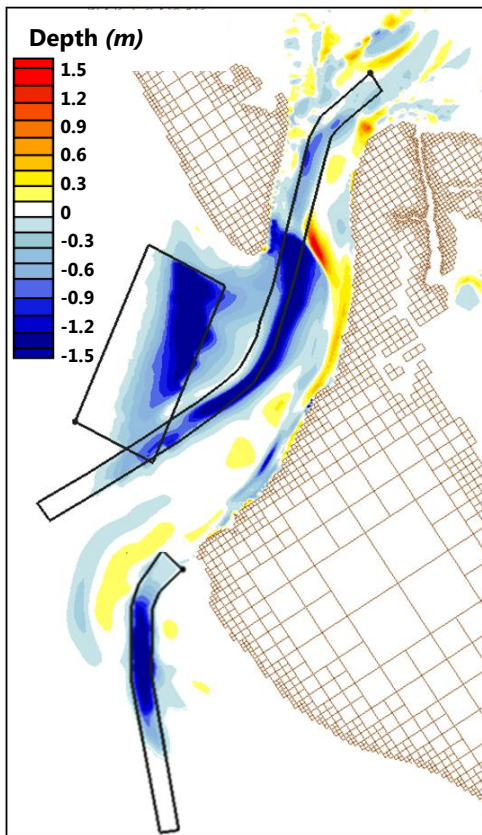


Figure 103: delta Depth D2-C-B vs NA

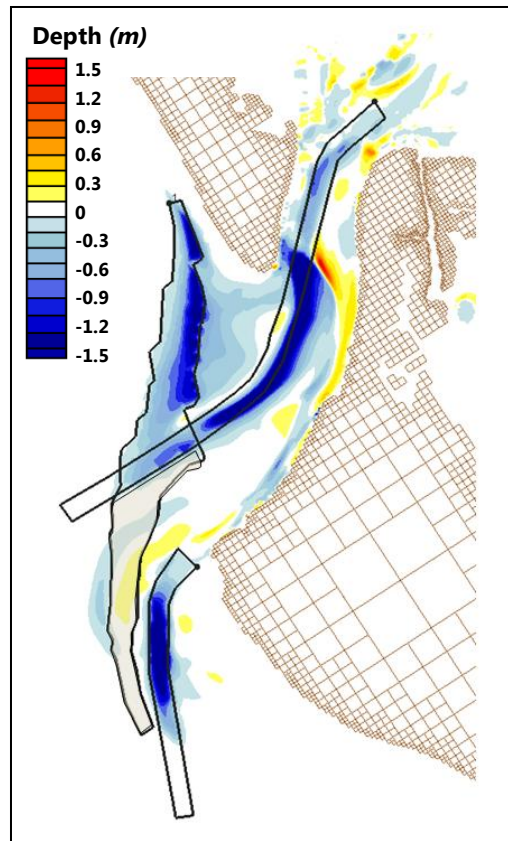


Figure 104: delta Depth D3*-C-B vs NA (note brown section of cut D3 was not dredged)

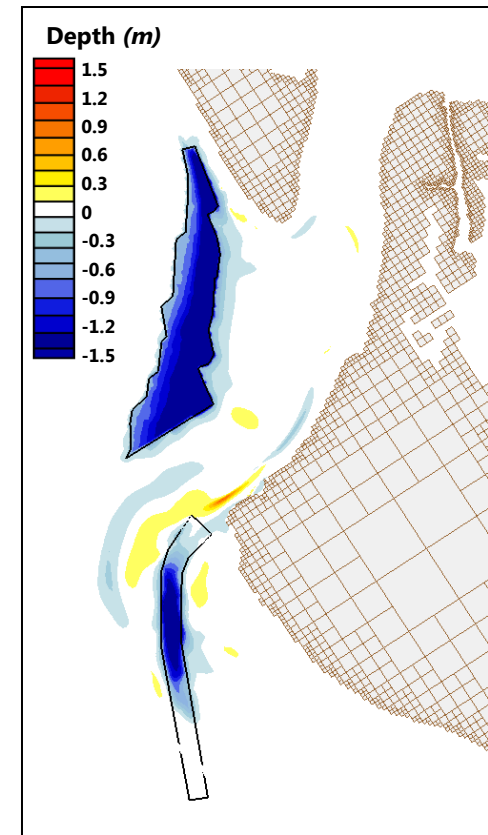


Figure 105: delta Depth: D3-B vs. NA**

6.1.3. Morphologic Comparisons among Alternatives

Morphologic Comparisons were made among dredging alternatives illustrated in Figure 106 through Figure 108. Essentially, these figures allow the reader to understand which locations will be more accretional and/or less erosional (warm colors) and which locations will be more erosional and/or less accretional among alternatives. When comparing Alternative D2-C-B with the “No Action” Alternative (Figure 106) it is easy to see that the regions in Cuts D2, C and B are more accretional (see: Figure 100) than the “No Action” Alternative. The most seaward extent of the existing navigational channel is slightly less accretional than the “No Action” Alternative and the more landward extent of the channel is slightly more accretional (Figure 106 and see Figure 103 for understanding of the behavior of the navigation channel). The same observations can be made for the comparison of the change in morphology for Alternative D3*-C-B with the “No Action” Alternative (Figure 107). Cuts C is highly accretional (see: Figure 101) whereas Cut B is slightly accretional. Cut D3* has very little accretion. The navigation channel behaves in the same manner as described previously (see figs: Figure 107, Figure 104). Comparison in morphology between Alternative D3**-B and the “No Action” Alternative (Figure 108) shows very little difference in morphology. The Cuts D3** and B are slightly less erosional/more accretional than the “No Action” Alternative and there exists slight erosion adjacent to the dredge cuts.

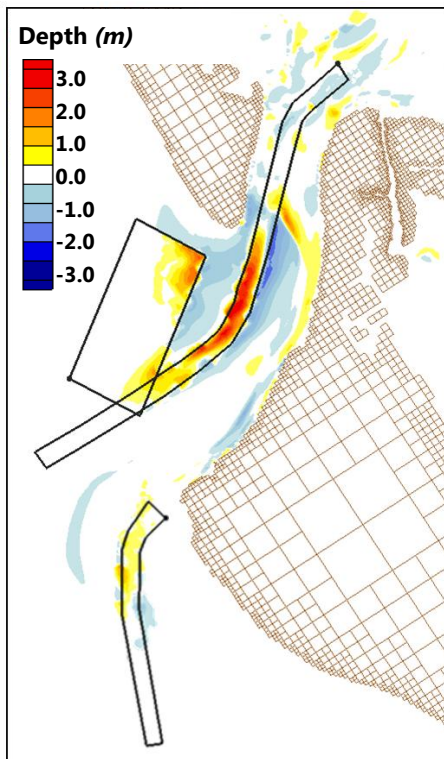


Figure 106: delta Morph: D2-C-B vs. N.A.

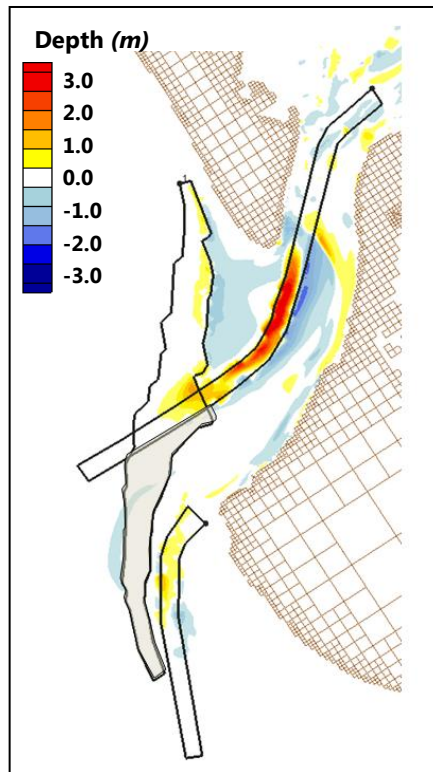


Figure 107: delta Morphology D3*-C-B vs. N.A.

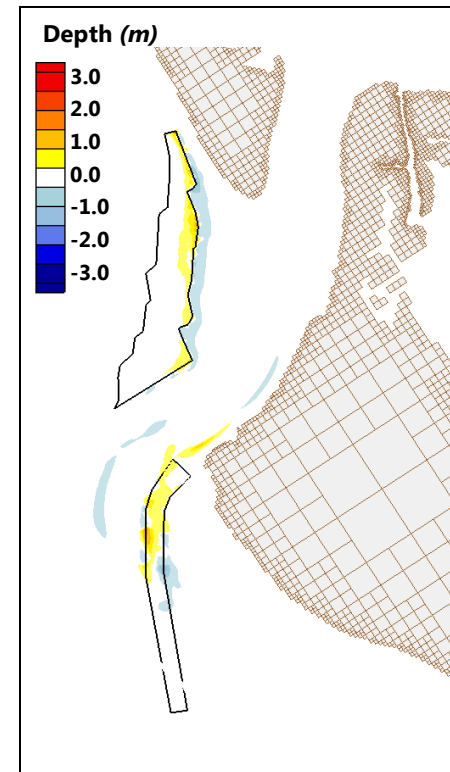


Figure 108: delta Morphology: D3-B vs. NA**

6.1.4. Time Integrated Sediment Transport Pathways

Sediment transport vectors were summed over the duration of the model run to determine integrated transport pathways for each alternative so that changes in sediment transport pathways relative to the “No Action” Alternative within the ebb shoal could be determined.

Figure 109 through Figure 111 show integrated transport pathways for the “No Action” Alternative. Figure 109 shows the cumulative summation of the sediment concentration and integrated transport vectors for the six-month run (May 2004 to November 2004). This figure shows at which locations sediments were most often suspended and at what magnitude and in which direction were they being transported. In this case, summation over the tidal cycle for a completely linear tide with no sub-harmonics would sum to zero ($\int_0^{2\pi} \sin(x) dx = 0$), however, most real tides have sub-harmonics and their integral over a tidal cycle is not equal to zero. This is known as a “residual tide” or “residual flow” and is strongly linked to sediment transport pathways in a tidal regime.

It is clear that the sediments are consistently suspended over the north lobe of the ebb shoal (Figure 109) and the strongest transport is toward and in the navigation channel (Figure 110). Examination of morphologic change (Figure 111) for the “No Action” Alternative shows clearly that transport of sediment toward the south east, over the north lobe, and transport into and in the navigation channel leads to accretion in the channel. Clearly, wave driven transport over the north lobe is responsible for the continual and relentless deposition of sediments into the navigation channel. Adjacent to the Siesta Key shoreline, sediment transport is toward the south, away from the shoreline due to dominance by wave energy.

Figure 112 through Figure 114 show integrated transport pathways for Alternative D2-C-B. Figure 112 shows again the cumulative summation of the sediment concentration and integrated transport vectors. Again, sediments are suspended on the north lobe and concentrations are higher directly east of Cut D2 due to the progression of wave energy. The highest sediment concentration and transport direction is into Cut C (Figure 113). Examination of morphologic change for Alternative D2-C-B shows that transport toward Cut C causes accretion of this cut. The sediment load is predominantly carried by the tide as well as wave energy in this location. At the most landward location of the navigation channel, wave energy sweeps sediments from the north lobe into the navigation channel, however, tidal currents move a great deal of sediment through Cut C, thus alleviating the sediment load in the navigation channel. Transport is also directed toward Cut D2 by the tide.

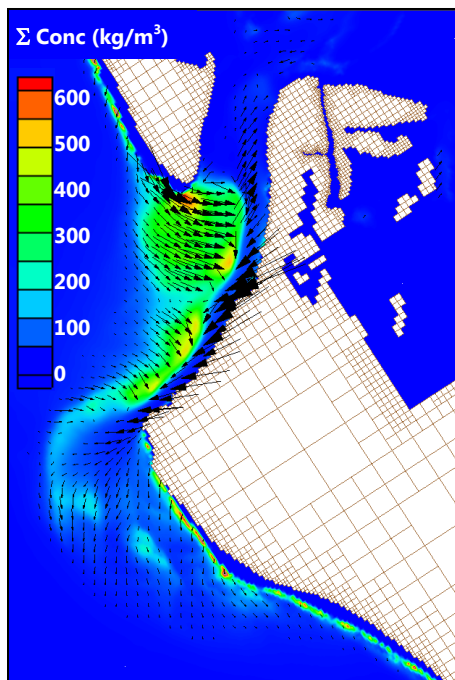


Figure 109: Integrated sediment transport concentration and transport vectors for the no action condition: May 2004 - November 2004 waves

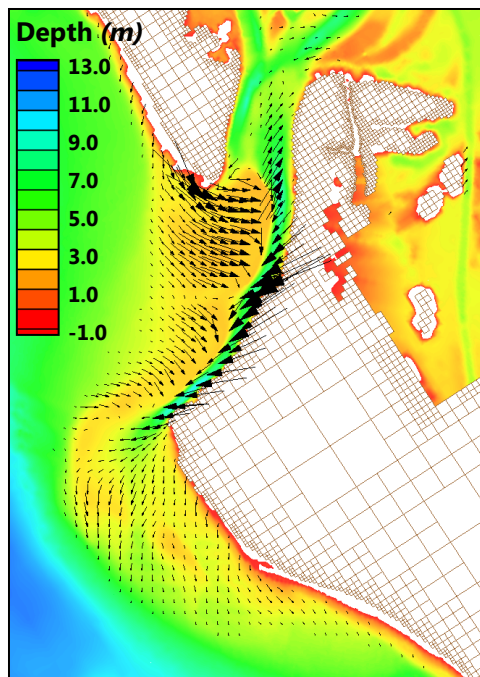


Figure 110: Integrated sediment transport vectors final bathymetry "No Action" Alternative November 2004

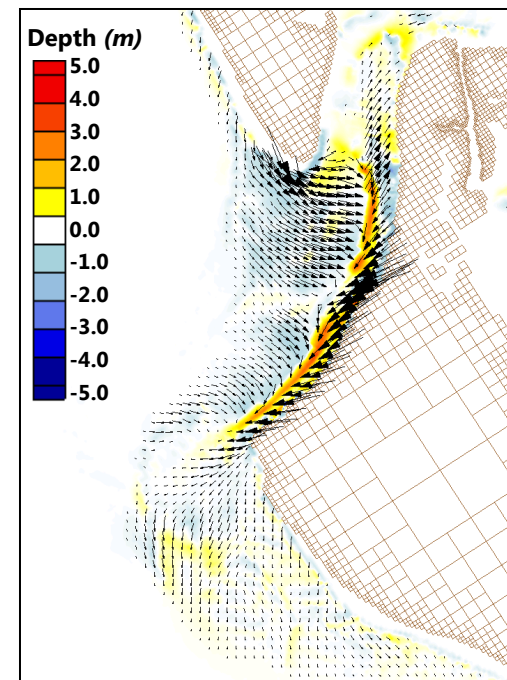


Figure 111: Integrated sediment transport vectors final morphologic change "No Action" Alternative November 2004

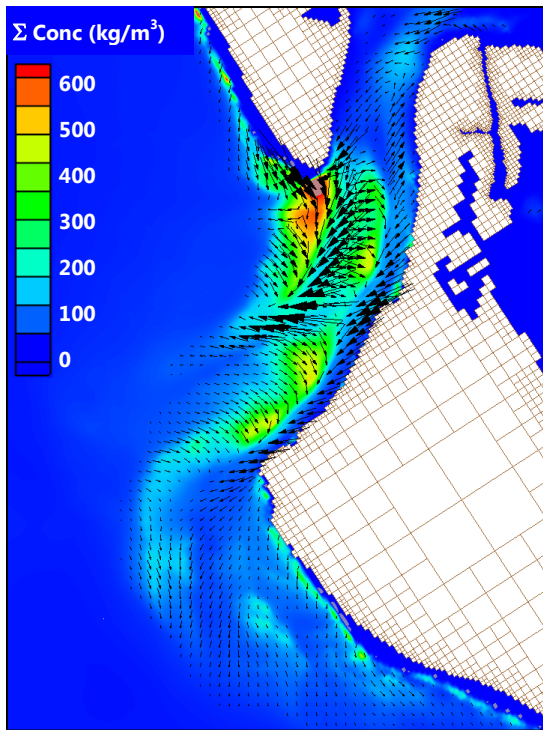


Figure 112 : Integrated sediment transport concentration and transport vectors for alternative D2-C-B: May 2004 - November 2004 waves

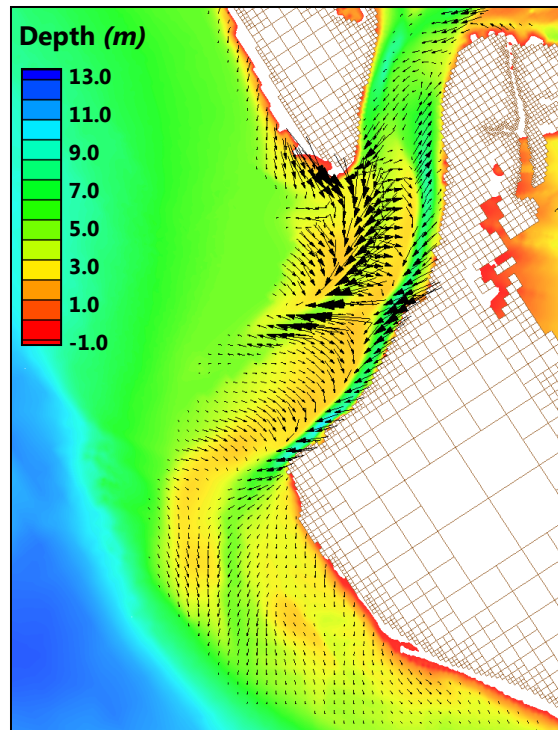


Figure 113: Integrated transport vectors for alternative D2-C B: May 2004 - 2004 waves and final bathymetry

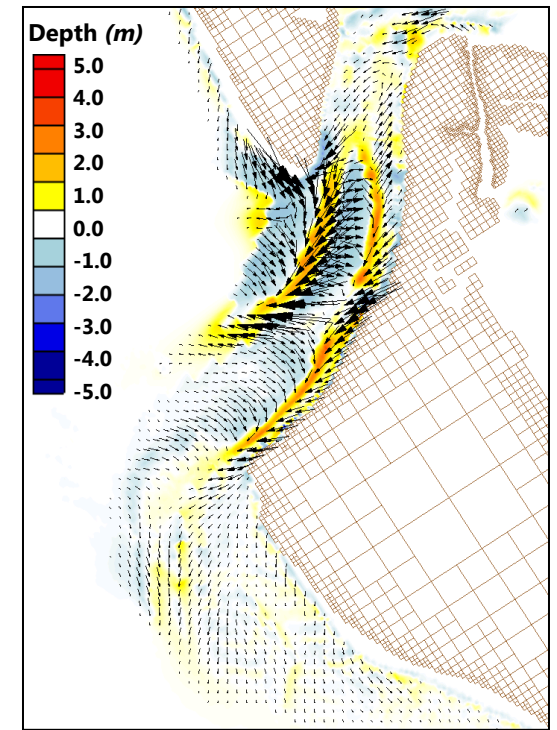


Figure 114: Integrated transport vectors for alternative D2-C B: May 2004 - 2004 waves and final morphologic change

Figure 115 through Figure 117 show integrated transport pathways for Alternative D3*-C-B. Figure 115 shows the cumulative summation of the sediment concentration and integrated transport vectors. Again, sediments are suspended primarily on the north lobe. Similar to Alternative D2-C-B, the highest sediment concentration and transport direction is into Cut C (Figure 116). Examination of morphologic change for Alternative D3*-C-B (Figure 117) shows that transport toward Cut C causes accretion of this cut. The sediment load is predominantly carried by the tide as well as wave energy in this location. At the most landward location of the navigation channel, wave energy sweeps sediments from the north lobe into the navigation channel, however, tidal currents move a great deal of sediment through Cut C, again, similar to Alternative D2-C-B alleviating the sediment load in the navigation channel.

Figure 118 through Figure 120 show integrated transport pathways for Alternative D3**-B. Figure 118 shows again the cumulative summation of the sediment concentration and integrated transport vectors. Again, sediments are suspended primarily on the north lobe. Examination of morphologic change for Alternative D3**-B (Figure 120) shows that transport toward the main ebb channel causes accretion in the channel. The sediment load is predominantly carried by the tide as well as wave energy in this location.

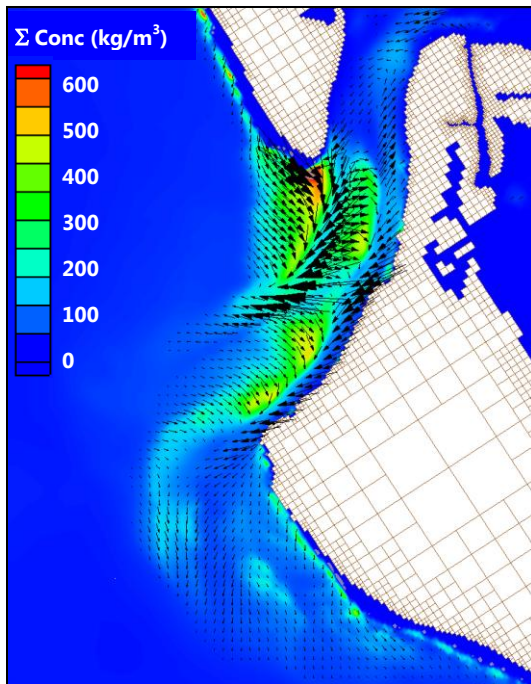


Figure 115: Integrated sediment transport concentration and transport vectors for alternative D3*-C-B: May 2004 - November 2004 waves (tip at location)

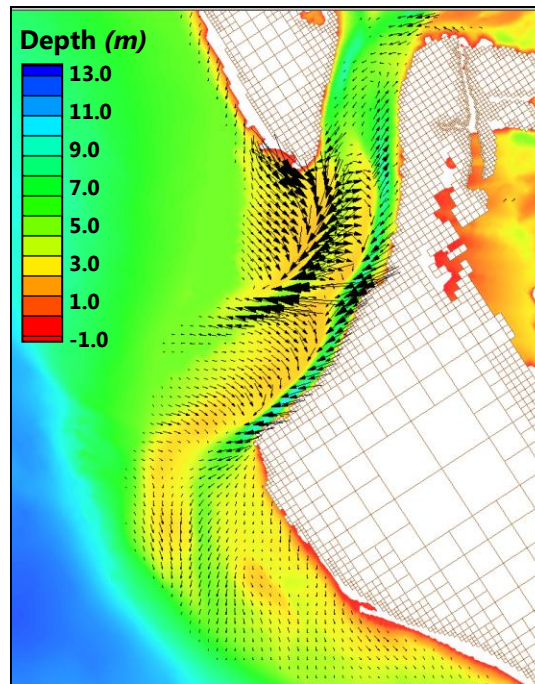


Figure 116: Integrated transport vectors for alternative D3*-C-B: May 2004 - 2004 waves and final bathymetry (tip at location)

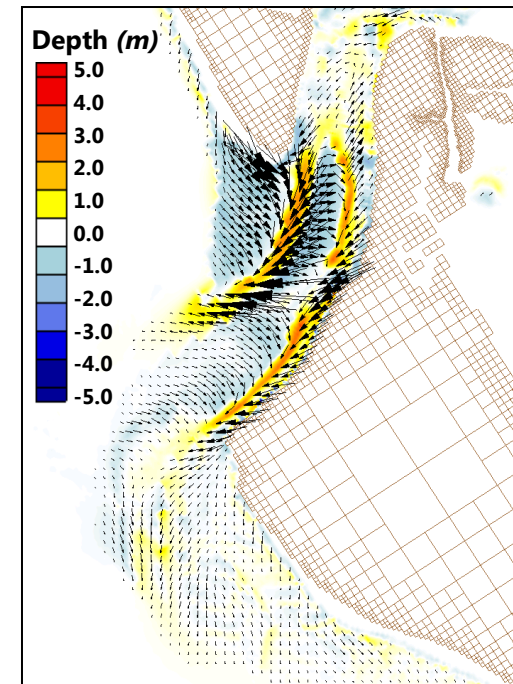


Figure 117: Integrated transport vectors for alternative D3*-C-B: May 2004 - 2004 waves and final morphologic change (tip at location)

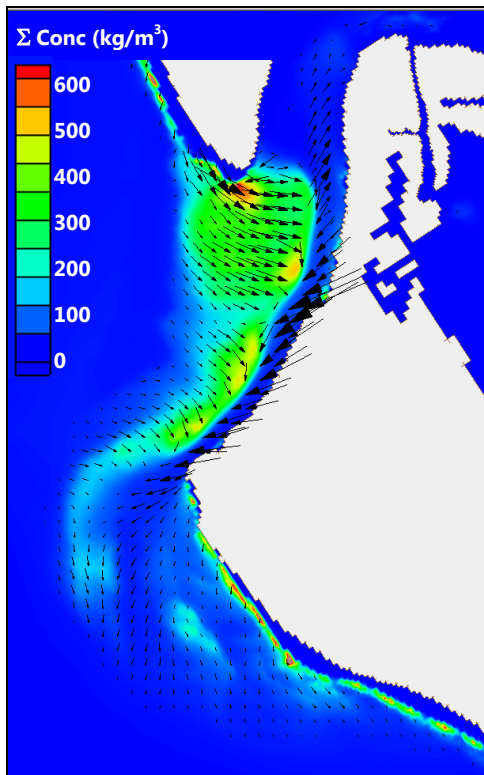


Figure 118: Integrated sediment transport concentration and transport vectors for alternative D3**-B: May 2004 - November 2004 waves (tip at location)

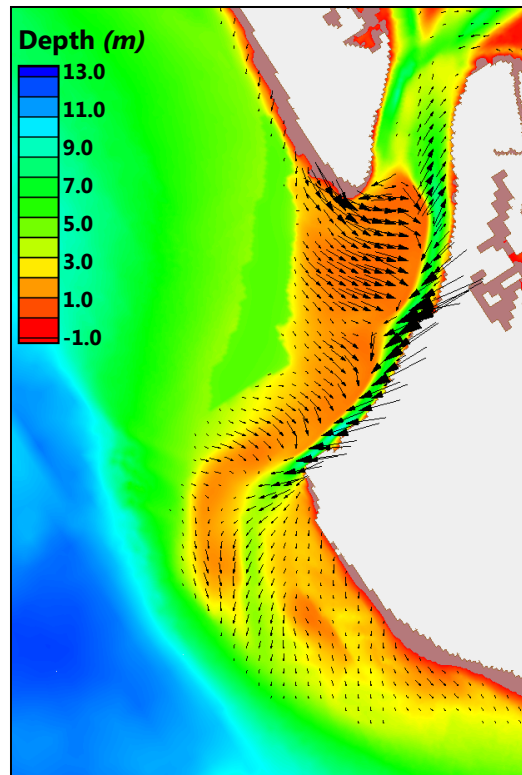


Figure 119: Integrated transport vectors for alternative D3**-B: May 2004 - 2004 waves and final bathymetry (tip at location)

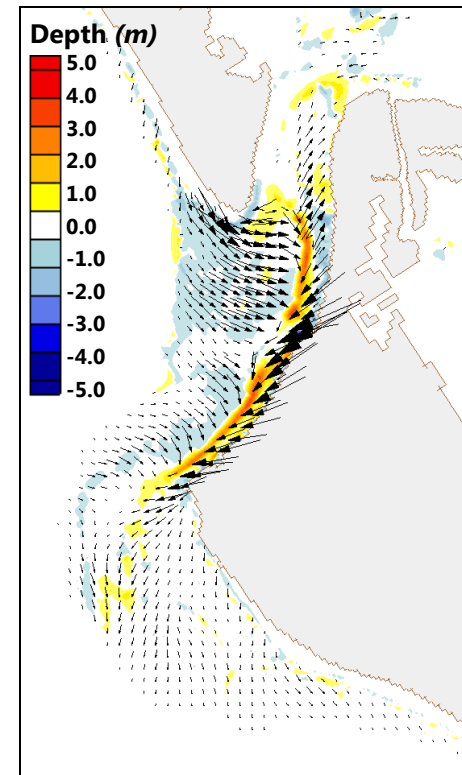


Figure 120: Integrated transport vectors for alternative D3**-B: May 2004 - 2004 waves and final morphologic change (tip at location)

Integrated (residual) transport vectors were decomposed into northing and eastings to see more clearly how sediments are being transported. Figure 121 and Figure 122 show transport direction for the “No Action” Alternative for east/west transport and north/south transport, respectively. As can be readily seen (Figure 121), transport is across the north lobe, to the east and into the navigation channel. Figure 122 shows transport predominately to the south everywhere on the shoal, including adjacent to Siesta Key, until the pathway ultimately turns east to the attachment point on Siesta Key.

Figure 123 shows the decomposition of the vectors for Alternative D2-C-B. Here, the most significant change from the “No Action” Alternative is in the east-west direction. Whereas sediment has continually been swept across the north lobe and into the navigation channel, here the tidal currents bisect the eastward transport of sediment, whereby sediments are brought into Cut C. Further up the inlet, transport direction is reversed out in an ebb dominated direction instead of inward toward the IGWW. Figure 124 shows predominant transport direction to the south, except in the vicinity of Cut D2 where there is slight transport to the north.

Figure 125 and Figure 126 show transport for Alternative D3*-C-B. Here transport is essentially the same as Alternative D2-C-B, however, there is very little transport moving toward Cut D3*.

Figure 127 and Figure 128 show transport for Alternative D3**-B. Here transport is essentially the same as the “No Action” Alternative.

Figure 129, Figure 130 and Figure 131 show the difference in morphology and the difference in transport vectors for the “No Action” Alternative and Alternative D2-C-B, Alternative D3*-C-B, and Alternative D3**-B, respectively. It is readily observable that most of the sediment from the north lobe moves into Cut C for the first two alternatives. There is slightly less accretion in the seaward extent of the navigation channel and slight accretion at the landward extent of the navigation channel from ebb-directed currents from the GIWW. Overall, for Alternatives D2-C-B and D3*-C-B presented here, the most significance in the change in transport over the ebb shoal is transport into, and replenishing Cut C instead of into the navigation channel. There is slight recharge of Cut D2 and minimal recharge of Cut D3*. Adjacent to Siesta Key, there is slight decrease in erosion at Cut B and slight decrease in transport to the southwest, away from Siesta Key for both alternatives examined. For Alternative D3**-B, there is very little difference between the “No Action” Alternative and the with project condition (Figure 131).

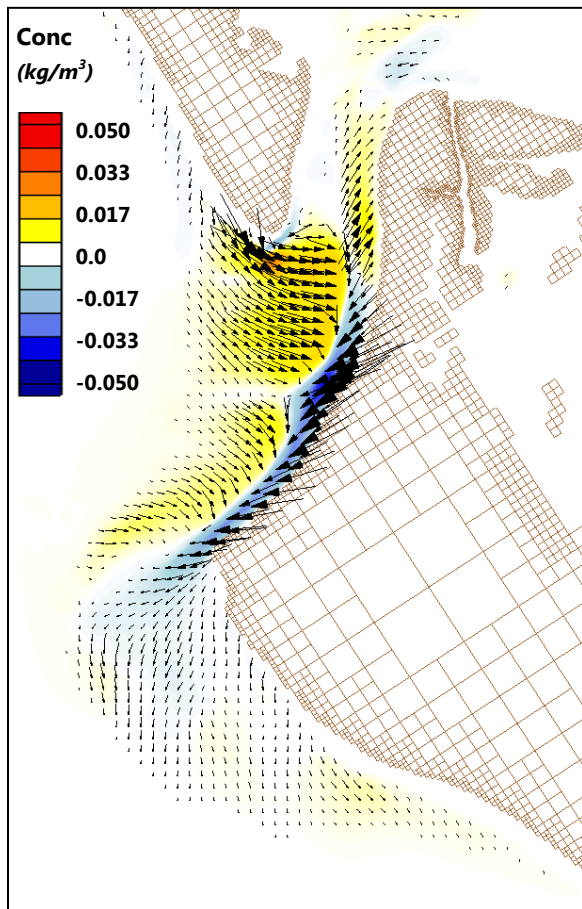


Figure 121: Residual sediment transport magnitude in X-Direction (Yellow=East, Blue=West) and total transport vectors for the no action condition: May 2004 - November 2004 waves (tip at location)

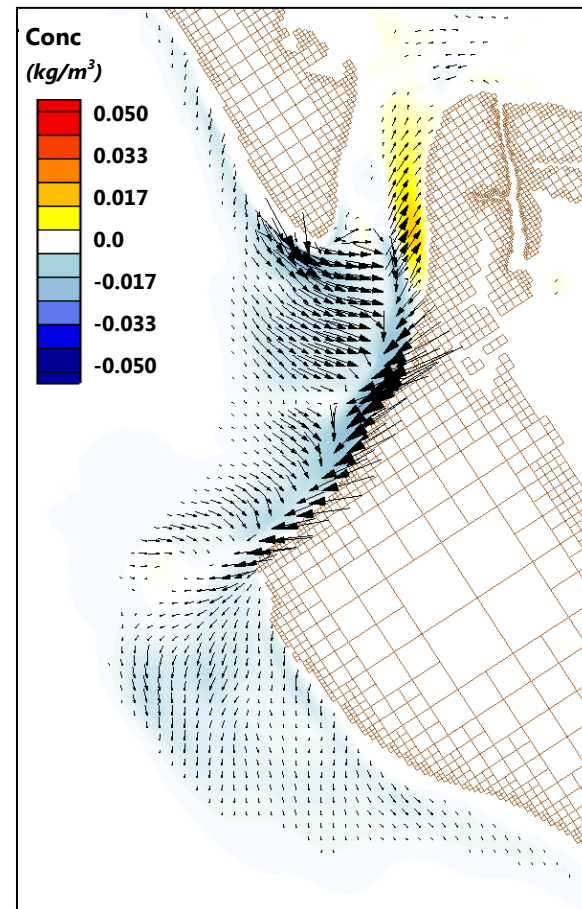


Figure 122: Residual sediment transport magnitude in Y-Direction (Yellow=North, Blue=South) and total transport vectors for the no action condition: May 2004 - November 2004 waves (tip at location)

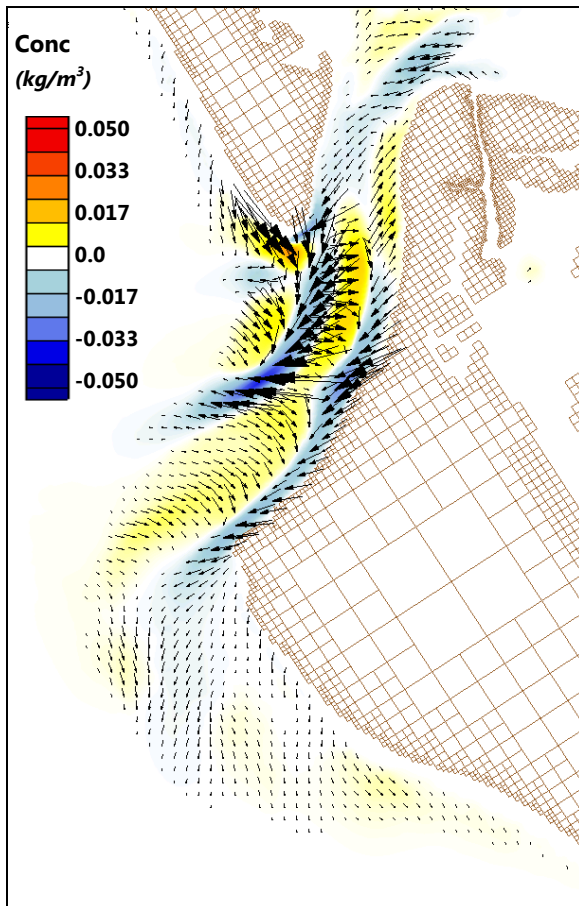


Figure 123 Residual sediment transport magnitude in X-Direction (Yellow=East, Blue=West) and total transport vectors for the D2-C-B Alternative: May 2004 - November 2004 waves (tip at location)

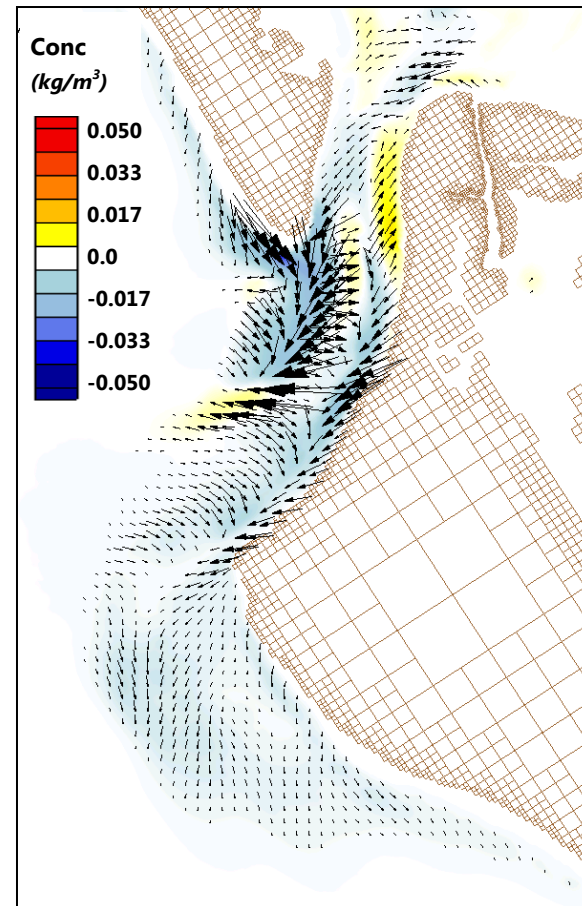


Figure 124: Residual sediment transport magnitude in Y-Direction (Yellow=North, Blue=South) and total transport vectors for the D2-C-B Alternative: May 2004 - November 2004 waves (tip at location)

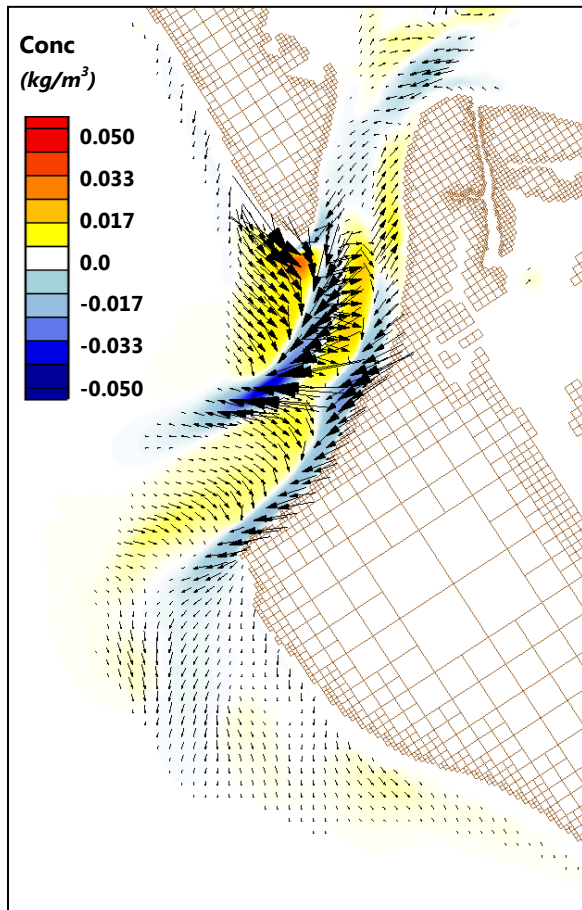


Figure 125 Residual sediment transport magnitude in X-Direction (Yellow=East, Blue=West) and total transport vectors for the D3*-C-B Alternative: May 2004 - November 2004 waves (tip at location)

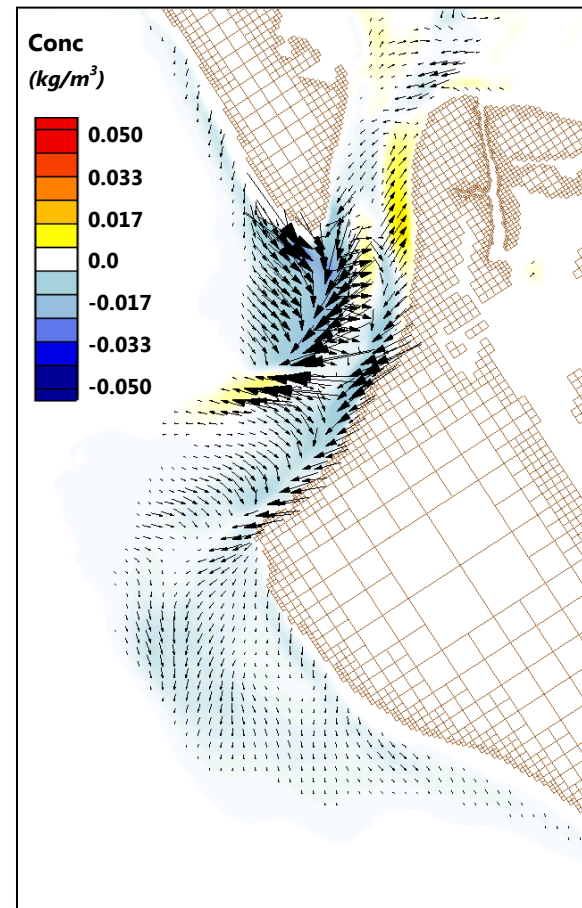


Figure 126: Residual sediment transport magnitude in Y-Direction (Yellow=North, Blue=South) and total transport vectors for the D3*-C-B Alternative: May 2004 - November 2004 waves (tip at location)

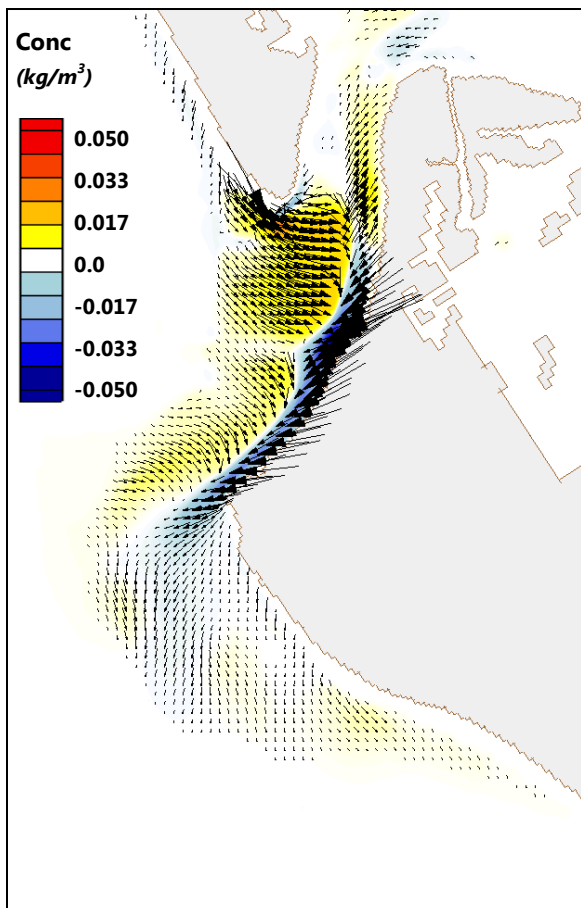


Figure 127 Residual sediment transport magnitude in X-Direction (Yellow=East, Blue=West) and total transport vectors for the D3-B Alternative: May 2004 - November 2004 waves (tip at location)**

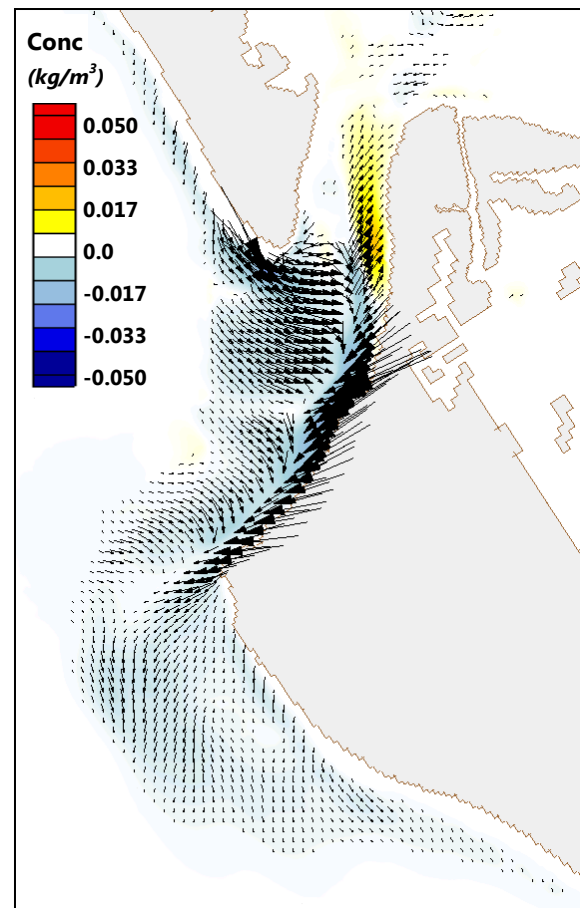


Figure 128: Residual sediment transport magnitude in Y-Direction (Yellow=North, Blue=South) and total transport vectors for the D3-B Alternative: May 2004 - November 2004 waves (tip at location)**

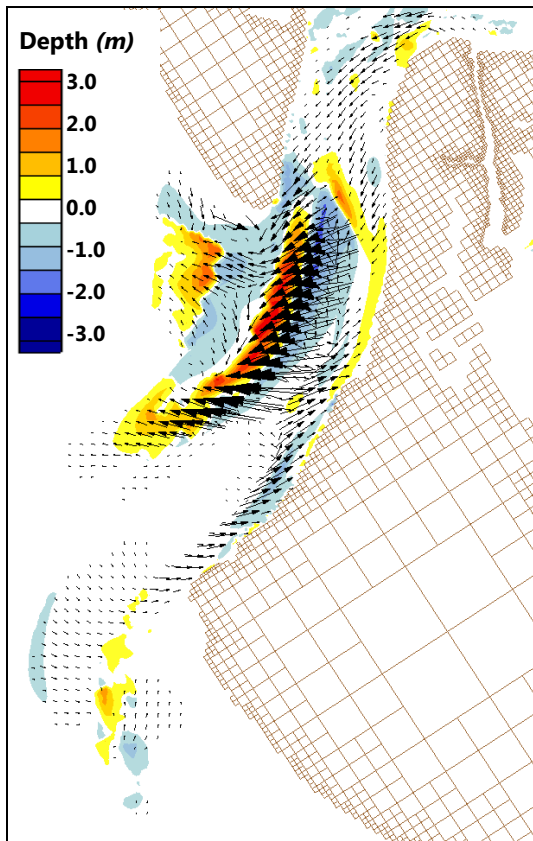


Figure 129: Difference in Morphology between D2-C-B and “No Action” Alternative, and difference between total transport vectors for the D2-C-B Alternative: May 2004 - November 2004 waves (tip at location)

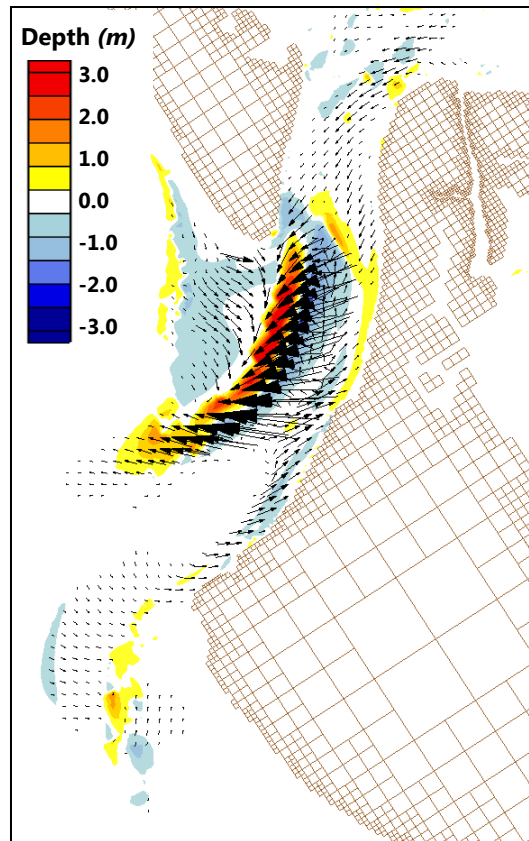


Figure 130: Difference in Morphology between D3*-C-B and “No Action” Alternative, and difference between total transport vectors for the D3*-C-B Alternative: May 2004 - November 2004 waves (tip at location)

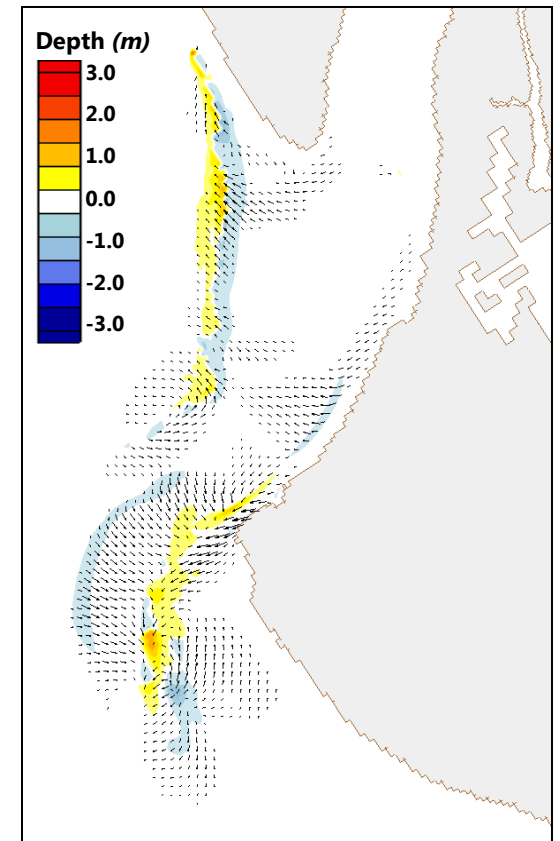


Figure 131: Difference in Morphology between D3-B and “No Action” Alternative, and difference between total transport vectors for the D3**-B Alternative: May 2004 - November 2004 waves (tip at location)**

SAJ sought to examine whether the volume losses in Lido Key were comparable with the volume gains in the Ebb Shoal at Big Sarasota Pass. Results here show that without the project, the gains in the ebb shoal are 50% of the losses on Lido Key. With the project, with either Alternative D2-C-B, or Alternative D3*-C-B, the gains in the ebb shoal are 111% and 101% of the losses on Lido Key (Table 13). These model results further illustrate what has been identified by several authors previously (Davis and Wang, 2004, Davis et al., 2007) that Big Sarasota Pass Ebb Shoal is, in fact, the recipient of sediment losses on Lido Key and that back-passing sediment from the Shoal back on the beaches of Lido Key is a reasonable sediment management strategy.

**Table 13: Volume losses and Gains on Lido Key and Big Sarasota Pass Ebb Shoal
(THOUSANDS OF CUBIC YARDS)**

NO CUT				D2-C-B CUT			
	GAINED	LOST	NET		GAINED	LOST	NET
Lido BEACH	26	-100	-74	Lido BEACH	31	-131	-101
EBB SHOAL	840	-800	40	EBB SHOAL	1,207	-1,095	112
RATIO SHOAL/BEACH			0.54	RATIO SHOAL/BEACH			1.11
NET CHANGE LIDO-SHOAL			-34	NET CHANGE LIDO-SHOAL			11
D3*-C-B CUT				D3**-B CUT			
	GAINED	LOST	NET		GAINED	LOST	NET
Lido BEACH	34	-122	-88	Lido BEACH	47	-116	-72
EBB SHOAL	1,217	-1,128	88	EBB SHOAL	903	-856	47
RATIO SHOAL/BEACH			1.01	RATIO SHOAL/BEACH			0.66
NET CHANGE LIDO-SHOAL			1	NET CHANGE LIDO-SHOAL			-24

6.2. 1.5 Year Runs

To estimate the ebb shoal response for the selected plan in the long-term, SAJ ran 1.5 year runs to further the understanding of how ebb shoal mining could potentially change morphology over a longer duration. Limitations in computer memory, processing speed and model capability dictates the maximum model duration to less than two years. Results become less detailed and smoothed over time and whereas it is possible to discern changes in ebb shoal planform are possible, details within the shoal are smoothed and the results are of limited use for understanding fine-scale morphologic change and heterogeneity within the shoal. The reader should refer to Table 11 and Table 12 for the initial bathymetric conditions and boundary conditions.

Morphologic change within Alternatives, and depth change and morphology change between Alternatives and the “No Action” Alternative were examined to determine the long-term response of the ebb shoal response after having mined sediment.

6.2.1. Morphology Change within Alternatives

Figure 132 through Figure 135 show the change in morphology for all of the alternatives after having run the model with the most updated bathymetry. Figure 132 shows the morphologic change for the “No Action” Alternative at the end of the 1.5 year run from 1 January 2005 through 1 June 2006. The results are very similar to those run with 2004 bathymetry in Figure 56 as well as the most updated bathymetry and 2004 storm waves (Figure 99). There is slight deflation of the northern lobe as wave energy transports sediment into the main navigation channel. Figure 133 shows the morphologic change for the D2-C-B Alternative over the same time period. Here as expected there is significant accretion in Cut C and in the main navigation channel. There is modest accretion in Cut D2 and between 3 and 6 ft deflation of the north lobe starting at the eastern edge of Cut D2, across the north lobe and to the main navigation channel. Figure 134 shows the morphologic change for the D3*-C-B Alternative. Again, there is significant accretion in Cut C and in the main navigation channel. There is little to no appreciable accretion in Cut D3* and between 3 and 6 ft deflation of the north lobe to the main navigation channel. Figure 135 shows morphologic change for the D3**-B Alternative. Deflation across the north lobe directly east of Cut D3** is visible and there is slight accretion in Cut D3**.

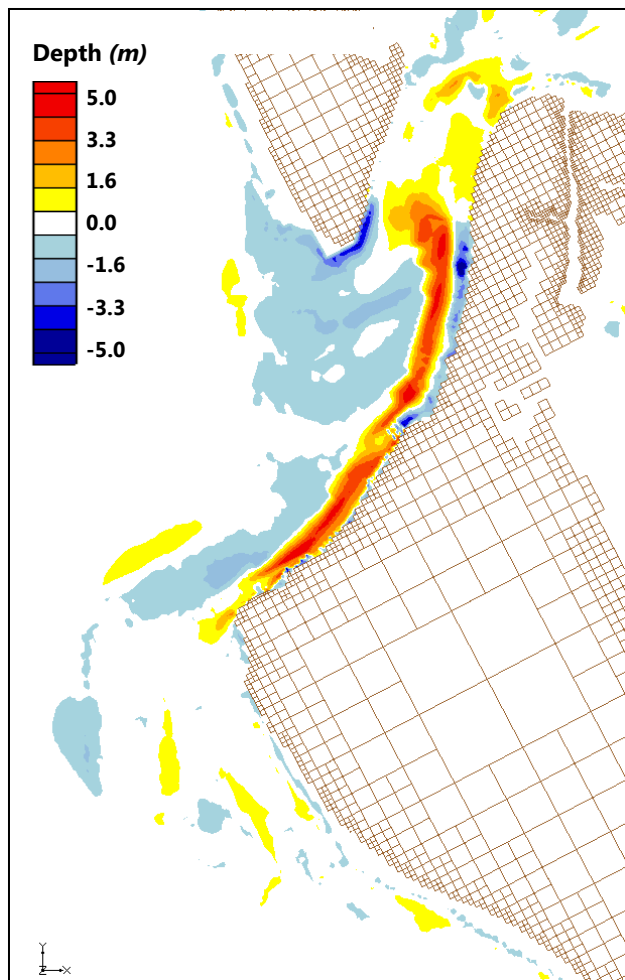


Figure 132: Morphology Change No Action

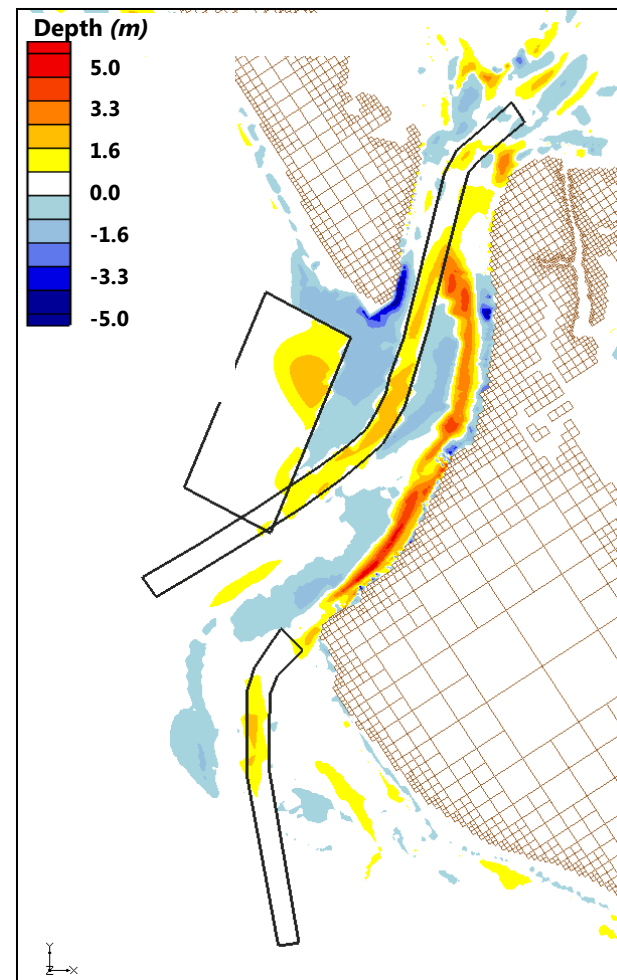


Figure 133: Morphology Change D2-C-B

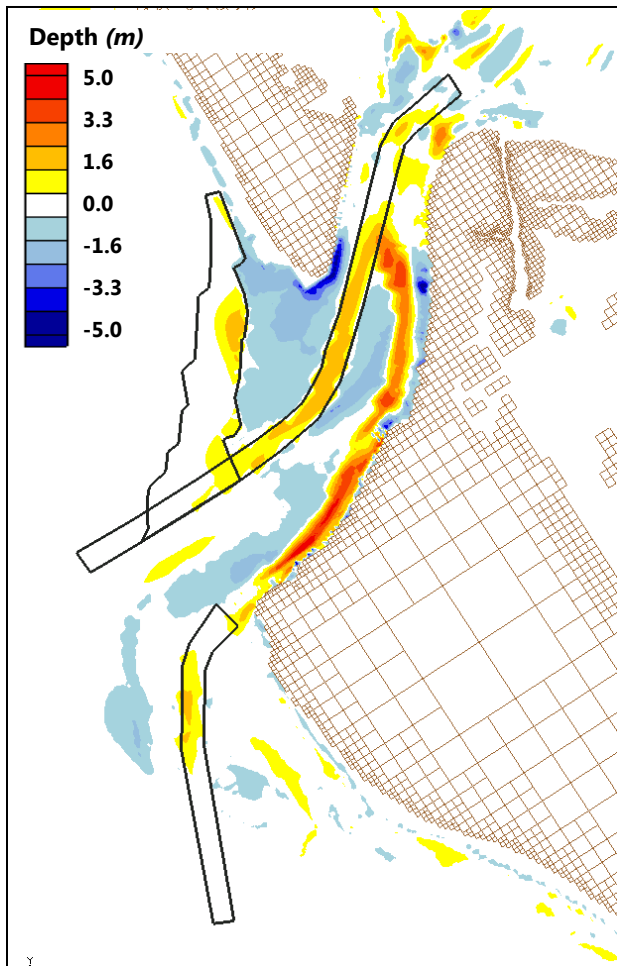


Figure 134: Morphology Change D3*-C B

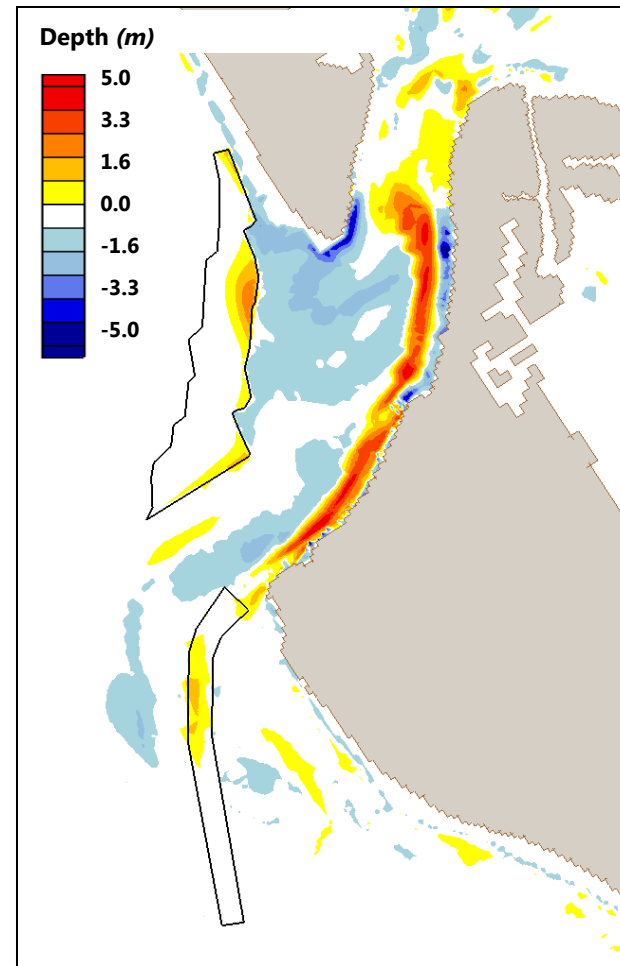


Figure 135: Morphology Change D3-B**

6.2.2. Depth Comparisons among Alternatives

Alternatives were compared by depth to understand how the bathymetry has changed over a 1.5 year duration due to ebb shoal mining relative to the “No Action” Alternative. In general, comparison with six-month runs (Figure 100, Figure 101 and Figure 102) show continued infilling into Cut C (Figure 136 and Figure 137), and that Cut has returned to almost 0.5 meters (1.64 ft) of the initial non-dredged condition. Cuts D2 and D3* are also within about 1 meter of the initial non-dredged condition as well. Cut D3** still remains up to 2 meters (6.56 ft.) from its original non-dredged depth (Figure 138).

In Figure 136, the regions in Cut D2, C and B are deeper due to the dredging activity itself, and in addition, the north lobe of the ebb shoal has deflated by approximately 1 meter due to sediment being moved into the dredge cuts. From Figure 133 it was shown that there has been appreciable accretion in Cut C and some into Cut D2, however, the volume of sediment deposited into these regions did not bring the bed elevation up to pre-mining conditions over the 1.5 year time period. The region of the navigation channel adjacent to the most seaward extent of Siesta Key is relatively deeper than the “No Action” Alternative due to sediment being redirected away from the navigation channel and toward Cut C.

From Figure 137 it can be shown that the regions in Cut D3* and B are deeper due to dredging activity, and the north lobe has deflated by up to 1 meter. Cut C has recovered to an extent where it is more shallow at the Cut than the initial pre-cut bathymetry. The navigation channel remains deeper than the "No Action" alternative due to sediment transport being redirected toward Cut C.

Figure 138 shows the depth comparison between Alternative D3**-C-B with the "No Action" Alternative. It is clear that the greatest difference in depth between alternatives is at the location of the dredge cuts themselves. Outside of these regions across the ebb shoal, there is little difference in bathymetry between both alternatives except at the flood channel at the southern tip of Lido Key. Cut D3** still remains up to 2 meters (6.56 ft.) deeper than the initial pre-dredged condition.

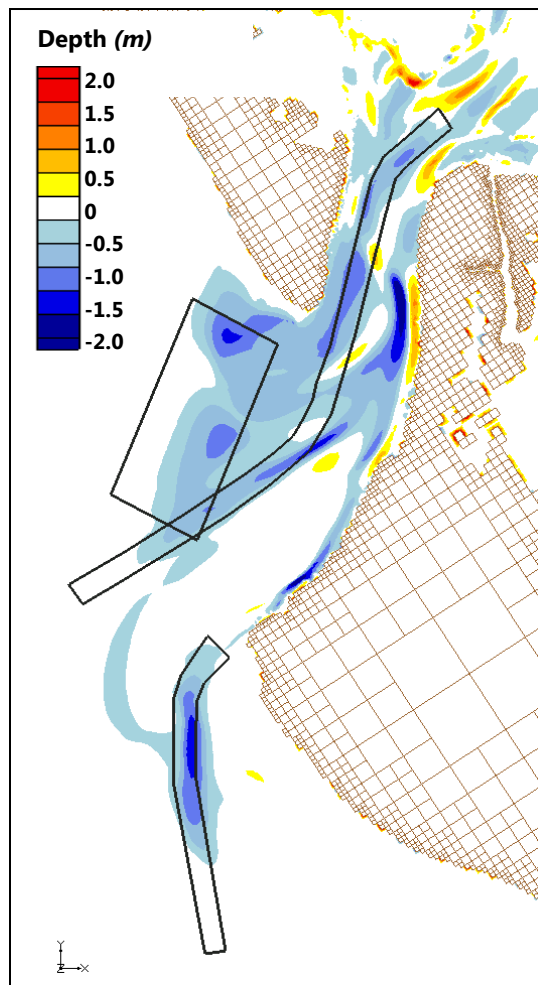


Figure 136: delta Depth D2-C-B vs NA

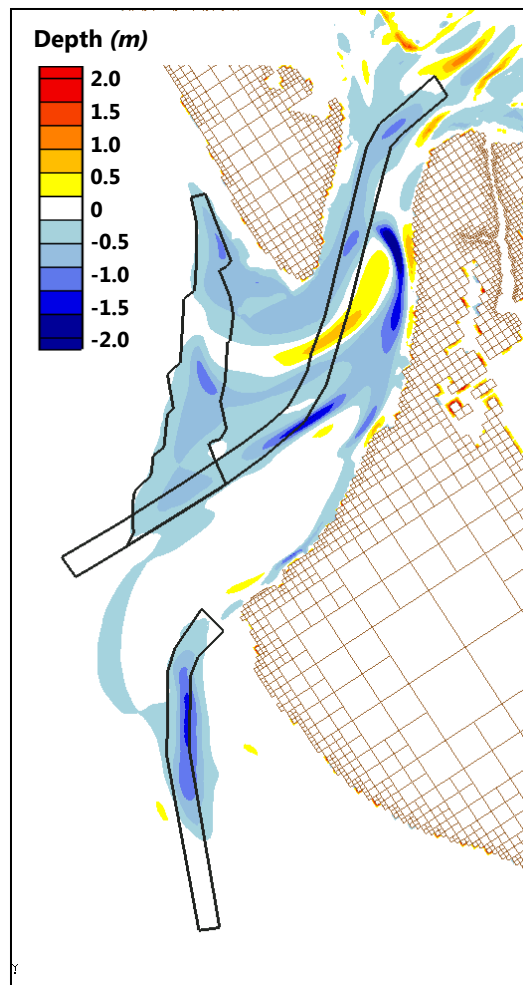


Figure 137: delta Depth D3*-C-B vs NA

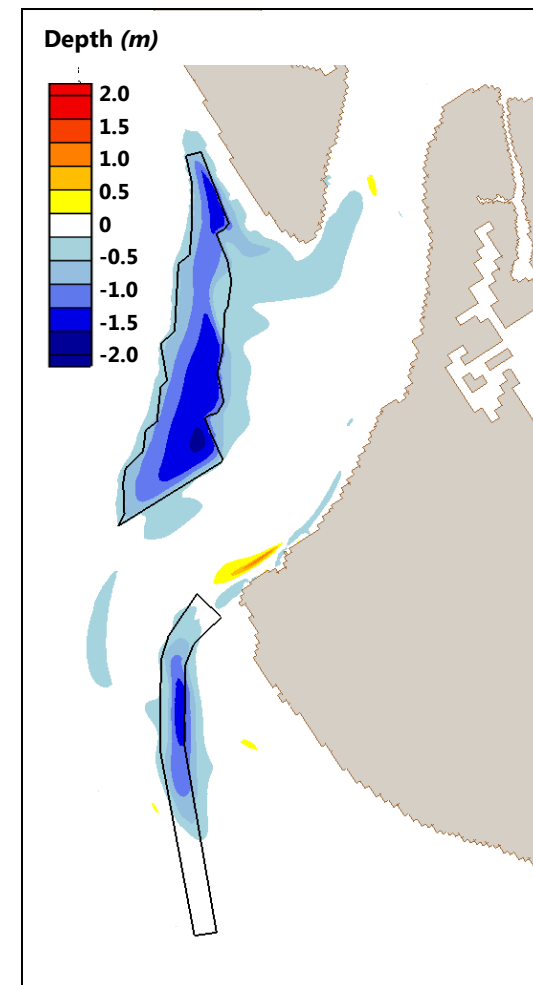


Figure 138: delta Depth: D3-B vs NA**

6.2.3. Morphologic Comparisons among Alternatives

Morphologic Comparisons were made between Alternatives and the "No Action" Alternative (Figure 139, Figure 140 and Figure 141). Essentially, these figures allow the reader to understand which locations will be more accretional and/or less erosional (warm colors) and which locations will be more erosional and/or less accretional among alternatives. When comparing Alternative D2-C-B with the "No Action" Alternative (Figure 139) it is easy to see that the regions in Cuts D2, C and B are more accretional (see: Figure 132) than the "No Action" Alternative. The navigation channel is less accretional than the "No Action" Alternative.

Similar observations can be made for the comparison of the change in morphology for Alternative D3*-C-B with the "No Action" Alternative (Figure 140). Cuts C is highly accretional (see: Figure 133) whereas Cut B is slightly accretional. Cut D3* is slightly more accretional than the "No Action" Alternative. The navigation channel behaves in the same manner as described previously because sediment is being redirected away from the navigation channel and toward Cut C.

There is very little difference between morphologic change for Alternative D3**-C-B and the "No Action" Alternative except for the eastern margin of Cut D3** and at Cut B (Figure 138).

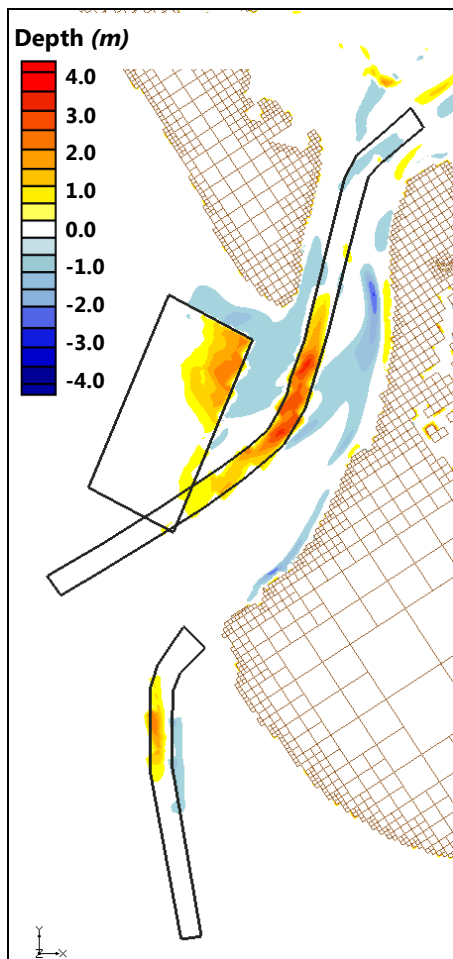


Figure 139: delta Morphology: D2-C-B vs. N.A.

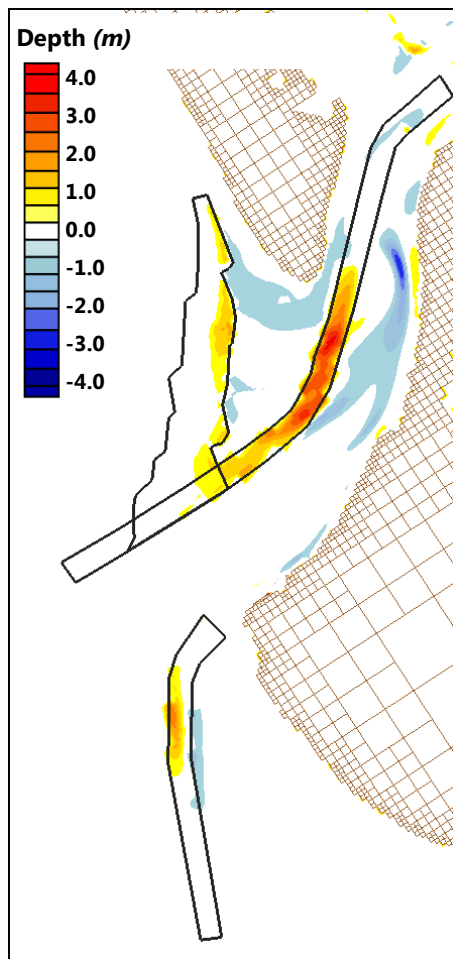


Figure 140: delta Morphology D3*-C-B vs. N.A.

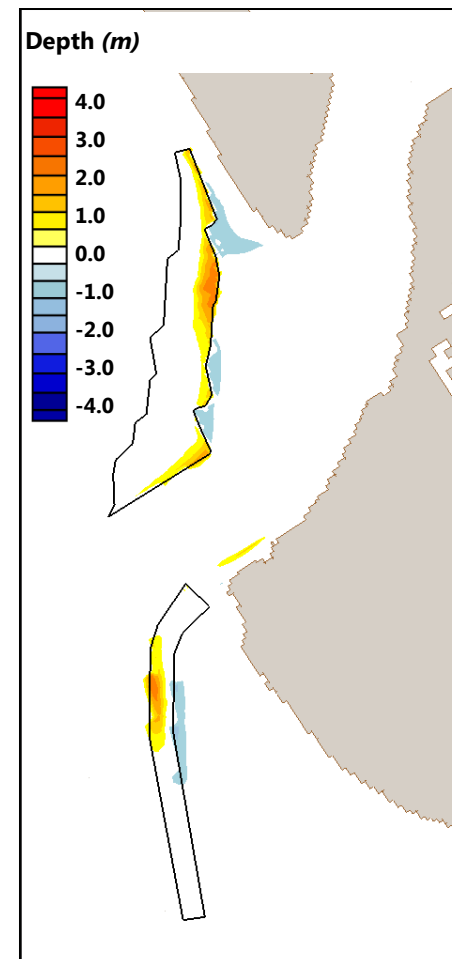


Figure 141: delta Morphology: D3-B vs. N.A.**

7. UPDATED SEDIMENT BUDGETS - FUTURE ALTERNATIVES

Sediment budgets were created for future scenarios as follows:

1. Future Without Nourishment
2. Future With-Project D2-C-B
3. Future With-Project D3*-C-B
4. Future With-Project D3**-B

The method proposed by Bodge (1993; Coastal Engineering Manual Part V-6) was used. See Section 2.1 for details.

7.1. Future Without Nourishment

The system of equations developed for the sediment budget applies values for left and right beaches from the perspective of a seaward-looking observer (**Figure 39**).

Using results from the Existing Sediment Budget,

$$\Delta V_{\text{shoal}} = 37,084 \text{ cy/yr}$$

$$\Delta V_R = -12,833 \text{ cy/yr}$$

The right-directed and left-directed transport rates solved in the Existing Sediment Budget were applied where:

$$R_1 = 17,802 \text{ cy/yr}$$

$$R_2 = 12,800 \text{ cy/yr}$$

$$L_1 = -1 * R_1$$

$$L_2 = -118,800 \text{ cy/yr}$$

Solving for

$$p_1 = (-m_2 L_2 + R_2 + \Delta V_r) / R_1 \quad (6)$$

$$p_2 = 1 + m_2 - \frac{R_1}{R_2} (1 + m_1 - p_1) + \Delta V_{\text{shoal}} / L_2 \quad (7)$$

The volume change at Siesta Key is solved as:

$$\Delta V_L = L_1 - p_2 L_2 - m_1 R_1 \quad (8)$$

To develop the Family of Solutions, the parameters m_1 , and m_2 ranged from 0 to 1:

m_1 = local inlet-induced transport from the left shoreline into the inlet (expressed as a fraction or multiple of the right-directed incident transport, R_1)

m_2 = local inlet-induced transport from the right shoreline into the inlet (expressed as a fraction or multiple of the left-directed incident transport, L_2);

7.1.1. Family of Solutions

To narrow the solutions, a family of solutions was created using knowledge of the region. First, it was specified that net transport into the system is 106,000 cy/yr based upon the sediment budget developed from the Inlet Management Program (2008). It is also assumed that shoaling into Big Sarasota Pass from Lido Key is greater than shoaling from Siesta Key. Further, it is assumed that bypassing from Lido Key is greater than 53,000 cy/yr based upon the sediment budget developed from the Inlet Management Program (2008). Finally, it was assumed, due to the significant amount of net transport from the north, that shoaling from Siesta Key is less than 20% of the total sediment volume entering the ebb shoal each year. These narrowed solutions are shown in Figure 142 where shoaling from the north into the inlet complex was ~ 20,000 cu yd/year and shoaling from the south into the inlet was ~17,000 cu yd/year. At the southern boundary of the study area at Point of Rocks, the net longshore sand transport was to the south at 0 cu yd/year. Transport through the shoal was ~98,000 cu yd/year with ~81,000 cu/yd year bypassed to Siesta Key. The finalized sediment budget is shown in Figure 143.

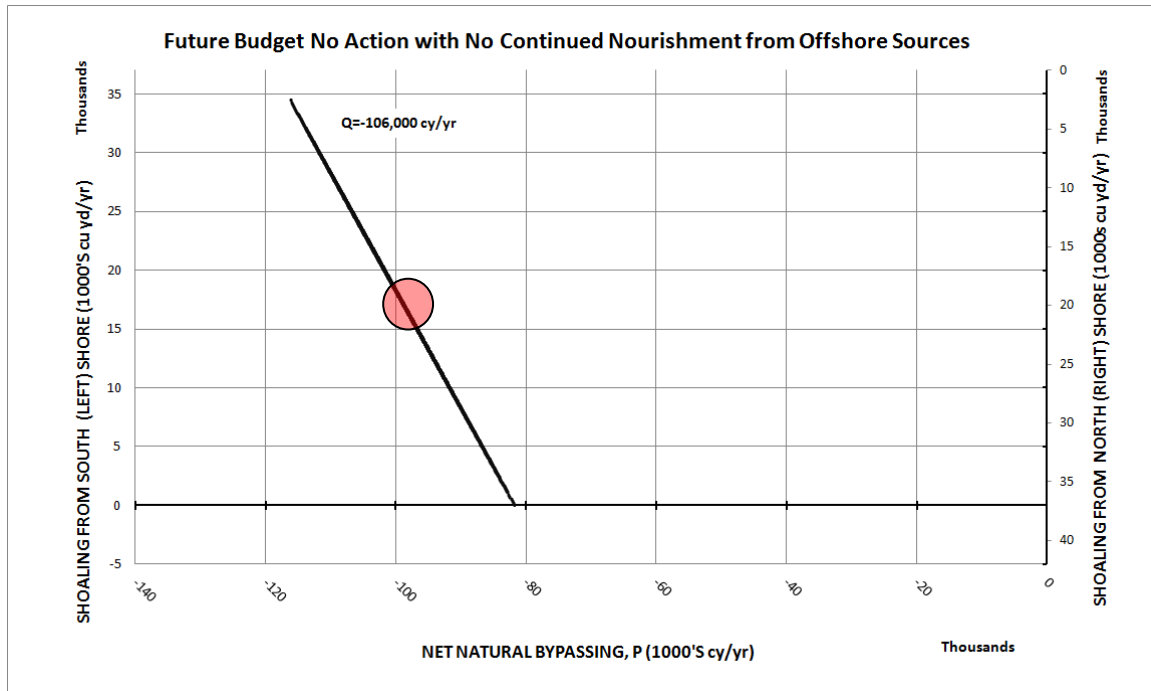


Figure 142: Future Sediment Budget No Action and No Continued Nourishment from Offshore; Narrowed Family of Solutions; Red dot indicates Mean Solution

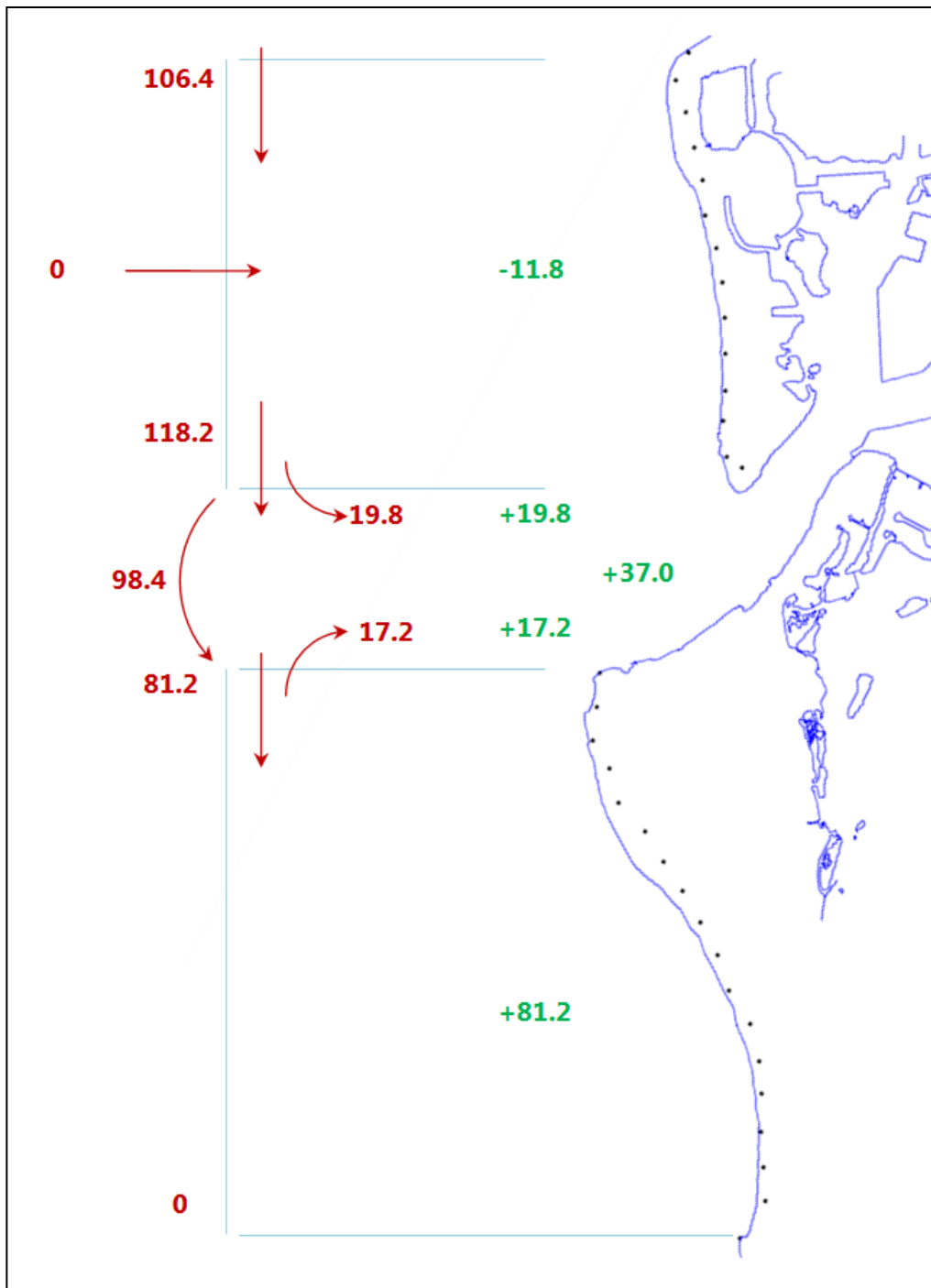


Figure 143: Finalized Sediment Budget Future Condition, “No Action” Alternative and No Offshore Inputs

7.2. Future With-project D2-C-B

Using the results from the CMS numerical model, (Table 15), the net change between the ebb shoal at BSP and Lido Key was 11,122 cy yd/year shoaled into BSP.

$$\Delta V_{\text{shoal}} = 11,122 \text{ cy/yr}$$

$$\Delta V_R = 0 \text{ cy/yr}$$

The right-directed and left-directed transport rates solved in the Existing Sediment Budget were applied as in the previous Section 7.1.

7.2.1. Family of Solutions

The family of solutions were developed using the same assumptions in the previous Section. The narrowed solutions are shown in Figure 144.

The mean solution, shown in Figure 144 has approximately 103,000 cy/yr moving through the inlet. Shoaling from the north into the inlet complex was ~2,500 cy/yr, and shoaling from the south into the inlet was ~8,600 cy/yr. Bypassing to Siesta Key was ~95,000 cy/yr. At the southern boundary of the study area at Point of Rocks, the net longshore sand transport was to the south at 0 cy/yr. The finalized sediment budget is shown in Figure 145. Assuming that 100,000 cy/yr is placed on Lido Key, 101,000 cy/yr erodes from Lido Key (from Table 15) and the net change to Lido Key is 1,000 cy/yr. Including shoaling into BSP, the net change to BSP is 12,100 cy/yr, 103,900 cy/yr moves through the inlet, but 8,600 cy/yr shoals from Siesta Key into BSP, thus the net bypassing to Siesta Key is 95,300 cy/yr.

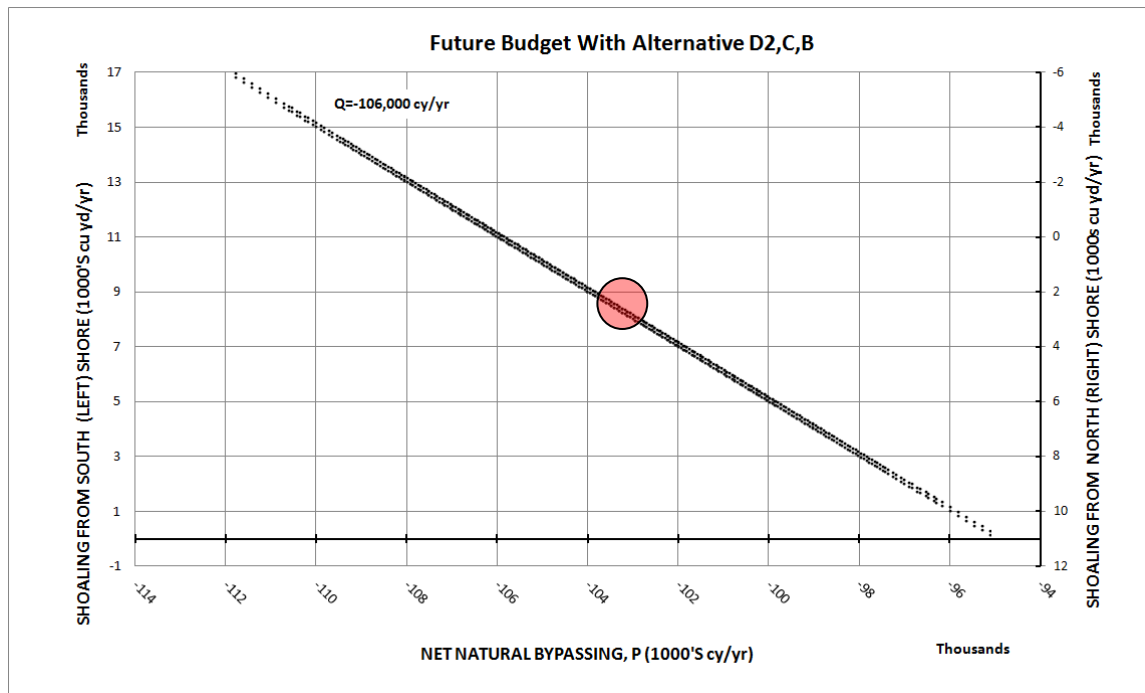


Figure 144: Future Sediment Budget Alternative D2-C-B; Narrowed Family of Solutions; Red dot indicates Mean Solution

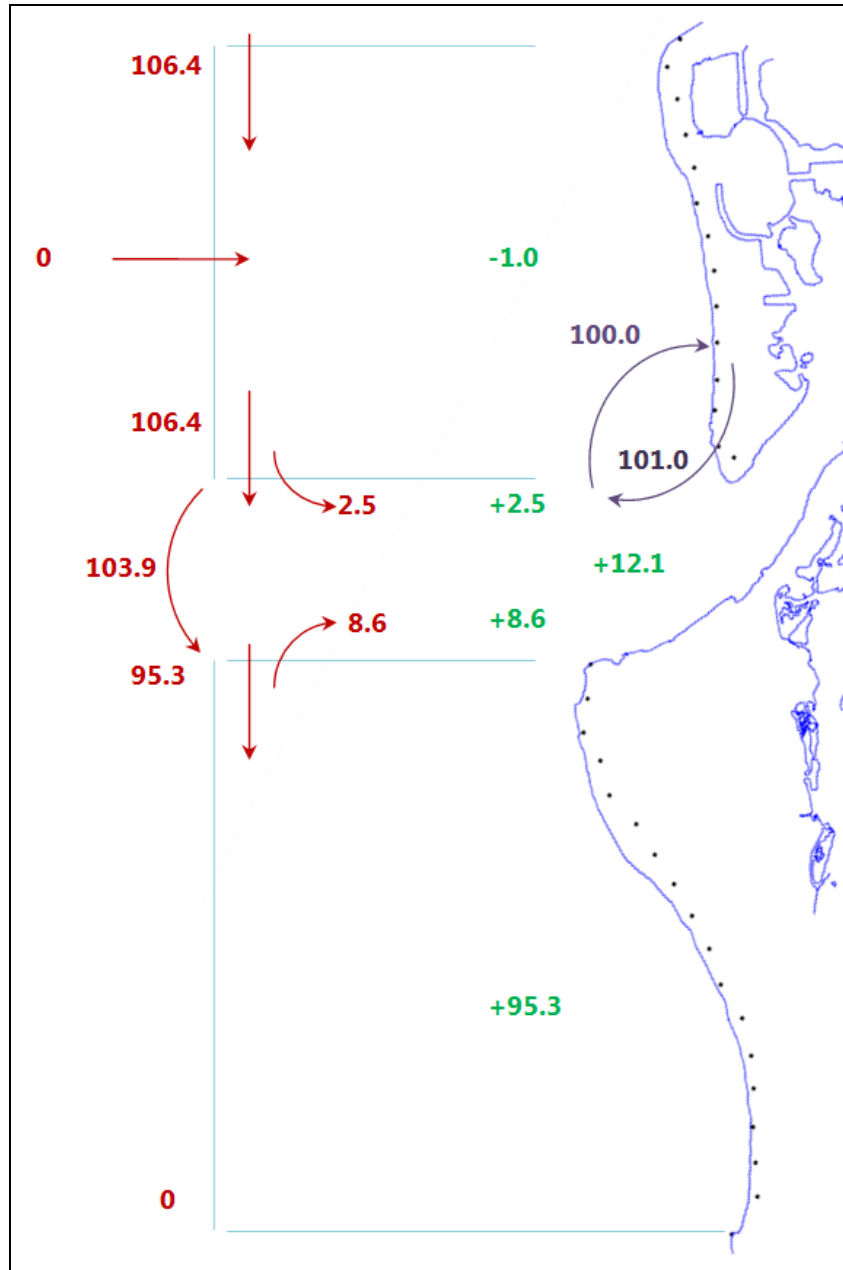


Figure 145: Solutions for Equations in Figure 6 from the Bodge Method (CEM IV-6; USACE 2008); Finalized Sediment Budget Future Condition, Alternative D2-C-B

7.3. Future With-project D3*-C-B

Using the results from the CMS numerical model, (Table 13), the net change between the ebb shoal at BSP and Lido Key was 0 cy/yr.

$$\Delta V_{\text{shoal}} = 0 \text{ cy/yr}$$

$$\Delta V_R = 0 \text{ cy/yr}$$

The right-directed and left-directed transport rates solved in the Existing Sediment Budget were applied as in the previous Section 7.1.

7.3.1. Family of Solutions

The family of solutions were developed using the same assumptions in the previous Section. The narrowed solutions are shown in Figure 146.

The mean solution, shown in Figure 146, has approximately 109,000 cy/yr moving through the inlet. Shoaling into the inlet was negligible for both shorelines. Approximately 106,000 cy/yr is bypassed to Siesta Key. At the southern boundary of the study area at Point of Rocks, the net longshore sand transport was to the south at 0 cy/yr. The finalized sediment budget is shown in Figure 147. Assuming that 100,000 cy/yr is placed on Lido Key, 88,000 cy/yr erodes from Lido Key (from Table 15) and the net change to Lido Key is 12,000 cy/yr. Including shoaling into BSP, the net change to BSP is -12,100 cy/yr, 109,500 cy/yr moves through the inlet, but 3,100 cy/yr shoals from Siesta Key into BSP, thus the net bypassing to Siesta Key is 106,400 cy/yr.

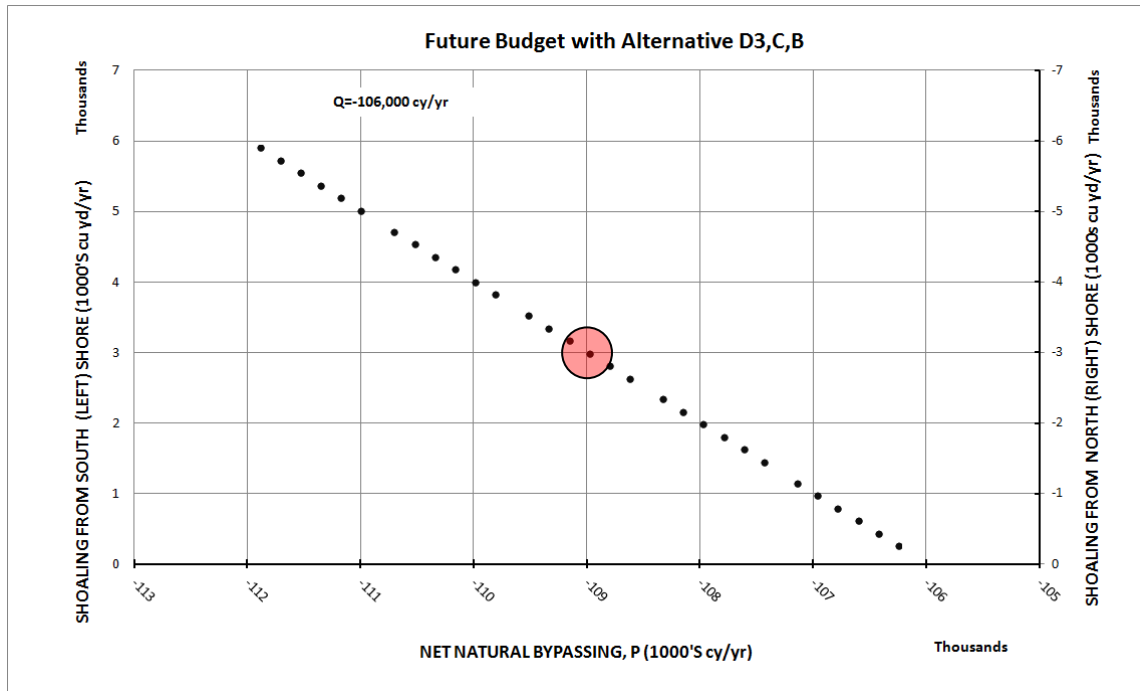


Figure 146: Future Sediment Budget Alternative D3*-C-B; Narrowed Family of Solutions; Red dot indicates Mean Solution

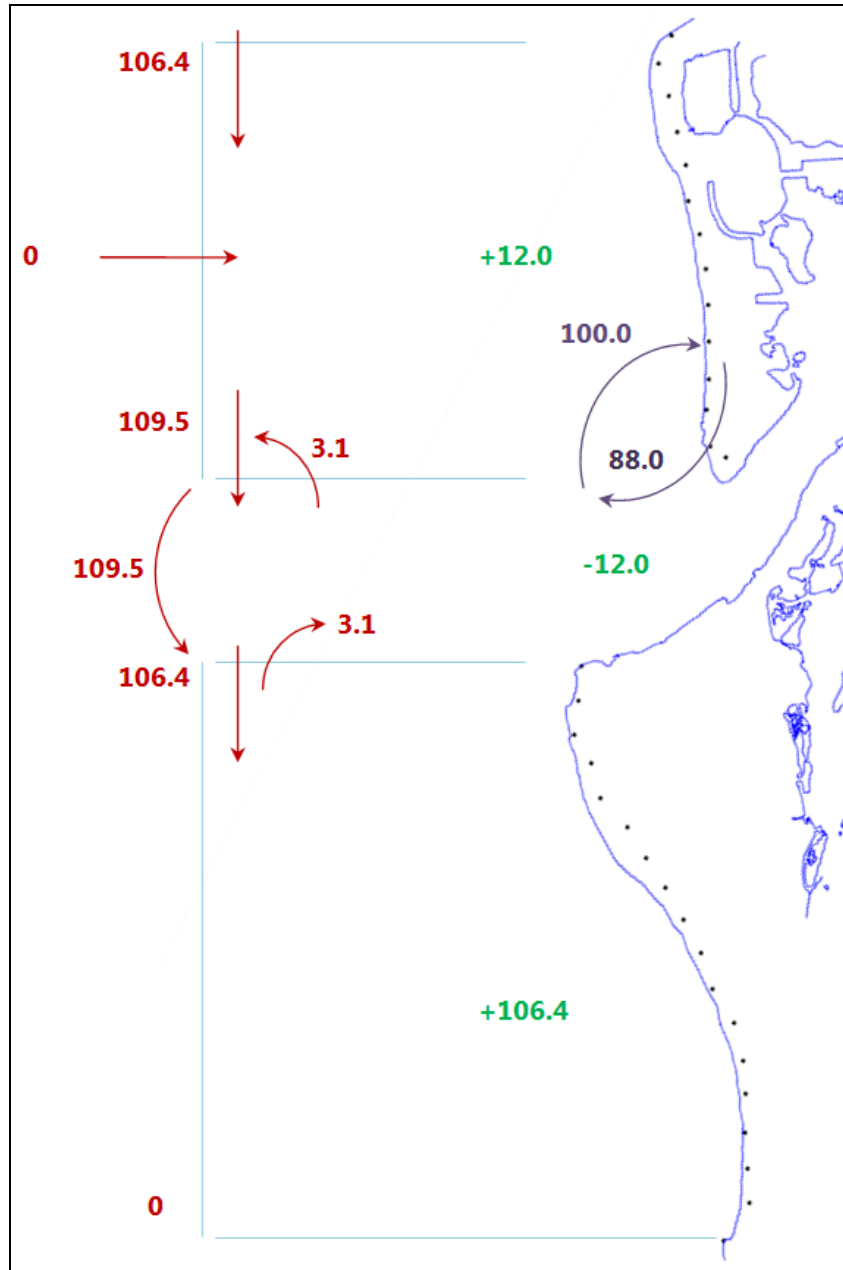


Figure 147: Solutions for Equations in Figure 6 from the Bodge Method (CEM IV-6; USACE 2008); Finalized Sediment Budget Future Condition, Alternative D3-C-B

7.4. Future With-project D3-B**

Using the results from the CMS numerical model, (Table 13), the net change between the ebb shoal at BSP and Lido Key was -24,388 cy/yr erosion on Lido Key.

$$\Delta V_{\text{shoal}} = 0 \text{ cy/yr}$$

$$\Delta V_R = -24,388 \text{ cy/yr}$$

The right-directed and left-directed transport rates solved in the Existing Sediment Budget were applied as in the previous Section 7.1.

7.4.1. Family of Solutions

The family of solutions were developed using the same assumptions in the previous Section. The narrowed solutions are shown in Figure 139.

The mean solution, shown in Figure 148, has approximately 149,500 cu yd/year moving through the inlet. Shoaling from the southern shoreline was 18,000 cy and shoaling from the northern shoreline was zero. At the southern boundary of the study area at Point of Rocks, the net longshore sand transport was to the south at 0 cu yd/year. The finalized sediment budget is shown in Figure 149. Assuming that 100,000 cy/yr is placed on Lido Key, a total of 72,000 cy/yr erodes from Lido Key (from Table 15), 47,000 cu yd/year of that sediment shoals into BSP, the remaining 25,000 cy/yr moves through the inlet to be bypassed to Siesta Key. The net change to Lido Key is 28,000 cy/yr. Including shoaling into BSP, the net change to BSP is -53,000 cy/yr., 149,500 cy/yr moves through the inlet, but 18,100 cy/yr shoals from Siesta Key into BSP, thus the net bypassing to Siesta Key is 131,400 cy/yr.

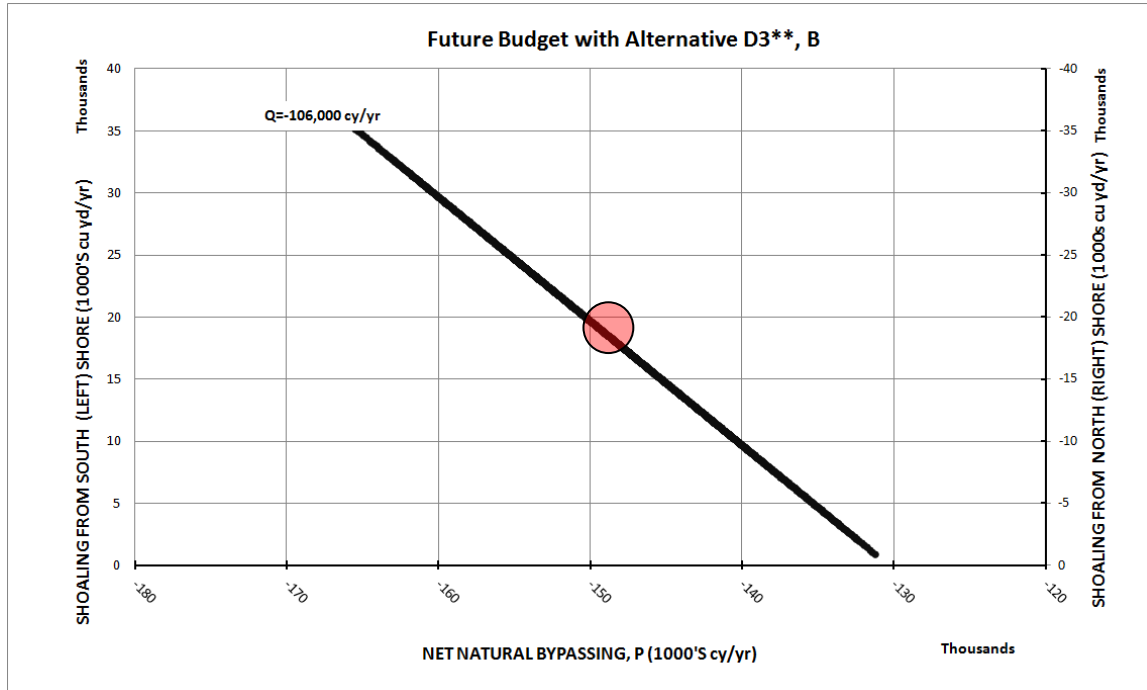


Figure 148: Future Sediment Budget Alternative D3*-C-B; Narrowed Family of Solutions; Red dot indicates Mean Solution

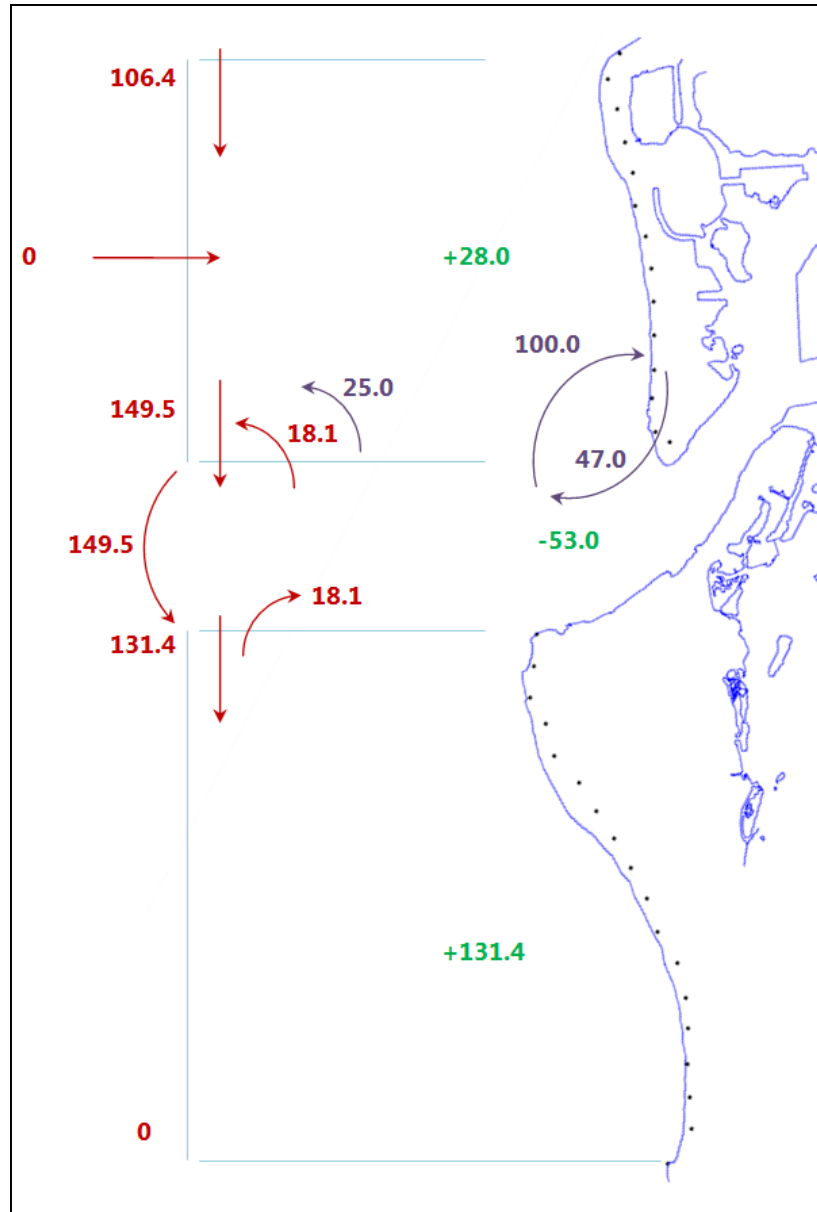


Figure 149: Solutions for Equations in Figure 6 from the Bodge Method (CEM IV-6; USACE 2008); Finalized Sediment Budget Future Condition, Alternative D3-B**

8. DISCUSSION

Big Sarasota Pass has existed with little change since the earliest available maps of the area; however, Lido Key and much of the GIWW have experienced considerable change over the last century. The morphodynamic conditions of Big Sarasota Pass have been influenced by both natural and anthropogenic factors. Both Lido Key and St. Armands Key did not exist 100 years ago and were, instead, a grouping of small islands called the Cerol Isles. During the 1920s, the shallows separating the Cerol Isles were filled by Mr. John Ringling, and the new island became Lido Key.

8.1. Ebb Shoal Volume, Ebb Shoal Growth and Excavation Volume

The total ebb shoal volume from 1955 to 2013 is greater than 20MCY, and its long-term yearly weighted average is 21 MCY. The proposed project would remove approximately 1.3 MCY from the shoal for initial construction, which is about 6% of the total ebb shoal volume measured in 2010 and 2013 which was 23.3 MCY (Figure 150).

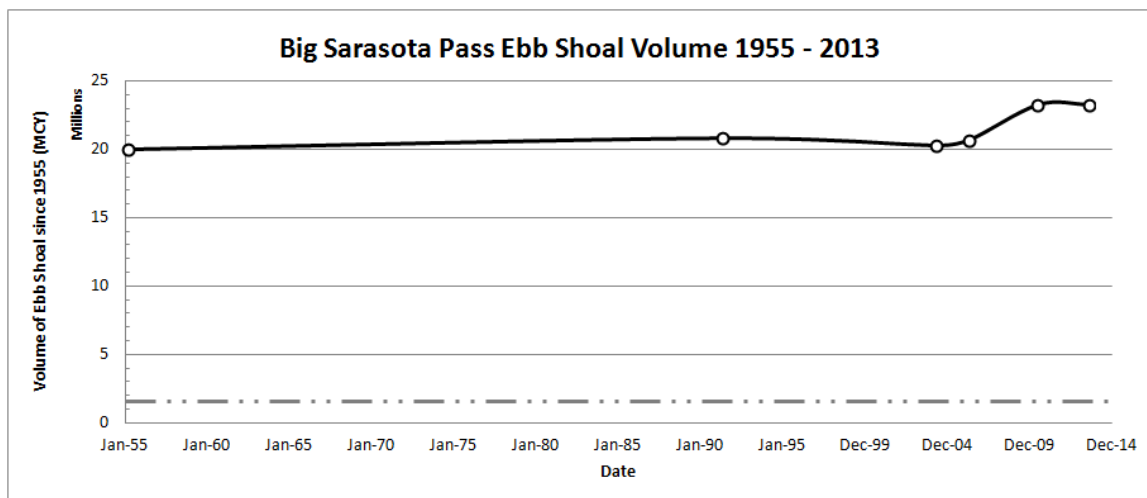


Figure 150: Volume of sediment using method by Walton and Adams (1979) at Big Sarasota Pass, change in volume from 1955 to 2013. Grey dotted line represents the volume to be removed from the ebb shoal by the Lido Key Shore Protection Project.

The volume of the ebb shoal has increased in the last decade by approximately 2.3 MCY from its long-term average of 21 MCY, which is most likely due to the influx of offshore sediments for nourishment projects on Lido and Longboat Keys (Figure 151). Here, a reduction in ebb shoal volume of 1.3 MCY would leave a surplus of sediment over the 2004 volume. The ebb shoal would have a volume of

approximately 22 MCY after removal which is 1MCY more than the long-term average of 21 MCY (Figure 151).

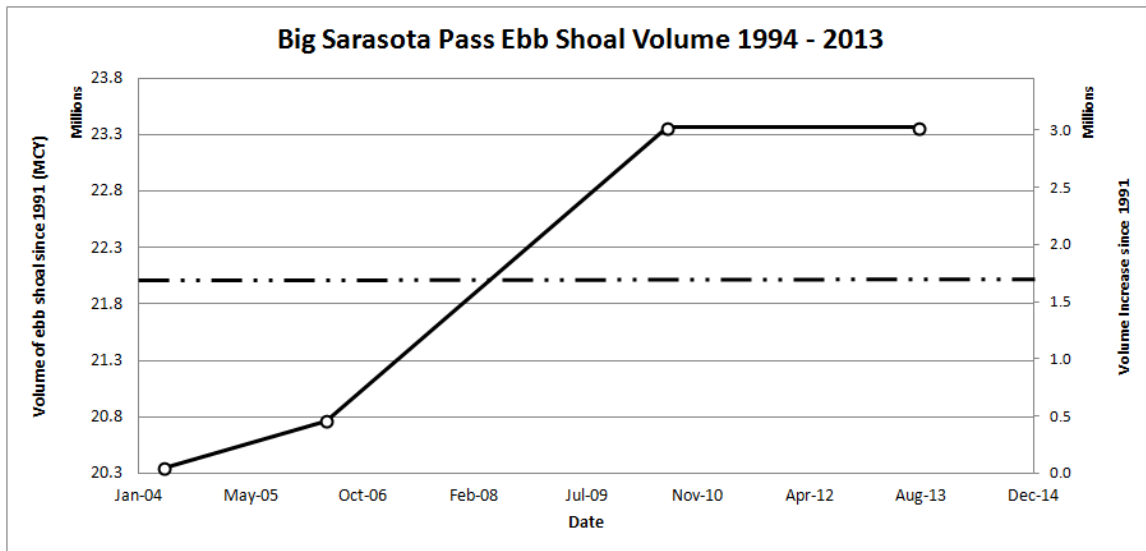


Figure 151: Ebb Shoal Growth in the past decade; 1.3 MCY reduction leaves a surplus of sediment

8.2. The Creation of Lido Key and the migration of the Main Ebb Channel

As discussed previously, the migration of the main ebb channel in Big Sarasota Pass caused the southward shift in the ebb shoal attachment point, erosion on the northern beaches of Siesta Key, and the confinement of the channel against the northern shoreline of Siesta Key. The infilling of the Cerol Islands and dredging of the GIWW have changed the tidal prism and flow structure of tidal currents through the inlet as well as the alongshore currents due to the creation of a new surf zone fronting Lido Key. These changes have lead to an increase in sediment transport to the southeast that has shifted the main inlet channel to the southeast against Siesta Key. SAJ used CMS to model the flow and sediment transport using the measured bathymetry from 1883 to qualitatively compare with flows and sediment transport from 2004 to gain further insight into how transport patterns and main ebb channel location have changed.

A CMS grid was developed using the bathymetry for Big Sarasota Pass in 1883 (Figure 10). The model was run for a six-month period using waves and water elevations from May to November 2004. These results were compared with the 2004 “No Action” Alternative presented in Section 3.4.

Sediment transport vectors were then summed over the duration of the model run to determine integrated transport pathways for each alternative so that changes in sediment transport pathways relative to both conditions in 1883 and the “No Action” from 2004 could be determined.

Figure 152 through Figure 154 show integrated transport pathways for the ebb shoal in 1883. Figure 152 shows the cumulative summation of the sediment concentration and integrated transport vectors for the six-month run. Here, sediments are transported over the northwestern portions of the shoal to the southeast. Figure 153 shows the integrated transport vectors over the bathymetry and Figure 154 shows sediment transport vectors over morphologic change for 1883. Overall, because flows can move through the gaps in the Cerol Islands, flow is not concentrated through the main channel of Big Sarasota Pass. Subsequently, there is not much sediment transport or morphologic change because flows are very diffuse and bed stresses are low. Sediments are suspended but are not readily advected to a new location and morphologic change is rather modest (Figure 154).

Figure 155 through Figure 157 show integrated transport pathways for the ebb shoal in 2004. Figure 155 shows the integrated transport vectors and the integrated sediment concentration. Compared to the 1883 condition (Figure 152), there is greater sediment concentration and transport in the surf zone fronting Lido Key and over the northern lobe. Figure 156 and Figure 157 show the integrated transport vectors over the bathymetry and morphologic change, respectively. Compared with the 1883 condition, sediment transport is highly directed toward and concentrated in the main ebb channel. In addition, the morphologic change for the modern time period is concentrated in the main channel (Figure 157).

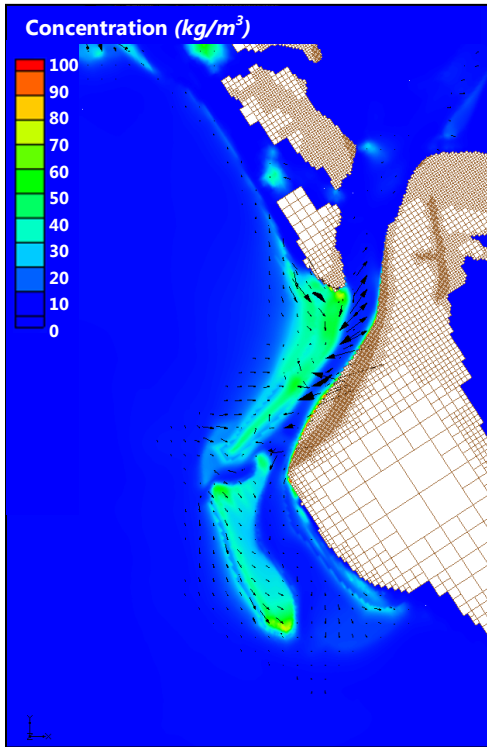


Figure 152: Integrated sediment transport concentration and transport vectors for 1883 bathymetry

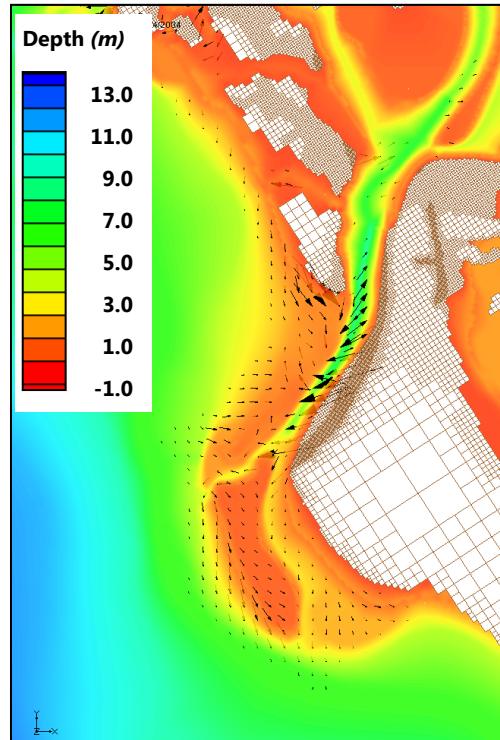


Figure 153: Integrated sediment transport vectors final bathymetry for 1883 bathymetry

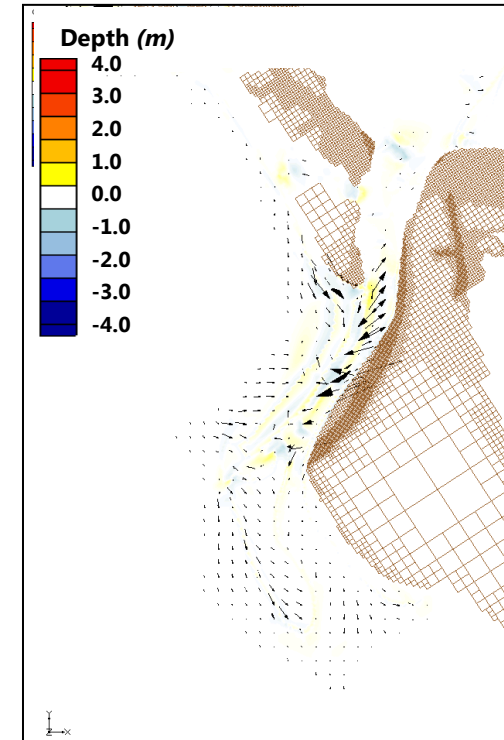


Figure 154: Integrated sediment transport vectors final morphologic change for 1883 bathymetry

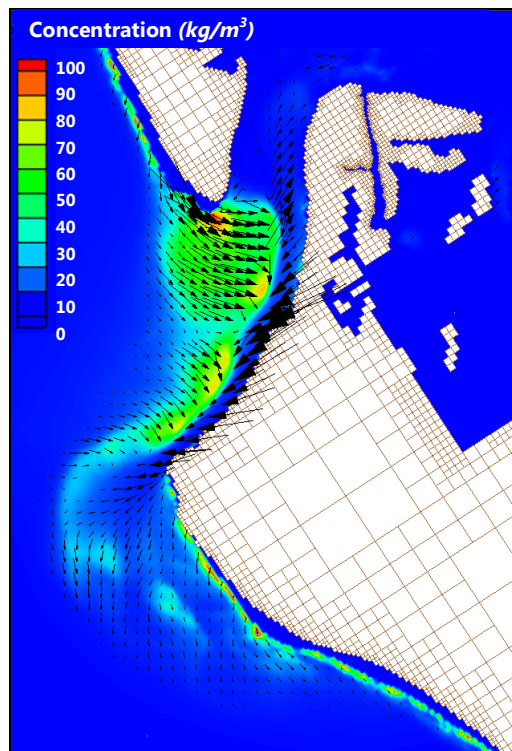


Figure 155: Integrated sediment transport concentration and transport vectors for 2004 bathymetry

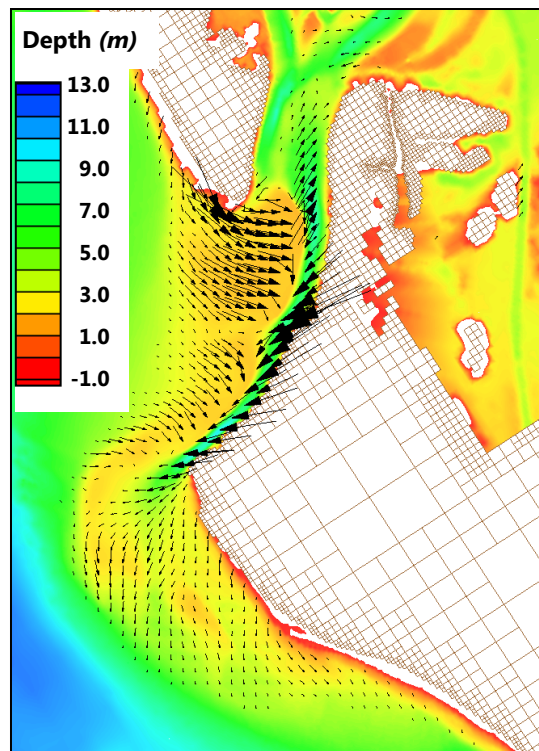


Figure 156: Integrated sediment transport vectors final bathymetry for 2004 bathymetry

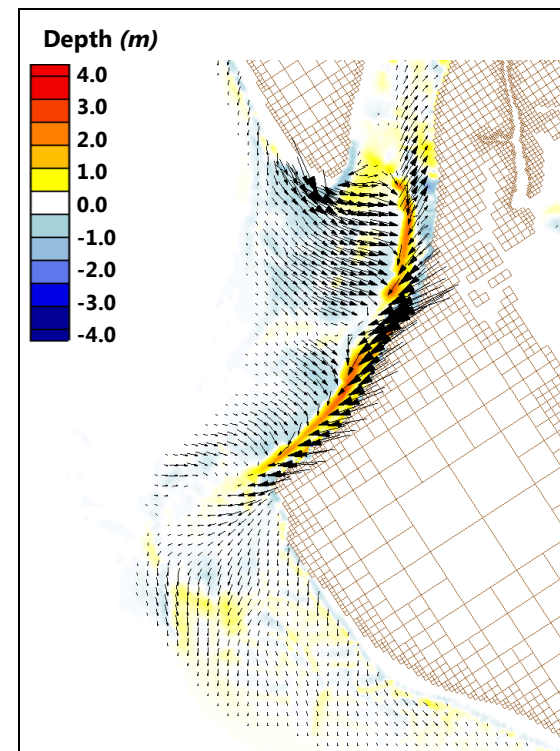


Figure 157: Integrated sediment transport vectors final morphologic change for 2004 bathymetry

Figure 158 compares the 1883 and 2004 bathymetry transport vectors and morphology. It can be readily observed that transport has increased at the southern end of Lido Key, which has increased erosion in this region. In addition, and most important, it is clear that transport has been increased toward the main ebb channel and transport has been increased toward the southwest, away from the most westerly tip of Siesta Key. The main ebb channel has eroded back into the northern shoreline of Siesta Key that had been land in 1883 (Figure 158 and Figure 159), and in response, the northern shoreline of Siesta Key was hardened with armoring structures. The Interim Report on Lido Key (USACE, 1962) notes that a swash channel occasionally breaks through to the north of the main channel, but is ineffective in that it does not remain open for a time period that would provide relief to the northern shoreline of Siesta Key. Overall, the expanse of the ebb shoal northwest of the main ebb channel has deflated and the region adjacent, directly to the west of the main ebb channel has shoaled. In addition, there is marked deposition and westward migration of the shoreline fronting the portion of Siesta Key directly north of Point ‘O Rocks 1883 (Figure 158 and Figure 159).

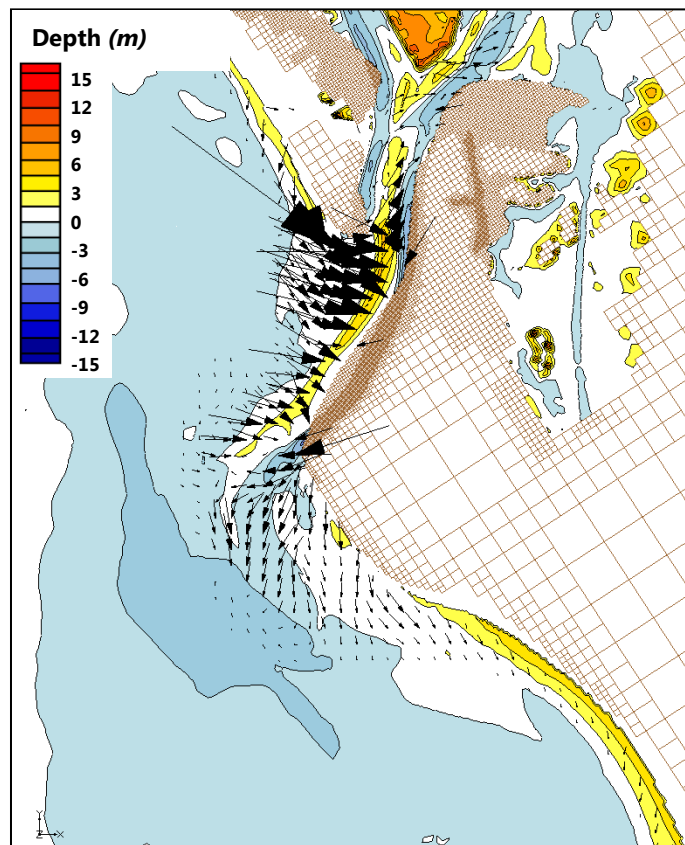


Figure 158: Difference in morphology and difference in total transport vectors between 1883 and 2004

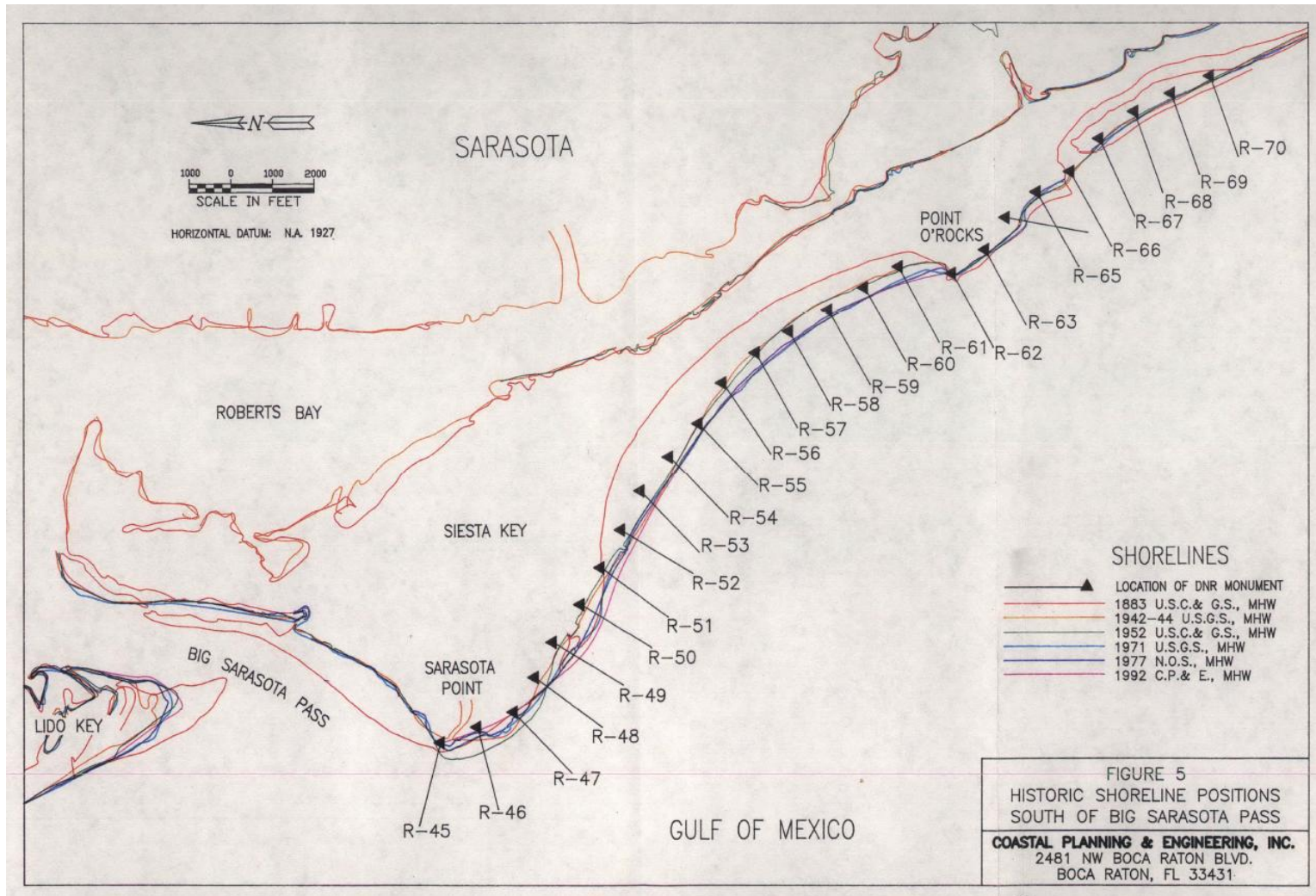


Figure 159: Shoreline change (from 1992 IMP CPE)

Examination of the differences in residual transport pathways between 1883 and 2004 have shown that alongshore sediment transport has increased at the southern end of Lido Key, which has increased shoreline erosion in this region. Because of the anthropogenically induced gradient in sediment transport at the south end of Lido Key, there exists a need to continually add sediment to maintain the beaches of Lido Key. In addition, it can be readily seen that transport has been increased toward the main ebb channel and transport has been increased toward the south, away from the most westerly tip of Siesta Key. The main ebb channel has eroded back into the northern shoreline of Siesta Key – which had been land in 1883, and in response, the northern shoreline of Siesta Key was hardened with armoring structures. A swash channel occasionally breaks through to the north of the main channel, but does not remain open for a time period that would provide relief to the northern shoreline of Siesta Key. Since the anthropogenic changes to the Cerol Islands and the GIWW, there is unyielding and constant transport to the south across the shoal, and the main ebb channel remains pinned to the north interior shoreline of Siesta Key. So long as the main ebb channel remains at that location, there is no relief for the beaches of Siesta Key which are north of the attachment point of the ebb shoal.

8.3. Selected Alternatives

Several alternatives were tested using the Coastal Modeling System to screen those that would be unacceptable in terms of for following four criteria: (1) the response and evolution of the inlet and ebb shoal morphology as a function of mining the ebb shoal at Big Sarasota Pass; (2) changes to the wave climate as a function of modified bathymetry at the borrow site; (3) response of the ebb tide channel (navigation channel) to due to the evolution of the inlet complex morphology; and (4) changes in sediment transport pathways that exchange sediments between the ebb shoal and adjacent beaches.

Alternatives were developed using those outlined in the Sarasota County Comprehensive Inlet Management Program Pig Pass and New Pass Management Alternatives, (2008). Alternatives were tested with the CMS to determine if any had adverse effects according to the four criteria described previously. The large contour Cut D3 was removed from the array of possible alternatives because it increased and focused wave energy on the shoreline at Siesta Key (Appendix A). Despite the fact that no adverse morphologic impact was seen at Siesta Key, the risk associated with an increase in wave energy at the region is unacceptable by stakeholders and was considered a justifiable reason to screen out this alternative. Alternatives D2, D1, C and B all had acceptable results from the CMS and did not cause adverse impacts to ebb shoal-inlet complex morphology, to the wave climate and to the navigation channel. None of these alternatives alone demonstrated the ability to yield the

required 1.3 MCY for the shore protection project at Lido Key. Three new alternatives were developed by first modifying the contour cut, D3 and then using different combinations of Cuts D3, D2, C and B to yield the amount of sediment needed for initial construction of the project and each was screened for impacts to adjacent beaches, ebb shoal morphology and impacts to navigation. One of the three new alternatives, D2-C-B, is no longer under consideration because Cut D2 unnecessarily creates artificial and unnatural contours in the ebb shoal. The corners of Cut D2 will infill rapidly as the ebb shoal returns to a more natural state with gently sloping contours. The two remaining alternatives that were considered further are consider Alternative D3*-C-B and Alternative D3**-B, only.

Alternative D3*-C-B would mine 1.45 MCY of sediment from the ebb shoal. The ending morphology for this Alternative included infilling of Cut C and slight infilling of Cut B. When compared with the morphologic change of the “No Action” Alternative, Alternative D3*-C-B induced slightly more ebb shoal deflation across the north lobe, where wave energy traverses Cut D3 without being attenuated. There is also ebb shoal deflation just to the east of Cut C where sediments are transported both into Cut C as well as into the main ebb channel. The downdrift attachment point at Siesta Key was unchanged from the “No Action” Alternative, and increases in wave energy were not significant except for the most southern extent of Lido Key due to the proximity of Cut D3 to the Lido Key. Further, there were no impacts to navigation. Integrated transport vectors showed a good deal of sediment transport being directed toward Cut C. Comparison with the “No Action” Alternative showed that transport was being redirected away from the main ebb channel and toward Cut C. This is significant for two reasons. First, it provides relief for the main ebb channel; the constant eastward pressure on the main ebb channel through Big Sarasota Pass is relieved by Cut C. Second, it results in the reduction of shoaled sediments in the main ebb channel. CMS modeling showed that for this alternative, 100% of the sediment that erodes from Lido Key will be deposited into the ebb shoal.

Alternative D3**-B would mine 1.38 MCY of sediment from the ebb shoal. The ending morphology for this Alternative included very little infilling, if any, of Cut D3** for six month runs and slight infilling of Cut B. When compared with the morphologic change of the “No Action” Alternative, Alternative D3**-B induced slightly more ebb shoal deflation across the north lobe, where wave energy traverses Cut D3 without being attenuated but very little change elsewhere throughout the ebb shoal complex. Increases in wave energy were insignificant except for the most southern extent of Lido Key due to the proximity of Cut D3 to the Lido Key and navigation was not impacted. Morphology and the location of the attachment point at Siesta Key were not changed from the “No Action” Alternative. Integrated sediment transport comparison with the “No Action” Alternative showed very little

difference except for lightly increased transport into cuts D3** and B themselves. Overall, option D3**-B is a very conservative option with regard to changes in the ebb shoal. This option induces very little change to the ebb shoal, carries very little risk, but also provides no opportunity to relieve the pressure of the main ebb channel against the north bank of Siesta Key. CMS modeling showed that for this alternative approximately 66% of the sediment that erodes from Lido Key moves into the ebb shoal and approximately 34% of what erodes at Lido Key will bypass the ebb shoal and move to Siesta Key.

8.4. Sediment Budgets

For the future project D3*-C-B sediment budget, it was shown that the most important source of sediment to downdrift beaches is the net flux into the system from northerly beaches. The CMS numerical model indicated that 100% of the erosion at Lido Key that originated from the nourishment placement would be returned to the ebb shoal. All of the incident transport from the north, 106,000 cy/yr is bypassed to Siesta Key. Cut C is essentially a settling basin for sediments that had been used for the nourishment of Lido Key and are returning to the ebb shoal.

For the future project D3**-B sediment budget, that the most important source of sediment to downdrift beaches is the net flux into the system from northerly beaches as well as a portion of the sediments that were removed or “unlocked” from Big Sarasota Pass ebb shoal and placed onto Lido Key. All of the incident flux into the system; 106,000 cy/yr is bypassed to Siesta Key. In addition, 36% (25,000 cy/yr) of the placement onto Lido Key is passed to the shoal. 18,000 cy/yr is shoaled into BSP from Siesta Key and, in total, approximately 131,000 cy/yr is bypassed to Siesta Key. Cut D3** (a contour cut), offers no place in which sediments can settle, and instead sediments are swept across the north lobe of the ebb shoal into the navigation channel in the same manner as the existing and “No Action” Alternative. Once sediments are transported to the main ebb channel, they are bypassed to the south lobe of the shoal.

8.5. Alternative Scenarios

Between options D3*-C-B, and D3**-B, there exist benefits and risks associated with each. The can be summarized in the Table 14 below.

Table 14: Alternatives Risks and Benefits

	Alternative D*-C-B	Alternative D**-B
Meets volume requirement for the project	Yes	Yes
Does not alter ebb shoal planform beyond the borrow sites	Yes	Yes
Does not change sediment transport pathways	No, sediment is redirected into Cut C. This is a change from the Existing and No Project Condition. There exists inherent risk in the alteration of sediment transport pathways, however major benefits can be provided by providing relief for the eastern migration of the main ebb channel which continues to cut into the northern shoreline of Siesta Key. Existing transport pathways across the northern lobe and into the main ebb channel are still intact.	Yes
Does not affect navigation	Yes. Improves navigation by redirecting sediment away from the main ebb channel. This seems counter-intuitive from the Bernoulli principle, however, flows remain strong enough to keep the main ebb channel from shoaling to a greater extent than the "No Action" Alternative	Yes. No excessive shoaling exists.
Does not significantly increase wave energy	Yes	Yes

Does not change the morphology at Siesta Key	Yes	Yes
Does not cause the attachment point for Siesta Key to move further to the southeast	Yes.	Increased transport to Siesta Key which will include some of the sediment mined from the ebb shoal and placed on Lido Key may cause the attachment point to migrate further to the east because of the increased sediment load
Does not cause downdrift effects as indicated by the sediment budget	Yes.	Yes. In fact, may significantly increase transport to downdrift beaches
Does not cause the volume of the ebb shoal to decrease over time	Yes. Numerical modeling indicates that close to 100% of the sediment removed from the ebb shoal will return to the ebb shoal.	No. Numerical modeling indicates that approximately 44% of the sediment removed from the ebb shoal will be bypassed south of the shoal.

With regard to project borrow site formulation and overall volumes, the project would remove at maximum 6% of the existing shoal volume. The ebb shoal at Big Sarasota Pass has traditionally been between 21 MCY and 24 MCY since 1883, and the project requires approximately 1.3 MCY from the shoal. There appears to be a strong correlation between the volume of sediment that has been transported to Sarasota County beaches from offshore and the growth of the ebb shoal, and since 2004, the ebb shoal has grown by 3 MCY. The volume as of August 2013 is approximately 23.3 MCY, which is significantly more than its long-term volume of 20 MCY. The project would use at most 56% of the accreted volume, which would leave a surplus at Big Sarasota Pass over the long-term yearly average ebb shoal volume of approximately 21 MCY.

To recap, it is found here that mining source sediment from the ebb shoal at Big Sarasota Pass is a viable option for the Shore Protection Project at Lido Key. A dredging configuration can be constructed which does not induce undesirable morphologic change at the ebb shoal, does not increase wave energy or affect navigation. Dredging configurations have been found that may potentially alleviate pressure on the interior north shoreline of Siesta Key, if desired. It has been found that sediment transport volumes to downdrift beaches will not be affected because

essentially, “new” sediment is brought into the system by “unlocking” that which has been sequestered in the ebb shoal at Big Sarasota Pass for decades. It has been found through historical volume analysis that the project seeks to remove 6% of the total ebb shoal volume. In addition, it has been found that the borrow volume constitutes 56% of the volume which has accreted to the ebb shoal in the past decade, most likely due to the introduction of sediment into the system from offshore sources. Judicious consideration of the risks and benefits associated with the two selected alternatives must be performed before final selection of the borrow configuration. However, at this point in the study analysis, it has been found that both Alternatives will meet the objectives of the Lido Key Shore Protection Project without negatively impacting ebb shoal morphology, wave energy, sediment transport pathways, navigation and downdrift beaches.

9. CONCLUSIONS

Historically, Lido Key is an artificial island that was filled in the 1920’s. The ebb shoal at BSP was more symmetrical before the infilling of Lido Key and dredging of the GIWW, as can be seen in the 1883 bathymetry, but by 1940’s ebb shoal and main ebb channel was skewed toward the south. By 1960 it was well established that increased erosion mid-island, accelerated erosion at the southern tip of Lido Key as well as the migration of the main ebb channel against the northern shoreline of Siesta Key was well underway due to increased gradient in alongshore transport which was most likely due to the creation of the surf-zone during the infilling of the Key. At present, currents due to wave forcing are pushing sediment into main ebb channel – pinning the channel to the north interior bank of Siesta Key.

The volume and planform shape of the ebb shoal at BSP (~21 MCY) has changed little since 1883. It was found from the analysis herein that it is possible to remove 1.3 MCY of sediment from the ebb shoal without changing the planform area of the shoal. Further, it was determined that the project would be mining approximately 6% of the entire shoal volume. The mining volume is 56% of the “excess” sediment above the historical average of 21 MCY that has accreted over the past decade. The present volume of the ebb shoal of BSP is 23.3 MCY. After dredging, the volume would be approximately 22 MCY.

Results from the CMS model have shown that it is possible to mine the ebb shoal without affecting sediment transport pathways that deliver sediment to downdrift beaches (Siesta Key). Further, it is possible to mine the ebb shoal without affecting navigation through the main ebb channel and without significantly increasing nearshore wave energy, especially in the vicinity of Siesta Key.

With regard to sediment transport and location of main ebb channel, sediment mining from BSP can be conducted in such a way to redirect transport away from the main ebb channel and toward Cut C. This action is expected to take pressure off the main ebb channel and possibly move the channel slightly to the north, away from the interior shoreline of Siesta Key.

Lastly, it was found that it is possible to mine the ebb shoal in a sustainable manner using Cut C as a deposition basin thus preserving the long-term average volume of the shoal by recapturing that sediment which had been mined from the shoal. Further, a deposition basin will serve as an added measure to keep the attachment point from translating further to the south along Siesta Key by serving as a buffer against large volumes of sediment moving through the ebb shoal over an unnaturally short time-frame.

10. REFERENCES

Antonini, G., D. Fann, and P. Roat. "A Historical Geography of Southwest Florida Waterways Volume One: Anna Maria Sound to Lemon Bay." Florida Sea Grant Publication SGE47. University of Florida, Gainesville, Florida (1993).

Bodge, K.R., 1993. Gross Transport Effects at Inlets. Proceedings of the 6th Annual National Conference on Beach Preservation Technology (Tallahassee, FL, Florida Shore & Beach Preservation Association), pp. 112–127.

Buttolph, A. M., Reed, C. W., Kraus, N. C., Ono, N., Larson, M., Camenen, B., Hanson, H., Wamsley, T., and Zundel, A. K. 2006. Two-Dimensional Depth-Averaged Circulation Model CMS-M2D: Version 3.0, Report 2, Sediment Transport and Morphology Change. Technical Report ERDC/CHL-TR-06-7, US Army Engineer Research and Development Center, Coastal and Hydraulics Laboratory, Vicksburg, MS.

Camenen, B., and Larson, M. (2007). A Unified Sediment Transport Formulation for Coastal Inlet Application. Contract Report ERDC/CHL-CR-07-1, US Army Engineer Research and Development Center, Coastal and Hydraulics Laboratory, Vicksburg, MS.

Coastal Planning & Engineering, Inc. Big Sarasota Pass Inlet Management Plan, Interim Report No. 2 Submitted to: City of Sarasota. October, 1992

Coastal Planning & Engineering, Inc. Lido Key Beach Renourishment Project New Pass Borrow Area Modeling Study City of Sarasota, Florida. Submitted to: City of Sarasota. June, 2008.

Coastal Tech., USF, CEC. Sarasota County Comprehensive Inlet Management Program Big Pass and New Pass Management Alternatives. Sarasota County. 2008

Davis, Richard A. and Ping Wang. "Sediments and Processes at Big Sarasota Pass, Sarasota Florida." 2004.

Davis, Richard A., Ping Wang, and Tanya Beck. "Natural and anthropogenic influences on the morphodynamics of Big Sarasota Pass, Florida." Coastal Sediments' 07 (2007): 1582-1588.

Kowalski, K. A., 1995, Morphodynamics of Big Sarasota Pass and New Pass ebb-tidal deltas, Sarasota County, Florida. Univ. South Florida, MS Thesis, 144 p.

Kraus, Nicholas C. "Engineering of tidal inlets and morphologic consequences." *Handbook of Coastal Engineering* 31 (2009).

Lin, L., Demirbilek, Z., Mase, H., Zheng, J., and Yamada, F. 2008. CMS-Wave: A Nearshore Spectral Wave Processes Model for Coastal Inlets and Navigation Projects. ERDC/CHL-TR-08-13, US Army Engineer Research and Development Center, Coastal and Hydraulics Laboratory, Vicksburg, MS.

Tolman, H. L., (2009) User manual and system documentation of WAVEWATCH III Version 3.14. Environmental Modeling and Analysis Branch, NOAA. MMAB Contribution No. 276

Truitt, Cliff. "Tidal Inlet Dynamics." Sarasota Bay National Estuary Program MML, Project 310.419 (1992).

USACE Coastal Engineering Manual. (2008) EM 1110-2-1100 (Part V) 31 Jul 03

USACE. Detailed Project Report On Sarasota Passes, Sarasota, Fla. U.S. Army Engineer District, Jacksonville. Corps of Engineers, Jacksonville, Fla. July 30, 1962

USACE. Beach erosion control study Sarasota County, Florida Interim Report on Lido Key. Dept of the Army. Jacksonville District, Corps of Engineers. Jacksonville Florida. 1968.

USACE. Lido Key Sarasota County, Florida Hurricane and Storm Damage Reduction Feasibility Report with Environmental Assessment. U.S. Army Corps of Engineers, Jacksonville District. (2004)

Walton, T., & Adams, W. (1976). CAPACITY OF INLET OUTER BARS TO STORE SAND. Coastal Engineering Proceedings, 1(15). doi:10.9753/icce.v15.

Wang, Ping, Tanya Beck, and Richard A. Davis. "Sarasota County Inlet Project." (2007).

Watanabe, A. 1987. 3-dimensional numerical model of beach evolution. Proceedings Coastal Sediments '87, 802-817.

Wu, W., Zhang, M., and Sanchez, A. 2010. An implicit 2-D shallow water flow model on unstructured quadtree rectangular mesh. Journal of Coastal Research, submitted.

11. APPENDIX A

11.1. Alternative D3

Alternative D3 would mine 2.7 million cubic yards from Big Sarasota Pass to -16' MLW along a contour cut at the western edge of the shoal. Figure 160 shows the bathymetry and ebb shoal morphology at the end of the six month model run from May 4, 2004 to November 4, 2004. Examination of the ending morphology shows that for the "No Action" case (Figure 160 left), the general deflation of the updrift shoal as the main channel infills with sediment that had originated on the shoal. There is erosion of the most northerly flood marginal channel at the southern tip of Lido Key and increased definition (erosion) of the flood marginal channels across the updrift shoal.

Examination of the ending morphology for Alternative D3 (Figure 160, right) shows very little infilling of Cut D3, which indicates that sediment bypassing is still occurring, and shows that the remainder of the shoal does not change relative to the "No Action" Alternative. The greatest difference between the two cases is the location of Cut D3.

Figure 161 and Figure 162 show differences both vertically and temporally between the "No Action" Alternative and Alternative D3, directly. In Figure 161, the most significant change spatially between both alternatives is the dredge site itself. The residual depression in bathymetry at Cut D3 can be readily seen which are approximately 3 ft to 16 ft deeper than the "No Action" Alternative. There is slight accretion at the western edge of the navigation channel due to the slight deflation of the north lobe of the ebb shoal, sediments picked up by waves in this region are deposited at the edge of the navigation channel. In Figure 162, the temporal change from May to November 4, 2004 can be seen for Alternative D3. Here the slight deflation of the northern lobe and infilling of the navigation channel are readily observed. Here, as demonstrated by Figure 161, there is a slight difference in the bathymetry at the location of the navigation channel, especially on the most south-westerly portion of the channel when comparing the "No Action" Alternative with Alternative D3.

Also calculated from the model results was the normalized cumulative wave energy throughout the model grid Figure 163. The most northwest point of Siesta Key receives 1.6 times more energy with the project than without. This result is due to the fact that Cut D3 allows more wave energy to the northwesterly portion of the shoal, directly to the east of the cut. The increased depth of Cut D3 decreases friction at that location, which in turn does not allow for wave attenuation as waves traverse the mining site.

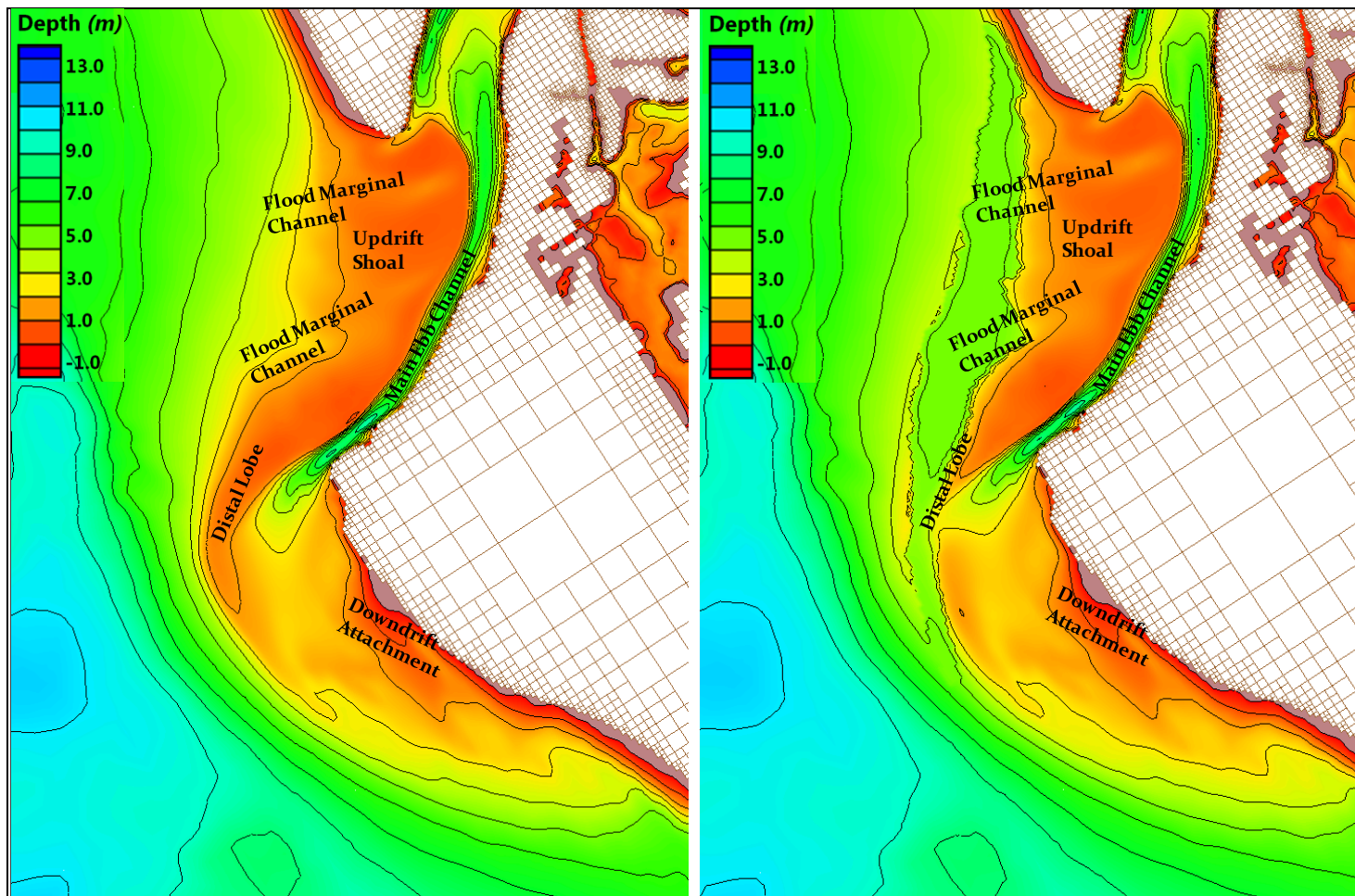


Figure 160: “No Action” Alternative (left), Alternative D3 (right); end state November 2004

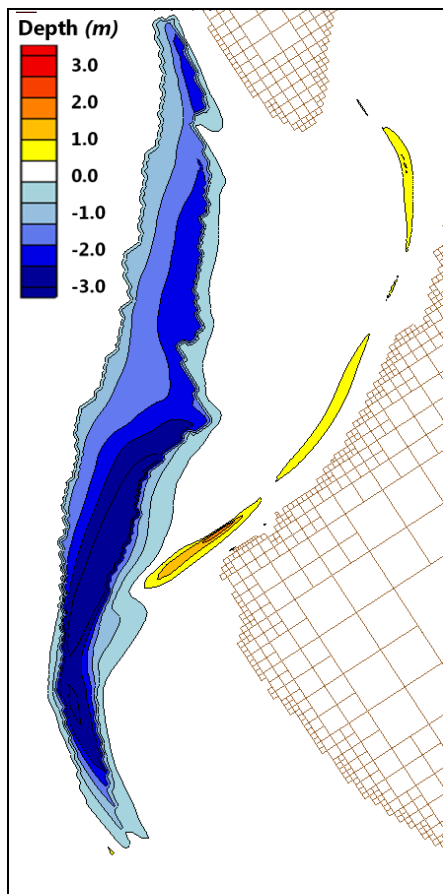


Figure 161: Spatial difference in bathymetry between “No Action” Alternative and Alternative D3 end state November 2004

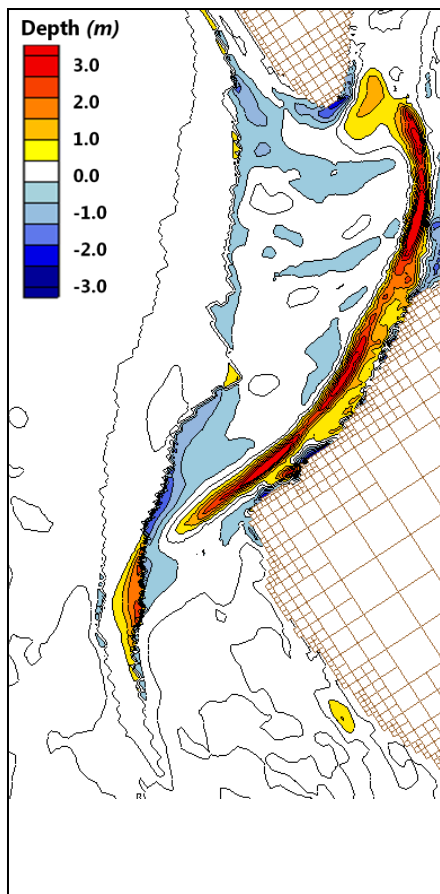


Figure 162: Temporal evolution of the Ebb Shoal; May 2004 - November 2004 Alternative D3

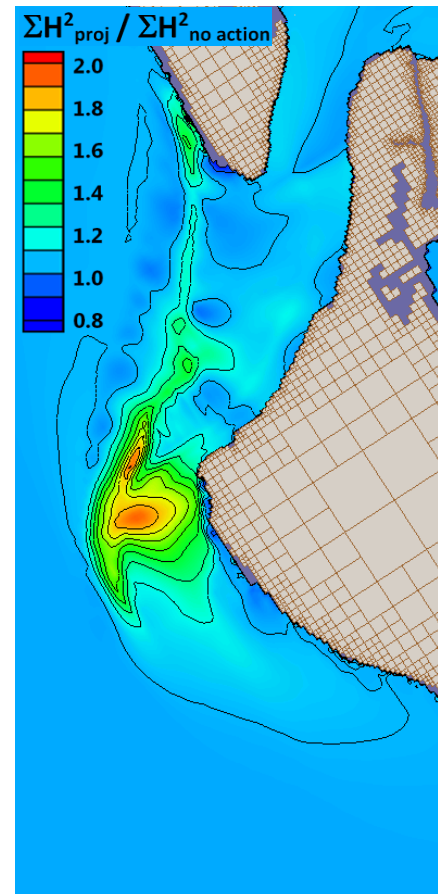


Figure 163: Cumulative Wave Energy May 2004 - November 2004 Alternative D3*-C-B

11.2. Alternative D2

Alternative D2 would mine 680 thousand cubic yards from Big Sarasota Pass to -12' MLW using a rectangular cut at the western edge of the shoal. Figure 164 shows the bathymetry and ebb shoal morphology at the end of the six month model run from May 4, 2004 to November 4, 2004. Examination of the ending morphology shows that for the "No Action" case (Figure 164, left), the general deflation of the updrift shoal as the main channel infills with sediment that had originated on the shoal. There is erosion of the most northerly flood marginal channel at the southern tip of Lido Key and increased definition (erosion) of the flood marginal channels across the updrift shoal.

Examination of the ending morphology for Alternative D2 (Figure 164, right) some infilling of Cut D2, which indicates that sediment bypass is still occurring, and shows that the remainder of the shoal does not change relative to the "No Action" Alternative. The greatest difference between the two cases is the location of Cut D2.

Figure 165 and Figure 166 show differences both spatially and temporally between the "No Action" Alternative and Alternative D2, directly. In Figure 165, the most significant change spatially between both alternatives is the dredge site itself. The residual depression in bathymetry at Cut D2 can be readily seen which are approximately up to 6 ft deeper than the "No Action" Alternative. There is no increase in accretion at the navigation channel for this alternative. In Figure 166, the temporal change from May to November 4, 2004 can be seen for Alternative D2. Here the slight deflation of the northern lobe and infilling of the navigation channel are readily observed. Again, it is important to recall that infilling of the navigation channel occurs in the "No Action" Alternative as seen in Figure 34 (main text). Here, as demonstrated by Figure 165, there is a slight difference in the bathymetry at the location of the navigation channel, especially on the most southwesterly portion of the channel when comparing the "No Action" Alternative with Alternative D2.

Also calculated from the model results was the normalized cumulative wave energy throughout the model grid Figure 167. Off the shoreline of Siesta Key fronting the Gulf of Mexico, there is no increase in wave energy (Figure 167).

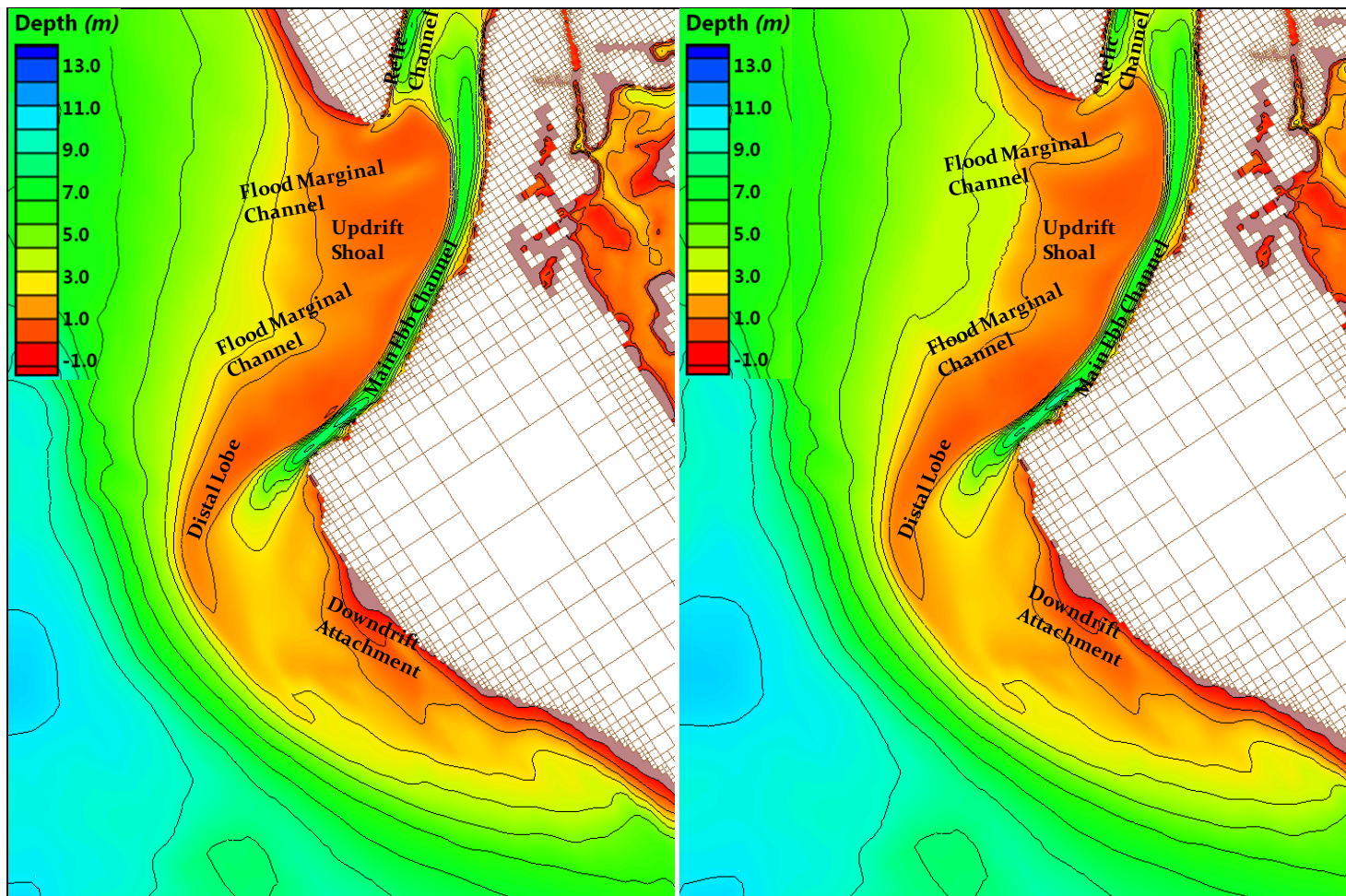


Figure 164: “No Action” Alternative (left), Alternative D2 (right); end state November 2004

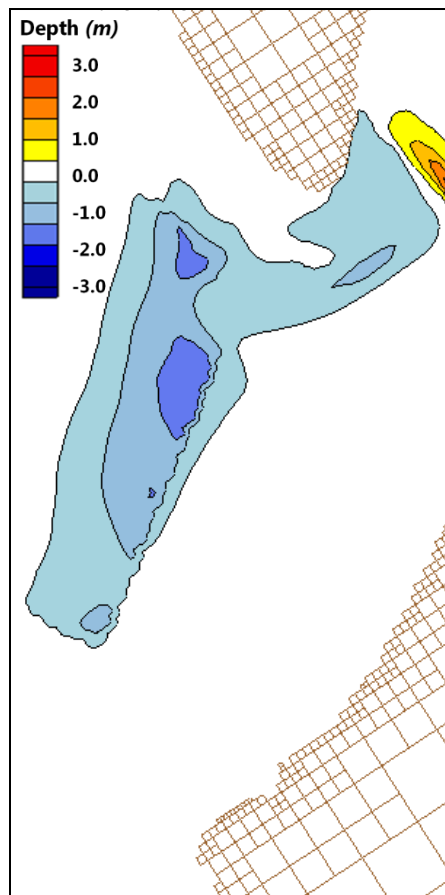


Figure 165: Spatial difference in bathymetry between “No Action” Alternative and Alternative D2 end state November 2004

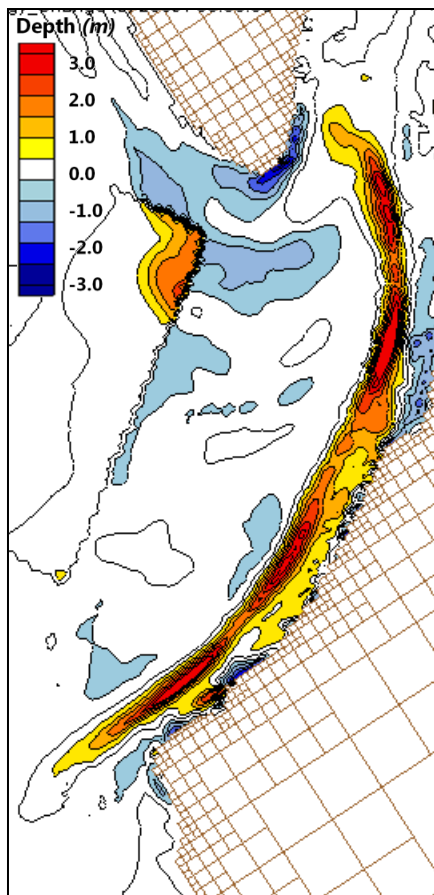


Figure 166: Temporal evolution of the Ebb Shoal; May 2004 - November 2004 Alternative D2

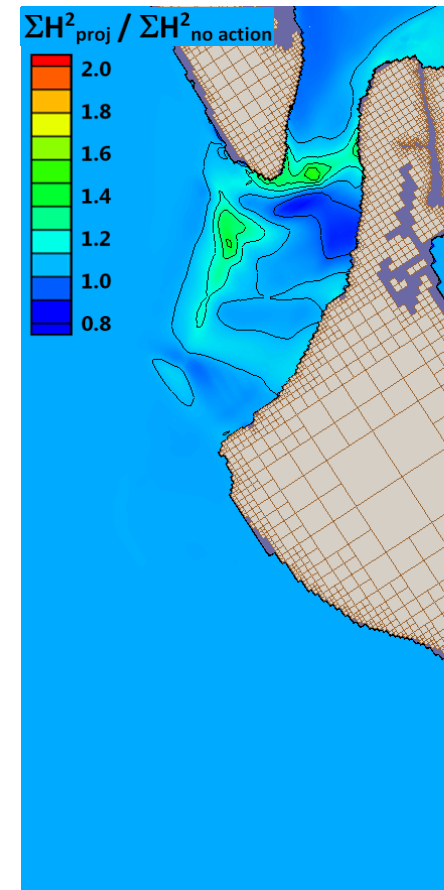


Figure 167: Cumulative Wave Energy May 2004 - November 2004 Alternative B+C+D2

11.3. Alternative C

Alternative C would mine 800 thousand cubic yards from Big Sarasota Pass to -12' MLW through the ebb shoal where ephemeral channels have appeared and re-appeared through time. Figure 168 shows the bathymetry and ebb shoal morphology at the end of the six month model run from May 4, 2004 to November 4, 2004. Examination of the ending morphology shows that for the "No Action" case (Figure 168, left), the general deflation of the updrift shoal as the main channel infills with sediment that had originated on the shoal. There is erosion of the most northerly flood marginal channel at the southern tip of Lido Key and increased definition (erosion) of the flood marginal channels across the updrift shoal.

Examination of the ending morphology for Alternative C (Figure 168, right) there is a great deal of infilling of Cut C, which will serve as a renewable dredge site. It is important to note that the remainder of the shoal does not change relative to the "No Action" Alternative. The greatest difference between the two cases is the location of Cut C.

Figure 169 and Figure 170 show differences both spatially and temporally between the "No Action" Alternative and Alternative C, directly. In Figure 169, the most significant change spatially between both alternatives is the dredge site itself. The residual depression in bathymetry at Cut C can be readily seen which are approximately up to 5 ft deeper than the "No Action" Alternative. There no increase in accretion at the navigation channel for this alternative, in fact, the navigation channel remains deeper for this alternative. The reason is that sediment that is moved by wave energy during the general deflation of the northern lobe is usually deposited in the navigation channel. Here, instead, it is deposited into Cut C. In Figure 170, the temporal change from May to November 4, 2004 can be seen for Alternative C. Here the slight deflation of the northern lobe, infilling into Alternative C and infilling of the navigation channel are readily observed.

Also calculated from the model results was the normalized cumulative wave energy throughout the model grid Figure 171. There is increased wave energy within cut C, but because Cut C is a relatively localized cut protected by the remainder of the ebb shoal and wave energy is allowed to dissipate before it comes close to Siesta Key.

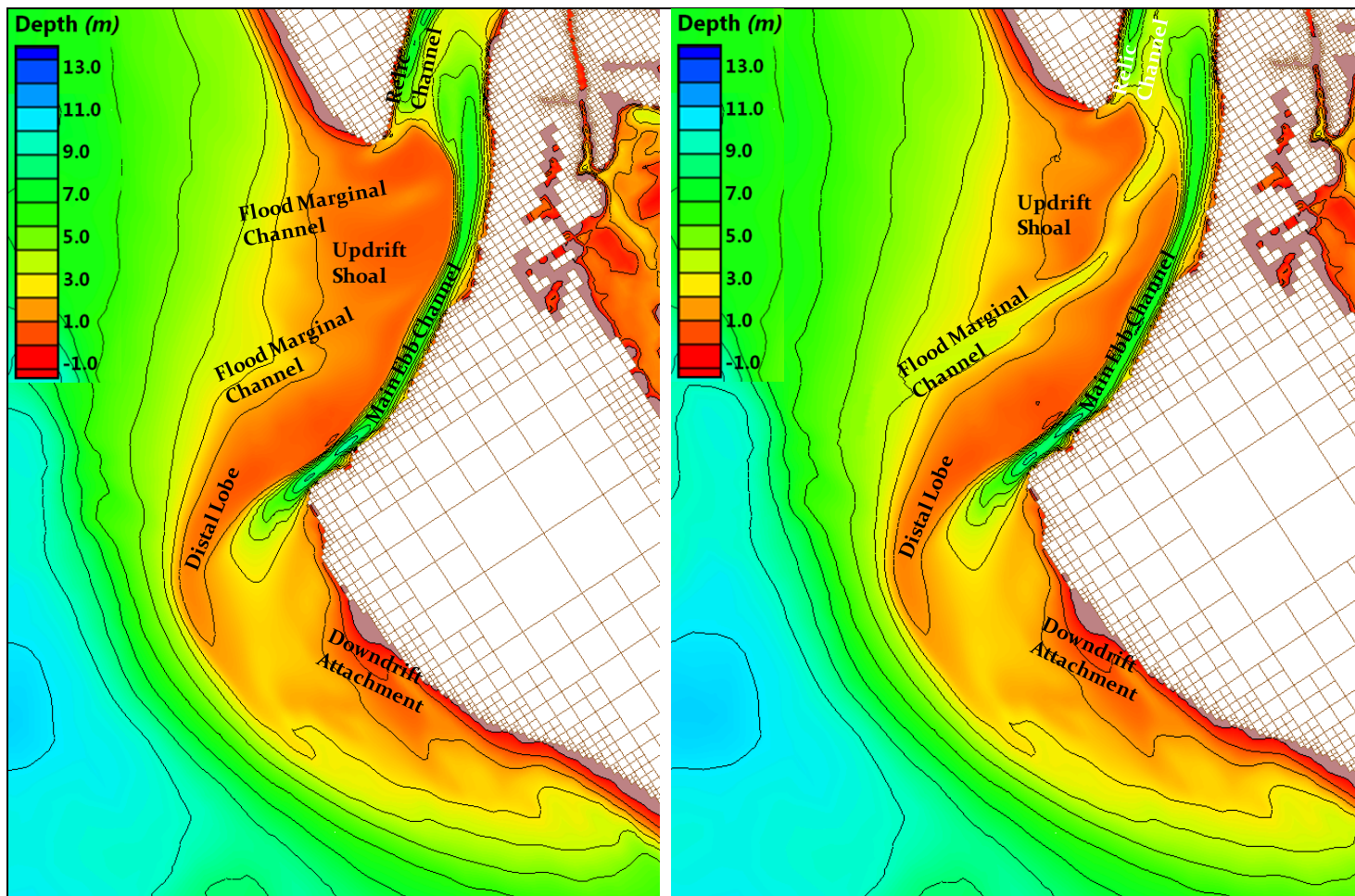


Figure 168: “No Action” Alternative (left), Alternative C (right); end state November 2004

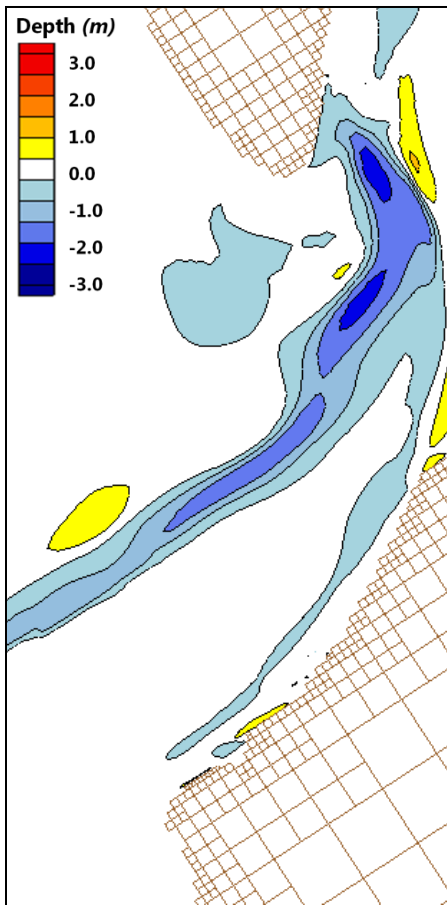


Figure 169: Spatial difference in bathymetry between “No Action” Alternative and Alternative C end state November 2004

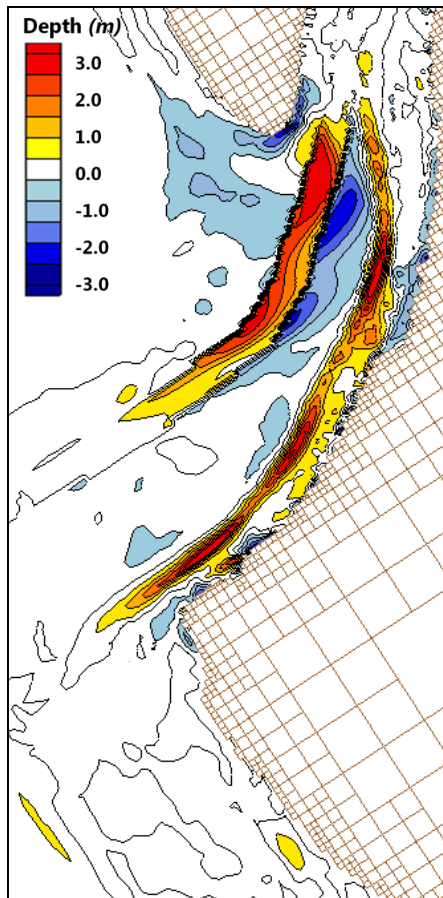


Figure 170: Temporal evolution of the Ebb Shoal; May 2004 - November 2004 Alternative C

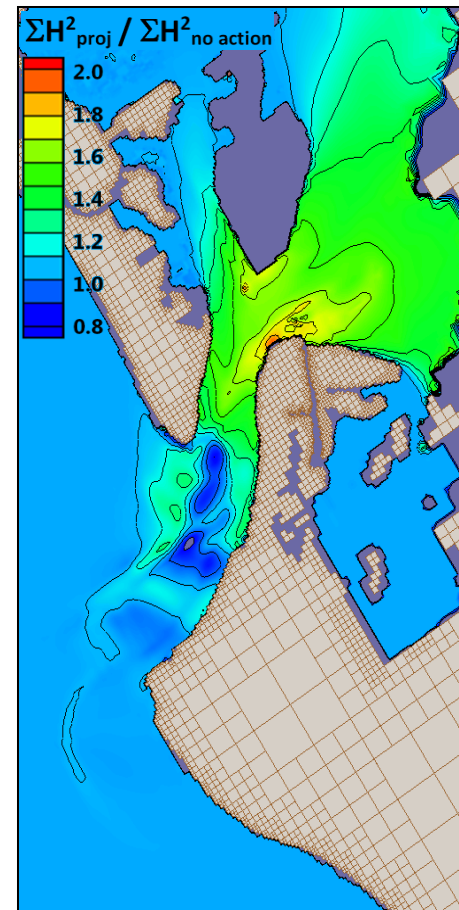


Figure 171: Cumulative Wave Energy May 2004 - November 2004 Alternative C

11.4. Alternative B

Alternative B would mine 250 thousand cubic yards from Big Sarasota Pass to -12' MLW through terminus of the navigation channel to the southwest through the outer shield. Figure 172 shows the bathymetry and ebb shoal morphology at the end of the six month model run from May 4, 2004 to November 4, 2004. Examination of the ending morphology shows that for the "No Action" case (Figure 172, left) the general deflation of the updrift shoal as the main channel infills with sediment that had originated on the shoal. There is erosion of the most northerly flood marginal channel at the southern tip of Lido Key and increased definition (erosion) of the flood marginal channels across the updrift shoal.

Examination of the ending morphology for Alternative B (Figure 172, right) there is relatively no infilling of Cut B. The remainder of the shoal does not change relative to the "No Action" Alternative. The greatest difference between the two cases is the location of Cut B.

Figure 173 and Figure 174 show differences both spatially and temporally between the "No Action" Alternative and Alternative B, directly. In Figure 173, the most significant change spatially between both alternatives is the dredge site itself. The residual depression in bathymetry at Cut B can be readily seen which are approximately up to 5 ft deeper than the "No Action" Alternative. There is no appreciable increase in accretion at the navigation channel for this alternative. In Figure 174, the temporal change from May to November 4, 2004 can be seen for Alternative B. Here the slight deflation of the northern lobe, infilling of the navigation channel are readily observed. Cut B remains relatively free of sediment.

Also calculated from the model results was the normalized cumulative wave energy throughout the model grid Figure 175. Offshore of Siesta Key, at the location of Cut B, wave energy is increased 1.5 times the "No Action" Alternative due to increased depth in the region.

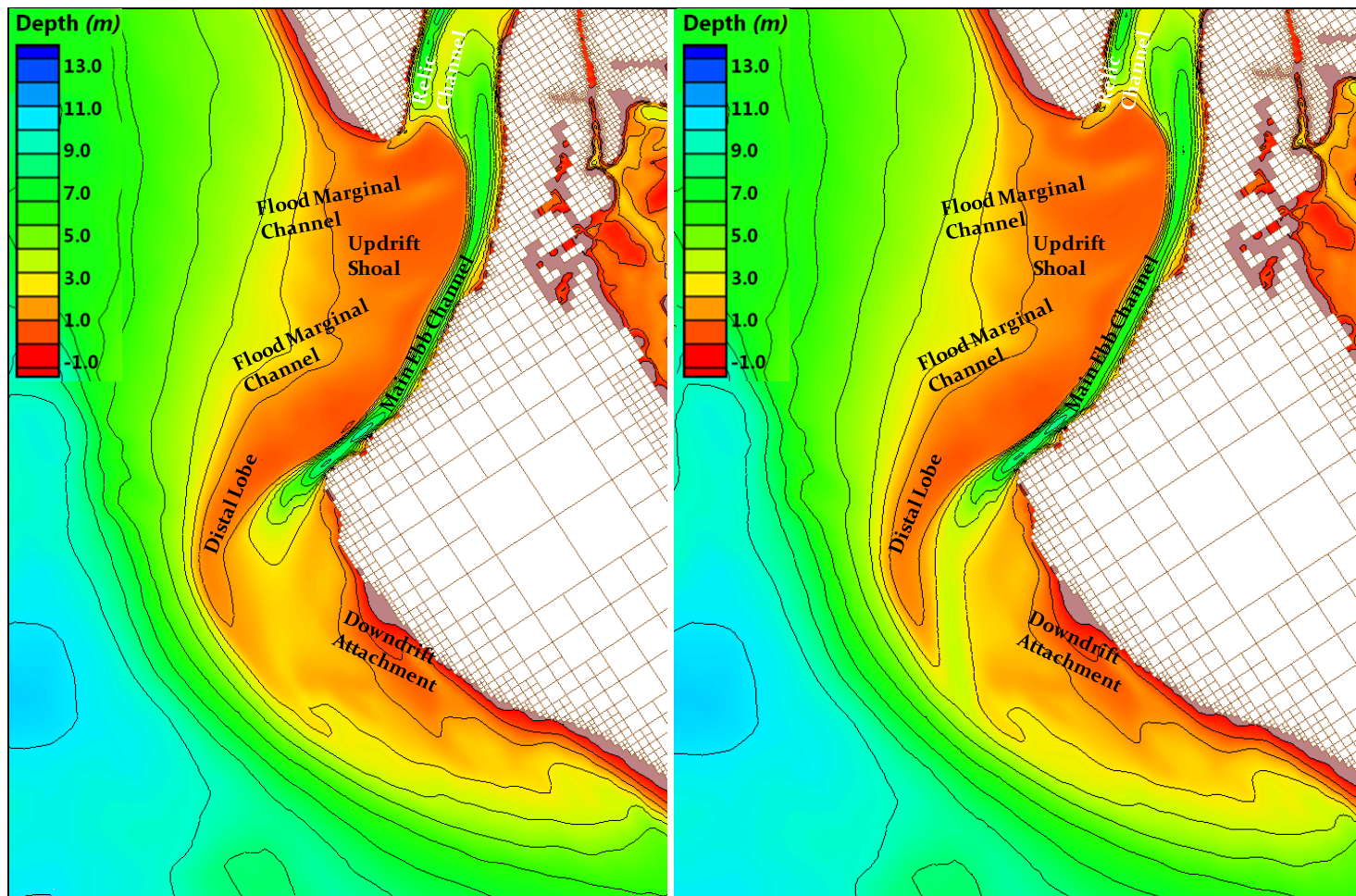


Figure 172: “No Action” Alternative (left), Alternative B (right); end state November 2004

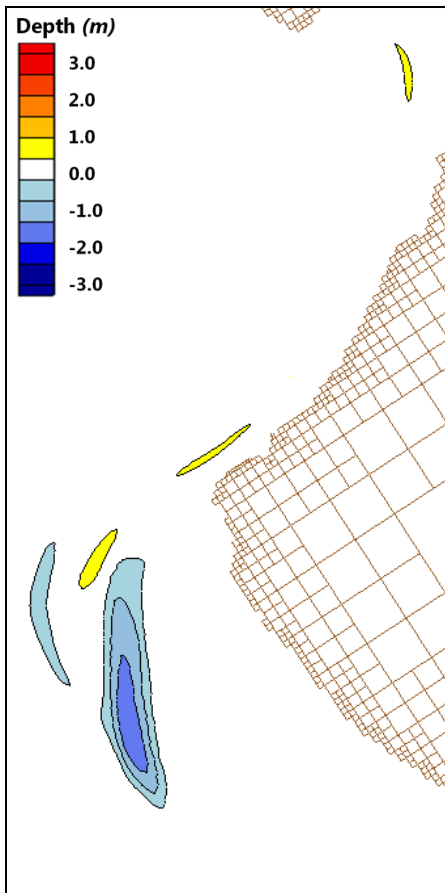


Figure 173: Spatial difference in bathymetry between “No Action” Alternative and Alternative B end state November 2004

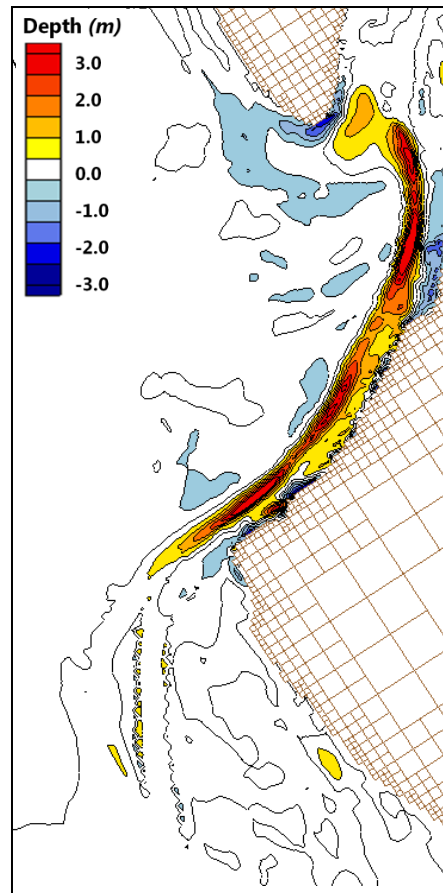


Figure 174: Temporal evolution of the Ebb Shoal; May 2004 - November 2004 Alternative B

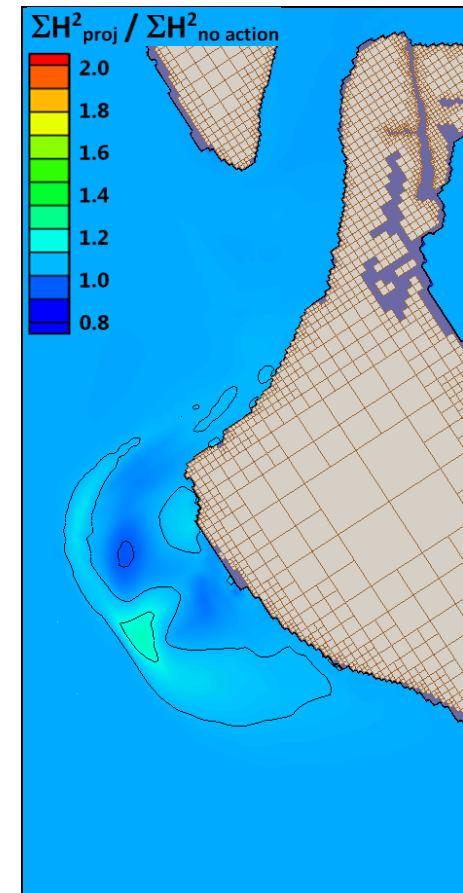


Figure 175: Cumulative Wave Energy May 2004 - November 2004 Alternative B

11.5. Alternative D1

Alternative D1 would mine 360 thousand cubic yards from Big Sarasota Pass to -12' MLW adjacent to the western edge of the existing navigation channel. Figure 176 shows the bathymetry and ebb shoal morphology at the end of the six month model run from May 4, 2004 to November 4, 2004. Examination of the ending morphology shows that for the "No Action" case (Figure 176, left) the general deflation of the updrift shoal as the main channel infills with sediment that had originated on the shoal. There is erosion of the most northerly flood marginal channel at the southern tip of Lido Key and increased definition (erosion) of the flood marginal channels across the updrift shoal.

Examination of the ending morphology for Alternative D1 (Figure 176, right) it is very difficult to see the infilling of Cut D1. The remainder of the shoal does not change relative to the "No Action" Alternative. The greatest difference between the two cases is the location of Cut D1.

Figure 177 and Figure 178 show differences both spatially and temporally between the "No Action" Alternative and Alternative D1, directly. In Figure 177, the most significant change spatially between both alternatives is the dredge site itself and in the navigation channel. The residual depression in bathymetry at Cut D1 can be readily seen which are approximately up to 5 ft deeper than the "No Action" Alternative. There no appreciable increase in accretion at the navigation channel for this alternative, in fact, the navigation channel remains deeper for Alternative D1. The reason is that sediment that is moved by wave energy during the general deflation of the northern lobe is usually deposited in the navigation channel. Here, instead, it is deposited into Cut D1. In Figure 178, the temporal change from May to November 4, 2004 can be seen for Alternative D1. Here the slight deflation of the northern lobe, infilling into Alternative D1 and infilling of the navigation channel are readily observed. Again, it is important to recall that infilling of the navigation channel occurs in the "No Action" Alternative as seen in Figure 34 (main text).

Also calculated from the model results was the normalized cumulative wave energy throughout the model grid Figure 179. To understand this figure, one must imagine standing on the shoreline, or being anchored at one location in a vessel for the entire six-month model run. Along the eastern edge of the navigation channel, increases in wave energy can be 1.3 times as much due to the wider navigation channel.

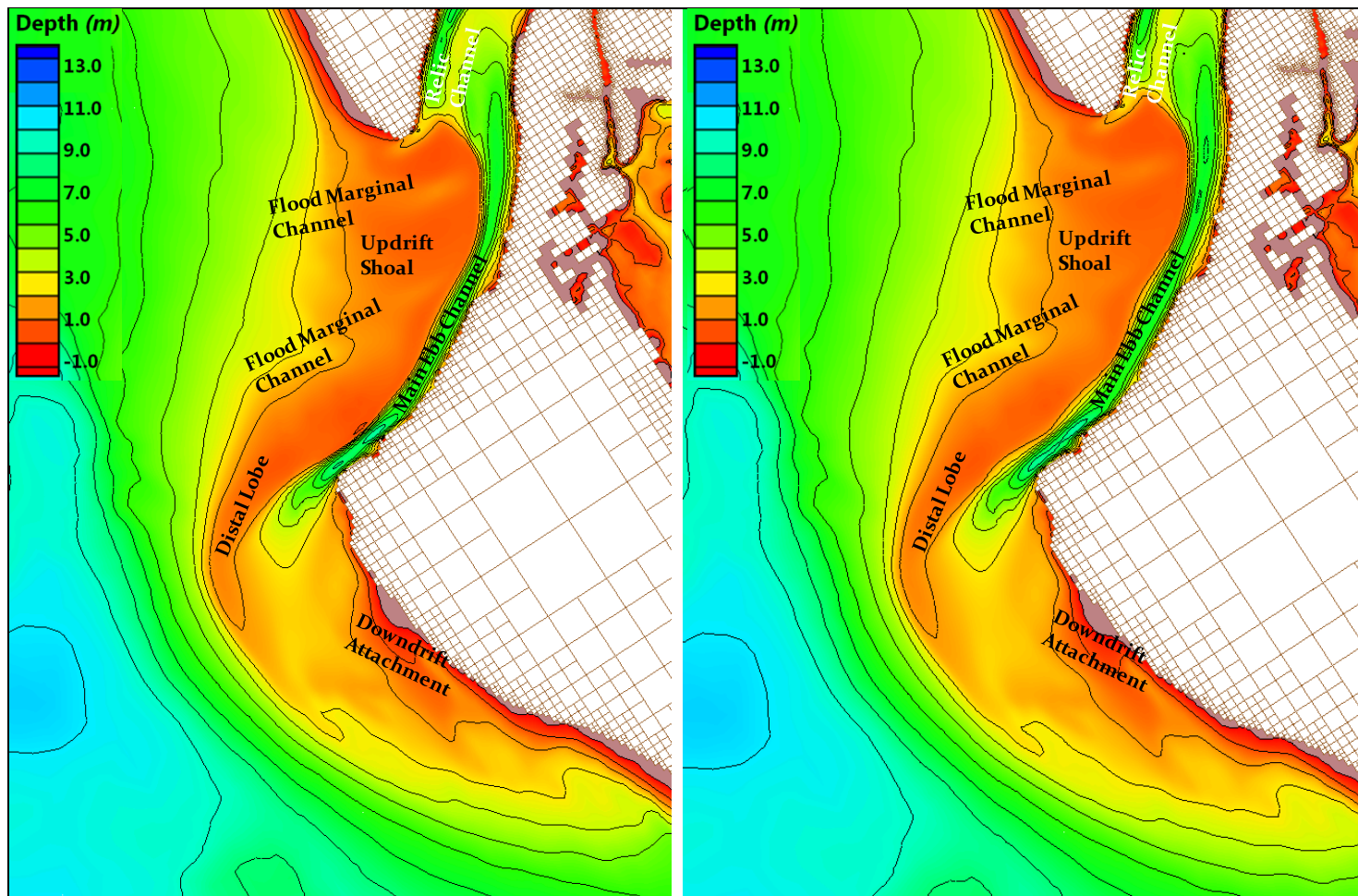


Figure 176: “No Action” Alternative (left), Alternative D1 (right); end state November 2004

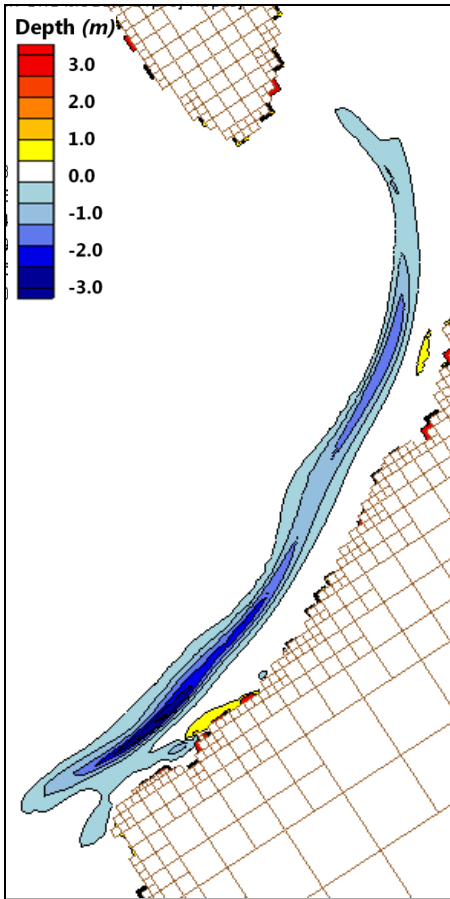


Figure 177: Spatial difference in bathymetry between “No Action” Alternative and Alternative C end state November 2004

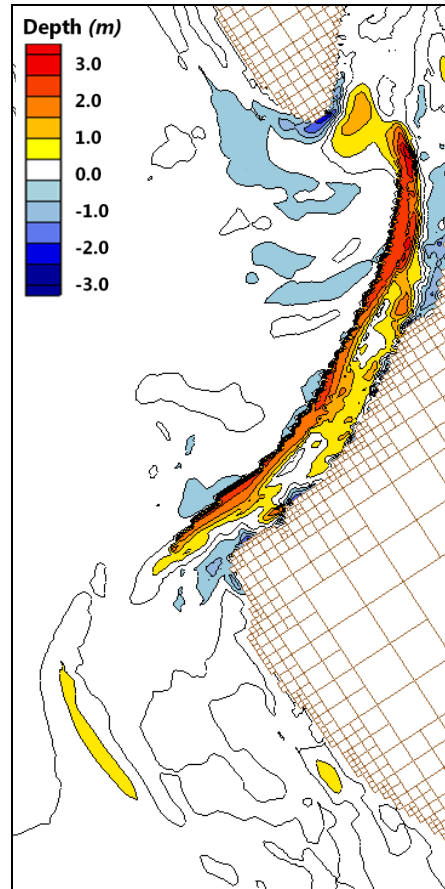


Figure 178: Temporal evolution of the Ebb Shoal; May 2004 - November 2004 Alternative C

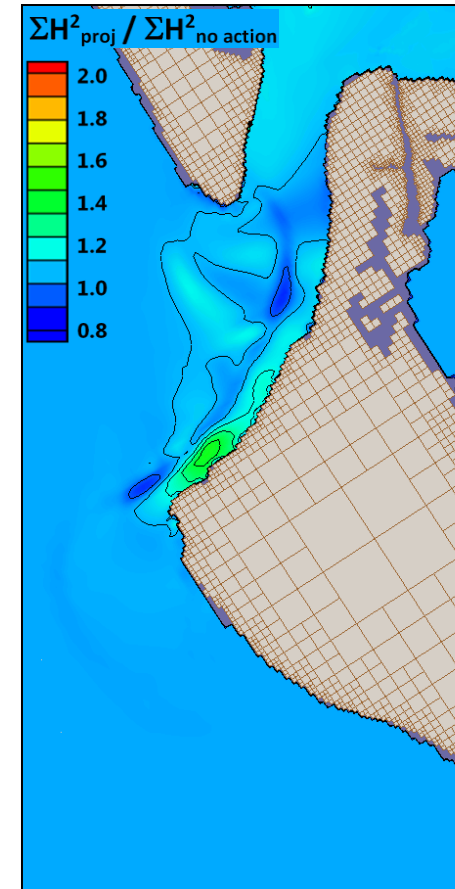


Figure 179: Cumulative Wave Energy May 2004 - November 2004 Alternativ